NOVEL HIGH WATER CONTENT HYDROGELS

BEVERLEY KAUR BENNING

Doctor of Philosophy

ASTON UNIVERSITY

September 2000

THESIS SUMMARY ASTON UNIVERSITY

NOVEL HIGH WATER CONTENT HYDROGELS

BEVERLEY KAUR BENNING

Submitted for the degree of
Doctor of Philosophy

September 2000

Hydrogels may be described as cross-linked hydrophilic polymers that swell but do not dissolve in water. The production of high water content hydrogels was the subject of investigation. Based upon copolymer compositions that had already achieved commercial success as biomaterials, new monomers were added or substituted in and the effects observed.

The addition of N-isopropyl acrylamide to an acrylamide-based composition that had previously been designed to become a contact lens, produced materials that showed smart effects in that the water content showed dependence on the temperature of the hydrating solution. Such thermo-responsive materials have potential uses in drug delivery, ultrafiltration and cell culture surfaces.

Proteoglycans in nature have an important role to play in structural support where a highly hydrophilic structure maintains lubricious surfaces. Certain functional groups that impart this hydrophilicity are present in certain sulphonate monomers, Bis(3-sulphopropyl ester) itaconate, dipotassium salt (SPI), 3-Sulphopropyl ester acrylate, potassium salt (SPA) and Sodium 2-(acrylamido)-2-methyl propane sulphonate (NaAMPS). These monomers were incorporated into a HEMA-based copolymer that had been designed initially as a contact lens and the resulting effects examined. Highly hydrophilic materials resulted that showed reduced protein deposition over the neutral core material. It is postulated that a sulphonate group would have a larger number of hydration shells around it than for example methacrylic acid, leading to more dynamic exchange and so reducing the adsorption of biological solutes.

A cationic monomer was added to bring back the net anionic nature of the sulphonate hydrogels and the effects studied. Ionic interactions were found to cause a reduction in the water content of the resulting materials as the mobility of the network decreased, leading to stiffer but less extensible materials. The presence of a net dominant charge, whether negative or positive, appeared to act to reduce protein deposition, but increasing equivalence in the amount of both charges served to present a more 'neutral' surface and deposition subsequently increased.

The grafting of hydrophilic hydrogel layers onto silicone elastomer was attempted and the results evaluated using dynamic contact angle measurements. Following plasma oxidation to reduce the surface energy barrier to aqueous grafting chemistry, it was found that the wettability of the modified elastomers could be significantly enhanced by such treatment. The SPA-grafted material in particular hinted at an osmotic drive for rehydration that may be exploited in biomaterials.

Keywords: hydrogel, ionic, sulphonate, hydrophilic, aqueous grafting, wettable, spoilation.

For my family

ACKNOWLEDGEMENTS

I would like to take this opportunity to show my appreciation to the following good folks:

I would like to thank Professor Brian Tighe for his guidance, enthusiasm and financial support throughout the course of this research. Additionally, for the opportunities to attend many conferences, particularly in New Orleans but also the group trips to the coast and other towns for various UK meetings.

To the members of the Biomaterials Research Unit who have made my time at Aston such an eye-opening and entertaining experience (the two usually occurring simultaneously). In particular Ais, whose humour and good sense (except after ten beers) could sometimes outmatch my own, Fi, for her lab know-how and with whom I rediscovered the pleasures of shopping and red wine, Mel, play-hard-work-hard-5"-heels girl and all three again for many good times – thanks guys!

Dr. Val Franklin for undertaking the *in vitro* ocular spoilation studies described in this thesis. Her time is much appreciated, as is the time and assistance from Dr. Steve Tonge for performing the dynamic contact angle analysis on the lens materials found in Chapter Seven. Dr. Rich Young, for getting the plasma rig working and plasma-oxidizing the relevant materials for me as the first step in my grafting forays, as well as being a source of chemistry-type knowledge on occasions too numerous to mention. Thank you for things both work-related and otherwise.

EPSRC and Vista Optics for the their financial support given under the Total Technology interdisciplinary higher degree scheme.

To my mates Sara and Vicky, for always being there as my remote sounding boards and entertaining trips away when I needed a break.

And finally my family, for the support, the distractions and a home.

LIST OF CONTENTS

LIST OF TABLES

LIST OF FIGURES

ABBREVIATIONS

EWC	Equilibrium water content	IPN	Interpenetrating network
DSC	Differential scanning calorimetry	DATr	N,N'-Diallyltartardiamide
AZBN	Azo-iso-butyronitrile	EGDMA	Ethylene glycol dimethacrylate
AMO	Acryloyl morpholine	NVP	N-Vinyl pyrrolidone
DMAEMA	Dimethylaminoethyl methacrylate	NIPA	N-Isopropyl acrylamide
AA	Acrylamide	T	Temperature
HPA	Hydroxypropyl acrylate	HEMA	Hydroxyethyl methacrylate
MPEGMA	Methoxy-poly(ethylene glycol) methacrylate	THFMA	Tetrahydrofurfuryl methacrylate
EEMA	2-Ethoxyethyl methacrylate	NaAMPS	Sodium 2-(acrylamido)-2-methyl propane sulphonate
SPA	3-Sulphopropyl ester acrylate, potassium salt	SPI	Bis(3-sulphopropyl ester) itaconate, dipotassium salt
Q	Reactivity of monomer	e	Charge on radical
S_T	Surface tension	E	Initial modulus
Ts	Tensile strength	Eb	Elongation to break
γ	Surface tension	θ	Contact angle
UV	Ultra-violet	PEG	Poly(ethylene glycol)

CHAPTER 1

Introduction

"Intelligence is quickness to apprehend
as distinct from ability,
which is capacity to act wisely on the thing apprehended."
Alfred North Whitehead, 1861-1947.

1.1 Hydrogels

Hydrogels may be described as cross-linked hydrophilic polymer networks which are swollen in but do not dissolve in water. The water contained within a hydrogel governs unique mechanical, surface and permeability properties that allow the material's use in a biological environment, particularly as a contact lens. The components of a hydrogel can be manipulated to change these properties to suit a certain application.

During the 1960's, Wichterle and Lim[1] identified the unique properties of a novel material suitable for biological use, notably as a contact lens. It showed a similarity to biological tissue with regard to water content, permeability to biological solutes and optical clarity. They produced the most widely known hydrogel, poly(2-hydroxyethyl methacrylate), or p(HEMA), which is able to swell in water by virtue of its hydroxyl group. This quickly replaced the structurally similar but hydrophobic material poly(methyl methacrylate) as the main lens material, which itself had replaced glass as a contact lens in the 1940's.

The plasticizing effect of water improved comfort for the wearer and the lens would subsequently be worn for a longer period of time. As the cornea is avascular, oxygen is supplied via the dissolved water in the hydrogel. Over the next half a century, other monomers were incorporated into hydrogels to increase the amount of water in the gel and to control the inherently poor mechanical properties of such a swollen structure.

In the 1970's, the major feature of claims in published patents was N-vinyl pyrrolidone (NVP). This monomer had already found use in another biomaterials field as a blood plasma expander[2] in the form of a linear water-soluble polymer (later abandoned) and more recently as a transdermal penetration enhancer[3]. The addition of NVP resulted in increased hydrophilicity of the material. However, the poor reactivity of NVP towards vinyl polymerisation in non-aqueous solution detrimentally affected the surface wettability and efficacy of a lens, which may subsequently affect corneal health. This has been the subject of a great deal of work in recent years in our group and will be discussed later.

Other patents in the late 1970's and early 1980's, including work performed at Aston University in the Biomaterials unit, described ways in which tough, stable acrylamide-based hydrogels could be prepared by bulk polymerisation[4]. Acrylamide conferred a structural advantage by allowing hydrogen bonding between polymer chains at high water content, thus increasing strength.

Until recently, only a small proportion of patents mentioned the importance of a coherent tear film to hinder the deposition of tear components. Fluorine-substituted monomers have been included in past patents to manipulate surface chemistry and control protein deposition[5]. Very few recognised and discussed the mechanisms of dehydration and attempted to reduce it, but a Johnson & Johnson patent[6] has included a zwitterionic monomer in a contact lens composition which was claimed to reduce thermally-induced water loss.

The chemistry of most of the materials in commercial use today is based upon the ideas described in the patents published in the 1970's. Methyl methacrylate remains a feature of many compositions, solely for its strengthening properties. Some commercial lens materials, components and water contents can be found in Table 1.1.

Trade name	USAN nomenclature	Material	% Water	Manufacturer
Medalist	Polymacon	HEMA	38	Bausch & Lomb
Hydrocurve II 55	Bufilcon A	HEMA/Acrylamide	55	PBH
Acuvue	Etafilcon A	HEMA/MA	58	Vistakon
Medalist 66	Hefilcon	HEMA/NVP	66	Bausch & Lomb
Permalens	Perfilcon	HEMA/NVP/MA	71	Coopervision
Frequency 73	Hefilcon	HEMA/NVP	73	Aspect
Permaflex	Surfilcon	MMA/NVP	74	PBH

Table 1.1 Monomer components and water content of some commercially available contact lens materials.

Hydrogels have many other applications in the biomedical field, including synthetic articular cartilage[7], wound dressings[8], skin adhesives[9] and in biotechnology as sensors and perm-selective membranes[10]. A review by Corkhill *et al*[11] discusses the many possible hydrogel applications, including some of those mentioned above.

In nature, biological surfaces are polar, with essentially an overall negative charge. Many constituents of biological fluids are also polar. As such, the use of charged monomers would have major effects on hydrogel bulk properties and their behaviour in a biological environment. As proteins in particular are sensitive to such charges, this can be an important factor in biocompatibility. In 1989, biocompatibility was defined as 'the ability of a material to perform with an appropriate host response in a specific application'[12] and this can still encompass the wide range of properties required for any implant.

1.2 Semi-Interpenetrating Polymer Networks (Semi-IPN)

An IPN has been defined as a combination of two polymers, each in network form, where at least one polymer has been synthesized and/or cross-linked in the presence of the other[13]. The class of IPN formed is dependent upon the method used to synthesize the IPN.

The simultaneous polymerisation of a solution of both monomers with their cross-linkers and initiators, by two different non-interfering methods produces a simultaneous, full IPN.

When a pre-formed polymer is dissolved in a hydrophilic monomer and cross-linking mixture and then polymerised, the network formed is called a semi-interpenetrating network (semi-IPN) and this is the type used in this work.

The primary polymer chain around which a hydrogel network is formed significantly modifies the behaviour of the hydrogel. The most obvious change relates to improved mechanical properties, as well as water binding and surface properties. IPN materials are stiffer and stronger than hydrogel copolymers of similar water content, but are less elastic. They also have noticeably lower polar components (γ_p) of surface energy, unlike copolymers of similar composition or equilibrium water content.

Gross optical properties relate to compatibility phenomena:

i. Solubility of the initial polymer and monomer mix, which can be assisted by use of a diluent,

ii. Compatibility of the polymer and the monomer,

iii. Compatibility of the polymer in the polymerised xerogel,

iv. Compatibility of the semi-IPN with water.

Translucence in hydrated systems is generally due to the preferential water clustering around the more hydrophilic moieties to the exclusion of hydrophobic blocks, causing light to scatter. Of course, optical properties would be of importance for applications such as a contact lens material but of lesser importance in e.g. wound dressings.

Although high water, optically clear semi-IPNs would be useful as contact lenses, translucent and opaque materials may be of use as wound dressings and synthetic articular cartilage.

1.3 Equilibrium Water Content

A cross-linked, hydrophilic polymer will swell when placed in water until equilibrium is reached. The water content of a fully hydrated and equilibrated hydrogel material is given as the equilibrium water content, EWC. This is quantified by the ratio of the water in the hydrogel to the total weight of the hydrogel, expressed as a percentage.

$$EWC\ (\%) = \frac{\text{Weight of water in hydrogel}}{\text{Total weight of hydrated hydrogel}} \times 100 \qquad \textit{Equation 1.1}$$

The water content is probably the single most important property of a hydrogel. It governs the mechanical properties, surface properties, permeability to biological solutes and behaviour at a biological interface. It results from a number of factors including: nature of monomers, cross-link density, temperature and pH of the hydrating solution.

Although highly important, the EWC is not the only structural aspect that must be taken into account. The water structure within the gel, chain stiffness and inter-chain forces are also capable of exerting a dominating influence.

For use as a biomaterial, there will be a necessary, dictated range of acceptable mechanical properties that will be governed somewhat by water. When applied as a

contact lens, the eyelid will physically challenge comfort and retention of visual stability during the blink cycle. The EWC can easily be varied by applying knowledge of monomer hydrophilicity or hydrophobicity and by varying the cross-link density.

1.4 The Structure of Water

The study of water binding was initially performed on cellulose acetate membranes[14,15]. Differential scanning calorimetry (DSC) was used to clarify that there were fours states of water and the semi-permeability of the membrane depended on the ratio of these states; completely free, free water weakly interacting with the polymer, bound water which can contain salts and bound water which rejects salts.

Work on synthetic polymers found that water could exist in more than one state. The water exists in a continuum of two extremes. Polar groups in hydrogel polymers interact more strongly with water than non-polar fragments. Water strongly associated to the polymer via hydrogen bonding is popularly referred to as 'bound' water. Water not taking part in direct hydrogen bonding and so with a greater degree of mobility is referred to as 'free' water. It has been suggested that the nature and relative amounts of the different states of water will affect the properties of hydrogels.

It is known that HEMA hydrogels have lower free to bound water ratios than NVP. A report by Lai[16] correlating water evaporation from hydrogel lenses with free and bound water found that higher free to bound water ratios gave a higher magnitude of lens dehydration.

Work published over the years supports the evidence for thermodynamically different classes of water within a hydrogel as a result of varying molecular interactions. The terms that have arisen in polymer chemistry to describe the different states of water depend upon the technique used for analysis, some of which are found in Table 1.2.

Bound Non-freezing		Free Freezing
Bound	Interfacial	Bulk
Primary bound	Secondary bound	Free bulk
Tightly bound	Loosely bound	

Table 1.2 Some classifications of water binding states.

Arguments also exist that are contrary to the model of thermodynamically different classes of water[17]. It has been proposed that the crystallisation of water in gels is a very gradual process that leads to the development of a meta-stable, non-equilibrium state; the internal structure of the gel can be described as an elastic solution in which the water molecules are distributed continuously over all possible orientations to and interactions with the polymer. There is no clear distinction between states.

An explanation for the two endothermic peaks produced by DSC on p(HEMA) hydrogels, at well below the melting of ice (usually associated with freezable bound) and at the freezing point of ice (associated with freezable free), claims that they are really the same peak interrupted by an exothermic peak caused by amorphous ice undergoing crystallisation just below the melting transition. The third claimed state, non-freezing water, is postulated as the fraction unaccounted for by DSC, perhaps because it is hidden in a broad continuum.

However, the theory of different states is widely accepted and is useful as a characterization technique to relate to the individual material.

Other techniques used to study water binding in hydrogels include ^{1}H nuclear magnetic resonance (NMR) spectroscopy[18-22], specific conductivity[23] and differential thermal analysis[24]. This work utilizes DSC to enable an easy, quantitative determination of the relative amount of freezing water to be made[25-28].

1.5 Differential Scanning Calorimetry (DSC)

Using calorimetric techniques, it has been found that only part of the total water within a gel will freeze.

Developed by Perkin-Elmer in 1964, DSC allows the percentage of freezing water to be calculated and also displays information about the water binding sites within the hydrogel through the shape of the melting endotherm. The freezing water fraction is calculated by measuring the energy required to maintain both the sample and a reference holder as the same temperature. For endothermic transitions, the energy input to the sample holder is increased, while for exothermic transitions, energy input to the reference is increased. A peak is displayed at a transition and the energy input to the sample or reference is measured directly as the area under the peak. The schematic for the measuring system is shown in Figure 1.1.

The ΔH of pure water is known (333.77 Jg^{-1}) and is believed to be approximately identical to the freezing water found in a hydrogel. This allows the calculation of freezing water to be made as described in section 2.4.

It has been noted that perhaps it is inappropriate to use 333.77 Jg^{-1} for the calculation, as the enthalpy of bound ice should be lower than ordinal ice with hexagonal packing[28]. But since there is no known method to isolate the captured bound ice, the slight possibility of error remains.

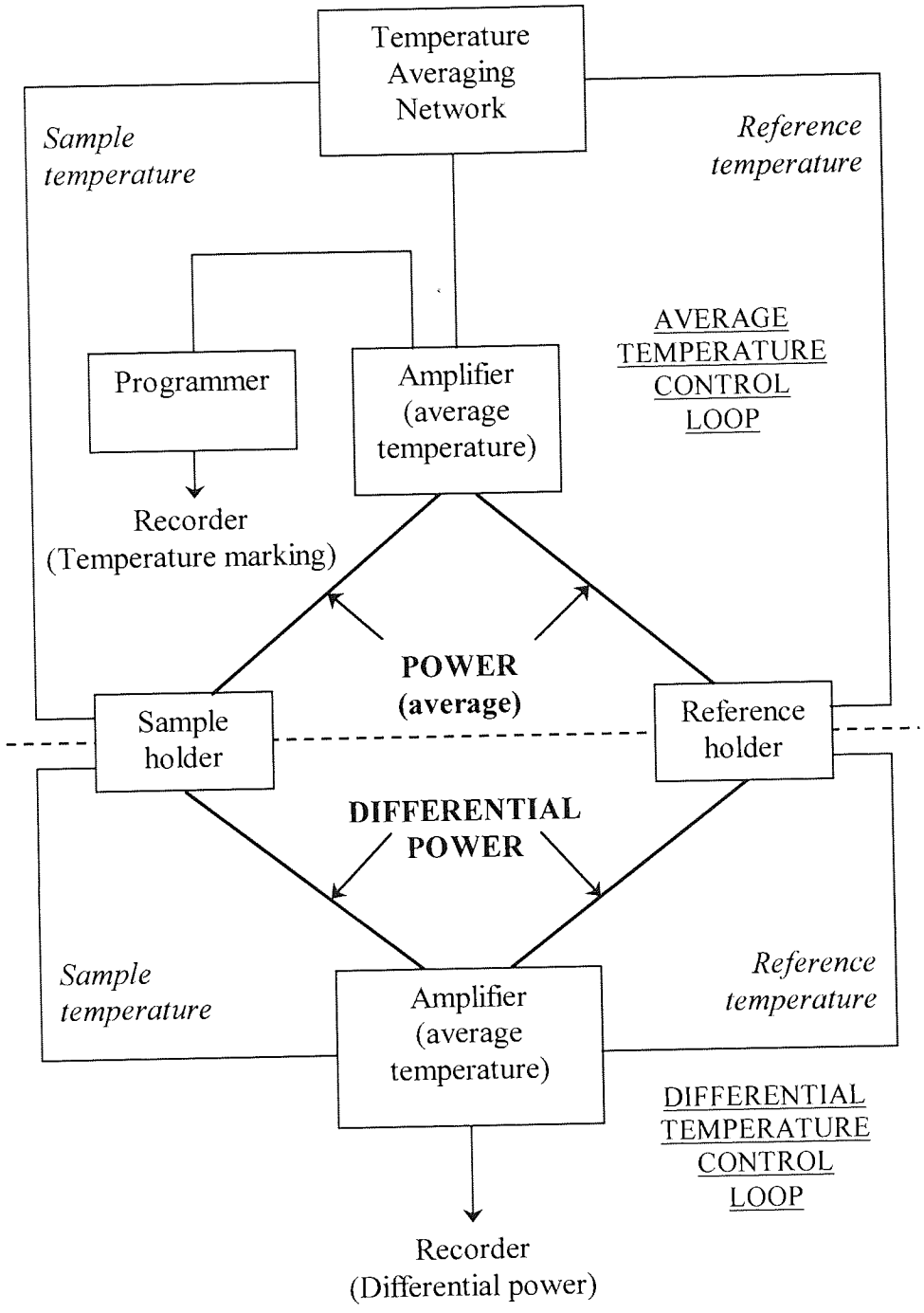

Figure 1.1 Schematic representation of a differential scanning calorimeter.

1.6 Wettability

In the 1970's, Holly and Refojo[29] looked at the wettability of pHEMA, the most widely used contact lens material. They found that water did not spread spontaneously on the material surface, despite the bulk water content of about 40%. Water would wet the gel if the adhesion of the gel to water was at least as strong as the cohesion of water, and this was not the case. A large hysteresis in the advancing and receding contact angles was found, indicating that the surface was capable of changing its free energy via the re-orientation of polymer chains.

As such, although a lens may be hydrophilic in that it contains water, this does not mean that the surface is automatically hydrophilic as well. The polymer chain at the lens-air boundary orientates itself into a position of lowest free energy, i.e., hydrophobic groups pointing out, hydrophilic groups buried into the lens. Efforts to reduce or even prevent chain rotation must be an integral part of controlling wettability and deposition.

The Wilhelmy plate technique has been used to examine the hysteresis of polymers by many researchers[30-32]. This requires a mechanical testing device, a balance and a means of graphical output. As the stage is raised, the sample is immersed in the test liquid, usually water. A meniscus is formed as the sample first contacts the liquid and as immersion continues, the contact angle becomes steady, producing a constant slope on the graphical output. After immersion reaches a pre-determined depth (8-12mm), the process is reversed; the wetting liquid is lowered and a constant slope due to the receding angle is obtained. The mechanics of the measurements are shown schematically in Figure 1.2. A straight-line approximation of the advancing and receding contact angles is made and extrapolated back to zero depth of immersion. The equations for determining the advancing (θ_A) and receding (θ_R) angles are given by,

$$\text{Cos}\,\theta = F / \gamma P \qquad \textit{Equation 1.2}$$

Where F = the wetting force at zero depth immersion (F_A, advancing) and withdrawal (F_R, receding), γ = the surface tension of HPLC Grade water (72.8 mN m^{-1}) and P = sample perimeter measured with a micrometer.

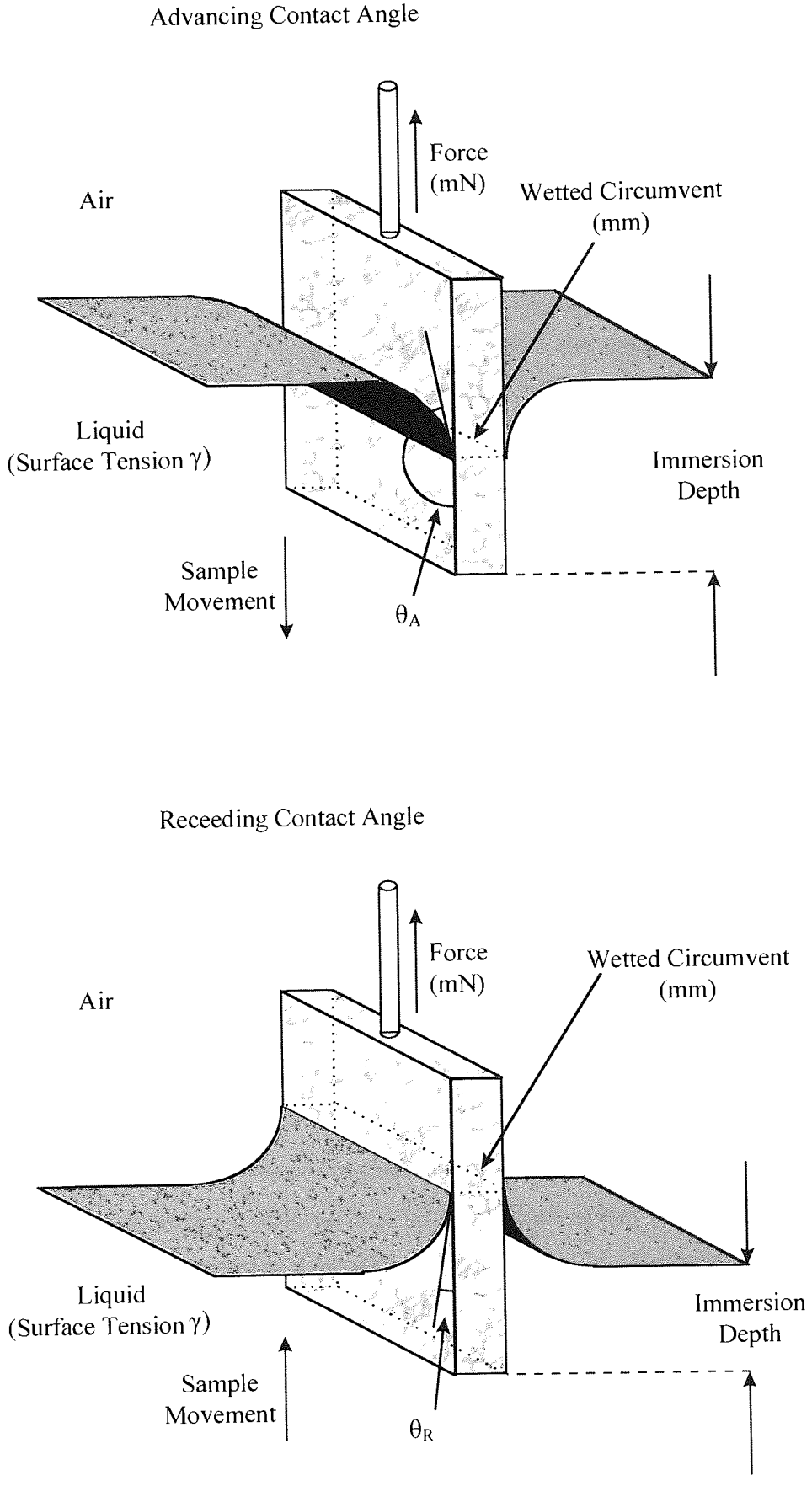

Figure 1.2 Advancing and receding contact angles.

Two types of hysteresis have been classified:

- Thermodynamic hysteresis, where the hysteresis curve is reproducible over many cycles and is independent of time and frequency.
- Kinetic hysteresis, where the curve changes with time and conditions.

Figures 1.3 and 1.4 show the hysteresis curves of poly(butadiene) and dehydrated pHEMA respectively, the first of which is an example of a thermodynamic hysteresis and the second of a kinetic hysteresis, where the effect of partial hydration on the second cycle can be seen.

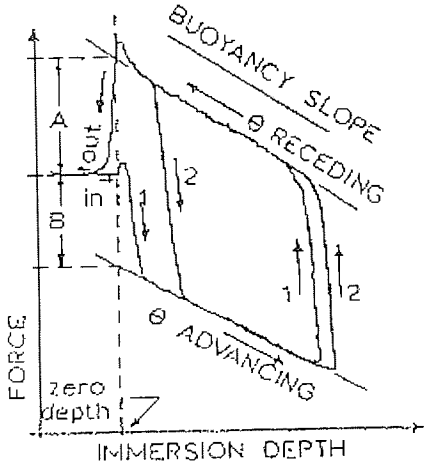

Figure 1.3 Hysteresis cycle for poly(butadiene).

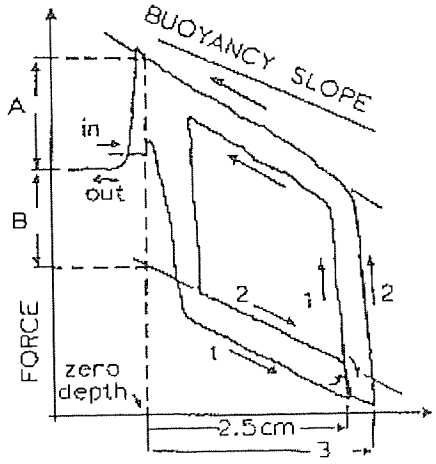

Figure 1.4 Hysteresis cycle for dehydrated pHEMA.

Morra *et al*[32] investigated the speed dependence of the technique and found that at low speed, the chains had time to conform and fairly constant slopes could be obtained with pHEMA. At high speed, the re-organisation of chains started to lag behind the advancing water front which 'saw' the unwetted gel surface as relatively hydrophobic. The surface conversion to a lower energy state could not keep up with the motion of the advancing wetting front and the interfacial tension between the gel and the water remained initially high immediately behind the advancing front.

The hydrophilic and hydrophobic functions of a hydrogel are not just affected by the bulk composition but by the microstructure of the polymer, i.e. sequence distribution and this

can also affect the observed hysteresis[33]. Surface characteristics must be closely controlled for coherent tear spreading as deposition by ocular components is aided by tear film break-up.

1.7 Contact Angle Measurements

Information may be obtained regarding the surface of the hydrogel by making contact angle measurements. Analysis of the interface between a drop of wetting liquid or vapour on a solid surface enables the surface free energy of solids to be obtained. The surface free energy is formed from polar and dispersive contributions that influence the compatibility of the material in biological environments. The polar component in particular is important in that it determines the wettability of a material.

Results are obtained by resolving the forces at a three-phase interface, formed either by a drop of liquid on a solid surface in air or by a drop of liquid or vapour on a solid surface immersed in a liquid. From almost two hundred years ago, the theories used to determine the surface free energy of polymers from contact angle measurements have been developed and are outlined below.

1.7.1 Dehydrated Surfaces

In 1805, Young[34] derived an equation to resolve the forces at the contact point of a sessile drop of liquid on a solid surface as shown in Figure 1.5.

$$\gamma_{sv} = \gamma_{sl} + \gamma_{lv}\cos\theta \qquad \textit{Equation 1.3}$$

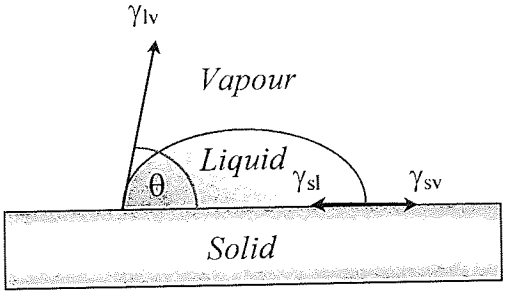

Where

γ_{sv} = solid-vapour interfacial free energy
γ_{sl} = solid-liquid interfacial free energy
γ_{lv} = liquid-vapour interfacial free energy

Figure 1.5 The components of solid surface free energy.

Nearly sixty years later, Dupre[35] reasoned that the reversible work of adhesion of a liquid and solid, W_a, could be expressed as

$$W_a = \gamma_s + \gamma_{lv} + \gamma_{sl} \qquad \textit{Equation 1.4}$$

These two equations may be combined to give the well-known Young-Dupre equation.

$$W_a = (\gamma_s - \gamma_{sv}) + \gamma_{lv} (1 + \cos\theta) \qquad \textit{Equation 1.5}$$

As it stands, this equation is not adequate to deal with the action of polar forces across the interface.

Owens and Wendt[36] determined the polar and dispersive forces to give an expression for the determination of the surface free energies of dehydrated polymer surfaces.

$$1 + \cos\theta = (2/\gamma_{lv}) ((\gamma_{lv}^{d}\gamma_s^{d})^{0.5} + (\gamma_{lv}^{p}\gamma_s^{p})^{0.5}) \qquad \textit{Equation 1.6}$$

This equation is able to relate the contact angle, θ, to the polar and dispersive components of the solid, γ_s^p and γ_s^d. Where the polar and dispersive components for two wetting liquids are already known, the polar and dispersive components for the solid can be determined by solving the simultaneous equations. The total free surface energy, γ_s^t, can be found by adding the values of the polar and dispersive components[37].

$$\gamma_s^t = \gamma_s^d + \gamma_s^p \qquad \textit{Equation 1.7}$$

The most widely used wetting liquids are distilled water and diiodomethane, due to their high total surface free energies and their balance of polar and dispersive components, shown in Table 1.3.

Liquid	γ_s^d (mN m^{-1})	γ_s^p (mN m^{-1})	γ_s^t (mN m^{-1})
Water	21.8	51.0	72.8
Diiodomethane	48.1	2.3	50.4

Table 1.3 Polar and dispersive components for water and diiodomethane

1.7.2 Hydrated Surfaces

The determination of surface energies in air has problems of reproducibility due to variations in removal of excess surface water and dehydration of the polymer. Two techniques have been developed to overcome these problems, Hamilton's method[38,39] and the captive air bubble technique, which allow the surface energy of a polymer to be determined in the fully hydrated state.

1.7.2.1 Hamilton's Method

This method involves measuring contact angles of n-octane drops on a solid surface whilst immersed in water, as shown in Figure 1.6.

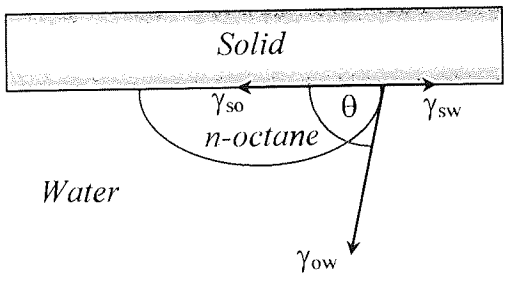

Where

γ_{sw} = solid-water interfacial free energy
γ_{ow} = octane-water interfacial free energy
γ_{so} = solid-octane interfacial free energy

Figure 1.6 The free energy components for Hamilton's method.

Fowkes[40] developed an equation to explain the work of adhesion at the solid-liquid interface, where the sum of the free surface energies of the two separate phases would be offset by the stabilization from dispersive forces (universal van der Waals forces) to give the interfacial free energy between the solid and the liquid.

$$\gamma_{sl} = \gamma_s + \gamma_{lv} - 2(\gamma_s^d \gamma_{lv}^d)^{0.5} \qquad \textit{Equation 1.8}$$

Tamai *et al*[41] extended Fowkes' work to include stabilization at the interface by non-dispersion forces, I_{sl}, such as hydrogen bonding and dipole interactions.

$$\gamma_{sl} = \gamma_s + \gamma_{lv} - 2(\gamma_s^d \gamma_{lv}^d)^{0.5} - I_{sl} \qquad \textit{Equation 1.9}$$

where

$$I_{sl} = 2(\gamma_{lv}^p \gamma_s^p)^{0.5} \qquad \textit{Equation 1.10}$$

Octane and water have surface free energies of 21.8 and 72.0mN m^{-1} respectively, the surface free energy of octane due to dispersion forces only (γ_{ov}^d). The surface free energy of water consists of dispersion forces (γ_{wv}^d) of 21.8mN m^{-1} and polar forces (γ_{wv}^p) of 50.2mN m^{-1}. Fowkes showed that the only forces that contribute to the interfacial free energy between two liquids are those forces that exist in both liquids. As octane and water have identical dispersion force contributions, octane underwater contact angles would have an identical value of solids that can only interact through dispersion forces but have higher values on solids that may interact via polar forces.

Equations 1.2 and 1.8 combine and reduce down to an equation that corresponds to the polar stabilisation energy between water and the solid.

$$I_{sw} = \gamma_{wv} - \gamma_{ov} - \gamma_{ow}\cos\theta \qquad \textit{Equation 1.11}$$

Where

I_{sw} = polar stabilization energy between water and the solid

γ_{wv} = surface tension of n-octane saturated water

γ_{ov} = surface tension between n-octane and water

γ_{ow} = surface tension between n-octane and water

Once the components γ_{ov} and γ_{ow} have been determined experimentally by Fowkes' method, I_{sw} may be calculated. Substituting the final value of I_{sw} into equation 1.10 enables the polar component of the surface free energy, γ_s^p, to be determined.

1.7.2.2 Captive Air Bubble Method

A bubble of air is used instead of a drop of n-octane in this method[42], which uses the same experimental procedure as Hamilton's method. Using data from both Hamilton's and the captive air bubble techniques, values for γ_{sv}, γ_{sv}^{p}, γ_{sv}^{d} and γ_{sw} can be determined[43].

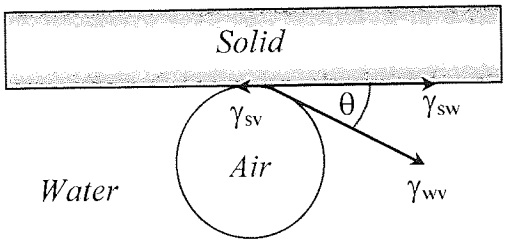

Where

γ_{sw} = solid-water interfacial free energy
γ_{wv} = water-vapour interfacial free energy
= surface tension of water
γ_{sv} = solid-vapour interfacial free energy
= solid surface free energy = γ_s

Figure 1.7 Individual free energy components for the captive air bubble technique.

Young's equation to the captive air bubble technique may be applied.

$$\gamma_{sv} - \gamma_{sw} = \gamma_{wv}\cos\theta \qquad \textit{Equation 1.12}$$

As γ_{wv} is equal to the surface tension of water, 72.8mN m^{-1}, and θ is obtained from the measurement shown in Figure 1.7, it is possible to determine $\gamma_{sv} - \gamma_{sw}$. For this technique, γ_{wv} = 72.8mN m^{-1}, γ_{ov} = 21.8mN m^{-1} and γ_{ow} = 51.0mN m^{-1}. The polar stabilisation component shown as Equation 1.11,

$$I_{sw} = \gamma_{wv} - \gamma_{ov} - \gamma_{ow}\cos\theta$$

then,

$$I_{sw} = 51.0(1 - \cos\theta) \qquad \textit{Equation 1.13}$$

The dispersive component of the solid, γ_{sv}^{d}, may be determined by the combination and rearrangement of Equations of 1.9 and 1.12.

$$\gamma_{sv}^{d} = (((\gamma_{sv} - \gamma_{sw}) - I_{sw} + \gamma_{wv})/2(\gamma_{wv}^{d})^{0.5})^{2} \qquad \textit{Equation 1.14}$$

The polar component of the solid, γ_{sv}^{p}, is obtained by rearranging Equation 1.10.

$$\gamma_{sv}^{p} = (I_{sw})^{2}/(4\gamma_{wv}^{p}) \qquad \textit{Equation 1.15}$$

A spreadsheet application has been programmed so that γ_{sv} - γ_{sw}, I_{sw}, γ_{sv}^{d}, γ_{sv}^{p}, γ_{sv} and γ_{sw} may be calculated upon entry of θ.

The Owens and Wendt equation (Equation 1.6) may also be used to determine the dispersive component of the surface free energy of hydrated hydrogels. The polar component obtained from Hamilton's method, together with the water/air contact angle, is substituted into the equation and the dispersive component calculated. Corkhill[44] has shown that the results obtained by the method and from Equation 1.14 are to within 0.2mN m^{-1} of each other.

1.8 Spoilation

The term spoilation encompasses the physical and chemical changes in the hydrogel contact lens and the various extraneous deposits which may impair the optical properties of the lens, or produce symptoms of discomfort and often intolerance to the wearer[45]. The principal of ocular spoilation is common to other instances where materials contact biological fluids, i.e. thrombosis at foreign surfaces, the formation of dental plaque in saliva. These all involve the adsorption of protein at a solid surface.

The build up of debris on a contact lens can reduce visual acuity and cause discomfort[46]. This debris is mainly proteinaceous in nature but also includes cholesterol mucopolysaccharides, lipoidal and ionic species. *In vivo* leaching of the remnants of polymerisation is also a cause of inflammation, but these artefacts should be eliminated from an expanded gel network prior to biological contact via hydration.

The critical surface tension of solid surfaces is sometimes used as an indicator of biocompatibility. This is defined as the surface tension of a liquid that will just wet the surface and spread[47]. Interfacial tension is the difference between the critical surface tension of the surface and the surface tension of the liquid. Some groups have suggested that for maximum biocompatibility, an interfacial tension of less than 5 mN m^{-1} is needed. Baier[48] found that implanted materials that exhibited thromboresistance were coated with a thin layer of glycoprotein which had a critical surface tension of 20-30 mN m^{-1} and the surface chemistry was dominated by methyl groups. Andrade found that highly hydrophilic surfaces minimised protein adsorption, which in turn prevented

thrombus formation due to a low interfacial energy. Ikada *et al*[47] stated that there were two ways for a polymer surface to be non-adhesive, which is why both types of surface could be relatively blood compatible. These are:

- Super-hydrophilic, water-like surface.
- Super-hydrophobic.

Protein adsorption is a thermodynamic process, one of two types:

- Hydrophilic, exothermic and reversible.
- Hydrophobic, endothermic and irreversibly bound.

The corneal epithelium has a surface tension of approx. 30mN m^{-1} but the natural wetting agents in tears (mucins) reduces the surface tension of water (72.8mN m^{-1}) to 40-46mN m^{-1} and increases the critical surface tension of the cornea to about 40mN m^{-1} by adsorption on to its surface, both effects to facilitate a continuous tear film.

Tear break-up facilitates deposition of tear components, first referred to as 'spoilation' over 20 years ago by Montague Ruben in his important text on soft contact lenses[49]. This process has implications for both comfort and corneal health and a mechanism for protein adsorption is displayed in Figure 1.8.

Mirejovsky *et al*[50] found that high water/ionic lenses absorbed large amounts of protein, predominantly lysozyme, and this caused a fall in the EWC and freezing water, which led to a fall in oxygen permeability. Lactoferrin, albumin and α-acid glycoproteins were detected after 5 days. Initially, adsorbed protein results in an increased surface wettability due to a decrease in the boundary layer effect. Once chemical conversion occurs, hydrophobic domains appear on the lens surface and further, disadvantageous spoilation occurs. Synthetic surfaces are unable to contribute to the dynamic exchange of adsorbed components that natural surfaces can.

The characteristics of some proteins used in this study are shown in Table 1.4.

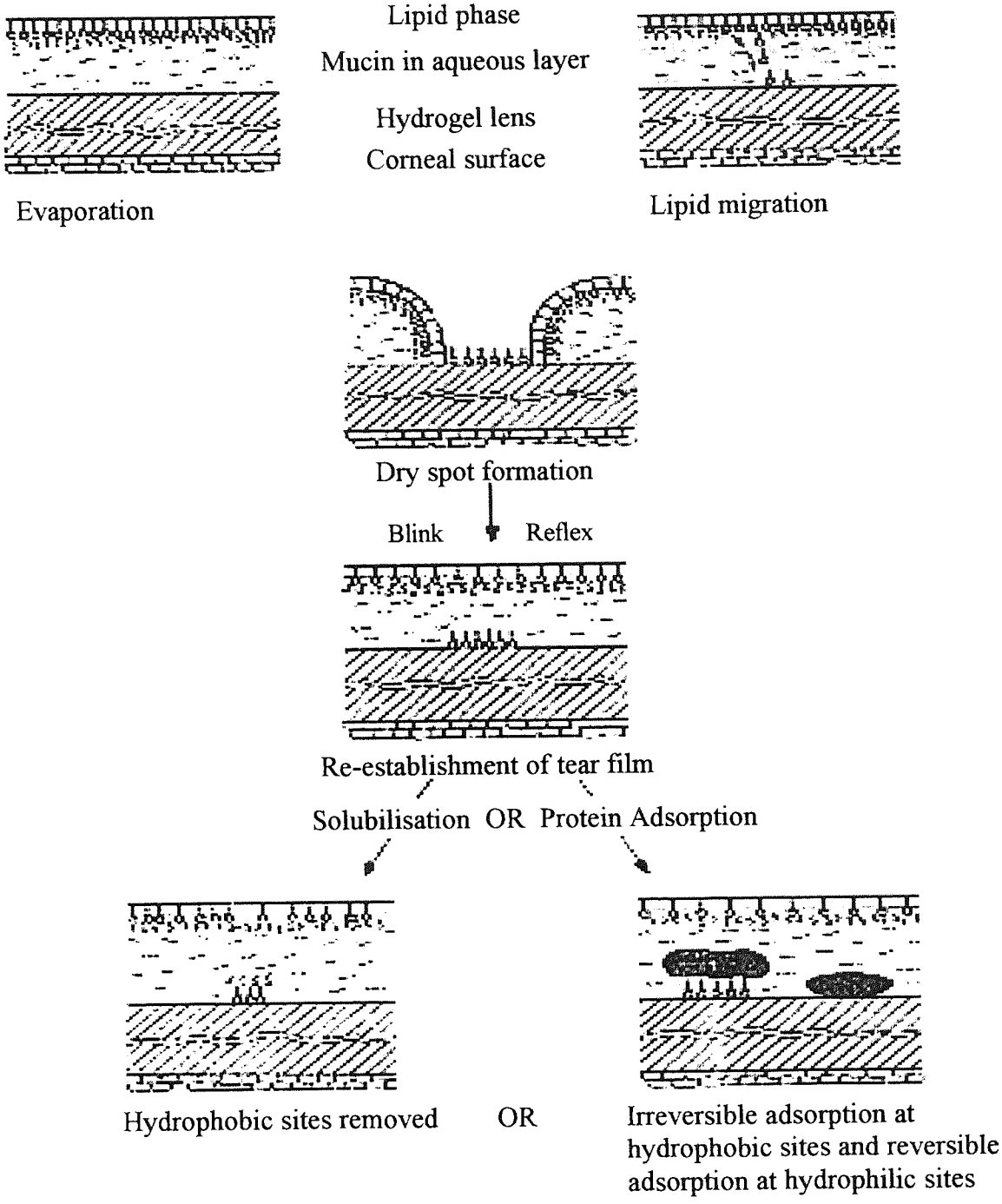

Figure 1.8 Schematic protein adsorption hypothesis[46].

Protein	Source	Molecular Weight	Relative Charge
Lysozyme	Chicken Egg	12,600	+ + +
Albumin	Human Serum	65,000	- - -
Lactoferrin	Bovine Colostrum	74,000	+ +
Insulin	Bovine Pancreas	6,000	0
Ferredoxin	Spinach	12,000	- - -

Table 1.4 Characteristics of the major proteins found in spoilation work.

Studies have shown that protein accumulation is highly material dependent and lipid deposition is primarily patient dependent. More protein is found deposited on ionic lenses over non-ionic and protein deposition increases with ionicity.

By using an artificial tear model and analysing 'spoiled' lens materials for protein and lipid deposits, comparative results are obtained to give an idea of lens performance. As primarily surface techniques, fluorescence (for measuring lipid levels) and UV (protein) give surface and bulk information respectively.

Lipids interact either via the carbonyl groups of fatty acids interacting with hydrogen bonding sites at the hydrogel surface, or via penetration into the hydrogel matrix because molecules have a greater solubility in the organic backbone than in water. Deposition arises with the regular collapse of the tear films and is independent from the ongoing interfacial process of protein adsorption[45]. Penetration of lipid into the polymer matrix modifies the interface and changes the course of biological conversion.

1.9 Copolymer Sequence Distributions

Work performed within this group over the years has shown that hydrogels with large, irregular domains of the same monomer type have a greater tendency to show non-specific protein adsorption than hydrogels with regular chemical variation[51,52]. A predictive mechanism was developed so that the formation of blocks could be avoided based on a given composition. This procedure could allow the optimal concentration of monomers to be used in the smart design of a hydrogel surface, which, as already discussed, has a major impact on biocompatibility. This is possible because, although the reactivity ratios for a pair of monomers are fixed, the concentrations may be varied to design a copolymer with short repeat units.

1.9.1 The Terminal Model of Copolymerisation

The standard kinetic treatment of free radical polymerisation is the terminal model of copolymerisation[54,55]. Here, the reactivity of an active centre is dependent only upon the monomer unit in the copolymer chain on which the radical is located. Four propagation

steps demonstrate the growth of the polymer chain and the consumption of monomer for two monomers.

$$\sim\sim\sim M_1\bullet + M_1 \longrightarrow \sim\sim\sim\sim M_1\bullet \qquad v_{1,1} = k_{1,1}\,[M_1\bullet\,][M_1] \qquad \textit{Equation 1.16}$$

$$\sim\sim\sim M_1\bullet + M_2 \longrightarrow \sim\sim\sim\sim M_2\bullet \qquad v_{1,2} = k_{1,2}\,[M_1\bullet\,][M_2] \qquad \textit{Equation 1.17}$$

$$\sim\sim\sim M_2\bullet + M_1 \longrightarrow \sim\sim\sim\sim M_1\bullet \qquad v_{2,1} = k_{2,1}\,[M_2\bullet\,][M_1] \qquad \textit{Equation 1.18}$$

$$\sim\sim\sim M_2\bullet + M_2 \longrightarrow \sim\sim\sim\sim M_2\bullet \qquad v_{2,2} = k_{2,2}\,[M_2\bullet\,][M_2] \qquad \textit{Equation 1.19}$$

Where

M = monomer

M• = monomer radical

k = rate constant

[ ] = concentration of species

The rate of consumption of the monomers can be expressed as,

$$-d[M_1]/dt = k_{1,1}[M_1\bullet][M_1] + k_{2,1}[M_2\bullet][M_1] \qquad \textit{Equation 1.20}$$

$$-d[M_2]/dt = k_{1,2}[M_1\bullet][M_2] + k_{2,2}[M_2\bullet][M_2] \qquad \textit{Equation 1.21}$$

The mole ratio of the monomers in the copolymer is given by,

$$\frac{d[M_1]/dt}{d[M_2]/dt} = \frac{k_{1,1}[M_1\bullet][M_1] + k_{2,1}[M_2\bullet][M_1]}{k_{1,2}[M_1\bullet][M_2] + k_{2,2}[M_2\bullet][M_2]} \qquad \textit{Equation 1.22}$$

If a steady state is reached immediately upon commencement of polymerisation, the total concentrations of $M_1\bullet$ and $M_2\bullet$ will remain constant and the rate of conversion of $M_1\bullet$ to $M_2\bullet$ will equal the rate of conversion of $M_2\bullet$ to $M_1\bullet$, i.e.,

$$k_{2,1}[M_2\bullet][M_1] = k_{1,2}[M_1\bullet][M_2] \qquad \textit{Equation 1.23}$$

The individual reactivity ratios of monomers M_1 and M_2 are defined as the ratio of the rates of reaction of a polymer chain ending in a radical of one type adding to itself, to the rate of its reaction with the second monomer in the copolymer system. As such,

$$r_1 = k_{1,1}/k_{1,2} \qquad \textit{Equation 1.24}$$

and

$$r_2 = k_{2,2}/k_{2,1} \qquad \textit{Equation 1.25}$$

Equation 1.22 reduces to,

$$\frac{d[M_1]}{d[M_2]} = \frac{[M_1]\,(1 + r_1[M_1]/[M_2])}{[M_2]\,(r_2 + [M_1]/[M_2])} \qquad \textit{Equation 1.26}$$

The reactivity ratios are a measure of which monomer a given radical has a preference to react with. If $r_1 > 1$, radical $M_1\bullet$ prefers to add monomer M_1 and if $r_1 < 1$, radical $M_1\bullet$ prefers to add M_2.

An ideal copolymerisation is where the radicals have the same preference of addition to each of the monomers and $r_1r_2 = 1$. The arrangement of the monomer units is completely random along the chain. When $r_1 = r_2 = 0$, each radical shows a strong preference for cross-propagation which results in the monomers alternating regularly regardless of the monomer feed ratio until one monomer is completely consumed. Where $r_1 = r_2 = 1$, neither radical centre shows a preference for either monomer and the rates of consumption are determined by the relative concentrations of monomer in the initial feed. If $r_1 >> r_2$, the polymerisation produces large blocks of M_1 with small segments of M_2 between the blocks until M_1 is completely consumed.

1.9.2 Computer Copolymer Sequence Distributions

The sequence distribution of a copolymer may be simulated using computer software to provide a fast analysis of a polymerisation of vinyl monomers based upon known reactivity ratios and variable concentrations. The program 'COPOL' provides analysis for binary systems and 'TERPOL' for ternary systems. Both methods are based on the terminal model of copolymerisation and make use of the Monte Carlo method of

statistical trials. An approximation relieves the need for producing the polymer and performing detailed structural analysis to resolve the sequence. Ashraf[51] has evaluated the accuracy of the simulations produced by the programs by providing experimental evidence with ^{13}C NMR and elemental analysis that appears to corroborate the simulated output, as being within 3% of one another.

1.9.3 The Alfrey-Price Q-e Scheme

To obtain a simulated sequence distribution, the monomer reactivity ratios must be known. Many have been determined experimentally but there are many monomers for which they have not. The Alfrey-Price[54] Q-e scheme may be used to approximate reactivity ratios without the need for lengthy experimental procedures. The scheme attempts to quantify reactivity by considering the polar and resonance stabilisation effects of the monomer and their influence on the copolymerisation process[56,57].

Two vinyl monomers are assigned values e_1 and e_2 to represent the charge on the end group of radical 1 and the double bond of monomer 2 respectively. Q and P denote the reactivity of the monomer and radical respectively. These four quantities would give a rate of reaction as shown in Equation 1.27,

$$k_{1,2} = P_1 Q_2 e^{-e_1 e_2} \qquad \textit{Equation 1.27}$$

This equation, applied to each of the propagation steps outlined in equations 1.16 to 1.19 are combined and re-arranged to give,

$$(k_{1,1}/k_{1,2}) = r_1 = (Q_1/Q_2)\, e^{-e_1(e_1-e_2)} \qquad \textit{Equation 1.28}$$

$$(k_{2,2}/k_{2,1}) = r_2 = (Q_2/Q_1)\, e^{-e_2(e_2-e_1)} \qquad \textit{Equation 1.29}$$

The division of the two relative reactivities leads to a simplified expression involving only the difference in polarity, which can be used to determine an unknown e value from which then a Q value may be established, where r_1 and r_2 are known.

$$r_1 r_2 = e^{-(e_1-e_2)^2} \qquad \textit{Equation 1.30}$$

1.10 Solvent Effects

Over the years, many researchers have taken note of the effect that solvents can have on the reactivity of monomers. In particular, the effect of water on N-vinyl pyrrolidone has been of great interest.

In 1954, Frank[58] carried out various physiochemical measurements on the water-NVP binary system. A viscosity plot found that there was strong interaction between water and NVP which deviated from ideal, but that the magnitude of the maximum viscosity was not as high as would be expected for hydrate formation. This also held for the heat of mixing.

A maximum polymerisation rate of NVP in water was reported at a monomer concentration of 75% by volume, which corresponded to an NVP/water molar ratio of 1:2, also the point of maximum viscosity for the system[59]. By extrapolating the heat generated per mole of NVP back to zero monomer concentration, a value that appeared to be the interaction energy of a weak hydrogen bond was found ($\approx$ 8 kJ mol^{-1}). As such, it was put forward that by hydrogen bonding with water, the reactivity of NVP increased by decreasing the electron density of the vinyl group. This increased the propagation velocity and hence the rate of polymerisation. Excess water was found to have a detrimental effect on the reaction medium.

Huglin and Rehab[60] investigated NVP and water in a copolymer system with butyl acrylate (BA). Above 25% water (and less than 35%), a dramatic increase in the r_{BA} value is seen. Again, there is good evidence that an NVP/water complex exists that is more reactive that NVP alone in homopolymerisation. They proposed that the strong NVP/water complex influenced r_{BA} as follows:

$$\text{----BA}\bullet + \text{BA} \rightarrow \text{-----BA}\bullet \qquad \equiv k_{1,1} \qquad \textit{Equation 1.31}$$

$$\text{----BA}\bullet + (\text{NVP}/H_2O) \rightarrow \text{-----VP}\bullet \qquad \equiv k_{1,2} \qquad \textit{Equation 1.32}$$

$$r_{BA} = k_{1,1} / k_{1,2} \qquad \textit{Equation 1.33}$$

NVP/water is reactive to its addition to -----VP• but is reduced in reactivity with BA• due to hydrophobic repulsion. As such, $k_{1,2}$ is decreased and r_{BA} increases. A rise in r_{NVP}

was not seen, as the expected increase (of the same degree as r_{BA}) was not of sufficient magnitude to be visible outside of the experimental error limits.

Both the polarity of the solvent and the extent of hydrogen bonding with monomers are the factors responsible for observed solvent effects in free radical polymerisation[61]. Perec[62] commented that the influence of solvents was particularly strong for copolymers where at least one of the comonomers might be associated by hydrogen bonding. For acrylamide, the equilibrium between the forms shown below shifts in solvents of different polarities and dielectric constants, which could influence the polarity of the double bond and the reactivity of the growing radical chain, as displayed in Figure 1.9.

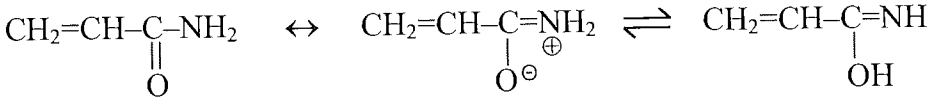

Figure 1.9 The tautomeric forms of acrylamide in solution.

It has been suggested that proton donor solvents protonate the carbonyl group of acrylamide, giving the terminal radical the charge distribution shown in Figure 1.10. The solvent effect could also have modified the auto-association of acrylamide and/or the association of acrylamide with the solvent.

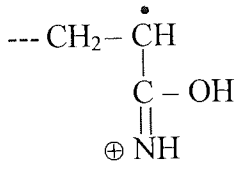

Figure 1.10 The protonation of a terminal acrylamide by a solvent.

For systems such as styrene/methyl methacrylate, styrene/acrylamide and methyl methacrylate/acrylamide, solvent effects have been due to the changes in polarization of the carbonyl or amide groups in the monomers bought about by the different polarities of the solvents[63]. For methacrylonitrile/styrene, polarization of the terminal methacrylonitrile radical was enhanced by increased solvent polarity which decreased its reactivity towards its monomer compared with styrene and so improved the alternating

tendency. The styrene terminal radical appears to be relatively insensitive to the medium.

The nucleophilic solvent N-methyl pyrrolidone (NMP) has also been found to increase the reactivity of the monomers NVP and methyl methacrylate[64,65]. With the known problems of NVP reactivity, the addition of NMP is expected to improve its incorporation into a growing polymer chain.

1.11 Ionicity in Nature

A contact lens designed for extended wear should ideally behave as an extension of the cornea; it should allow the cornea to respire without due physiological stress, resist the deforming force of the eyelid and permit the maintenance of a continuous tear film on the lens whilst minimising the accumulation of lipoidal and denatured protein deposits.

An accepted and popular contact lens material used for daily and weekly wear is Etafilcon, based on HEMA and a small amount of methacrylic acid. The acidic moiety increases the hydrophilicity of the HEMA material by 20%, making a more comfortable lens with increased oxygen permeability. Although adding an anionic charge has been found to increase the degree of spoilation of the material, the type of spoilation is sometimes more important.

An anionic charge is common in nature. The charged glycosaminoglycans in particular are of major structural importance in vertebrate animals. Important examples include the chondroitin sulphates and keratan sulphates of connective tissue, the dermatan sulphates of skin and hyaluronic acid. Glycosaminoglycans are found covalently attached to a core protein to form proteoglycan macromolecules, which are found in all connective tissue and extracellular matrices and on the surface of many cells, particularly epithelial cells. The high hydrophilicity imparts the required viscoelastic properties of joints and other structures subject to mechanical deformation, e.g., cartilage, whose proteoglycan contains both keratan sulphate and chondroitin sulphate chains, whose structures are presented in Figure 1.11.

The sulphonate groups have such importance in binding water that, to impart a similar moiety into a contact lens material could have very beneficial consequences - a high water contact, a wettable surface and resistance to dehydration.

In tears, mucins play a lubricating role. The carbohydrates that are attached to the proteins backbone of mucin are 12 residues in length and are made up of the same five monosaccharides:

- N-Acetyl Galactosamine
- N-Acetyl Glucosamine
- Galactose
- Fucose
- N-Acetyl Neuraminic acid (Sialic acid)

The sugar groups (apart from the linking galactose and terminal fucose or sialic acid) may bear ester sulphate groups.

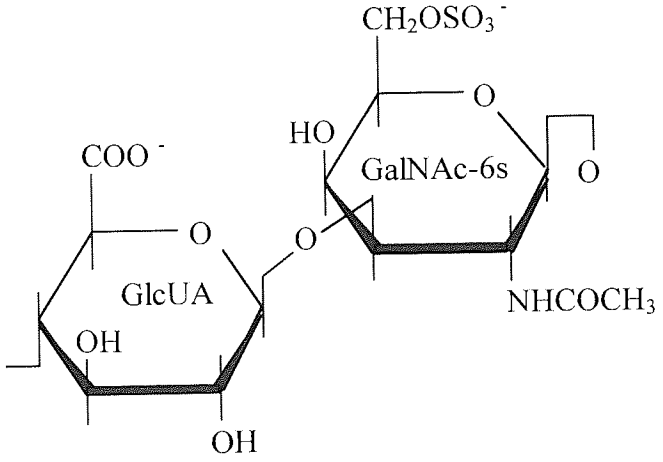

Chondroitin 6-Sulphate

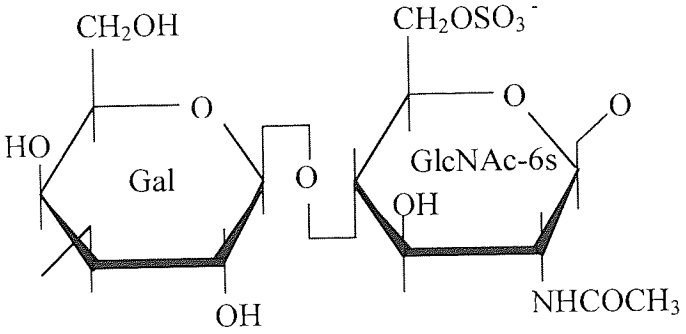

Keratan Sulphate

Figure 1.11 The repeating unit sulphated disaccharide of some glycosaminoglycans. GlcUA = D-glucuronic acid, GalNAc-6s = N-acetyl-D-galactosamine, GlcNAc = N-acetyl-D-glucosamine & Gal = D-galactose. For clarity, hydrogens are not shown.

Hyaluronic acid has other functions in the body than as a structural component. The polymer is very soluble in water and is present in synovial fluid of joints and in the vitreous humor of the eye. It appears to act as a viscosity-increasing agent or lubricating agent in these fluids and its structure is shown in Figure 1.12. A polar molecule having a lubricant role may be of relevance when considering the lubricating role tears have on a contact lens (or corneal) surface.

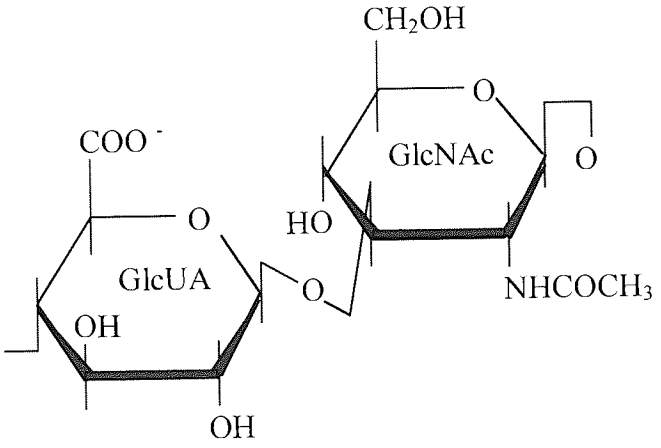

Figure 1.12 Structure of hyaluronic acid. GlcUA = D-glucuronic acid & GlcNAc = N-acetyl-D-glucosamine. For clarity, hydrogens are not shown.

1.12 Polymerisation

In this study, hydrogels are produced in sheet form to facilitate production and testing. This work makes use of free-radical polymerisation by thermal initiation. The initiation step is promoted by azo-iso-butyronitrile (AZBN), which undergoes first order thermal decomposition[65] at 50°C to produce two radicals as shown in Figure 1.13. This radical may then go on to a radical addition reaction with a monomer containing a vinyl bond, yielding a double bond.

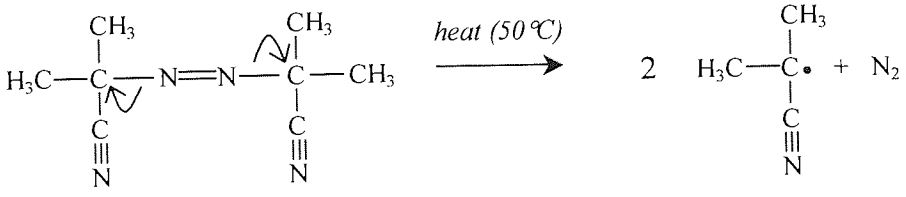

Figure 1.13 Initiation: the thermal decomposition of azo-iso-butyronitrile.

AZBN does not undergo induced dissociation or chain transfer and the decomposition rate is only slightly dependent on the medium. The termination rate relates inversely to the viscosity of the medium.

It has been suggested that NMP is able to form a stable solvent cage around the AZBN primary radical which decreases the reactivity. This has the effect of extending the half-life of the radical and increases the probability of mutual combination of reactive species.

1.13 Scope of Study

With the advent of the silicone hydrogel for extended wear, the surface problem of wettability has not yet been resolved. The lenses are in eyes and patients do not complain of discomfort[66]. But mucin balls are known to develop[67], caused by the shearing force between the eyelid and the material. The long-term effects of this have yet to be discovered, as the materials have only been available for a year. Otherwise, the oxygen requirement of the cornea appears to have been satisfied, as has on-eye lens movement and tear exchange. A wettable surface is obtained by plasma-treatment to create oxidized regions or to deposit a hydrophilic coating, but long-term efficacy is a problem and the materials are still not wettable enough. Until hydrogel chemistry is better understood, the surface problem will remain.

This thesis is concerned with the investigation of high water content hydrogels, which show more similarity to the water content of the cornea (approx. 81%) and which would therefore, naturally be assumed to be more compatible than low water content materials. Neutral materials based on acrylamide from an old patent composition[4] will be modified with newer monomers and the effects studied. The majority of the work will seek to appreciate the effect of charge, anionic alone and both anionic and cationic together, on another hydrogel copolymer that has been worn as contact lens and is based upon the commonly used monomer in contact lens wear, HEMA. *In vitro* spoilation techniques will be used to investigate the effect of charge on the uptake of biological substrates into and onto the hydrogels. The addition of polyurethanes will be investigated in an attempt to obtain optically clear, strong biomaterials.

Hydrogel technology and known chemistry will be applied in attempts to surface graft a silicone material to improve the wettability by a significant amount. By understanding the 'traditional' hydrogel-layer coating, it should be possible to naturally progress to a more ideal extended wear contact lens.

CHAPTER 2

Materials And Experimental Techniques

"...only her scepticism kept her from being an atheist."

Jean-Paul Sarte, 1905-1980,

Les Mots (1964).

2.1 Reagents

All reagents used are shown in Tables 2.1 and 2.2, with structures shown in Figure 2.1.

Monomers were purified by reduced-pressure distillation before use and stored in a refrigerator where appropriate.

Table 2.1 Specifications of polymers, cross-linking agents, initiator and diluent employed.

Polymer	Abbrev.	Properties	Supplier
Polyester-based polyurethane (aromatic), Cat. #5706	PU5	Tensile strength = 36.3 N mm^{-2} Modulus at 100% = 27.4 N mm^{-2} Eb = 120% Viscosity = 200-500 MPa s^{-1}	B. F. Goodrich
Polyester-based polyurethane (aromatic), Cat. #5715	PU6	Tensile strength = 55 N mm^{-2} Modulus at 100% = 9.2 N mm^{-2} Eb = 450% Viscosity = 100-200 MPa s^{-1}	B. F. Goodrich
Ethylene glycol dimethacrylate*	EGDMA	198.2	BDH
Azo-iso-butyronitrile*	AZBN	164.21	BDH
N,N'-Diallyl-tartardiamide*	DATr	288.25	Aldrich
N-Methyl pyrrolidone	NMP	99.13	Fisher Scientific

Notes

Where marked *, material stored in refrigerator.

Table 2.2 Monomers utilized, molecular weights and suppliers.

Reagent	Abbrev.	M.Wt.	Supplier
Acrylamide	AA	71.1	Park Scientific
N-Isopropyl acrylamide	NIPA	113.2	Polysciences
N,N-Dimethyl acrylamide*	NNDMA	99.13	Aldrich
N-Vinyl pyrrolidone*	NVP	111.1	Vickers
Acryloyl morpholine*	AMO	141.2	Aldrich
Hydroxypropyl acrylate*	HPA	130.1	Aldrich
Methacrylic acid*	MA	86.1	Aldrich
Methyl methacrylate*	MMA	100.1	Vickers
Poly(ethylene glycol)$_n$ methyl ether methacrylate*, av. M_n=200	$MPEG_{200}MA$	300 (av.)	Polysciences
Hydroxyethyl methacrylate*	HEMA	130.1	Vista Optics
Dimethylaminoethyl methacrylate*	DMAEMA	157.2	Sigma
Tetrahydrofurfuryl methacrylate*	THFMA	170.2	Aldrich
2-Ethoxyethyl methacrylate*	EEMA	158.2	Vickers
2-Methoxyethyl methacrylate*	MEMA	144	Aldrich
Sodium 2-(acrylamido)-2-methyl propane sulphonate	NaAMPS	229	Lubrizol Corporation
Bis(3-sulphopropyl ester) itaconate, dipotassium salt	SPI	450	Raschig
3-Sulphopropyl ester acrylate, potassium salt	SPA	232	Raschig

Notes

* indicates reagent stored in refrigerator below 5°C.

Figure 2.1 Structures of chemicals employed

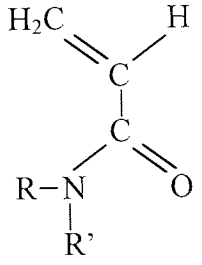

R = H	R' = H	Acrylamide	AA
R = H	R' = $CH(CH_3)_2$	N-Isopropyl acrylamide	NIPA
R = CH_3	R' = CH_3	N,N-Dimethyl acrylamide	NNDMA

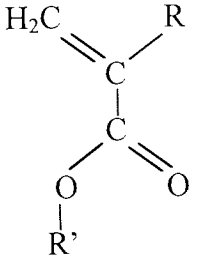

R = H	R' = $CH_2CH_2CH_2OH$	Hydroxypropyl acrylate	HPA
R = CH_3	R' = CH_2CH_2OH	Hydroxyethyl methacrylate	HEMA
R = CH_3	R' = CH_3	Methyl methacrylate	MMA
R = CH_3	R' = $CH_2CH_2N(CH_3)_2$	Dimethylaminoethyl methacrylate	DMAEMA
R = CH_3	R' = $CH_2CH_2OCH_2CH_3$	2-Ethoxyethyl methacrylate	EEMA
R = CH_3	R' = $(CH_2CH_2O)_nCH_3$	Poly(ethylene glycol)$_n$ methyl ether methacrylate, av. M_n=200	$MPEG_{200}MA$
R = CH_3	R' = H	Methacrylic acid	MAA

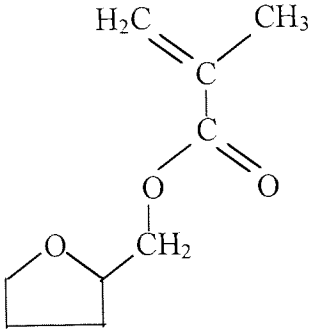

Tetrahydrofurfuryl methacrylate THFMA

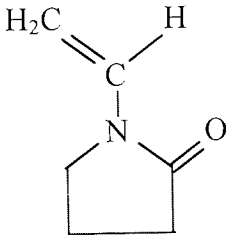

N-Vinyl pyrrolidone NVP

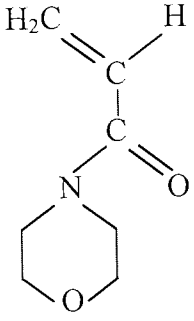

Acryloyl morpholine AMO

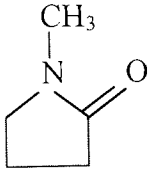

N-Methyl pyrrolidone NMP

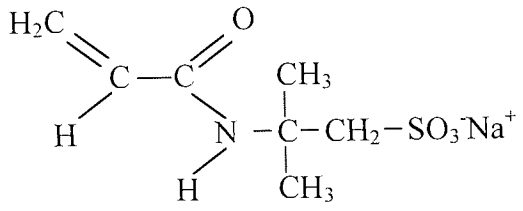

Sodium 2-(acrylamido)-2-methyl propane sulphonate NaAMPS

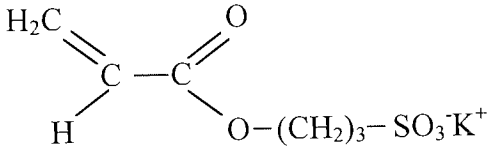

3-Sulphopropyl ester acrylate, potassium salt SPA

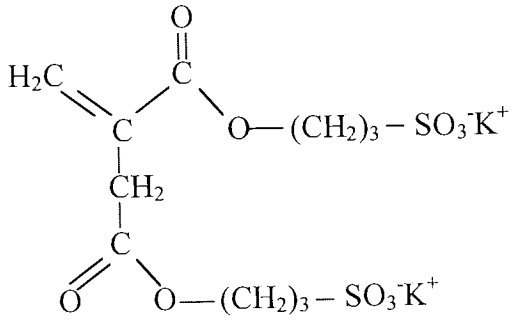

Bis(3-sulphopropyl ester) itaconate, dipotassium salt SPI

Ethylene glycol dimethacrylate EGDMA

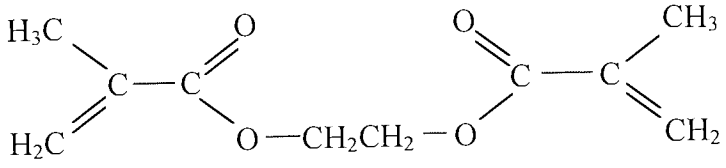

N,N'-Diallyltartardiamide DATr

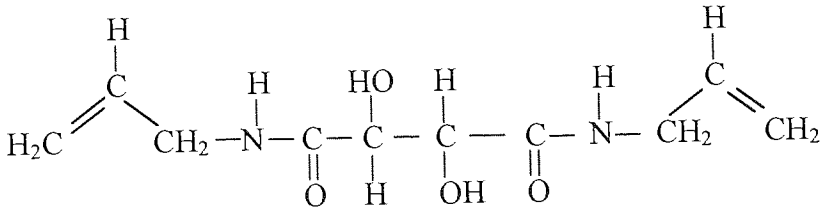

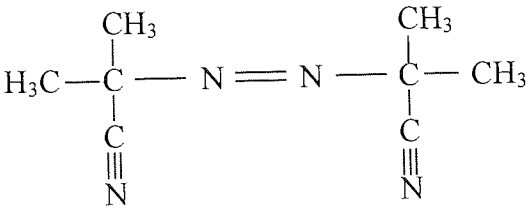

Azo-iso-butyronitrile AZBN

2.2 Preparation of Membranes

Membrane sheets were produced by polymerisation of a monomer mixture in a glass mould[68], shown in Figure 2.2. Two glass plates, approximately 10cm by 15cm in size, were each covered by Melinex (polyethylene terephthalate) and separated by two polyethylene gaskets, each one 0.2mm thick. Spring clips would hold the mould together. A homogeneous monomer mixture was injected into the mould cavity by insertion of a G22 syringe needle into the cavity space between the Melinex sheets.

The compositions were typically made up to 5g in mass and the desired cross-linker and initiator added as a percentage of that mass, i.e. % w/w. In this work, the cross-linker DATr was added at 0.8% w/w. If necessary, a solvent was added to the mixture to encourage homogeneity to an amount not more than 20% of the total mass. The mixture was degassed with a slow stream of nitrogen prior to injection.

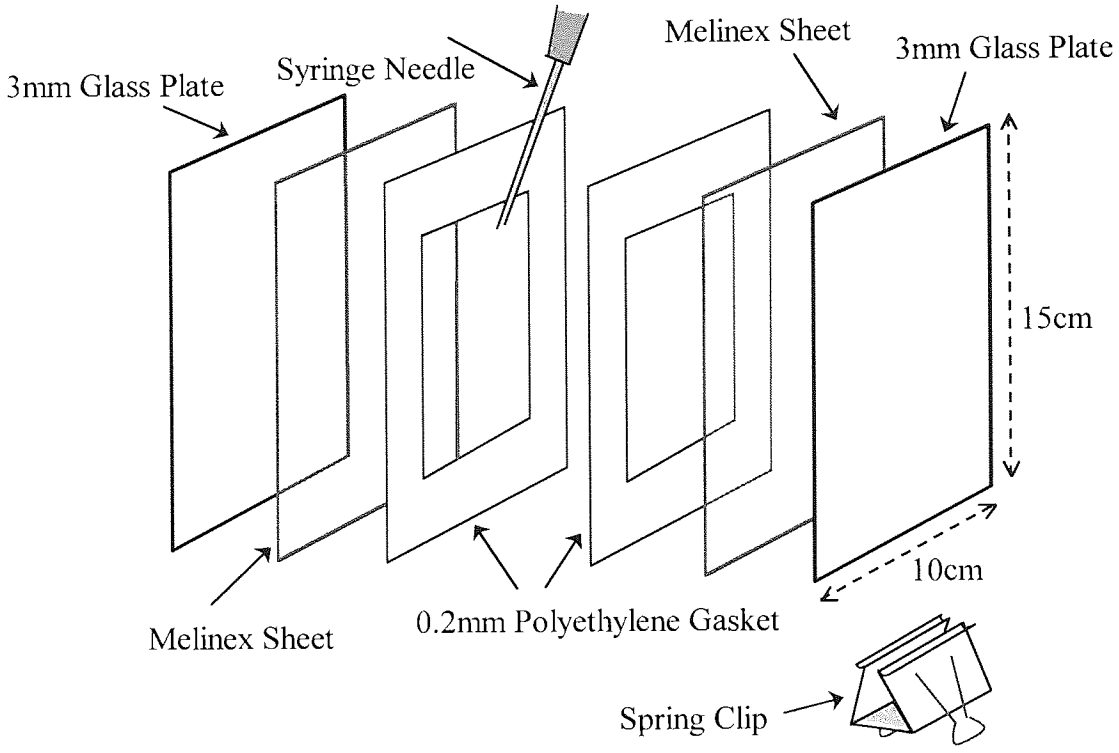

Figure 2.2 Diagram of a membrane mould (exploded view).

The injected mould would be placed in an oven at 60°C for three days followed by a three hour post-cure at 90°C. The membrane was then removed from the mould and separated from the Melinex sheets. It was allowed to hydrate in distilled water (approx. pH 6.2) for at least seven days, changing the water daily. Previous experience had shown that this procedure allowed equilibrium hydration to be reached and the extraction of any water-soluble residual monomers.

2.3 Equilibrium Water Content

The equilibrium water content (EWC) was calculated by determining the weight difference between the hydrated and dehydrated material. Small samples of hydrogel were cut using a cork borer and blotted carefully with slightly damp filter paper to remove excess surface water.

After weighing, the samples were dehydrated to constant weight in a microwave (approx. 20min at medium-high) and re-weighed. The EWC was calculated from a minimum of five samples from each membrane and the final value expressed as an average.

$$EWC\ (\%) = \frac{\text{Weight of water in hydrogel}}{\text{Total weight of hydrated hydrogel}} \times 100 \qquad \textit{Equation 1.1}$$

2.4 Differential Scanning Calorimetry

Differential scanning calorimetry (DSC) was used to calculate the percentage of freezing water in a hydrogel. Thermograms as seen in Figure 2.3 were obtained using a Perkin Elmer differential scanning calorimeter, DSC 7, connected to a liquid nitrogen cooling accessory. The program was run using Perkin Elmer Pyris software 2.01 on Windows NT 4.0 on an interfaced P-133 PC.

A sample of the hydrogel was cut from the membrane using a size 1 cork borer and excess water carefully blotted with damp filter paper (to prevent absorption from the sample). The disc was weighed and then sealed in an aluminium pan to prevent water evaporation. The pan was then placed in the sample holder of the thermal analyser.

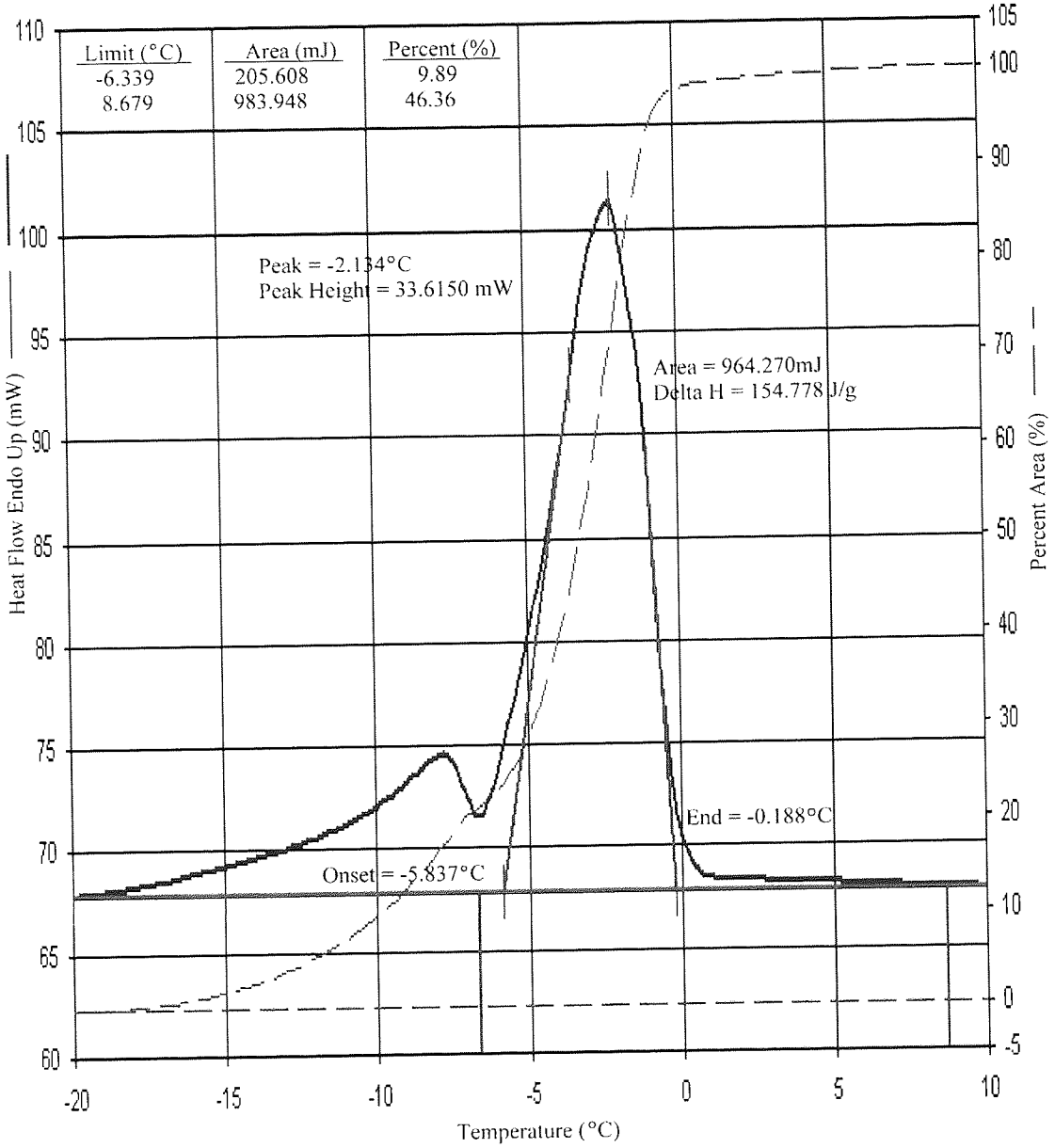

Figure 2.3 An example of a thermogram obtained by DSC.

The method was designed to cool the sample to a level that would freeze any super-cooled water and reach equilibrium, before being slowly heated to produce clear endothermic peaks in the region of the melting point of water and was as follows:

1) Cool from 20°C to -70°C at 100°C min^{-1}
2) Hold for 5min at -70°C
3) Heat from -70°C to -25°C at 20°C min^{-1}
4) Heat from -25°C to 20°C at 10°C min^{-1}

The area under the endothermic peak(s) corresponds to the energy required to melt the freezing water in the sample. The weight of the sample is known, as is the energy required to melt 1g of pure water is known (333.77 Jg^{-1}) and so the software, using Equation 2.1, can calculate the percentage of freezable water in the sample.

$$\text{Freezing water (\%)} = \frac{\text{Energy required to melt water in 1g sample}}{\text{Energy required to melt 1g of pure water}} \times 100 \qquad \textit{Equation 2.1}$$

The final freezing water value was an average of at least two samples from one hydrogel material.

2.5 Mechanical Properties in Tension

Materials were tested in their fully hydrated state using a Hounsfield HTi tensometer interfaced with an IBM 55SX computer. The tensometer was fitted with a 10N load cell attached to the instrument crosshead which was able to move in a vertical plane only. From the load cell, a clamp was suspended by a chain and hanged directly above a lower clamp permanently fixed to the tensometer. Samples to be tested were placed into the clamps in the vertical position. The crosshead would move at an entered speed until the sample being assessed broke completely.

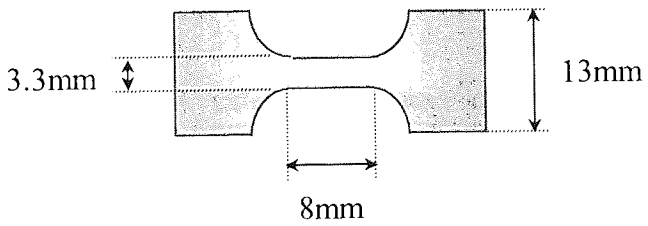

Figure 2.4 Dimensions of a hydrogel sample used in mechanical testing in tension.

The sample was cut into a dumbbell shape, shown in Figure 2.4, with a specially designed metal cutting tool to give a test area of 3.3mm x 8mm. Prior to testing, the test material had been equilibrated in distilled water to ensure complete hydration.

The test piece was measured for its thickness using a micrometer and then placed between the clamps. Under conditions of room temperature and pressure, the sample of known thickness was subjected to the pulling force of the test until the material broke. A

test speed of 10mm min^{-1} was used, theoretically slow enough to allow the chains of the polymer material to uncoil and give representative mechanical properties for the material[69]. Throughout the test, the sample was kept in a hydrated state (i.e. 100% humidity) by the repeated, regular application of a fine mist of water, dispensed onto its surface by an atomiser.

The computer software produced an graphical output, an example of which is seen in Figure 2.5, and calculated the Young's modulus (E), tensile strength at break (Ts) and elongation to break (Eb) using the following equations:

$$\text{Young's modulus (E)} = \frac{\text{stress}}{\text{strain}} \quad \text{MPa} \qquad \textit{Equation 2.2}$$

where

$$\text{stress} = \frac{\text{load}}{\text{cross-sectional area}} \qquad \textit{Equation 2.3}$$

and

$$\text{strain} = \frac{\text{extension of gauge length}}{\text{original gauge length}} \qquad \textit{Equation 2.4}$$

$$\text{Tensile strength (Ts)} = \frac{\text{load at break}}{\text{cross-sectional area}} \quad \text{MPa} \qquad \textit{Equation 2.5}$$

$$\text{Elongation at break (Eb)} = \frac{\text{extension of gauge length}}{\text{original gauge length}} \times 100\% \qquad \textit{Equation 2.6}$$

Each material was tested at least five times and the final values stated given as an average.

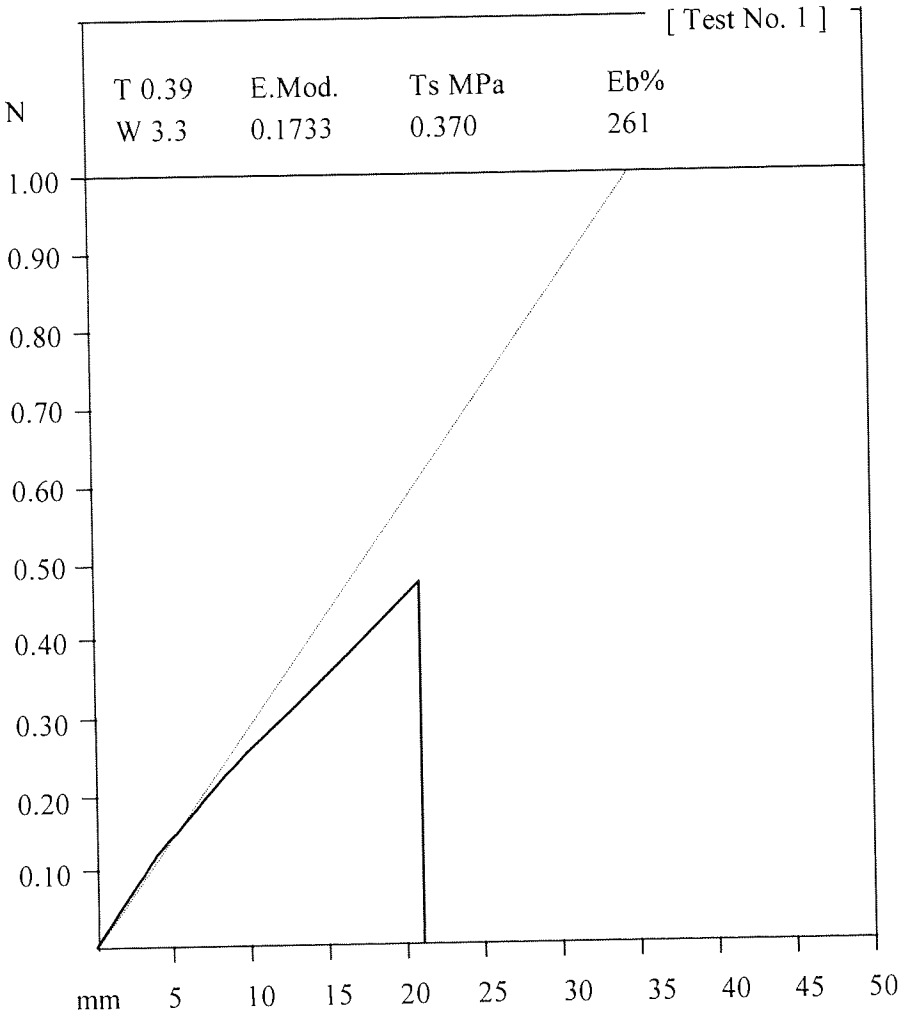

Figure 2.5 An example of a stress-strain curve obtained from a tensometer.

2.6 Contact Angles

The surface energies of hydrogels can be calculated using the equations explained in Chapter One,

(a) in the dehydrated state using the sessile drop technique and,
(b) in the hydrated state using the Hamilton and captive air bubble techniques.

The contact angles were measured using a contact angle measuring system by GBX. This consists of a computer-controlled stage that presents the backlit sample to a video camera, feeding the display live to an interfaced computer. A photograph could be taken

of a drop on the surface of the sample and the software used to take contact angle measurements from the image on-screen.

2.6.1 Sessile Drop Technique

A size 8 cork-borer was used to cut discs out of a 'clean' hydrogel membrane (surface cleaned with Teepol detergent and thoroughly rinsed in distilled water followed by an overnight soak). The discs were then dehydrated in a microwave and kept in a desiccator until tested.

A disc was then mounted horizontally on a slide and placed on the GBX stage. An automated syringe was used for this technique, being able to dispense a controlled volume of water onto the surface of the material and so reducing user variation. A 1µl drop size was used. The use of the computer-controlled stage ensured that the same force was used each time for the placement of the drop, again helping to reduce user variation.

The software was set to take a photograph immediately following the placement of a drop and from this image, contact angle measurements were made using the software.

2.6.2 Hamilton's Method

Discs were cut from the hydrated hydrogel membrane using a size 7 cork-borer. Surface water was removed from one face of the hydrogel by careful blotting before being mounted on a glass slide with a slight dais in the centre. The slide was then inverted and the sample suspended in an optically perfect glass cell as shown in Figure 2.6. The cell was filled with distilled water and a drop of n-octane placed on the surface of the hydrogel using a G25 syringe needle whose point had been removed to obtain drop symmetry. The contact angle between the n-octane and the hydrogel was measured using the software.

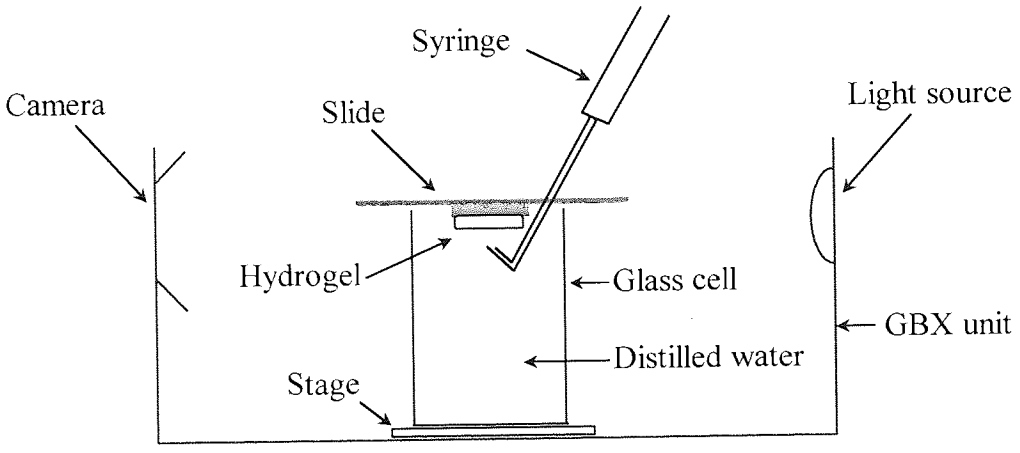

Figure 2.6 Diagram of hydrogel sample ready for inverted contact angle measurements.

2.6.3 Captive Air Bubble Technique

This technique differs from Hamilton's only in that air bubbles are used in place of n-octane.

2.6.4 Dynamic Contact Angle Measurement

Dynamic contact angles for hydrogel materials are obtained by using a Cahn Dynamic Contact Angle 300 Series Analyser, interfaced to an IBM computer. A schematic of the set-up can be seen in Figure 2.7.

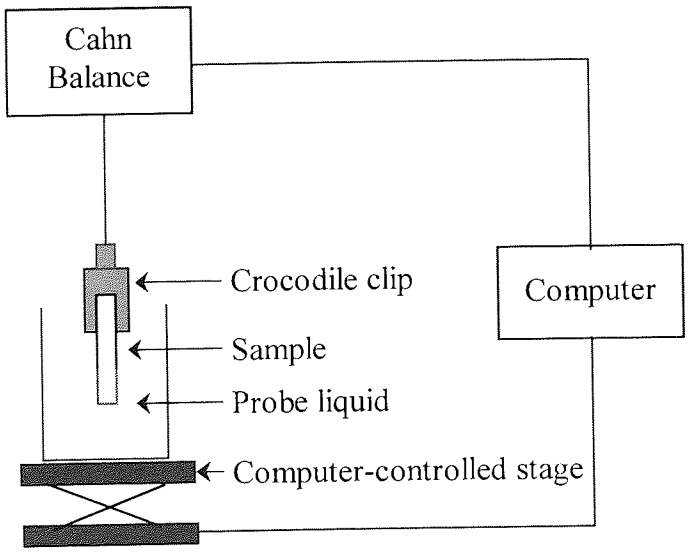

Figure 2.7 Schematic diagram of the dynamic contact angle analyser.

The analyser was used to determine the values of the advancing and receding contact angles of silicone hydrogel materials that had undergone various surface treatments to render them more wettable. The samples were cut into strips 10mm x 3.3mm using a cutter attached to a press. The thickness of the strip was measure with a micrometer and the value noted.

The hydrated sample was suspended from the balance by a wire and crocodile clip and allowed to hang in a vertical setting with the lowest edge approximately 3mm above the level of the liquid, HPLC-grade water. The instrument would have an immersion depth and number of cycles programmed prior to the experiment.

Once the sample was in place, it was lowered into the probe liquid at a rate of 0.1mm/s to a depth of ~10mm, from where it was immediately raised at the same rate until it returned to its original position and a check made that the sample had no contact with the meniscus of the liquid at this point. The procedure was repeated for the required number of cycles, the minimum being three for each sample.

Computer software plotted the results obtained as force vs. immersion depth. A simple equation relates the wetting force to the cosine of the contact angle,

$$\text{Cos}\,\theta = F / \gamma P \qquad \textit{Equation 2.7}$$

where

F = force of meniscus at the solid/liquid/vapour interface, measured directly by the Cahn balance at immersion (advancing) and withdrawal (receding).

P = perimeter of the sample in contact with the probe liquid.

γ = surface tension of the probe liquid.

The software, using this equation, calculates the values of advancing and receding contact angles automatically.

A typical dynamic hysteresis profile is illustrated in Figure 2.8.

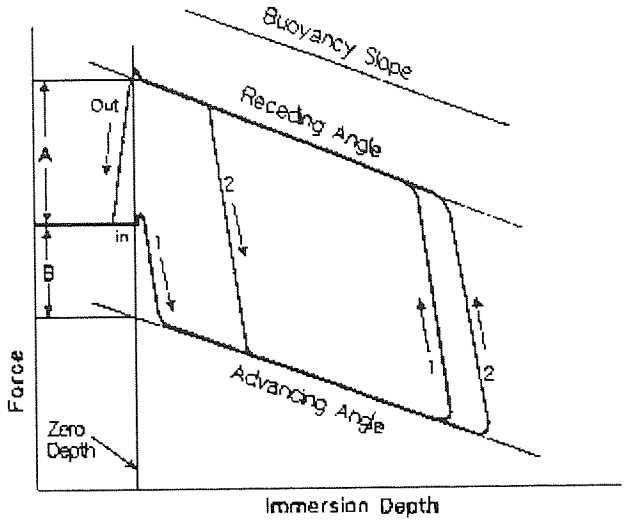

Figure 2.8 A typical dynamic hysteresis curve illustrating a two-immersion cycle.

2.7 Static Surface Tension

Static surface tension (γ) can be measured using either the DuNouy ring or the Wilhelmy plate and is the amount of energy required to expand the surface by unit area. Both methods are based on the forces involved at the air-interface and record the maximum force acting on the ring or the plate. The DuNouy ring is suspended from the Cahn balance used for dynamic contact angle measurement and immersed in the probe liquid. The stage is lowered until the ring pulls free of the liquid and at the point that it pulls free, the force required to raise it reaches a maximum and is displayed on the balance as a static surface tension. An average of at least five measurements were taken.

This technique was applied to the wetting liquid remaining in the beaker following a dynamic contact angle measurement. From it, one could obtain an indication of surface stability and any possible leaching of components from the material, which may have affected the dipping forces measured. A noticeable decrease would result in the measured surface tension of the liquid the greater the degree of leaching of polar monomers. The surface tension for pure water is 72.8 dyn cm^{-1} or 0.0728 N m^{-1}.

2.8 Copolymer Sequence Distribution

A computer program is used to simulate the effect of monomer reactivity on sequence distribution, 'COPOL' for a binary system and 'TERPOL' for a ternary system.

The reactivity ratios of monomer 1, M_1, and monomer 2, M_2, are entered and a simulation of the reaction sequence obtained. The reactivity ratios are defined as the ratio of the rates of reaction of a polymer chain ending in a radical of one type adding itself, to the rate of its reaction with the second monomer in the copolymer system, i.e.

$$r_1 = k_{1,1} / k_{1,2} \qquad \textit{Equation 2.8}$$

and

$$r_2 = k_{2,2} / k_{2,1} \qquad \textit{Equation 2.9}$$

where r_1 and r_2 are the reactivity ratios of monomers M_1 and M_2 respectively. All conversions were done to 100%.

2.9 *In Vitro* Ocular Spoilation

The *in vitro* ocular spoilation model was developed at Aston in order to assess the degree of deposition of various proteins and lipids on biomaterials[53].

The tear substitute was based on a 1:2 (v/v) solution of foetal calf serum diluted with phosphate-buffered saline as a base. This was then 'spiked' with additional components such as mucin, lactoferrin and lysozyme in order to mimic the composition of tears.

Controlled spoilation may be carried out by the 'shaker' model or the 'drop and dry' model. The 'shaker' model was used in this study. Glass beads were placed in a vial to provide an irregular surface on which the sample could sit, allowing contact with air and the artificial tear solution. The tear solution was added to a level just below the top surface of the glass beads. The prepared vials were then placed on a flatbed shaker operating at 200 cycles/minute. The tear solution in the vials was replaced every 24 hours to maintain a fresh supply of protein and lipid components.

The sample was cut from a hydrated hydrogel membrane using a size 6 cork borer to give a disk of 10mm diameter.

The deposition of both lipids and proteins was monitored at regular intervals over a period of 28 days to mimic a three-week period of extended wear.

Lipid deposition was monitored on a modified Hitachi F-4500 fluorescence spectrophotometer. This is a non-destructive technique that relies on the fluorescence of lipoidal species (via the conjugation present in cholesterol esters and fatty acids) following excitation by UV light. Lenses were placed in distilled water in a specially designed quartz cell, which allowed reproducible orientation of the disc to the incident light beam to be achieved. An excitation beam wavelength of 360nm was used and the height of the resulting emission peak monitored over the 400-600nm range.

Protein adsorption was measured at 280nm using a Hitachi UV spectrometer. The test sample was placed right at the bottom of the UV cell, which was filled with distilled water for position consistency and the absorbance was measured against distilled water. The progressive accumulation of protein on the hydrogel was then calculated by referral to a standard Beer-Lambert curve. Multiplying the values obtained by 1.5 converted the units from mg/sample to mg/lens.

CHAPTER 3

Neutral Hydrogels Based On Acrylamides

"I do not believe that any peacock envies another peacock his tail, because every peacock is persuaded that his own tail is the finest in the world. The consequence of this is that peacocks are peaceable birds."

Bertrand Russell, 1872-1970.

3.1 Introduction

Work in the late 1970s and early '80s focused on hydrophilic monomers that contained functional groups capable of conferring strength via internal bonding. As such, unsaturated carboxylic acids and amides that can potentially form hydrogen bonds were suitable candidates for evaluation. These bonds would effectively act as secondary cross-links that would play a part in controlling the degree of swell and hydrophilicity of a hydrated hydrogel.

Pedley's[70] study of hydrophilic monomers resulted in a patent publication entitled simply 'Hydrogels' with named co-inventors Larke and Tighe[4]. It described a material suitable for use in biomedical applications, particularly a contact lens, incorporating acrylamide, hydroxypropyl acrylate and N-vinyl pyrrolidone. The molar ratios of monomer given in examples were 35-55, 55-20 and 10-30 molar parts respectively and gave hydrogels of at least 72% equilibrium water content. The materials had been designed to produce good sequence distributions which will be discussed later in this chapter. He found that high water contents and good deformational properties could be obtained for acrylamide-hydroxypropyl acrylate (AA-co-HPA) copolymers, HPA being more hydrophilic than its analogue HEMA due to a chain mobility facilitated by the lack of an α-methyl group. N-vinyl pyrrolidone (NVP) was added to improve the balance of water content and strength.

Middleton[71] took this further by incorporating styrene and a small amount of methacrylic acid. Styrene had a low reactivity ratio, similar to NVP, would increase the rate of gelation and lend clarity and strength. Methacrylic acid in small amounts would add a negative charge to aid spoilation prevention. This work led to the publication of another patent entitled 'Hydrogel-forming Polymeric Materials'[72].

A major disadvantage of acrylamide is that it is a solid material with a relatively low solubility in many of the commercial monomers used to produce hydrogels. As a result of this, the patents incorporating it relied on a relatively high proportion of NVP.

Acrylamide is however readily soluble in water and a small amount may be included in the monomer mixture to aid homogeneity. Excess amounts of solvent would only serve to reduce the monomer concentrations to unacceptable levels for efficient polymerisation

and form weak networks. It has been found that incorporating water up to 10% by weight into 50:50 (mol:mol) acrylamide-methacrylic acid could cause an increase of approximately 30% in water content after 28 days hydration. This is believed to be caused by the direct association of water molecules with the functional groups of acrylamide prior to polymerisation which results in decreased hydrogen bonding between chains and hence a more expanded network. Water also results in a higher proportion of acrylamide integration, possibly by aggregating units of acrylamide units together ready for addition as blocks into a polymer chain.

Previous work in our laboratories has deemed it acceptable for levels up to 20% w/w of solvent to be added. In this work, 10% w/w water and 10% w/w N-methyl pyrrolidone will be used for reasons discussed in Chapter One.

Goulding[73] found that a large drift in water content appeared in acrylamide hydrogels between one and seven months of hydration, negating the assumption that an equilibrium could be achieved typically after seven days for all hydrogels. Chemical analysis indicated that the acrylamide content had decreased. Acrylamide groups of a copolymer are known to slowly hydrolyse to give acrylic acid, relaxing hydrogen bonds between like units and causing the water content to increase. This is only likely to occur in the presence of strong acids or bases, and acrylamide shows resonance stability in water. The distilled water used in this work was typically of pH 5.4-6.3. Alternatively, the change could be due in part to low molecular weight poly(acrylamide) units leaching out of the polymer. More likely is the gradual, increased strain on inter-chain hydrogen bonds by water molecules clustering around polar groups to such an extent that they rupture, thus allowing further solvation.

A group of acrylamides that have an increasing role to play in the biomaterials field are the N-alkyl acrylamides, some of which are shown in Figure 3.1. In 1984, the first observation of a discontinuous phase transition with temperature of a non-ionic, N-isopropyl acrylamide (NIPA) gel was reported[74]. This occurred in pure water at 33°C, significantly in the vicinity of physiological temperature. A subsequent study[75] of two N-alkyl acrylamides found that N-n-propyl acrylamide underwent a discontinuous volume change at ~25°C and N-cyclopropyl acrylamide underwent a continuous volume change at a higher temperature region (40-50°C).

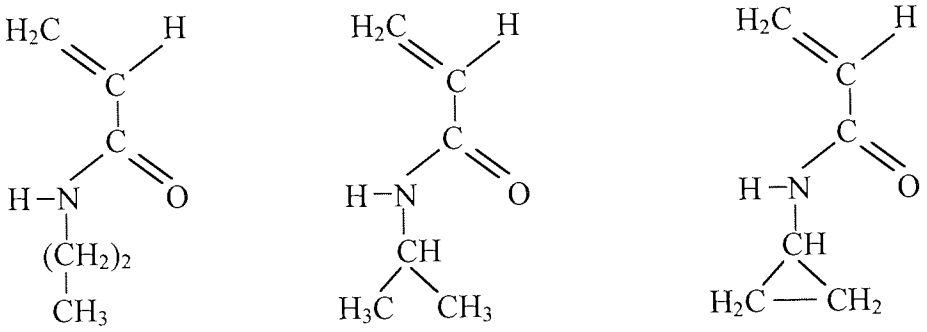

N-n-Propyl acrylamide N-Isopropyl acrylamide N-Cyclopropyl acrylamide

Figure 3.1 The structure of some N-alkyl acrylamides.

It is presumed that the hydrogel whose hydrophobic group has a larger surface area undergoes a discontinuous volume phase transition in water at lower temperatures due to the strength of the hydrophobic interaction. Hence, in order of decreasing hydrophobicity, the monomers are N-n-propyl acrylamide, N-isopropyl acrylamide, N-cyclopropyl acrylamide.

This transition temperature is known as a lower critical solution temperature (LCST) and for NIPA gels is in the region 32-34°C.

As explained by Otake *et al*[76], when hydrophobic solutes are introduced to water, one of two things can occur:

- Hydrophobic hydration, where water molecules form a cage-like structure around hydrophobic solutes causing non-polar molecules to become soluble in water, and
- Hydrophobic interaction.

As the temperature is increased the number of water molecules structured around hydrophobic solutes decreases which promotes hydrophobic interaction. Phase separation occurs and the material turns opaque in appearance, indicating a heterogeneous structure of an aggregated polymer network, as the hydrophobic interactions become dominant and bound water becomes free. Temperature may be used

to control the balance of these interactions and it is this that substantiates their usefulness as a biomaterial.

Fourier-Transform Infrared Spectroscopy (FT-IR) analysis of the C-H stretching region suggests that N-isopropyl groups and the polymer backbone both undergo conformational changes and become more ordered upon heating above the LCST[77].

Possible uses include an alternative to ultrafiltration, absorption of heavy metal and other ions from aqueous solution[78], purification and recovery of pharmaceutical products from solution, immobilization of enzymes and cells, novel cell culture surfaces[79] where cells spontaneously detach simply by reducing the temperature to below the LCST or temperature-modulated drug delivery. Caffeine has been loaded into NIPA hydrogels and its release studied by other workers[80] to find that an increased NIPA content causes a higher release of the drug due to a larger magnitude of swellability. The inclusion of small amounts of acidic comonomers, such as methacrylic acid, also forms materials that have uses in pH-specific membrane separations[81].

The biocompatibility of a well-designed hydrogel should barely be influenced by residual monomer and catalyst fragments, as the permeability of the expanded gel network should mean that un-polymerised material is eliminated prior to living tissue contact. An exception to this generalisation is found in the case of NVP. Not only does NVP form 'blocky' sequences within copolymer networks, but gives rise to extra-network oligomeric material formed towards the end of the polymerisation which diffuses slowly out of the network. Both give potential problems in extended wear, since blocks of NVP are highly lipophilic and the oligomers gradually leach into the eye.

The use of acryloyl morpholine[82] (AMO) as an alternative to NVP has been examined by various researchers in our laboratories. Although structurally similar, the radical reactivity ratio of AMO is less disadvantageous in these types of copolymerisations than NVP. This is of particular significance when the copolymer involves HEMA, as it typically does in the contact lens field and will be discussed in Chapter Four.

As the AA/HPA/NVP hydrogel copolymer has been developed and accepted for use as a biomaterial and a contact lens, the substitution of AA for NIPA will be a natural

progression to a biomaterial suitable for rapid drug delivery, particularly ocular delivery if the dimensional changes can be managed. NIPA is more soluble in other monomers than acrylamide and is less prone to undergo hydrolysis by virtue of the steric hindrance of the isopropyl substituent. AMO in place of NVP will be an important modification to the acrylamide contact lens composition by reducing the lipophilicity of the material.

3.2 Composition of Copolymer Hydrogels

All of the monomers used in this study have historically been used in accepted biomaterial hydrogel compositions, either by our group or other research/commercial groups. There is substantially complete conversion, with only trace amounts of unreacted monomer eluted from the hydrated material. This has been previously confirmed by elemental analysis on dehydrated and hydrated polymers.

A computer program may be used to simulate the polymerisation between two or three monomers ('COPOL' or 'TERPOL' respectively) and a theoretical sequence distribution obtained. To do this, the reactivity ratios of monomer pairs must be entered. These can be calculated from a monomer's Q and e value. The pertinent values for this work are given in Table 3.1.

For those monomers where Q and e values are not quoted (marked *) they have been approximated[83] as shown in Appendix A. For NIPA, the values were calculated using a simple linear least squares evaluation. As values are assigned based upon monomer reactivity and polarity, the values for HPA (being a mix of isomers) were estimated to be similar to the values for the structurally comparable monomer glycidyl acrylate.

Various authors all accept that true reactivity ratios can only be calculated experimentally and have discussed the shortcomings of using Q and e values to calculate reactivity ratios, i.e. the effect of experimental error[56,57]. However, as a model to provide simple monomer assessment, they remain useful, particularly when used in conjunction with other research.

Monomer	Q value	e value
Acrylamide	0.23	0.54
N-Isopropyl Acrylamide*	0.59	1.14
Hydroxypropyl Acrylate*	0.48	1.28
N-Vinyl Pyrrolidone	0.088	-1.62
Acryloyl Morpholine	0.39	0.08

Table 3.1 The Q and e values of monomers used.

The compositions given in Table 3.2 form the basis of the work in this chapter, which is essentially that of monomer substitutions rather than series. Composition 1 is identical to that given in the patent, whilst no. 2 also falls within its bounds but is not specified. Modifications investigated are as follows:

- To observe the effect of replacing N-vinyl pyrrolidone with acryloyl morpholine.
- To observe the effect of replacing acrylamide with N-isopropyl acrylamide.

Solvent addition includes 10% by weight of water and 10% by weight of N-methyl pyrrolidone. N,N'-Diallyl-tartardiamide (DATr) as cross-linker was added to 0.8% w/w and 0.5% w/w of azo-iso-butyronitrile (AZBN) was added as initiator.

Composition	Molar %				
	AA	NIPA	HPA	NVP	AMO
1	35		55	10	
2	35		55		10
3	55		35	10	
4	55		35		10
5		35	55	10	
6		35	55		10
7		55	35	10	
8		55	35		10

Table 3.2 The monomer composition of acrylamide-based hydrogels studied.

DATr has a lower reactivity ratio than EGDMA and was used because this lower reactivity ratio would make it more compatible with the low reactivity of NVP.

The design of the original hydrogel was such that the amount of NVP was enough to increase hydrophilicity without the unfavourable effect of blocky sequence formation, as can be seen from Figure 3.2. In fact, NVP is shown to alternate. A study on the AA-NVP copolymer has shown that NVP is more reactive towards the copolymerisation process than AA[84], also with AZBN as initiator.

In this type of copolymer (with AA and HPA), the substitution of NVP for AMO appears to make no significant improvement in the sequence distribution (Figure 3.3) of the other two. AMO is shown to occasionally produce small blocks, but not of any notable size. As such, it may be assumed that the benefit of such a substitution would lie in reducing the lipophilicity of the material.

By increasing the proportion of AA from 35 mol% to 55 mol% and reducing the proportion of HPA from 55 mol% to 35 mol%, a change in the distribution of AA and HPA unit size is seen (Figure 3.4). HPA is more likely to be incorporated in smaller blocks, almost always alternating, whilst AA is incorporated over a larger sequence size distribution. This trend is repeated for the 55 mol% AA material with AMO (Figure 3.5).

35 mol% monomer A, Acrylamide
55 mol% monomer B, Hydroxypropyl Acrylate
10 mol% monomer C, N-Vinyl Pyrrolidone

r(AB) = 0.715 r(AC) = 0.814 r(BA) = 0.809
r(BC) = 0.133 r(CA) = 0.012 r(CB) = 0.002

Sequence Length	Acrylamide	Hydroxypropyl Acrylate	N-Vinyl Pyrrolidone
1	314	377	200
2	103	135	-
3	32	66	-
4	16	33	-
5	4	11	-
6	-	6	-
7	-	2	-
8	-	1	-
10	-	1	-

Figure 3.2 Computer-simulated sequence analysis of Composition 1.

35 mol% monomer A, Acrylamide
55 mol% monomer B, Hydroxypropyl Acrylate
10 mol% monomer C, Acryloyl Morpholine

r(AB) = 0.715 r(AC) = 0.46 r(BA) = 0.809
r(BC) = 0.264 r(CA) = 1.759 r(CB) = 0.894

Sequence Length	Acrylamide	Hydroxypropyl Acrylate	Acryloyl Morpholine
1	374	309	156
2	97	153	16
3	27	65	4
4	11	35	-
5	-	11	-
6	-	6	-
7	1	2	-
8	-	2	-
9	-	1	-
10	-	2	-

Figure 3.3 Computer-simulated sequence analysis of Composition 2.

55 mol% monomer A, Acrylamide
35 mol% monomer B, Hydroxypropyl Acrylate
10 mol% monomer C, N-Vinyl Pyrrolidone

r(AB) = 0.715 r(AC) = 0.814 r(BA) = 0.809
r(BC) = 0.133 r(CA) = 0.012 r(CB) = 0.002

Sequence Length	Acrylamide	Hydroxypropyl Acrylate	N-Vinyl Pyrrolidone
1	206	462	200
2	101	80	-
3	54	18	-
4	30	6	-
5	21	-	-
6	16	-	-
7	10	-	-
8	5	-	-
9	3	-	-
10	3	-	-
13	2	-	-
16	1	-	-

Figure 3.4 Computer-simulated sequence analysis of Composition 3.

55 mol% monomer A, Acrylamide
35 mol% monomer B, Hydroxypropyl Acrylate
10 mol% monomer C, Acryloyl Morpholine

r(AB) = 0.715 r(AC) = 0.46 r(BA) = 0.809
r(BC) = 0.264 r(CA) = 1.759 r(CB) = 0.894

Sequence Length	Acrylamide	Hydroxypropyl Acrylate	Acryloyl Morpholine
1	233	393	165
2	130	94	16
3	56	28	1
4	35	6	-
5	13	1	-
6	14	1	-
7	6	-	-
8	3	-	-
9	4	-	-
10	1	-	-
12	2	-	-
14	1	-	-

Figure 3.5 Computer-simulated sequence analysis of Composition 4.

The substitution of AA for NIPA leads to different outcomes again. Comparing Figure 3.6 and 3.8 illustrate the effect of increasing the NIPA/decreasing the HPA content with NVP as comonomer. At the 55 mol% level of HPA, the monomer is incorporated in a relatively blocky manner and a large fragment of HPA is seen to be polymerised last. This is also the case with AMO in place of NVP (Figure 3.7 and 3.9).

Reducing the HPA content to 35 mol%/increasing the NIPA to 55 mol% leads to smaller fragments being incorporated and so produces a more preferable polymer sequence. The r values show that the reactivity of AA with HPA and HPA with AA are similar, 0.715 and 0.809 respectively. The r value of NIPA with HPA however is much greater that that of HPA with NIPA, 1.441 and 0.68 respectively, and this is what produces the increased simulated HPA sequence length in the NIPA hydrogels with 55 mol% NIPA.

35 mol% monomer A, N-Isopropyl Acrylamide
55 mol% monomer B, Hydroxypropyl Acrylate
10 mol% monomer C, N-Vinyl Pyrrolidone

r(AB) = 1.441 r(AC) = 0.288 r(BA) = 0.68
r(BC) = 0.133 r(CA) = 0.001 r(CB) = 0.002

Sequence Length	N-Isopropyl Acrylamide	Hydroxypropyl Acrylate	N-Vinyl Pyrrolidone
1	334	228	200
2	101	126	-
3	31	57	-
4	9	29	-
5	2	15	-
6	3	8	-
7	1	10	-
8	-	3	-
9	-	2	-
10	-	2	-
11	-	1	-
12	-	3	-
31	-	1	-

Figure 3.6 Computer-simulated sequence analysis of Composition 5.

35 mol% monomer A, N-Isopropyl Acrylamide
55 mol% monomer B, Hydroxypropyl Acrylate
10 mol% monomer C, Acryloyl Morpholine

r(AB) = 1.441 r(AC) = 0. 451 r(BA) = 0.68
r(BC) = 0.264 r(CA) = 0.719 r(CB) = 0.894

Sequence Length	N-Isopropyl Acrylamide	Hydroxypropyl Acrylate	Acryloyl Morpholine
1	231	264	171
2	85	126	13
3	46	60	1
4	19	33	-
5	5	10	-
6	3	7	-
7	2	2	-
8	-	5	-
9	2	1	-
10	1	1	-
14	-	2	-
17	-	2	-
45	-	1	-

Figure 3.7 Computer-simulated sequence analysis of Composition 6.

55 mol% monomer A, N-Isopropyl Acrylamide
35 mol% monomer B, Hydroxypropyl Acrylate
10 mol% monomer C, N-Vinyl Pyrrolidone

r(AB) = 1.441 r(AC) = 0.288 r(BA) = 0.68
r(BC) = 0.133 r(CA) = 0.001 r(CB) = 0.002

Sequence Length	N-Isopropyl Acrylamide	Hydroxypropyl Acrylate	N-Vinyl Pyrrolidone
1	234	273	200
2	125	82	-
3	67	35	-
4	34	12	-
5	26	6	-
6	10	5	-
7	2	1	-
8	1	1	-
10	1	-	-
11	3	2	-
12	2	-	-
13	-	1	-

Figure 3.8 Computer-simulated sequence analysis of Composition 7.

55 mol% monomer A, N-Isopropyl Acrylamide
35 mol% monomer B, Hydroxypropyl Acrylate
10 mol% monomer C, Acryloyl Morpholine

r(AB) = 1.441 r(AC) = 0.451 r(BA) = 0.68
r(BC) = 0.264 r(CA) = 0.719 r(CB) = 0.894

Sequence Length	N-Isopropyl Acrylamide	Hydroxypropyl Acrylate	Acryloyl Morpholine
1	181	367	164
2	79	82	15
3	50	28	2
4	35	10	-
5	23	2	-
6	13	3	-
7	5	1	-
8	7	-	-
9	5	-	-
10	5	1	-
11	1	-	-
12	3	-	-
14	1	-	-
15	1	-	-
16	1	-	-

Figure 3.9 Computer-simulated sequence analysis of Composition 8.

3.3 Water-Binding Properties of Acrylamide and N-Isopropyl Acrylamide Hydrogels.

3.3.1 Results and Discussion

The effects that the proportions of AA:HPA and NIPA:HPA together with either NVP or AMO have on the equilibrium water content (EWC) and the ratio of freezing and non-freezing water are presented in Table 3.3. All materials have an EWC in the range of high 70's to mid 80%.

Increasing the proportion of acrylamide (and so decreasing the proportion of HPA) whilst keeping the amount of NVP constant appeared to give an increase in EWC of only 2% maximum. This could be seen in the corresponding rise in freezing water. However, the materials incorporating AMO in place of NVP saw this same increase due mainly to an increase in the non-freezing water. These materials had marginally lower EWCs than their NVP-containing equivalents.

Copolymer Composition (*% molar parts*)	EWC (%)	% Freezing Water	% Non-freezing Water
AA : HPA : NVP			
35:55:10	85.5	78.8	6.7
55:35:10	87.6	81.7	5.9
AA : HPA : AMO			
35:55:10	84.7	81.1	3.6
55:35:10	86.7	81.6	5.1
NIPA : HPA : NVP			
35:55:10	84.5	77.0	7.5
55:35:10	88.9	81.6	7.3
NIPA : HPA : AMO			
35:55:10	78.0	69.3	8.7
55:35:10	87.0	79.6	7.4

Table 3.3 Water-binding properties of acrylamide-based hydrogels expressed as percentage by mass.

The proportions of non-freezing water in the AA materials are very low compared to the other materials that will feature in this thesis and are slightly lower than those for the NIPA materials.

Increasing the amount of NIPA in the material causes an increase in the EWC of up to 5% where polymerised with NVP and up to 10% with AMO. The proportion of non-freezing water is slightly higher than the equivalent AA gels, probably due to a lower amount of water exclusion (due to hydrogen bonding) caused by the more sterically hindering isopropyl group. The AMO materials again show less hydrophilicity than their equivalent NVP gels in a lower EWC.

This representation displays gravimetric bulk results and does not easily indicate the water-binding properties of a single monomer unit, which changes in size as the molecular weights of the monomers change. As such, reworking the figures to mol water/mol monomer repeat unit based on monomer feed ratio gives a clearer indicator of hydrophilicity (assuming the monomer feed is forming a 'perfect' polymer chain), as shown in Table 3.4.

The AA-containing hydrogels all show similar bulk water properties in that increasing the proportion of AA causes almost no change in the moles of water attributed to a mole of polymer repeat unit. This would be expected as the EWCs were similar, the total weight of 35mol% AA/55mol% HPA and 55mol% AA/35mol% HPA are similar and the difference in molecular weight between NVP and AMO is not large.

NIPA on the other hand, is a much larger molecule than AA and changes in the quantity added will affect the size of the polymer repeat unit to a more significant degree. By increasing the amount of NIPA, a much higher ratio of water to polymer is achieved, mainly in the form of freezing water. At the 55 mol % level of NIPA, a higher amount of water is retained due to its higher proportion in a mole of the polymer unit.

Copolymer Composition (% molar parts)	Mol water / Mol monomer	Mol freezing water / Mol monomer	Mol non-freezing water / Mol monomer
AA : HPA : NVP			
35:55:10	35.2	32.5	2.8
55:35:10	37.6	35.1	2.5
AA : HPA : AMO			
35:55:10	34.0	32.6	1.4
55:35:10	35.8	33.7	2.1
NIPA : HPA : NVP			
35:55:10	37.0	33.8	3.2
55:35:10	52.9	48.6	4.3
NIPA : HPA : AMO			
35:55:10	24.7	21.9	2.8
55:35:10	45.3	41.5	3.8

Table 3.4 Water-binding properties of acrylamide-based hydrogels expressed as mol water/mol monomer repeat unit.

3.4 The Effect of Temperature on the Equilibrium Water Content

3.4.1 Method

The potential for NIPA-containing materials to be used in rapid drug delivery has been mentioned at the start of this chapter. As typical storage conditions for any material should be at room temperature (20°C), the materials were subjected to 5°C increments from 20°C up to 40°C (to incorporate physiological temperature of approx. 37°C) to investigate the dependence of the materials on temperature. At each temperature, the materials were allowed to reach equilibrium using a thermostatically controlled water bath before the water content was determined gravimetrically. A period of one hour appeared to be sufficient for this. The hydrogel had been equilibrated in water at room temperature for at least one week prior to the experiment. In addition, to demonstrate the thermo-reversible nature of NIPA-based materials, one material was taken from 40°C down to 20°C in 5°C stages (composition 5).

3.4.2 Results and Discussion

The temperature dependence of the EWC of NIPA-based hydrogels is clearly displayed in the following graphs. The reversible nature of the materials is shown with a single example in Figure 3.10.

The relatively small decrease seen with increasing temperature in the AA materials is that associated with an increased energy in the system preventing stable hydrogen bonding from occurring and so reducing the EWC. Where AA is present at the 55 mol% level, the effect of temperature is reduced and this is seen comparing Figure 3.10 to 3.11 and 3.12 to 3.13. It has been pointed out in the literature that the pyrrolidone ring of NVP affects thermal properties more than the amide group of AA[84]. When taking into account the proportions of monomer to each other, AA has less of a damping effect on the 10 mol% of NVP at the 35 mol% level than at the 55 mol% level. This is also the case when AMO is present.

At temperatures of ≥35°C, the NIPA-based materials showed signs of opacity, indicative of phase separation. Over the range of temperature, the balance of hydrophilic and hydrophobic interactions is seen to change. Above the LCST, the hydrophobic interactions become dominant. These materials do not show a sharp transition as poly(NIPA) does. However, the fine structure in the 30-35°C region has not been resolved in this work and may be a point for further study. A difficulty lies in measuring the water content to such accuracy using the current procedure, as speed of measurement, room temperature and humidity would affect the result.

Increasing the proportion of NIPA in the material decreases the magnitude of the change in EWC. The 55 mol% NIPA hydrogels has associated with it approx. 53 mole water/mole of monomer repeat unit whereas the 35 mol% NIPA hydrogel has just 37 mole water/mole monomer repeat unit (Table 3.4). With increased hydrophilicity of the copolymer, the polymer chains are better solvated and the solvent is more strongly bound, although this only supported by a single unit increase in the corresponding moles of non-freezing water/mole monomer repeat unit. Better solvation may be the cause of fewer water molecules being released during chain collapse, shown clearly between the materials involving NVP as comonomer and to a lesser extent with AMO below 35°C.

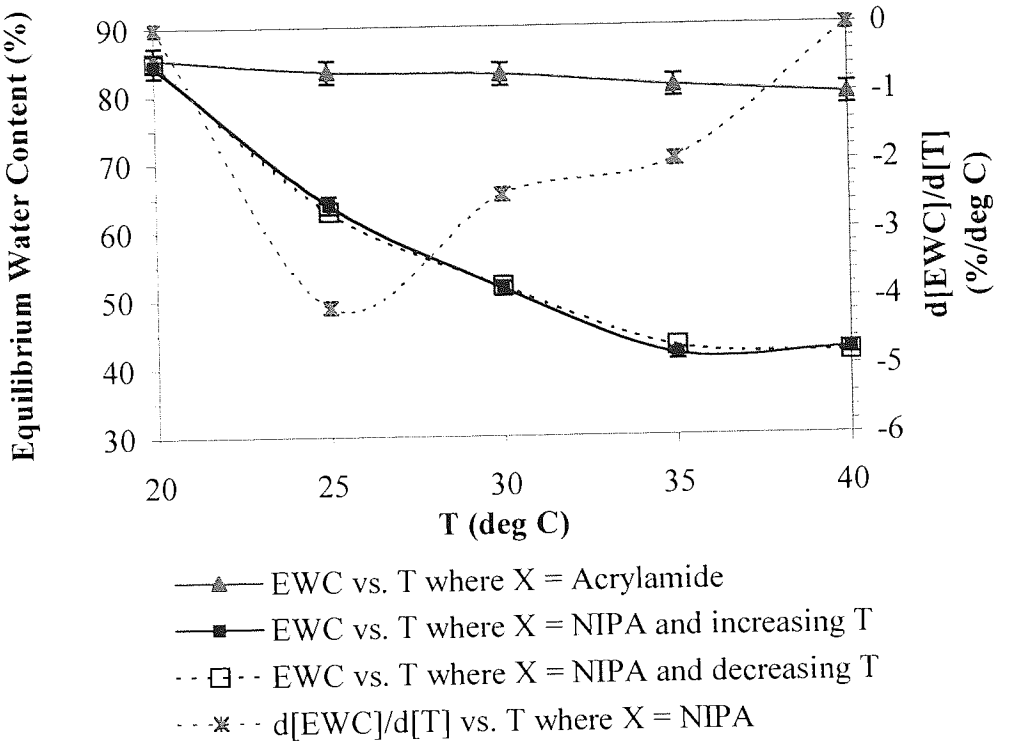

Figure 3.10 Effect of temperature on the EWC of X/HPA/NVP (35/55/10 molar pts) hydrogel (composition 1 & 5).

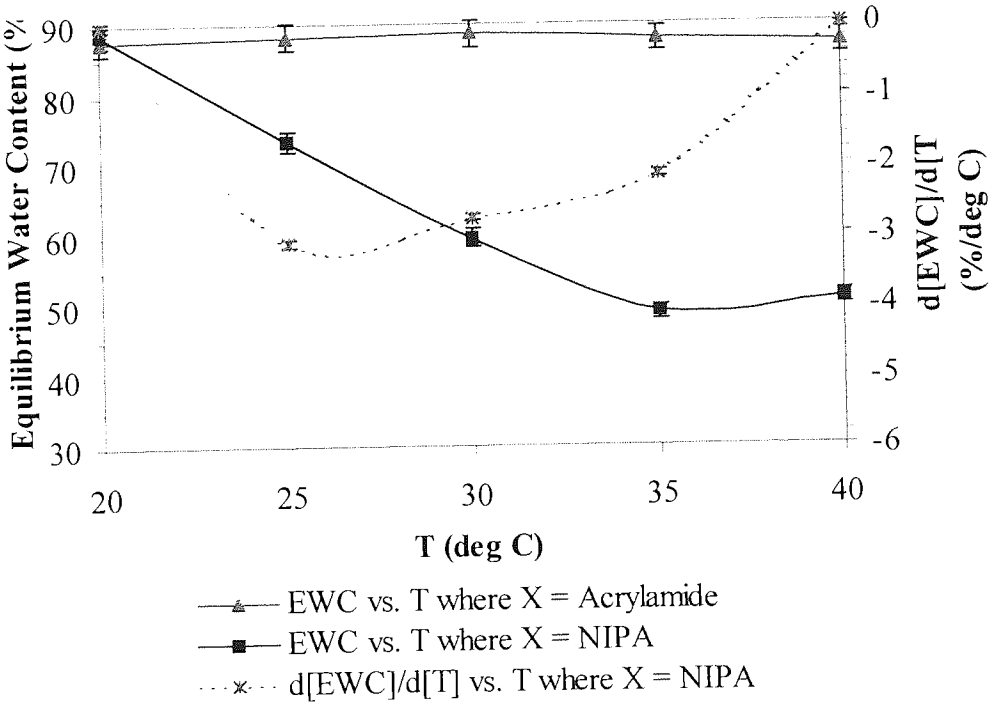

Figure 3.11 Effect of temperature on the EWC of X/HPA/NVP (55/35/10 molar pts) hydrogel (composition 2 & 6).

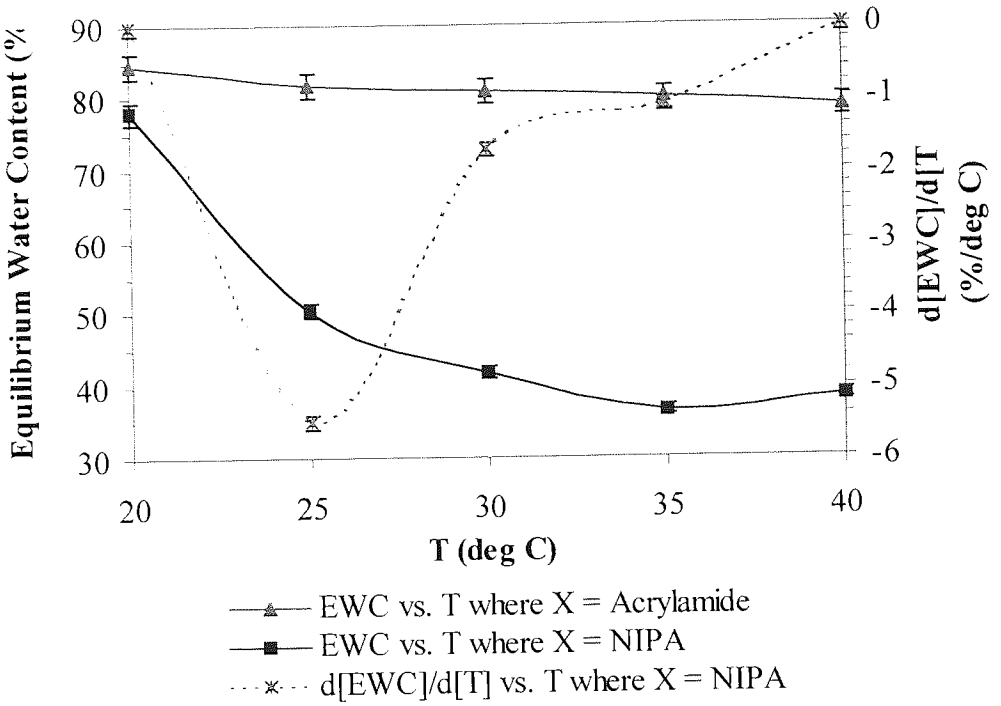

Figure 3.12 Effect of temperature on the EWC of X/HPA/AMO (35/55/10 molar pts) hydrogel (composition 3 & 7).

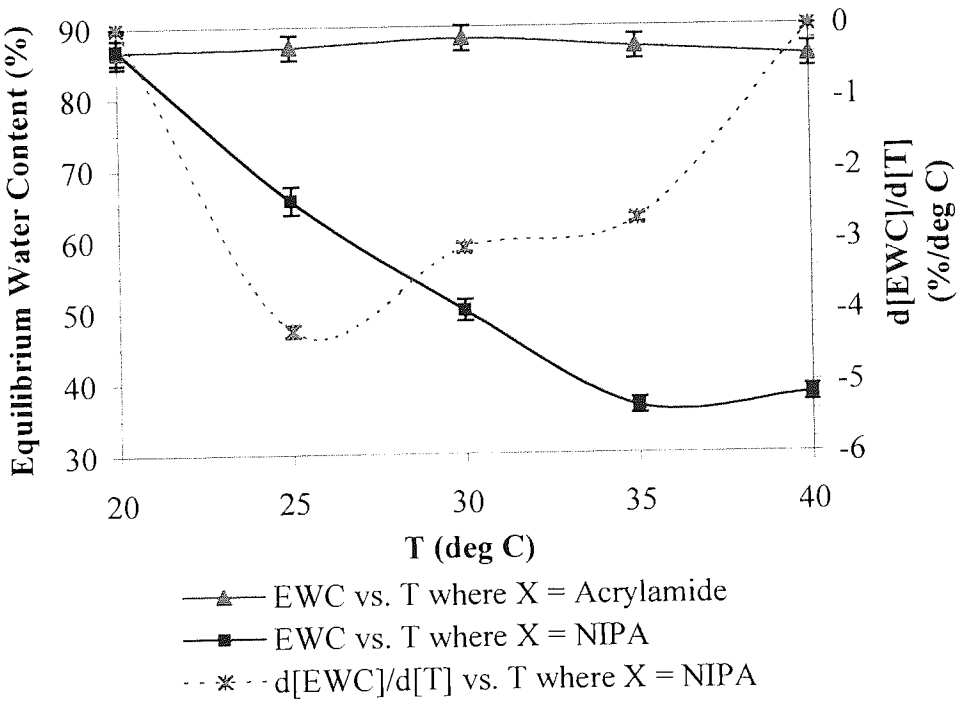

Figure 3.13 Effect of temperature on the EWC of X/HPA/AMO (55/35/10 molar pts) hydrogel (composition 4 & 8).

The rate of change in EWC for the NIPA-based gels has been shown by a plot of δ[EWC]/δ[T]. A higher NIPA content results in a slower rate of change for both NVP- and AMO-containing materials. A 'skin layer' effect has been proposed by Kaneko *et al*[85], which forms as the temperature rises; the surface of the gel dehydrates (or becomes more hydrophobic) immediately on the surrounding temperature change which blocks the flow of water out of the gel. The hydrodynamic internal pressure gradually increases and water accumulates near the surface of the gel because of this pressure. When the internal pressure becomes too large, the water is transported by convection out of the gel. By incorporating a higher proportion of other hydrophilic monomers, only a weak skin layer is formed, allowing faster gel contraction with a rise in hydrostatic internal pressure.

Substituting NVP for AMO has the effect of increasing the magnitude and rate of EWC change with temperature, comparable between Figures 3.10 and 3.12 and Figures 3.11 and 3.13. The slightly lower hydrophilicity displayed by the AMO materials over the NVP materials may aid the release of water upon the conformational changes to hydrophobic bonding because of AMOs higher readiness to release associated water. Alternatively, NIPA may be more able to self-associate and exclude water where AMO is present over NVP.

3.5 Mechanical Properties of Acrylamide-based Materials

3.5.1 Results and Discussion

The results of mechanical tests on the hydrogels are displayed in Table 3.5. It can be seen that all of the materials show relatively low values of Young's Modulus, which is a measure of the materials stiffness. As the hydrogels are almost all over 80% water content, the plasticising effect of the water is responsible for this apparent weakness. The expected large effect of internal hydrogen bonding increasing stiffness does not appear to feature, possibly due to the hydrogel being pre-swollen by including a diluent which has prevented the N-H and C=O from close interaction.

The materials containing 55 mol% NIPA have slightly lower value of elasticity than the others. By referring to the water binding values, the moles of water/mole of monomer repeat unit are much higher for these two hydrogels and so the plasticising effect is seen.

As the water properties do not indicate a clear difference and the error margins are relatively large, it may be tentatively postulated that incorporating AA does have a hydrogen bonding advantage over NIPA that marginally increases the resistance of the polymer chain to rotation and unravelling on a pulling force.

Copolymer Composition (*% molar parts*)	E (MPa)	Ts (MPa)	Eb (%)
AA : HPA : NVP			
35:55:10	0.08 ± 0.01	0.11 ± 0.02	156 ± 24
55:35:10	0.07 ± 0.01	0.11 ± 0.00	180 ± 16
AA : HPA : AMO			
35:55:10	0.07 ± 0.01	0.11 ± 0.04	154 ± 39
55:35:10	0.07 ± 0.01	0.13 ± 0.02	183 ± 24
NIPA : HPA : NVP			
35:55:10	0.05 ± 0.01	0.08 ± 0.02	150 ± 23
55:35:10	0.04 ± 0.00	0.06 ± 0.01	121 ± 17
NIPA : HPA : AMO			
35:55:10	0.06 ± 0.01	0.09 ± 0.03	153 ± 40
55:35:10	0.04 ± 0.00	0.11 ± 0.03	205 ± 31

Table 3.5 Mechanical properties of acrylamide-based hydrogels.

The AA materials show higher values of tensile strength than do the NIPA materials, which could be an indication of a better network formation. The simulated sequence distributions show that AA polymerises in a more ideal manner than NIPA with HPA and NVP or AMO as co-monomers.

3.6 Conclusions

Acryloyl morpholine in place of N-vinyl pyrrolidone appears to have no detrimental effect upon the water-binding properties of acrylamide-based hydrogels. As a contact lens material, an AA/HPA/AMO copolymer would be expected to reduce lipid deposition on the surface of the lens. AMO appears to produce sequence distributions similar to where NVP is involved with AA and HPA as comonomers.

Where acrylamide was included at 55 mol%, this material showed improved thermal stability over the 35 mol% level material. Such stability is required for a lens material to prevent dimensional changes from occurring upon insertion of a lens into the eye.

The use of N-isopropyl acrylamide with comonomers already proven suitable for biomaterial applications and its temperature sensitivity make it a material with many possible functions. For a more consistent rate of water loss from the hydrogel from the range 20-40°C, those incorporating NIPA at the 55 mol% level would appear suitable for rapid drug delivery or filtration applications. Also, HPA at 35 mol% gives a more preferable simulated sequence distribution than at 55 mol%. As NVP has been used as a skin permeation enhancer, an NIPA/HPA/NVP patch could be applied for topical delivery if backed onto an impermeable sheet with a skin-adhesive skirt. If toxicologically acceptable, the materials could be used as a cell culture platform that responds to temperature.

The acrylamide hydrogels appear to show marginally more resistance to chain rotation and deformation on an applied pulling force than N-isopropyl acrylamide materials. This could be due a more ideal network formation and/or a higher degree of hydrogen bonding acting as secondary cross-links.

CHAPTER 4

Hydrogels Containing Anionic Monomers

"Audentis Fortuna iuvat."

(Fortune assists the bold)

Virgil, 70-19BC,

Aeneid.

4.1 Introduction

Ionic monomers are introduced into hydrogels primarily as a means to increase the water content of the material. As a contact lens, increased water means increased comfort, but this brings about the associated problems discussed in Chapter One. The most well known ionic contact lens is Etafilcon A (HEMA and methacrylic acid). The incorporation of methacrylic acid raises the water content of a HEMA-only material by approx. 20% to 58%.

In recent years, new monomers have become available that have a sulphonate functionality that imparts a negative charge once hydrated. These monomers have fairly flexible side chains with a terminal sulphonate moiety but differ structurally from one another. Their structures are displayed in Figure 4.1 below.

Bis(3-sulphopropyl ester) itaconate,
dipotassium salt
SPI

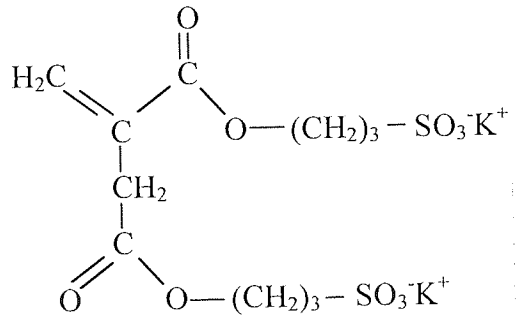

Sodium 2-(acrylamido)-2-methyl propane
sulphonate
NaAMPS

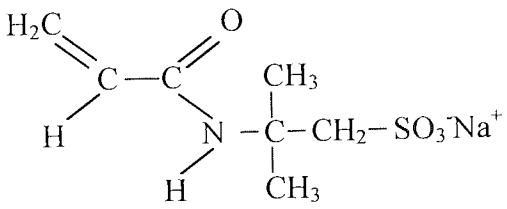

3-Sulphopropyl ester acrylate,
potassium salt
SPA

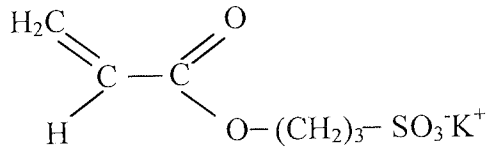

Figure 4.1 The chemical structures of SPI, NaAMPS and SPA.

As can be seen above, SPI is almost twice the molecular mass of SPA and has dual acid functionality. It is interesting to note that NaAMPS has an amide bond structure (CONH) that, in proteins, is the bond that links amino acids together and in that context is called a peptide bond. The CONH region is highlighted in Figure 4.1. The similarities of the functional groups of these monomers and the glycosaminoglycans in Figures 1.9 and 1.10 should also be mentioned. The glycosaminoglycans have roles in lubrication and as nature is able to use charged species, usually anionic species, these monomers may have a part to play in biomaterials.

One of the earliest studies on sulphonate monomers[86] including NaAMPS looked at the reactivity with NVP. The NaAMPS/NVP monomer pair showed evidence of an alternating tendency. The copolymerisations were carried out in aqueous solution in the presence of AZBN at 60°C. Another monomer investigated was a zwitterion, SPE, shown in Figure 4.2. This had been shown to form an intra-chain association which had the effect of excluding water. Previous work in our laboratory has shown that incorporation of SPE into HEMA-based materials resulted in phase-separated, opaque materials and hence was unsuitable for lens chemistry[87]. The materials also showed anti-polyelectrolyte behaviour.

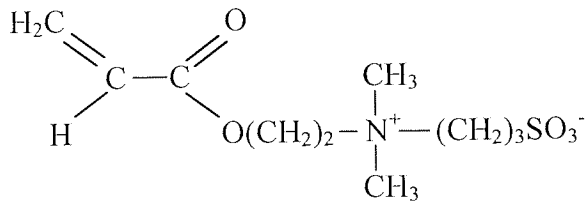

Figure 4.2 The structure of N,N'-dimethyl-N-methacryloxy-ethyl-N-(3-sulphopropyl)-ammonium betaine, SPE, M_r = 279.

Other researchers have found that NaAMPS also has an alternating tendency with acrylamide. Of particular interest in most research is the swell factor that may be obtained with polyelectrolyte gels containing the highly ionic sulphonates[88,89].

A low water content, non-ionic hydrogel material composed of HEMA, NVP, methyl methacrylate (MMA) and a PEG-methacrylate has been used as the basis of a proprietary material that has been through clinical trials and is commercially supplied through

optometrists in Europe. This material has been used successfully in eyes for ten years and is composed of monomers that are typically used in contact lenses. The three major components of the hydrogel were entered into the TERPOL simulation and the sequence distribution obtained, which can be seen in Figure 4.3. The block of NVP at the end of the sequence is typical of this monomer.

The size of the polyethylene glycol (PEG) unit was n=200, although larger molecular weight PEG's have been shown to reduce protein adsorption due to the more mobile and more hydrophilic surface presented, although longer chains have the consequence of increased calcium ion interaction in biological solutions[90].

The effects on water binding, mechanical properties, surface energies and spoilation profiles were investigated on incorporation of a charged, anionic species to this proprietary composition, hereafter known as Copolymer X.

Both water and N-methyl pyrrolidone were added at 10% w/w each where a sulphonate monomer was included in the copolymer. The reactivity of HEMA and NVP is known to be poor, with large blocks of NVP formed at the end of polymerisation. This is illustrated clearly in Figure 4.4, which shows the simulated reactivity of the two monomers that are popular comonomers in the production of high water content contact lenses (Hefilcon), despite the known reactivity problem and the resultant effects on performance. Work in our labs has attempted to replace NVP with AMO and the advantage of this replacement to the sequence distribution of the monomers is shown in Figure 4.5. However, in this study, the use of NVP continues but with the addition of solvents that have been reported to improve its reactivity.

64.8 Mole % of Monomer A, HEMA...represented by O
15.9 Mole % of Monomer B, NVP.....represented by X
19.3 Mole % of Monomer C, MMA.....represented by *

r(AB)= 32.678 r(AC)= 1.676 r(BA)= 0.006
r(BC)= 0.004 r(CA)= 0.319 r(CB)= 3.95

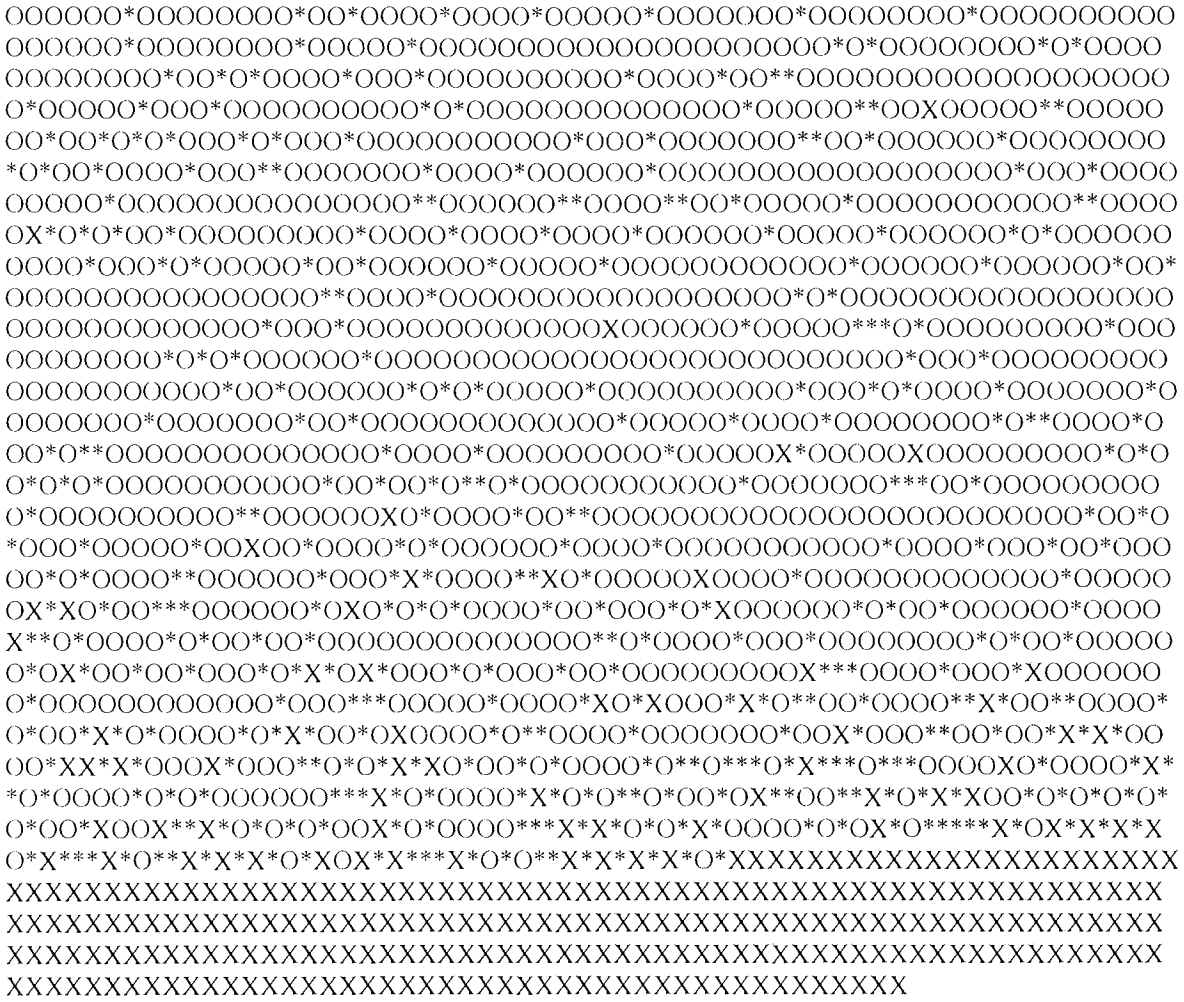

Sequence Length	HEMA	NVP	MMA	Sequence Length	HEMA	NVP	MMA
1	93	69	280	13	3	0	0
2	45	1	33	14	3	0	0
3	26	0	12	15	1	0	0
4	41	0	0	16	2	0	0
5	19	0	1	18	2	0	0
6	21	0	0	20	2	0	0
7	9	0	0	21	1	0	0
8	8	0	0	25	1	0	0
9	6	0	0	27	1	0	0
10	6	0	0	30	1	0	0
11	6	0	0	246	0	1	0
12	3	0	0				

Figure 4.3 Computer-simulated sequence distribution of the three major monomers in a successful contact lens material: HEMA, NVP and MMA.

70 mol% Monomer A, HEMA...represented by O
30 mol% Monomer B, NVP.....represented by X

r(AB) = 32.678 r(BA) = 0.006

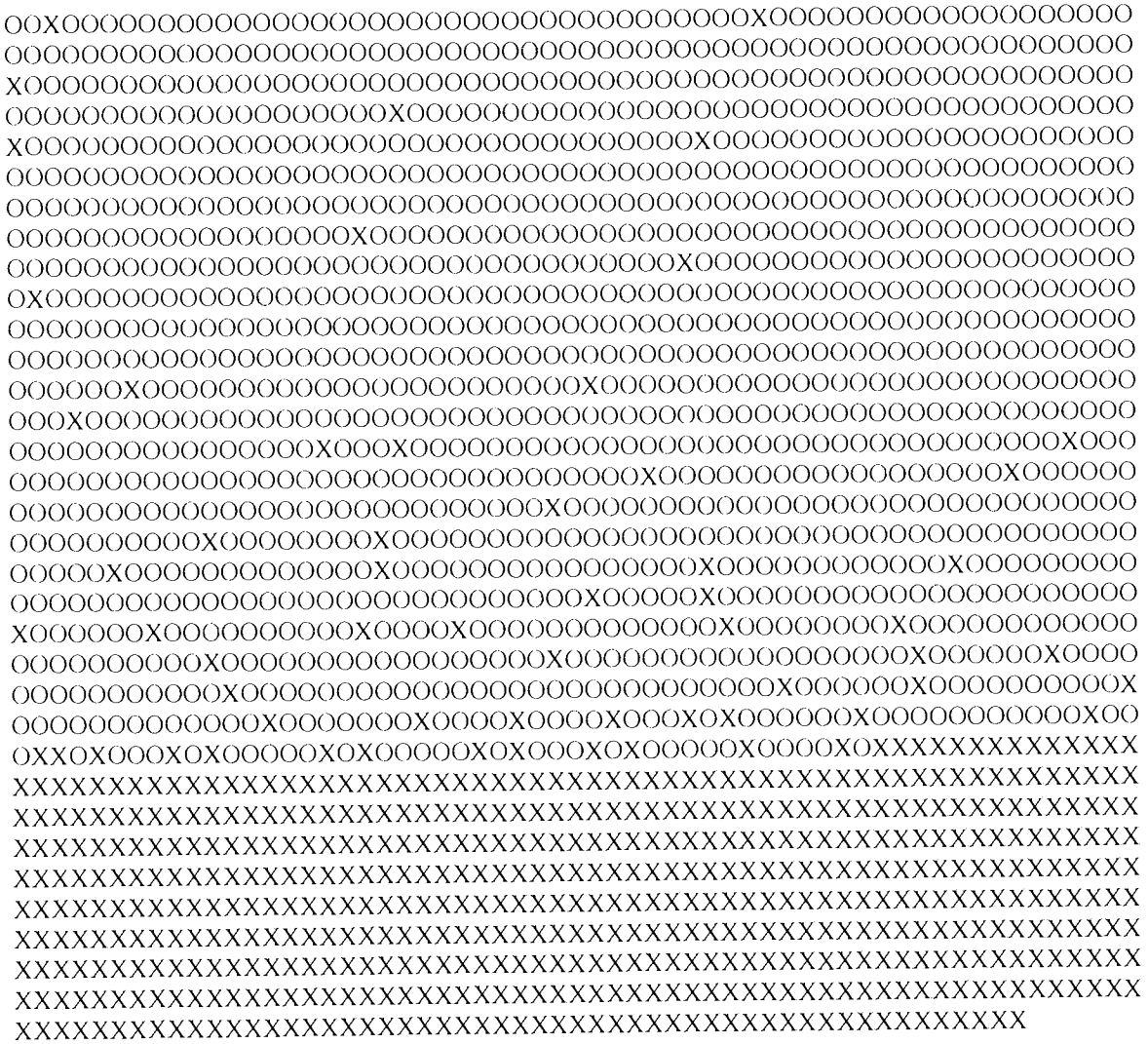

Sequence Length	HEMA	NVP	Sequence Length	HEMA	NVP	Sequence Length	HEMA	NVP
1	7	591	15	1	0	36	2	0
2	1	0	16	1	0	38	1	0
3	5	0	17	1	0	39	1	0
4	4	0	18	2	0	40	1	0
5	4	0	22	2	0	44	1	0
6	4	0	23	1	0	71	1	0
7	1	0	24	1	0	75	1	0
8	2	0	28	1	0	78	2	0
10	2	0	31	1	0	158	1	0
11	1	0	34	2	0	181	1	0
12	1	0	35	1	0	539	0	1
13	3							

Figure 4.4 Computer-simulated sequence distribution of HEMA:NVP 70:30 mol%.

70 mol% Monomer A, HEMA...represented by O
30 mol% Monomer B, AMO.....represented by X

r(AB) = 3.799 r(BA) = 0.211

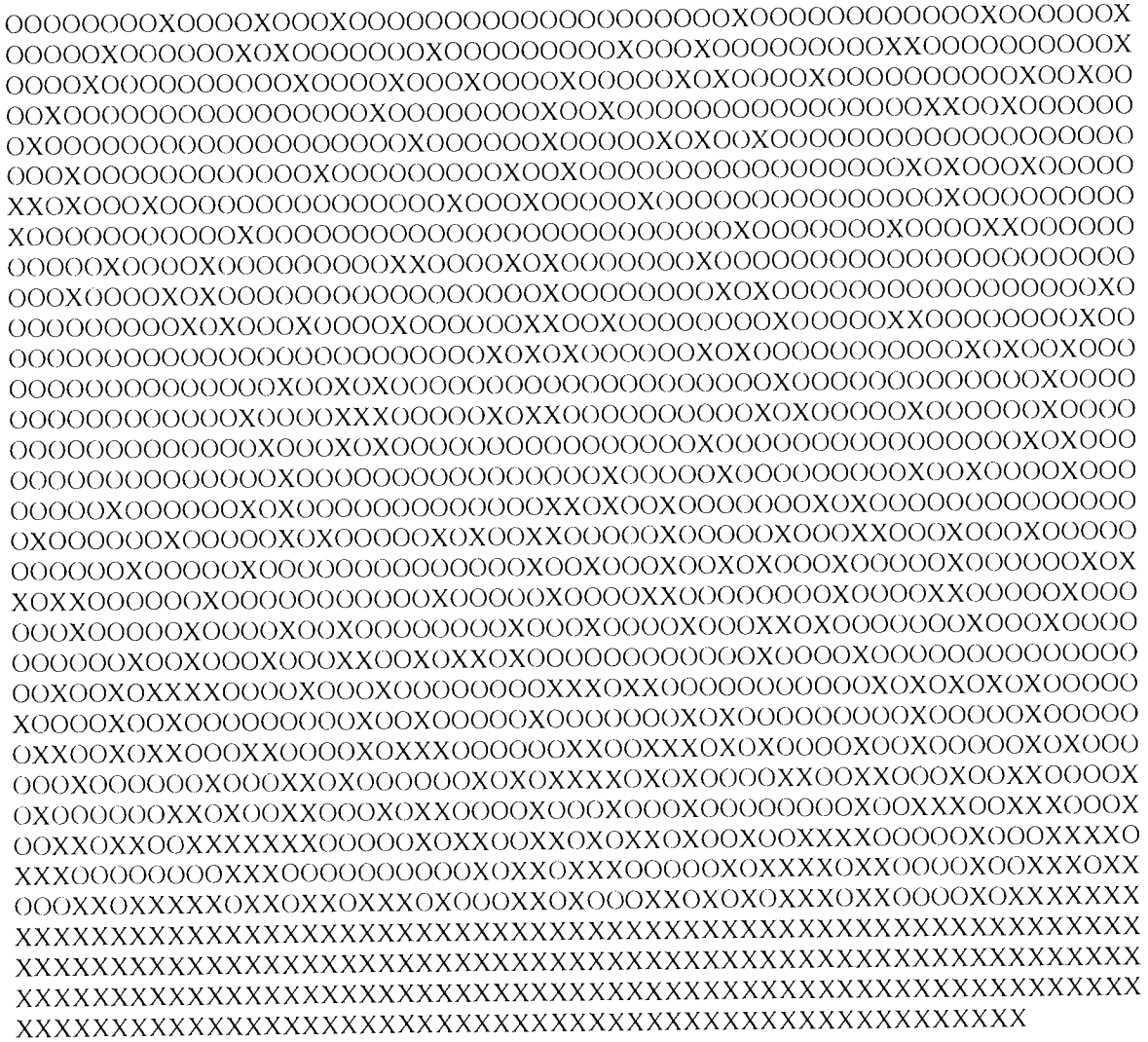

Sequence Length	HEMA	AMO	Sequence Length	HEMA	AMO
1	71	207	13	2	0
2	33	44	14	1	0
3	30	12	15	3	0
4	27	5	16	7	0
5	25	1	17	6	0
6	17	0	19	1	0
7	7	1	20	2	0
8	11	0	22	1	0
9	8	0	25	2	0
10	7	0	27	1	0
11	6	0	237	0	1
12	3	0			

Figure 4.5 Computer-simulated sequence distribution of HEMA:AMO 70:30 mol%.

4.2 Results and Discussion

The monomers SPI, NaAMPS and SPA were incorporated from 0% to 9.2% by mass into the base material and the effects analysed. The mole incorporation of the anionic monomers is shown in Table 4.1 below. It is important to remember that the moles of effective charge for SPI is double the moles of monomer.

Weight of sulphonate monomer added (%)	Mole % of sulphonate monomer per unit of copolymer (based on feed ratio)		
	SPI (M_r = 450)	SPA (M_r = 232)	NaAMPS (M_r = 229)
0.5	0.15	0.3	0.3
1.0	0.3	0.6	0.6
2.5	0.8	1.5	1.5
4.8	1.5	2.9	3.0
9.2	3.0	5.7	5.8

Table 4.1 Mole % of sulphonate monomers added to base composition.

4.2.1 Water-Binding Properties of Hydrogels Containing Anionic Sulphonate Monomers

The incorporation of SPI into the base material had the effect of causing the equilibrium water content to rise rapidly up to 2.5% by weight and then more slowly up to 9.2% by weight. This is shown graphically in Figure 4.6. The water content reached almost 70% on the highest level of anion added. The increase could be attributed to the increase in the freezing water component of the materials which reached a little over 50%. This rise caused a corresponding slight decrease in the non-freezing water over the same range to a minimum of approx. 18%.

On addition of SPA, the water content increased more consistently to a level just over 85% at 9.2% weight incorporation, shown in Figure 4.7. Again this rise corresponded to the increase in freezing water, which rose to approx. 80%. This then appeared to cause the non-freezing water component to fall to a level of 6%.

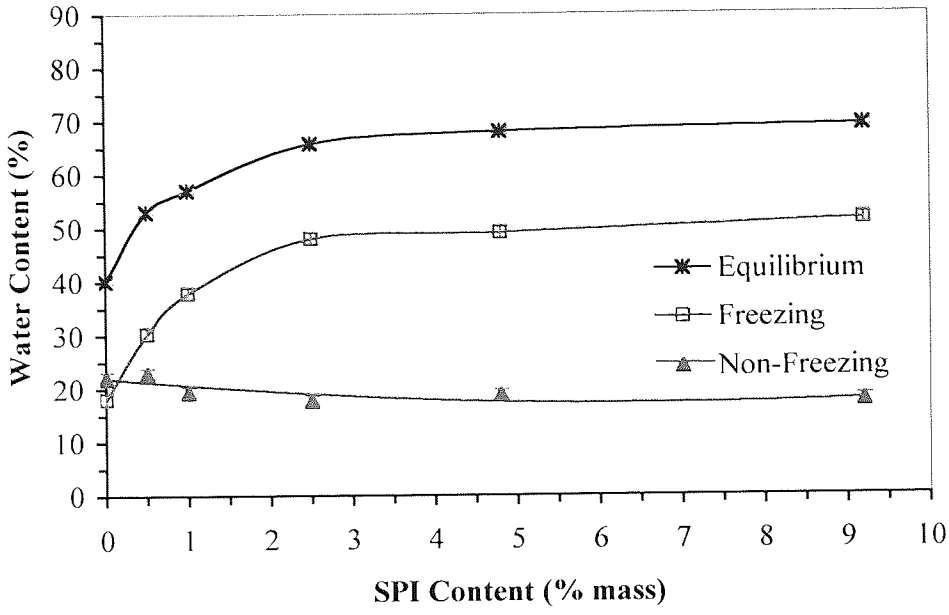

Figure 4.6 The water-binding properties of Copolymer X hydrogels containing increasing weight % of SPI.

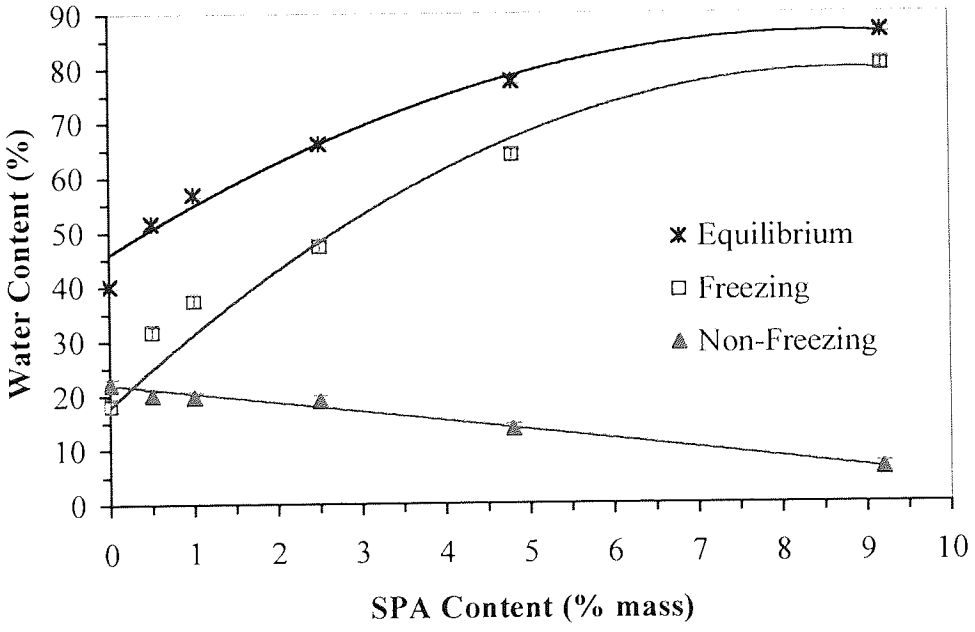

Figure 4.7 The water-binding properties of Copolymer X hydrogels containing increasing weight % of SPA.

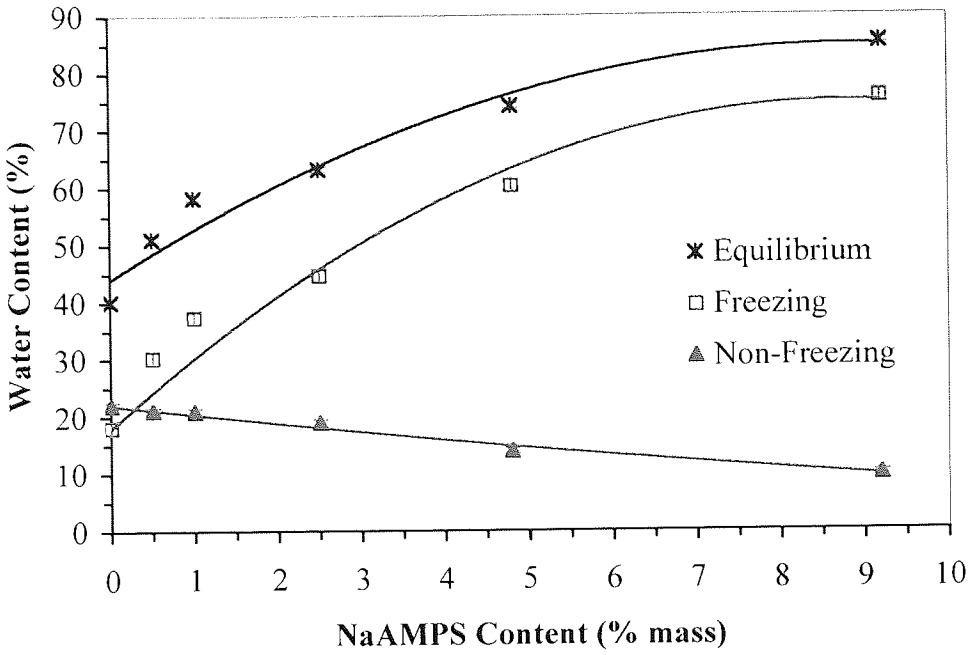

Figure 4.8 The water-binding properties of Copolymer X hydrogels containing increasing weight % of NaAMPS.

The addition of NaAMPS led to a water-binding profile similar to SPA in its magnitude of values, seen in Figure 4.8. A maximum equilibrium water content of 85% was obtained over the range. The freezing water component reached 76%, whilst the resultant non-freezing water content fell to 10%.

It was expected that SPI would show similar hydrophilicity to SPA at equivalent weight % levels, by virtue of it possessing two terminal sulphonate groups, and so more charged area to interact with water. The mole % incorporation of SPI was approximately half that of SPA at equal weight %, as shown in Table 4.1, but the double charge on SPI made the mole amount of charge equal to that of SPA at equal weight %.

At 2.5% by weight SPI, the equilibrium water content was within a 2% range of the equivalent weight of SPA. Above this however, the equilibrium water contents of SPA copolymers outstrip those of SPI up to a maximum of 17% at comparable weight % and moles of charge %.

Alternatively, SPI at 3.0 mole % (≡ 9.2% w/w) should have meant that almost twice the sulphonate groups as SPA at 2.9 mole % (≡ 4.8% w/w) and also NaAMPS at 3.0 mole %

(≡ 4.8 w/w) were present. However, the equilibrium water contents show that those for SPA and NaAMPS are higher, due in the main to the freezing water being over 10% higher than in the SPI copolymer.

The re-working of these values to moles of water per mole of monomer repeat unit (based on feed ratio) gives a truer indication of water binding at a more molecular level. Figures 4.9 to 4.11 show the water-binding properties of SPI, SPA and NaAMPS respectively, in terms of mole amounts.

As is clear from Figure 4.9, which shows the trend for moles of water per mole of SPI copolymer repeat unit, the curves show the same shape as for the gravimetrically determined water contents. The addition of SPI causes an increase in the total moles of water per mole of monomer repeat unit from 5 up to just over 18. The slight fall in non-freezing water % seen in Figure 4.6 is actually a slight increase in the moles of non-freezing water per mole of monomer repeat unit.

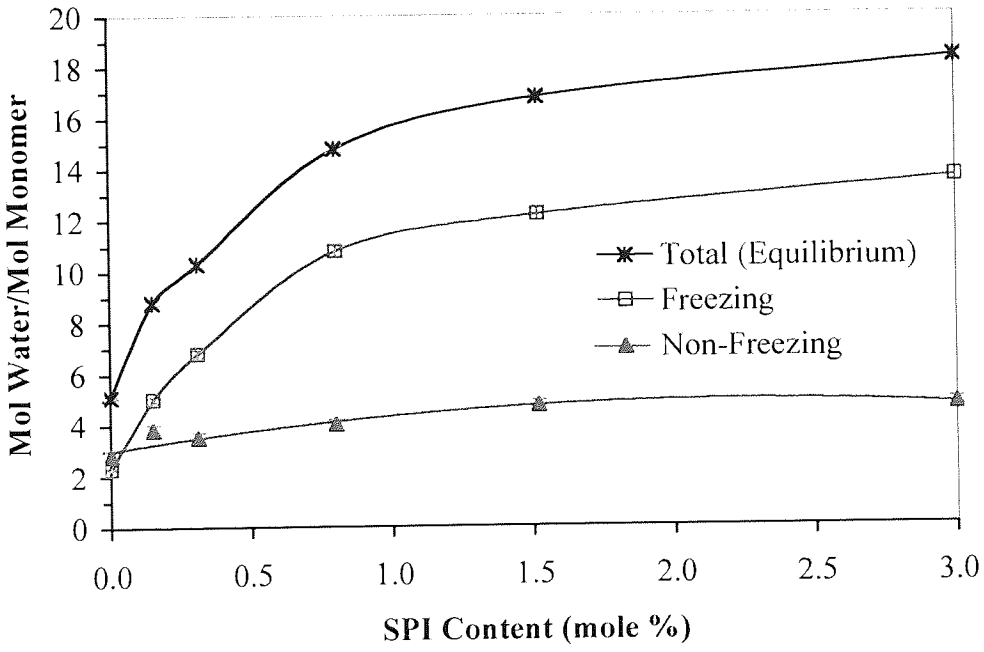

Figure 4.9 The water-binding properties expressed as per mole of monomer for Copolymer X hydrogels containing increasing mol% of SPI.

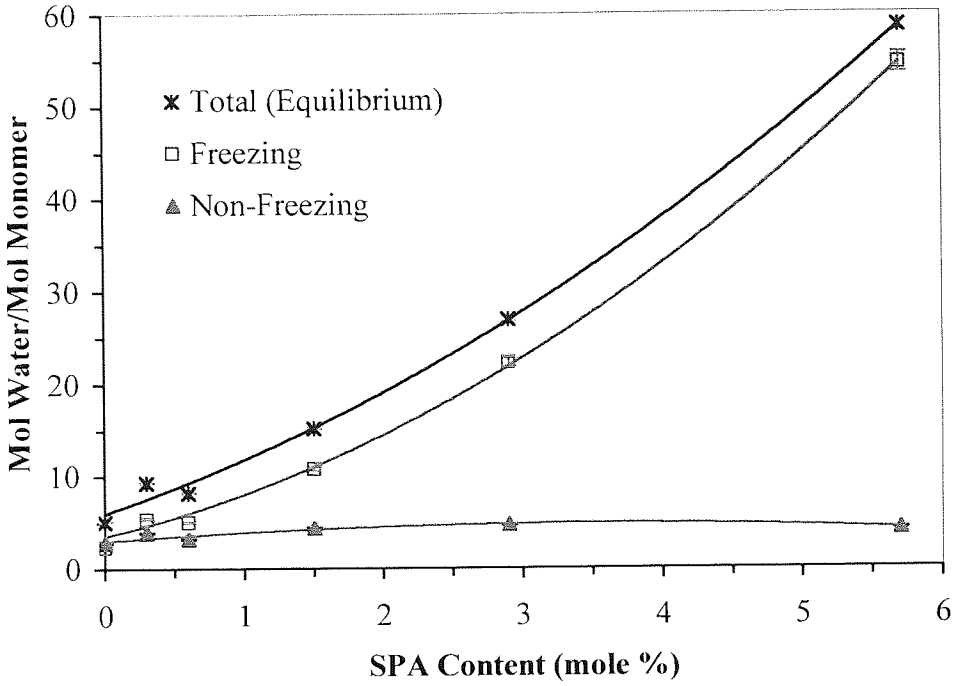

Figure 4.10 The water-binding properties expressed as per mole of monomer for Copolymer X hydrogels containing increasing mol% of SPA.

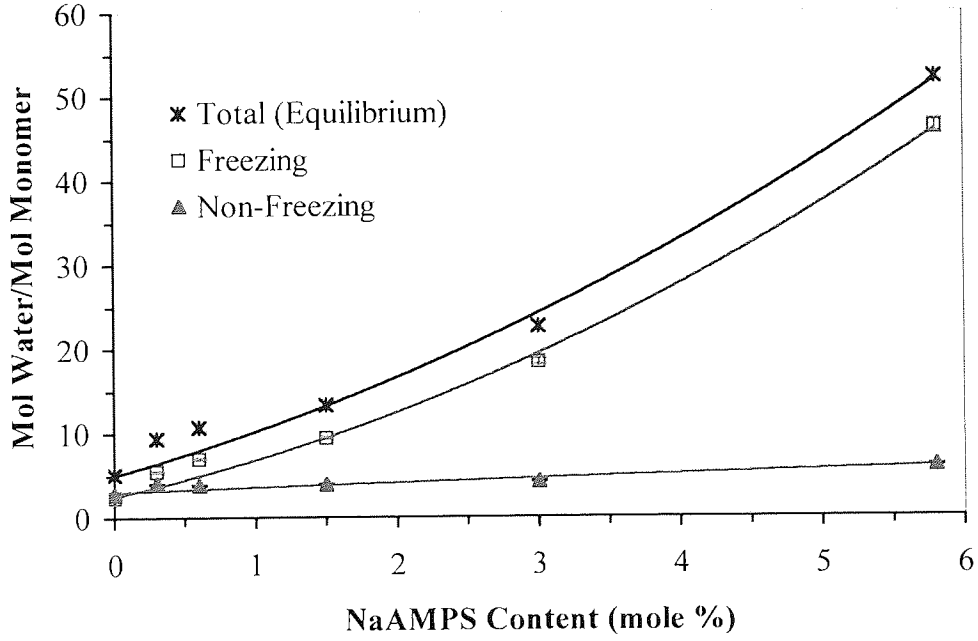

Figure 4.11 The water-binding properties expressed as per mole of monomer for Copolymer X hydrogels containing increasing mol% of NaAMPS.

In comparison, the significant decline in non-freezing water in excess of 10% seen on increased amounts of SPA and NaAMPS in Figures 4.7 and 4.8 respectively is shown in

Figures 4.10 and 4.11 to be an almost constant but slight increase in the moles of non-freezing water per mole of monomer, similar in scale to that seen in SPI copolymer. NaAMPS actually showed a little more water strongly associated to the copolymer than the other two.

What Figures 4.10 and 4.11 show, more importantly, is the substantial water-binding ability that SPA and NaAMPS have over SPI, and SPA being better able to attract freezing, plasticising water than NaAMPS.

The different profile obtained for SPI copolymers suggests that there is a different type of water binding occurring than in SPA and NaAMPS in response to the dual functionality. It could be possible that because an SPI molecule in a polymer chain has a negative group on either side of that chain, as does an SPI molecule in an adjacent chain, the sulphonate groups are unable to find individual space due to the bulk of sulphonates causing steric hindrance. The long chains on either side of the polymer chain would reduce the mobility of the copolymer chains, so reducing the EWC. As such, the sulphonate groups may be forced to 'share' water molecules between them, as indicated by the relative low level of water molecules per mole of polymer and resulting in the copolymer swelling in water to a lesser extent than SPA and NaAMPS copolymers. These monomers, once incorporated, may be more able to find a position in a hydrating medium to attract water to each sulphonate group alone.

The suspicion that the pH of the hydrating distilled water (measured to be in the range pH 5.8 – 6.3) was affecting the degree of charge present in the copolymers was investigated. The pK_a of SPI has been measured as being three, the same as that for SPA. Discs of two copolymers where SPI had been incorporated at the 4.8% and 9.2% w/w were allowed, in the first instance, to reach equilibrium in HPLC-grade water (deionised and pH 7). A second set of discs were boiled first in a 1% bicarbonate solution and then also allowed to equilibrate in HPLC-grade water. The resultant equilibrium water contents are shown in Table 4.2.

These results show that there was no pH-dependency affecting the water-binding results for the SPI copolymers compared to the SPA and NaAMPS copolymers. Boiling in bicarbonate solution caused the EWC to increase by up to 3%, bringing the water

properties closer to, but still below, those of SPA. As such, the molecular implications of the inclusion of SPI on the hydrophilicity of the copolymers, in comparison to the mono-functional SPA, remain uncertain.

Weight of SPI (%)	Equilibrium Water Content of SPI copolymers (± 0.3)		
	In distilled water (pH ≈ 6)	In HPLC-grade deionised water (pH ≈ 7)	In HPLC-grade water, post 1% bicarbonate boil
4.8	68.0	68.1	72.1
9.2	69.1	69.4	71.8

Table 4.2 Equilibrium water content of SPI copolymers in different types of hydrating water, average of at least three samples.

The large size and therefore dominance of the sulphonate groups, which appear to have a preference for loosely bound, freezing water over strongly bound, non-freezing water, is why water is unable to interact with groups that are able to strongly bind water. The result has been to keep the levels of non-freezing water in all of the copolymers relatively low.

4.2.2 Surface Free Energy Properties of Hydrated Hydrogels Containing Anionic Monomers

For all sulphonates copolymers, the incorporation of levels up to 1% by weight cause a primary increase in the total surface energy that is due to the presentation of polar groups at a surface which can bind water and so wet the surface better, as shown in Figures 4.12 through 4.14. This is a result, in each case, of a rise in the polar component of the surface energy and a fall in the dispersive component. The dispersive component arises primarily from non-polar group contributions to the surface energy, such as α-Me groups and $-CH_2-$ groups and so is reduced upon incorporating a polar group.

In water, the polar groups would be in the most energetically favourable position by rotating about the polymer backbone and presenting out into the liquid. Up to 1% weight incorporation of a sulphonate monomer, a rapid rise is the polar component is seen which is attributed to the change from non-ionic to ionic, with significantly increased polarity as a result.

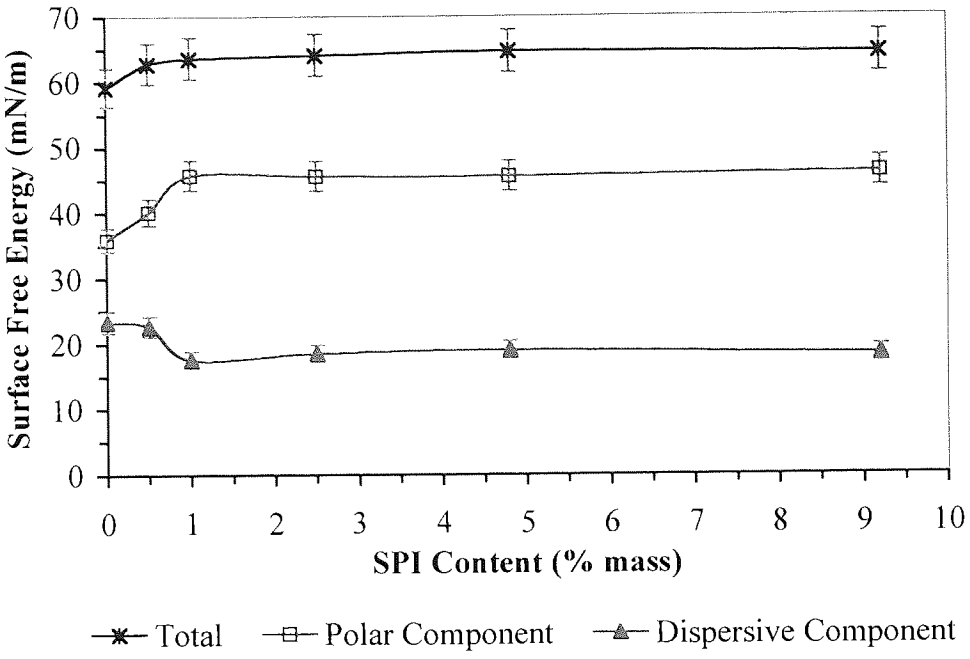

Figure 4.12 The components of surface free energy of hydrogels containing increasing amounts of SPI in the hydrated state.

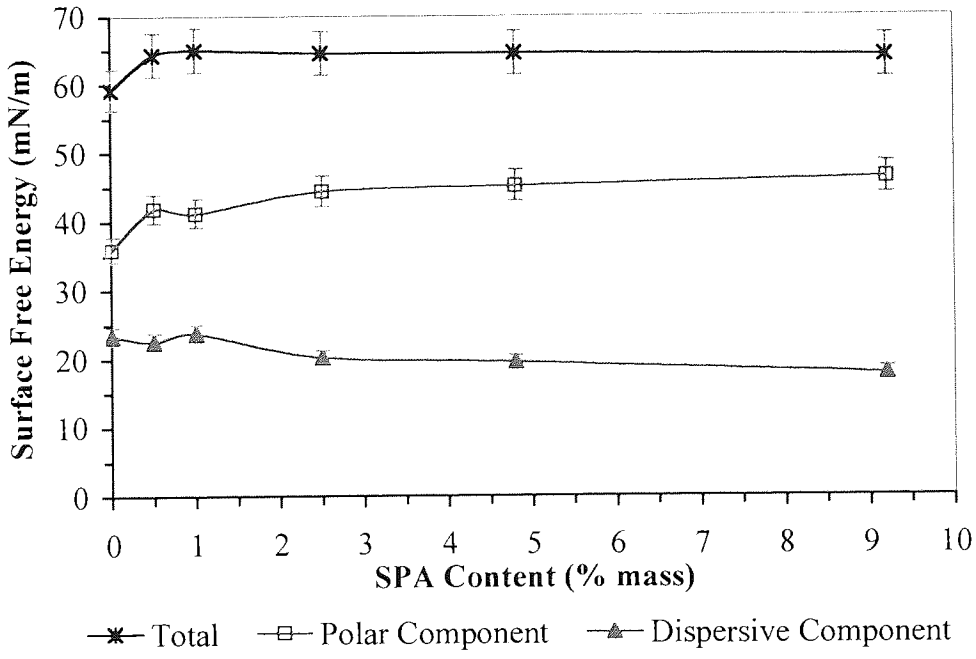

Figure 4.13 The components of surface free energy of hydrogels containing increasing amounts of SPA in the hydrated state.

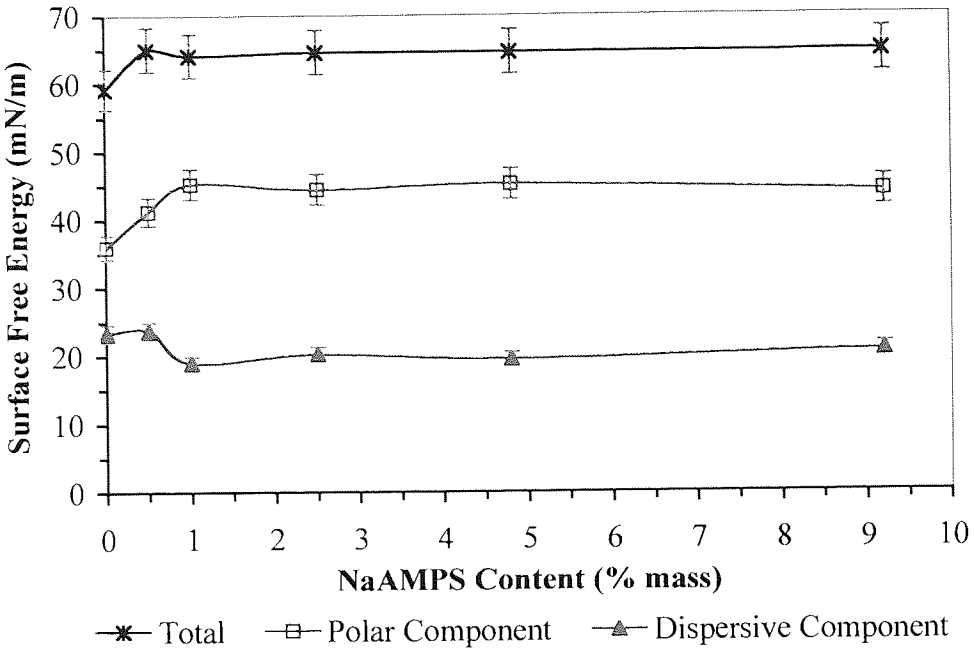

Figure 4.14 The components of surface free energy of hydrogels containing increasing amounts of NaAMPS in the hydrated state.

At levels over 1% w/w sulphonate monomer, it appears that a constant level of surface energy is achieved. Increased sulphonate concentration and likely increased presentation of sulphonate groups at the surface has not been reciprocated by increased polar components that may be ascertained by this technique. The limitations are due to the reliance on a bubble of relatively large size determining the interfacial molecular interaction of small size.

4.2.3 Mechanical Properties of Hydrated Hydrogels Containing Anionic Monomers

For each measurable property, the mechanical results for each set of sulphonate-containing monomer are plotted on the same set of axes.

Figure 4.15 shows the initial modulus of the materials varying with the ionicity of the hydrogel. The modulus indicates the degree of stiffness of the material. With increasing incorporation of a hydrophilic monomer, it would be expected that the stiffness would decrease due to an increase in the amount of plasticising, freezing water content. This is the case with all three sulphonates.

What can be seen for the profiles of the curves is that, again, SPI copolymers differ from SPA and NaAMPS. Additionally, the profile of the stiffness of SPI materials is the exact opposite of that for the water binding profile, that is, a plateau appears to be reached in the total water content and a corresponding area of stability is reached in the initial modulus of the materials. This effect is also seen in the tensile strength and elongation at break curves for SPI, in Figures 4.16 and 4.17 respectively.

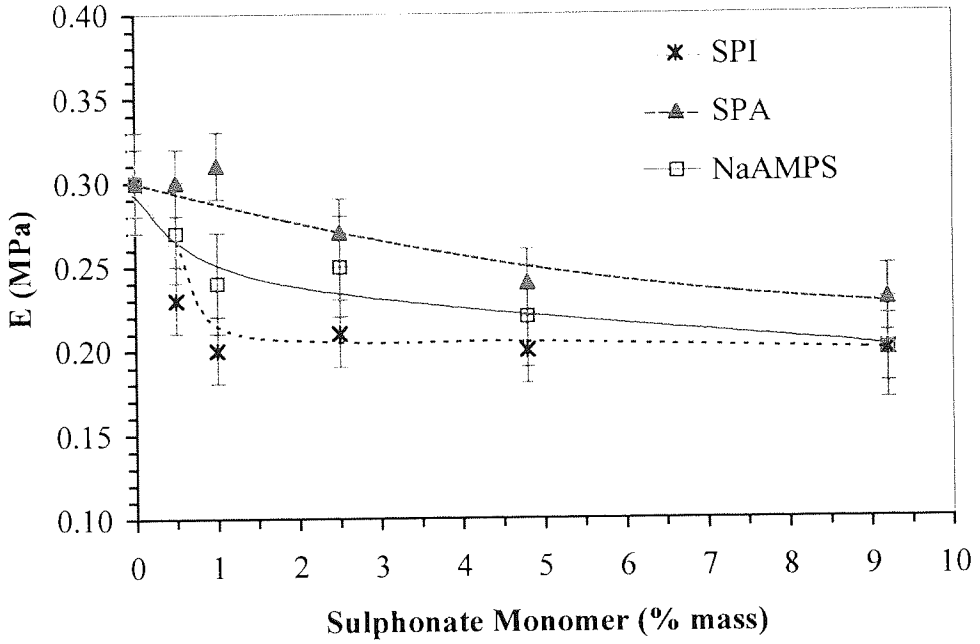

Figure 4.15 The initial modulus of hydrogels containing increasing amounts of SPI, SPA and NaAMPS.

It appears therefore that increasing amounts of SPI does not have much effect on inter-chain interactions. As the equilibrium water contents are lower than the corresponding copolymers including SPA and NaAMPS, it would have been expected that the SPI materials would have been stiffer, additionally because the presence of 3-sulphopropyl ester groups on either side of the copolymer chain would hinder chain rotation on application of a pulling force. This not being the case, the results may be an indication of poor network formation, in that where SPI is added, the chain is terminated.

SPA copolymers have similar mechanical features as NaAMPS copolymers, with mechanical properties decreasing as water content increases. For SPA, the materials show higher stiffness than NaAMPS (Figure 4.15) but for tensile strength and elongation

at break, NaAMPS materials show higher values, seen in Figures 4.16 and 4.17. As the water bonding properties are near enough equal at like for like levels of monomer inclusion, the differences must be due to structural interactions.

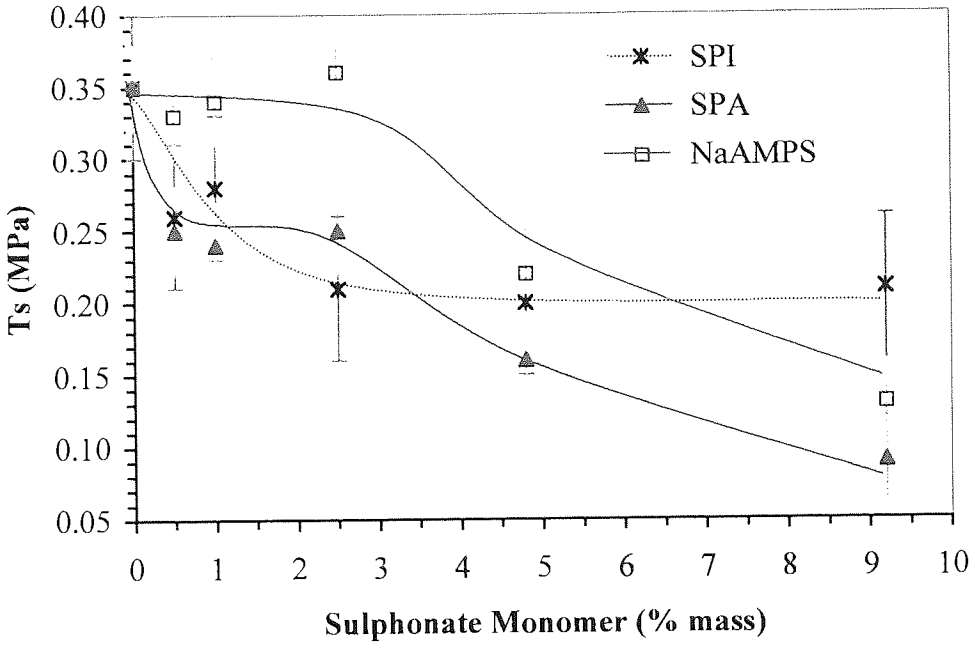

Figure 4.16 The tensile strength of hydrogels containing increasing amounts of SPI, SPA and NaAMPS.

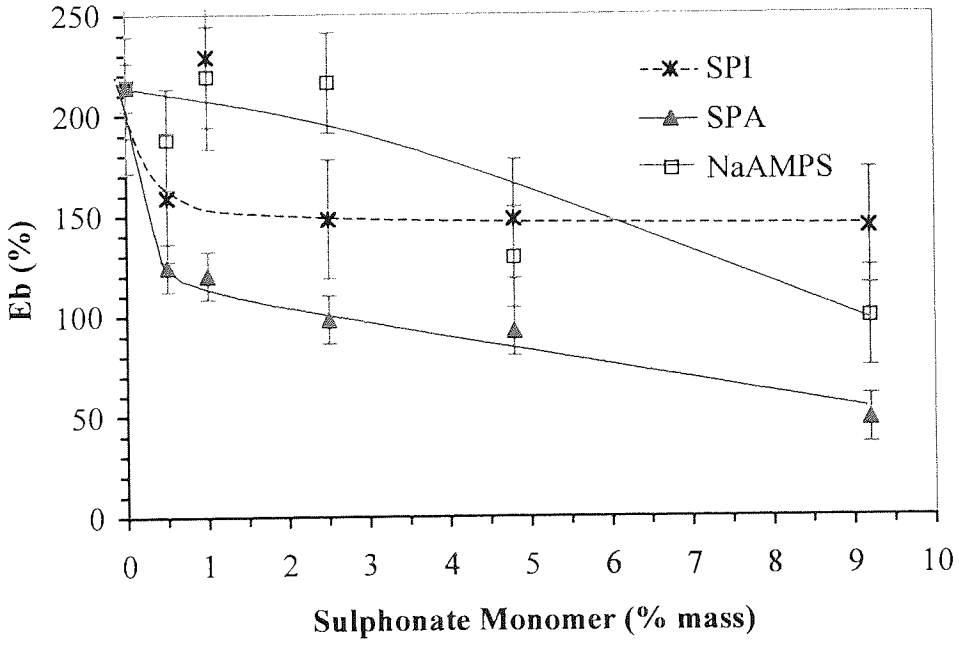

Figure 4.17 The elongation to break of hydrogels containing increasing amounts of SPI, SPA and NaAMPS.

The decreases in Ts and Eb seen with increasing SPA and NaAMPS corresponded to increasing brittleness of the materials, irrespective of the increases in plasticising water.

The ability of NaAMPS to extend further than SPA with a pulling force is postulated to be due to internal hydrogen bonding between polar groups on opposing NaAMPS molecules on different chains. This has the effect of a secondary cross-link and its structural advantage over SPA is due to the possession of a hydrogen-bonding amide bond, shown below in Figure 4.18.

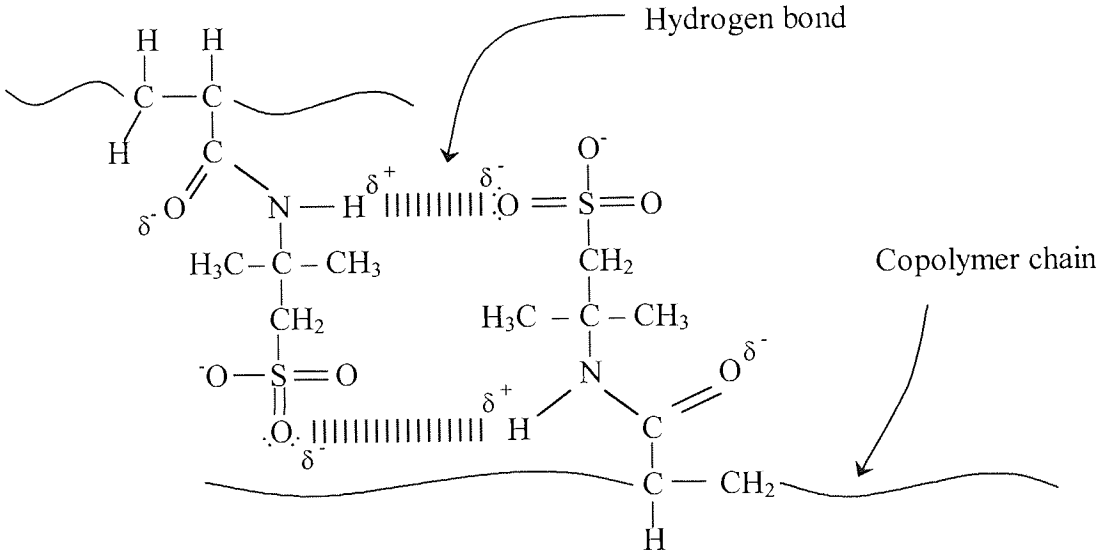

Figure 4.18 Proposed hydrogen bonding between NaAMPS molecules on opposite polymer chains.

As the copolymer chains unravel, in NaAMPS copolymers, both cross-links and hydrogen bonds are acting to maintain material integrity.

4.2.4 Spoilation Properties of Hydrated Hydrogels Containing Anionic Monomers

The popular daily disposable and weekly disposable hydrogel material Etafilcon A, is composed of HEMA and approximately 4% methacrylic acid. This material is known to attract and bind positively charged proteins from tears, in particular lysozyme. Despite this, successful wear has been achieved but not without the problems associated with high water content materials.

The Copolymer X material has also been successfully worn in eyes for about ten years. The incorporation of sulphonate monomers into this core material and its effects on the spoilation levels of both protein and lipid present in an artificial tear solution are now examined.

Figure 4.19 shows the total protein deposition on SPI copolymers. It is clear that the incorporation of charge has had a beneficial effect on total protein adsorption. This would be the effect of the negative charge electrostatically repelling the negatively charged protein albumin. However, increasing negativity causes increasing deposition, no doubt due to the attraction of the positive proteins lysozyme and lactoferrin.

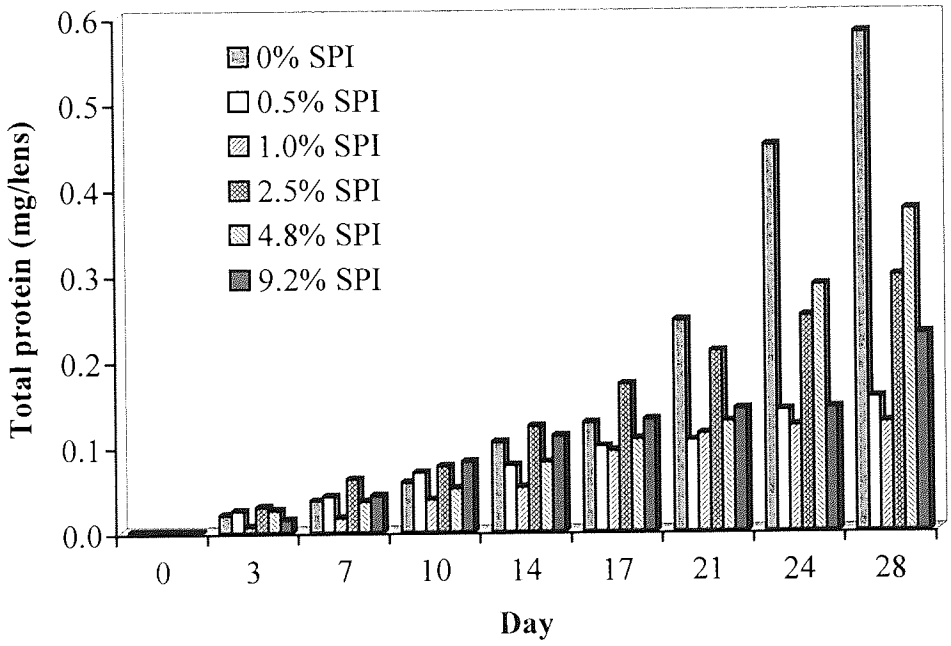

Figure 4.19 The total protein spoilation profile of hydrogels containing increasing amounts of SPI.

Similar trends are seen for both SPA and NaAMPS copolymers, in Figures 4.20 and 4.21 respectively, when incorporated up to the 2.5% by weight level. At the 4.8% level of incorporation, the hydrogels perform worse than the base material until the 28th day for SPA and 24th day for NaAMPS. No samples containing 9.2% by weight of these monomers survived the duration of the tests as the materials suffered with brittleness at such high water content.

The spoilation shows a good lag time for all three monomers, with the performance of SPI appearing to be slightly superior to the other two.

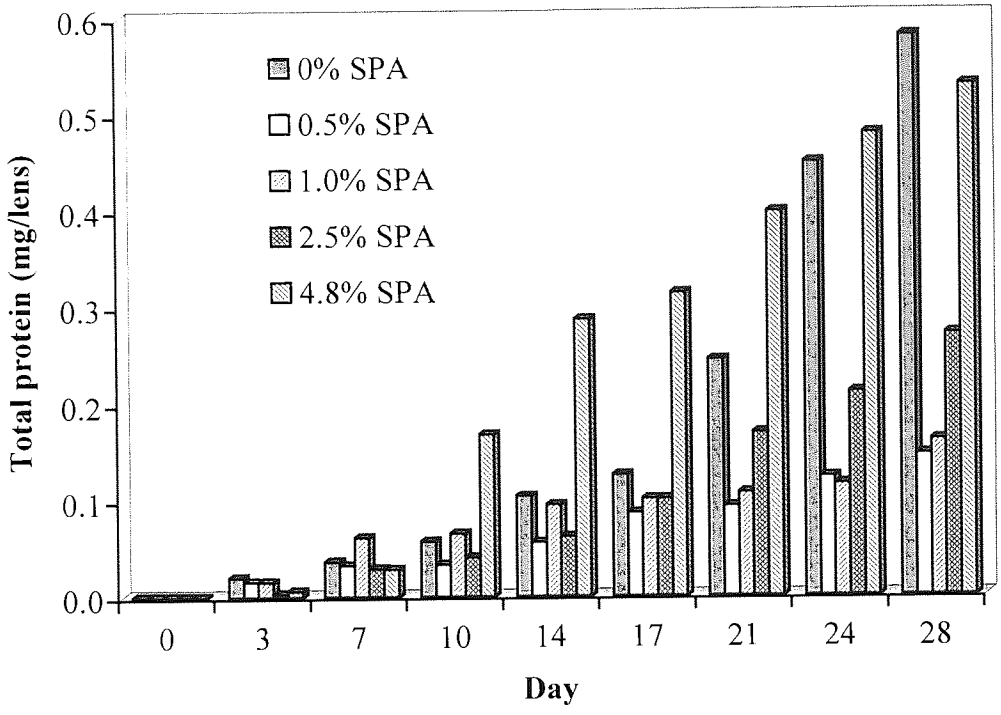

Figure 4.20 The total protein spoilation profile of hydrogels containing increasing amounts of SPA.

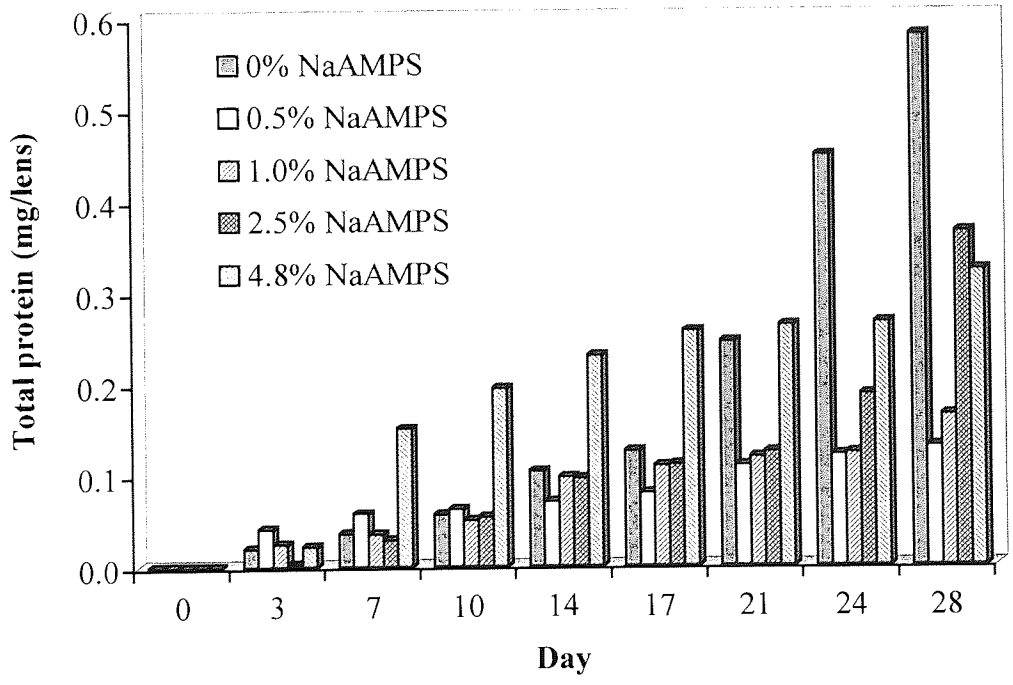

Figure 4.21 The total protein spoilation profile of hydrogels containing increasing amounts of NaAMPS.

An important fact to remember when interpreting these types of results is that the technique allows accumulation, which is not necessarily the true type of adsorption that is being investigated. To test the degree of strongly associated protein to the hydrogels, copolymers were selected for washing for about 15s in ReNu™, a soft contact lens cleaning solution from Bausch & Lomb that contains a positively charged antibacterial agent. The total protein at 28 days found in the 1.0% by weight SPI copolymer decreased by 44% and in the 1.0% by weight NaAMPS copolymer by 32%.

UV analysis provides a means to examine the total protein in and on the surface of a hydrogel and is unable to differentiate location. Fluorescence spectroscopy allows the amounts of protein to be found on the surface of the hydrogel, expressed as amount of fluorescence.

With increasing amounts of SPI, the effect on the surface protein spoilation is shown in Figure 4.22. Increasing charge is seen to increase the deposition somewhat. The difference seen between the 4.8% and 9.2% samples may have been due to temperature variations over the days of testing, as these were tested at different times.

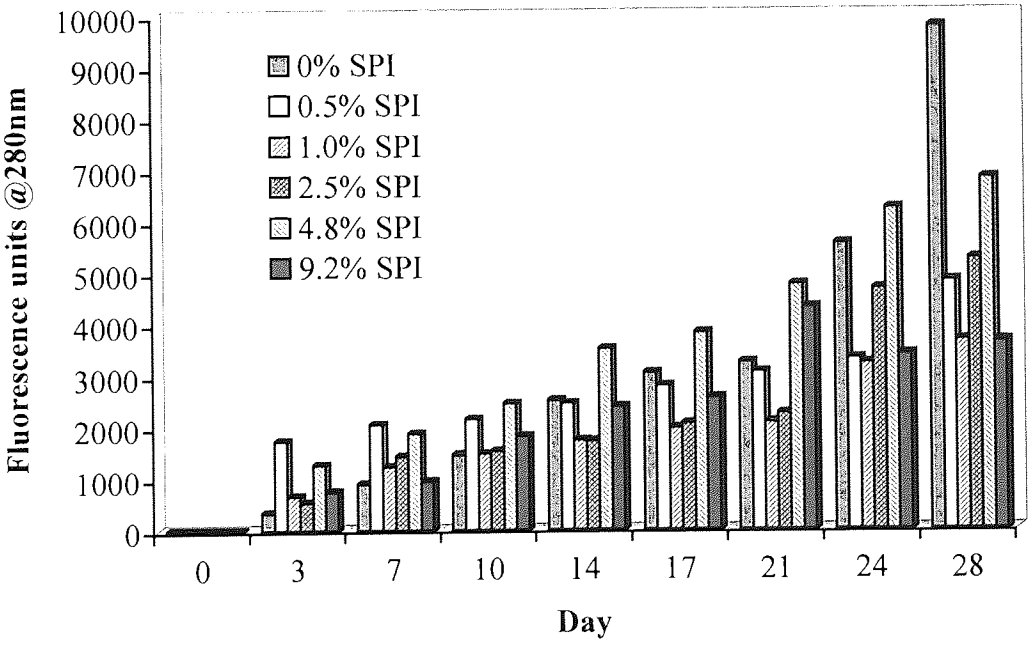

Figure 4.22 The surface protein spoilation profile of hydrogels containing increasing amounts of SPI.

Towards the later stages of the test, the copolymers incorporating charge appeared to show less spoiling in comparison to the base material. Again, the protein does not appear

to be irreversibly bound as a 15s wash in ReNu™ resulted in the fluorescence reading for the 1.0% SPI copolymer at 28 days falling by 71%.

Figure 4.23 displays the surface protein deposition for SPA copolymers. The 9.3% by weight SPA copolymer was too brittle to survive the duration of the test. The high spoilation seen with the 4.8% SPA copolymer could also be explained by sample fragility, with deposition occurring at a higher rate than expected because of surface irregularities. A SPA material was not washed and so an expected improvement cannot be shown.

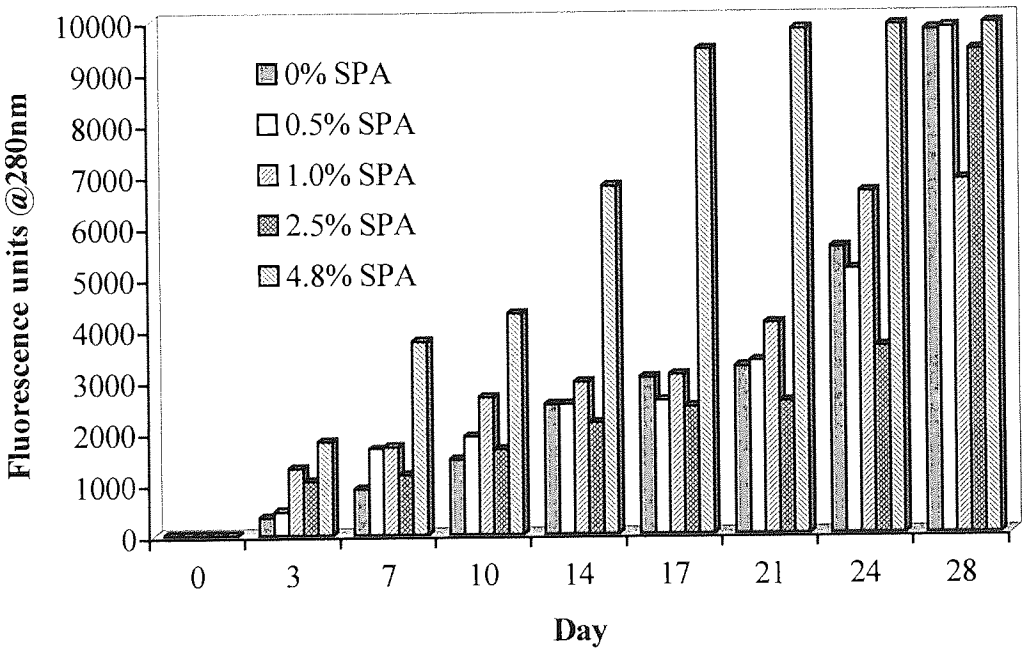

Figure 4.23 The surface protein spoilation profile of hydrogels containing increasing amounts of SPA.

The build up towards the end of the test was noticeably more than the equivalent SPI copolymers. It appears that SPI copolymers are better at resisting surface deposition than SPA copolymers. In general, the addition of SPA resulted in slightly more/less or almost the same surface deposition than the base copolymer and in contrast to the SPI materials, no clear advantage against the base material was seen at any point over the test period.

SPA copolymers have significantly higher water binding properties than SPI at the 4.8% and over, but this does not explain the SPA copolymers at below 4.8% spoiling more at the surface later in the test than the equivalent SPI copolymers. Again, SPI materials behaved in a manner different to SPA.

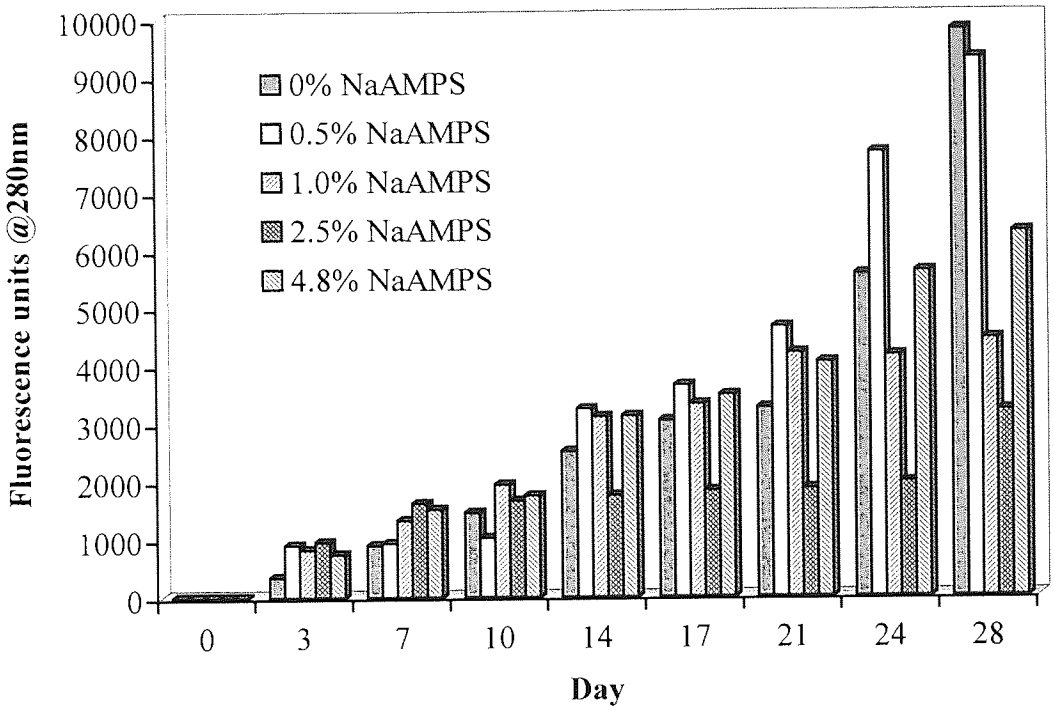

Figure 4.24 The surface protein spoilation profile of hydrogels containing increasing amounts of NaAMPS.

The surface deposition of NaAMPS copolymers, shown in Figure 4.24, shows similarities with that of SPI copolymers. At 0.5% NaAMPS, the copolymer shows more spoilation than the base material, but at higher levels of NaAMPS, the spoilation is better than with no charge towards the latter stages of the test.

Excepting the 4.8% NaAMPS material, increasing the concentration of NaAMPS appeared to decrease the surface deposition of protein, particularly after 14 days, but to say that this is a real result cannot be guaranteed due to inherent variability of the technique with enhanced accumulation rather than pure electrostatic interactions playing a significant role. The results of a clean in ReNu™ of the 1.0% NaAMPS copolymer resulted in a reduction in the fluorescence at 28 days of 29%, indicating the reversible nature of the deposition acquired.

The improved surface resistance of NaAMPS hydrogels over SPA could be due to the main structural dissimilarity – that of the amide bond present in NaAMPS. It is perhaps this structure, close to the polymer backbone and able to interact with water that causes the improvement.

The surprising levels of protein adsorption for the neutral material Copolymer X would normally have been attributed to ionicity. As HEMA is well-known to undergo a disproportionation reaction to produce methacrylic acid, poly(HEMA) will possess differing degrees of ionicity depending on the amount of acid it contains. Optical grade HEMA was used in this work in an effort to reduce the impurity, with no further purification performed. The levels of protein spoilation however, suggest that more than 2% methacrylic acid is present, a very high value of impurity, as Acuvue, with 3.8% methacrylic acid, has been found to deposit a total protein amount of about 0.55 mg/lens over 28 days. As such, accumulation rather than biological deposition was probably the main factor accounting for the result, or there was some other unknown factor acting.

Fluorescence spectrophotofluorimetry can be used to obtain comparative data on the relative degree of lipid spoilation. By applying an incident beam at 360nm wavelength, the conjugated species fluorescence and the intensity of the resultant peak determined. Conjugated double bonds are present in the majority of lipids found in tears, such as in cholesterol and cholesterol esters.

In stark contrast to the protein spoilation results, it appears from Figures 4.25 through 4.27 that the presence of sulphonate groups causes an increase in lipid deposition over the material containing no charged species. This contradicts the results obtained by Jones *et al*[91] comparing high water content non-ionic lenses and ionic contact lenses that contained methacrylic acid, with the negativity coming from carboxylate groups. In this case, the ionic lens resulted in less lipid deposition than the non-ionic material. This raises the interesting notion that the type of negativity and the size of the ionic species may have important implications in the type and degree of spoilation.

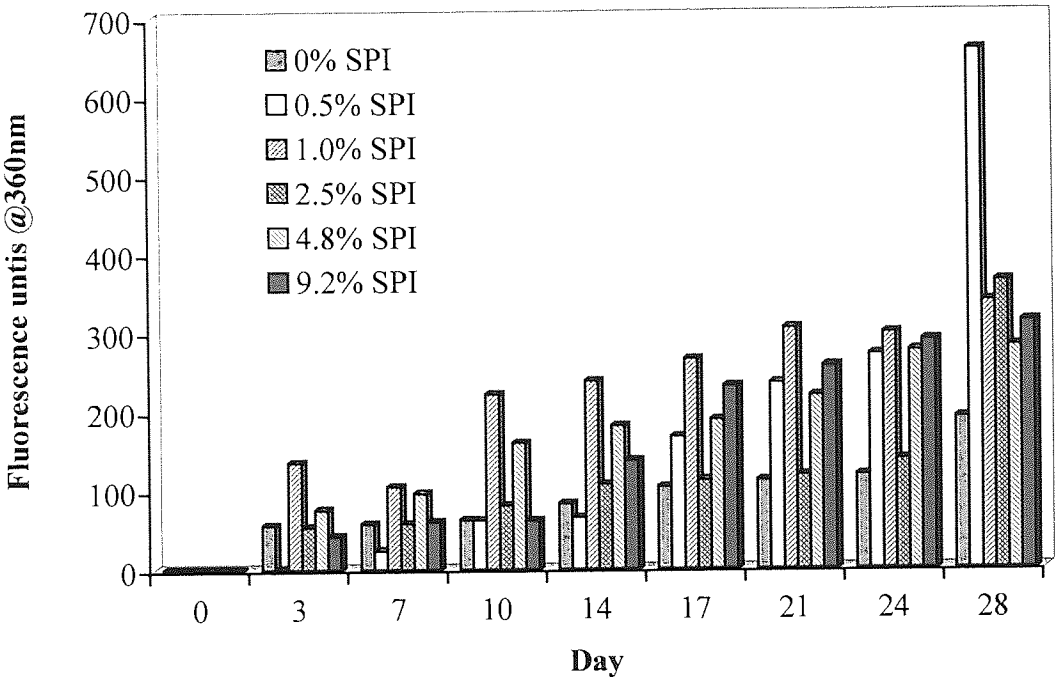

Figure 4.25 The surface lipid spoilation profile of hydrogels containing increasing amounts of SPI.

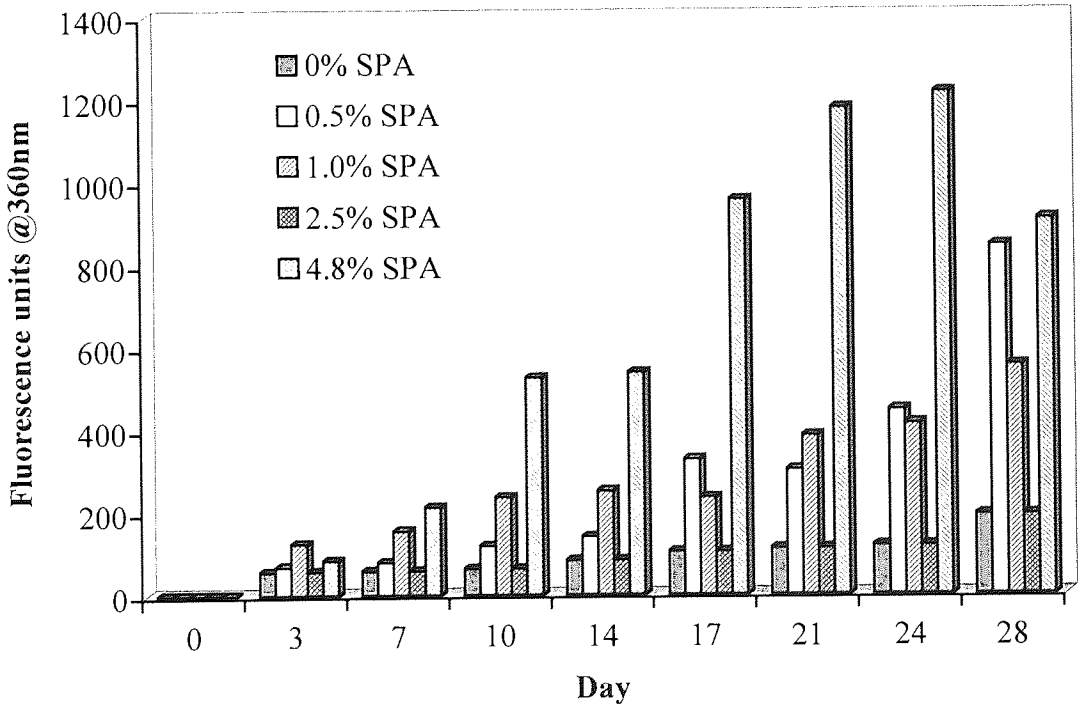

Figure 4.26 The surface lipid spoilation profile of hydrogels containing increasing amounts of SPA.

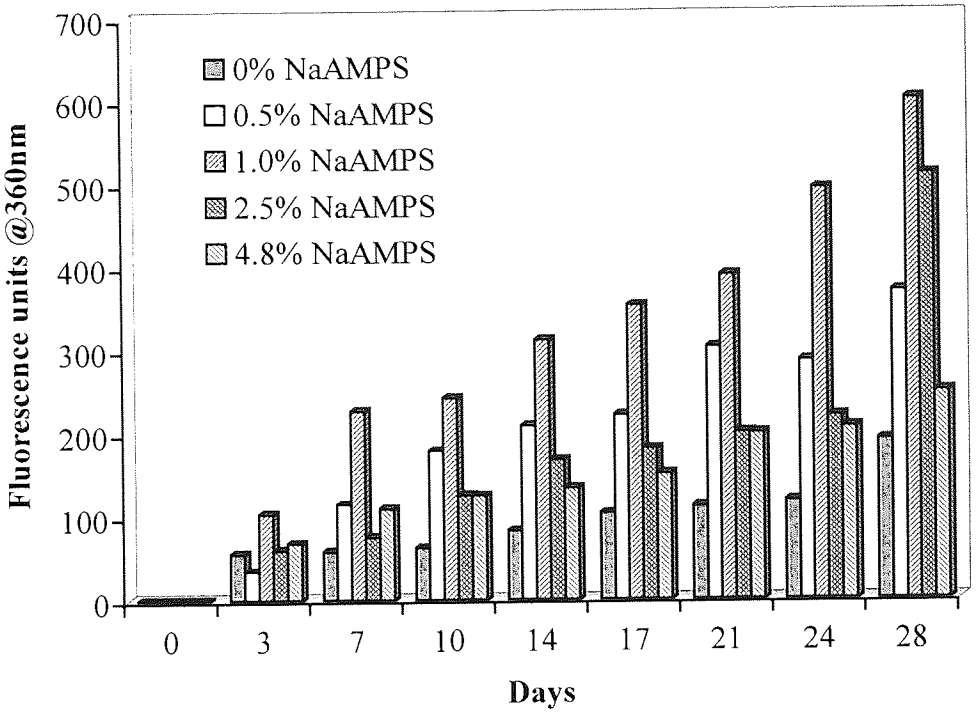

Figure 4.27 The surface lipid spoilation profile of hydrogels containing increasing amounts of NaAMPS.

It can also be seen that increasing the concentration of sulphonate monomer has a tendency to decrease to deposition typically at levels over 1.0% by weight. The lipid deposition at all levels of incorporation however remains higher than the neutral base copolymer. Again, the exception is the 4.8% SPA copolymer, for reasons stated earlier (i.e. fragility).

It could be that an optimum degree of charge exists for optimal lipid deposition to a hydrogel surface. At levels below and above this, either the non-ionic features of the other comonomers or the increased hydrophilicity and wettable surface resulting from the increasing sulphonate concentration and expression act in a manner that is not pro-lipid deposition.

The reversible nature of this deposition was again demonstrated when a wash in ReNu™ caused the surface lipid spoilation of SPI and NaAMPS at the 1% level, on the 28th day, to fall by 53% and 18% respectively.

4.3 Conclusions

The addition of sulphonate monomers to a non-ionic core material has significantly increased the hydrophilicity of the resultant hydrogels. The hydrophilicity series for the sulphonate monomers investigated has been found to be:

$$SPI < NaAMPS < SPA$$

A consequence of the high water contents reached at the highest level of SPA and NaAMPS incorporation is a corresponding decrease in mechanical properties, an inherent problem associated with hydrogels. However, NaAMPS appears to retain its elasticity and stiffness to a better degree than SPA by virtue of internal hydrogen bonding that has been postulated earlier.

The unexplainable differences between SPI and SPA, mono- and bi-functional sulphonates respectively, do not lend themselves to experimental error and the mechanical trends for SPI support the water binding properties, i.e., as the concentration of SPI increases, stiffness decreases as water content increases and then stiffness remains relatively constant as water content stabilises. Even though the monomers were added at equal weight percents, the higher molecular weight of SPI and dual charge meant that almost equal levels of sulphonate groups were present for each comparable copolymer. Obviously, the distribution and molecular conformations would be different and have had clear effects on the copolymer properties. The precise molecular implications of SPI in hydrogels have yet to be revealed.

The surface properties for the copolymers were all of a similar magnitude, with the water content and the presence of ionic species and not so much the concentration of ionic species being the deciding factors in the size of the total surface energies. This is shown graphically in Figure 2.8. The concentration of sulphonates is shown to have a small effect on the fine detail of surface energy which is water-binding driven. Increasing hydrophilicity through higher amounts of freezing water causes a natural increase in the polar component of surface free energy and a consequential fall in the dispersive component.

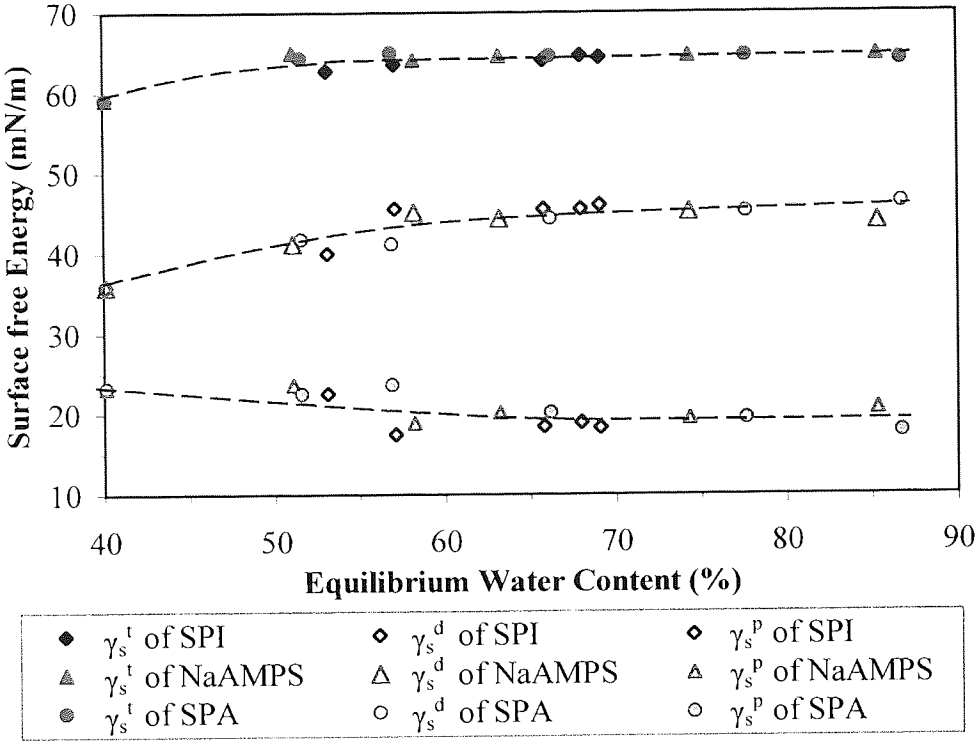

Figure 4.28 The equilibrium water content of the sulphonate-containing hydrogels vs. the surface free energies and their components.

The addition of sulphonate monomers has been show to cause lower levels of protein deposition than the non-ionic base material, with spoilation increasing with increasing sulphonate concentration. The levels of total protein spoilation for all materials over 28 days typically fall about 0.2 ± 0.1mg/lens, without cleaning. Figure 4.29 shows the average total protein spoilation for daily wear lenses worn on an extended wear basis by patients using the ReNu™ cleaning system[92,93]. The materials include HEMA, HEMA and methacrylic acid copolymer (Acuvue) and HEMA, poly(vinyl alcohol) and methacrylic acid copolymer (Focus). As can be seen, Acuvue (Etafilcon A) shows an average protein deposition of approx. 0.52 ± 0.15mg/lens, with cleaning.

The charge on a sulphonate group is a much larger and more polar entity than the charge that would be found on a carboxylate group. With this in mind, hydration shells would form around the sulphonates, with the water in the immediate vicinity of the charge being more strongly associated to the sulphonate than the water towards the outer edge of the shell.

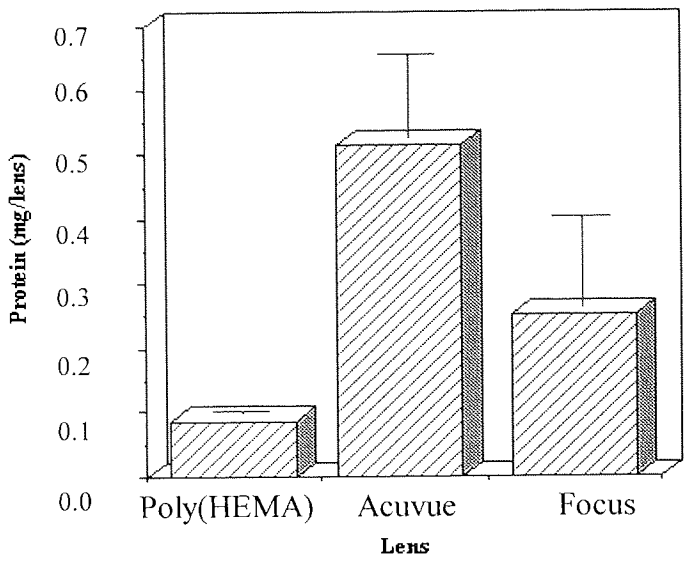

Figure 4.29 Average total protein spoilation for some daily wear lenses worn on an extended wear basis by patients using the ReNu™ cleaning system.

With this range of water association, more dynamic exchange would be expected to occur which would result in more dynamic exchange of adsorbing proteins. Sulphonate-containing copolymers would therefore be expected to show less deposition than carboxylate copolymers and this appears to be the case. Conversely, there is evidence that sulphonate monomers attract more lipid than do carboxylate monomers as incorporating methacrylic acid has been shown to show lower amounts of lipid deposition, as shown in Figure 4.30. Sulphonate monomers in this work results in lipid deposition that exceeds that of the 0% sulphonate material.

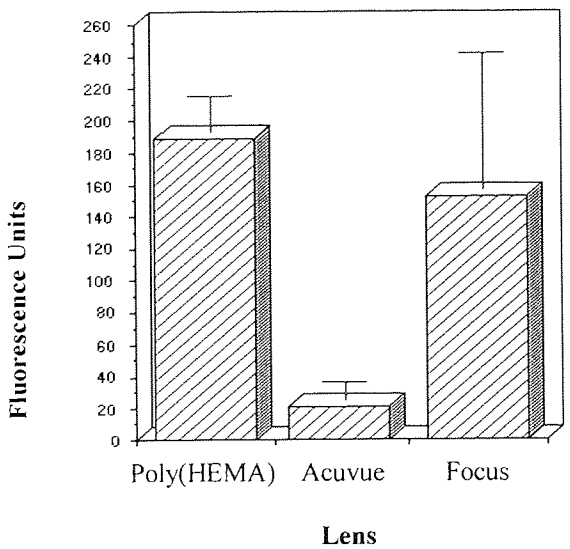

Figure 4.30 Average surface lipid deposition of selected daily wear lenses worn on an extended wear basis, using the ReNu™ cleaning system.

CHAPTER 5

Hydrogels Containing Anionic And Cationic Monomers

"It is better to know nothing
than to know what ain't so."
Henry Wheeler Shaw (Josh Billings),
1818-1885, Proverb.

5.1 Introduction

It well known that the high water/ionic lens material Etafilcon A based on HEMA and 5% methacrylic acid adsorbs large amounts of protein, predominantly positively charged lysozyme.

Work described in the previous chapter has indicated that the incorporation of sulphonate monomers to produce high water content ionic hydrogels does not show detrimental protein deposition over the non-ionic material based on HEMA/NVP/MMA/MPEGMA. In fact, protein deposition was reduced substantially at levels up to 2.5% by weight of sulphonate compared to the lower EWC non-ionic hydrogel.

At Aston, French[94] showed that low levels of cationicity in poly(HEMA) hydrogels could reduce the deposition of positively charged proteins without adversely affecting the uptake of other proteins. The basic monomers investigated were N-vinyl imidazole (NVI) and dimethylaminoethyl methacrylate (DMAEMA). When entered into the reactivity ratio equations, NVI was less reactive to vinyl polymerisation than DMAEMA and from Table 5.1, it can be seen that the Q and e values for DMAEMA are very similar to those of methyl methacrylate (MMA) which has been shown to alternate with HEMA and NVP in Figure 4.3.

Monomer	Q value	e value
Methyl Methacrylate	0.78	0.40
N-Vinyl Imidazole	0.11	-0.68
Dimethylaminoethyl Methacrylate	0.68	0.48

Table 5.1 Q and e values for MMA, NVI and DMAEMA.

The cyclic nature of NVI is shown in Figure 5.1 and this could increase the strength of a hydrogel because of its bulky nature restricting chain rotation. Levels of NVI or DMAEMA up to 20% by weight were added to materials and the deposition results did not discount their use in biomaterials. The small amount of literature on cationic hydrogels for biomaterials stems from the fact that nature tends to negativity with, for example, the internal cell wall of blood vessels carrying a negative charge.

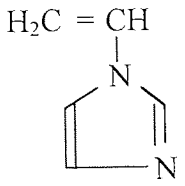

Figure 5.1 The structure of NVI.

Other basic monomers have been added to HEMA/AMO copolymers. Of the five tested from NVI, DMAEMA, pyridine-N-oxide, 4-vinyl pyridine and dimethylaminoethyl acrylate, DMAEMA resulted in the most hydrophilic copolymer and as a result showed the most variation in mechanical properties. DMAEMA also showed a lower hysteresis than the structurally similar DMAEA by virtue of its α-methyl group restricting the chain mobility.

The type of charge present in a hydrogel copolymer would affect the type and degree of protein deposition. As the negative charge of methacrylic acid is well-known to adsorb large amounts of lysozyme and cationicity has been shown to decrease the adsorption of positively charged proteins, the effect of anionic and cationic monomers in the same material would be of interest, particularly if an optimal charge balance could be attained for minimal deposition.

Specific protein deposition studies show that charge alone does not dictate the degree of spoilation and sensitivity to ionicity, but that size and the resulting charge density play important parts. A wash in ReNu for protein-specific, spoiled materials has shown that the high charge density of the negative protein ferredoxin made it the most difficult protein to remove. The high charge density of positive lysozyme made it the least deposited protein, before the levels of the lower charge density of positive lactoferrin. As ReNu also contains a positive charged antibacterial agent, this would be expected to adsorb to an anionic surface[95] and subsequently modify it when such a lens material is washed prior to insertion and so a dual charge would exist on the material.

Although the monomers added are basic, the potential to show basicity is determined by the pH of the hydrating medium. As the pH of the distilled water is about 6.2, whilst having no formal charge, the monomers are able to show a degree of ionicity. Because of this, when monomers such as NVI and methacrylic acid were added to poly(HEMA),

even small amounts of the acid were able override the contribution made by NVI to spoilation. Water acts as a protic acid and donates a proton to the amine that then allows the protonated nitrogen atom to express a positive charge.

The sulphonate hydrogels showed good potential as biomaterials in the previous chapter, as the charge did not cause an increase in protein deposition, probably due to the lower charge density of the sulphonate moiety and the size causing more layers of hydrating water. This is in comparison to the high charge density of methacrylic acid and the smaller size of the hydrating shell, which would be expected to result in higher adsorption (although directly comparable materials were not investigated here).

As such, in an effort to investigate the effect of adding a basic monomer to sulphonate containing copolymers was made by incorporating DMAEMA and the resulting copolymers characterised.

5.2 Results and Discussion

Dimethylaminoethyl methacrylate (DMAEMA) was added in increasing amounts to the core Copolymer X composition also containing 2.5% by weight of a sulphonate monomer; SPI, SPA or NaAMPS. The ratio of the cationic DMAEMA to the anionic sulphonate monomer is shown below in Table 5.2 for each amount of DMAEMA added.

Weight of DMAEMA added (%)	Mole % of DMAEMA (per monomer repeat unit)	Molar ratio DMAEMA:Sulphonate monomer		
		SPI (Mol% = 0.8)	SPA (Mol% = 1.4)	NaAMPS (Mol% = 1.5)
0.25	0.2	1 : 4.00	1 : 7.00	1 : 7.50
0.5	0.5	1 : 1.60	1 : 2.80	1 : 3.00
1.0	0.9	1 : 0.89	1 : 1.56	1 : 1.67
2.0	1.8	1 : 0.44	1 : 0.78	1 : 0.83
3.0	2.7	1 : 0.30	1 : 0.52	1 : 0.56
4.0	3.6	1 : 0.22	1 : 0.39	1 : 0.42

Table 5.2 The molar ratios of anionic and cationic monomers added to hydrogels.

The dominant charge (in terms of mole incorporation) is indicated along the top region of the graphs that follow. For each molecule of SPI, two charges are designated.

5.2.1 Water-Binding Properties of Hydrogels Containing Anionic Sulphonate Monomers With Increasing Amounts of DMAEMA

The increasing addition of DMAEMA to sulphonate-containing hydrogels generally had the effect of decreasing the EWC of the copolymers, initially at a high rate and then with much smaller decreases on higher levels of integration. This smaller effect corresponded to the materials where the cationic charge was potentially the dominant charge (in terms of quantity) in the material.

Although adding an ionic monomer increased the total ionicity of the material, this ionicity was obviously not reciprocated by an increase in the EWC. As such, internal interactions between negative and positive groups acting as internal cross-links, would be restricting chain mobility and so reducing the volume available to plasticising water.

In the SPI copolymer, a reduction of over 10% was seen in the EWC where DMAEMA is added up to 1% by weight, shown in Figure 5.2. These hydrogels, assuming that both ionic species are carrying a charge, contain more molar amounts of negative charge than positive, although more moles of DMAEMA are present than SPI at 1%, as seen from Table 5.2. The copolymers with 2%-4% DMAEMA showed decreasing EWC but very gradual. The major driver for the change in the EWC observed was clearly the reduction in the amount of freezing water and subsequently the non-freezing water was seen to be gradually increasing.

The two curves for freezing and non-freezing water, converge rapidly up to 1% DMAEMA and then more gradually, but do not meet over the range tested. This trend is seen for the SPA and NaAMPS materials also, with a small exception on the outset of DMAEMA addition and will be discussed in a moment.

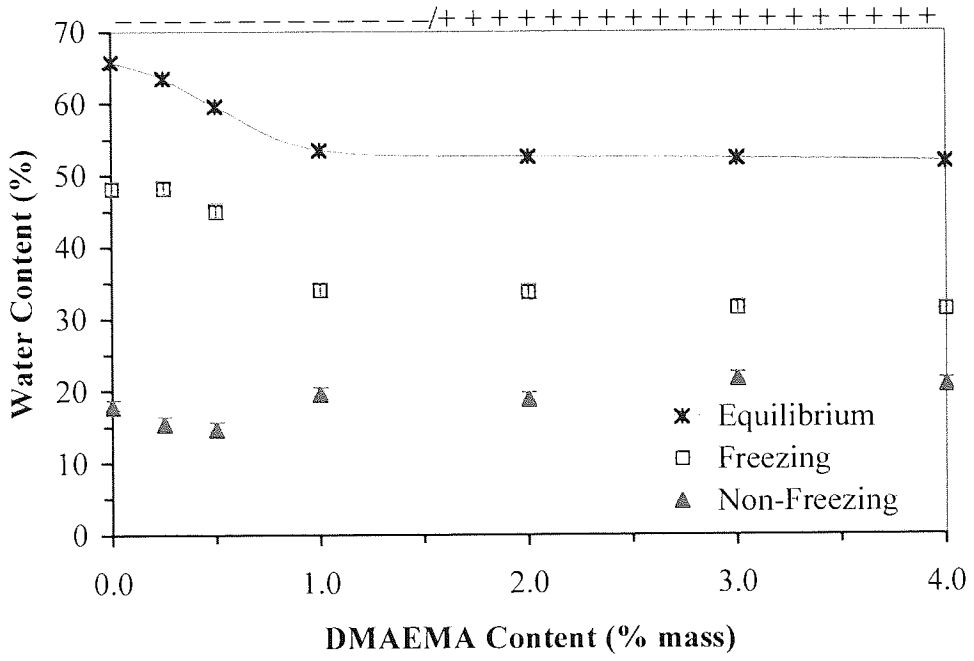

Figure 5.2 The water-binding properties of hydrogels containing 0.8 mol% SPI and increasing amounts of DMAEMA.

For both SPA and NaAMPS copolymers, it can be seen in Figures 5.3 and 5.4 respectively that the EWC increases on addition of 0.25% by weight of DMAEMA and subsequently decreases from that point onwards, rapidly up to 2.0% and more slowly thereafter. Because the increase occurred in two separate series, it is more likely to be a real effect. The increase in the freezing water and decrease in non-freezing water were the individual components accounting for this rise.

A possible reason for this could be the effect of a small amount of positive DMAEMA on the sodium ion associated with the negative sulphonate. A small amount of the cationic monomer could have resulted in a decrease in the charge shielding around the sulphonate charge allowing more water to cluster around the charge and increase the water content.

The SPA and NaAMPS copolymers including DMAEMA were of higher EWC than the equivalent SPI copolymers, for levels of DMAEMA up to and including 1% by weight. Over this amount, all of the sulphonate-containing monomers had almost identical water-binding properties.

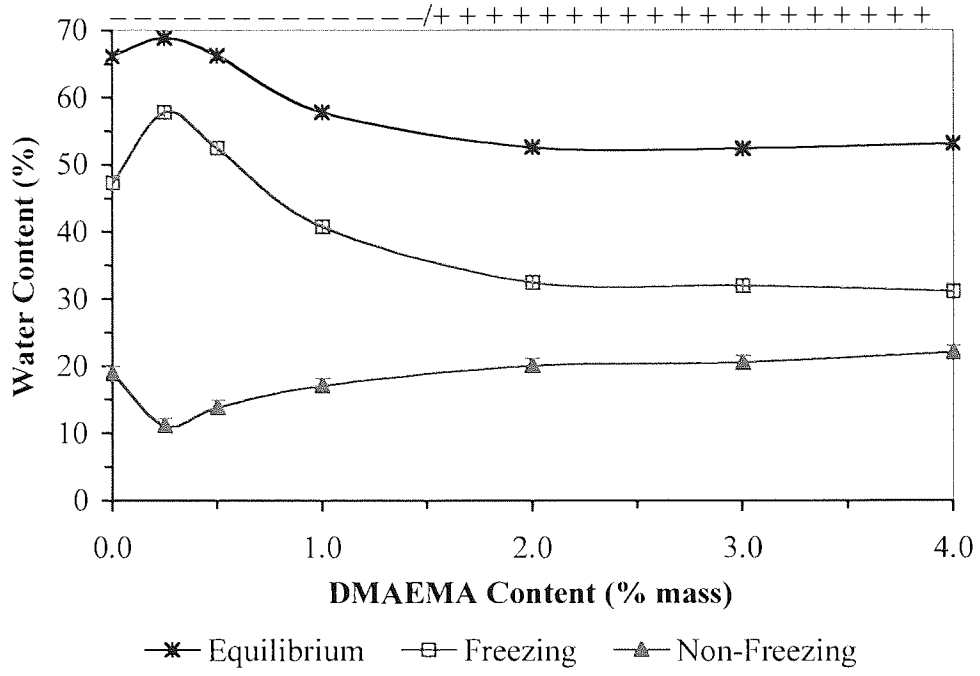

Figure 5.3 The water-binding properties of hydrogels containing 1.4 mol% SPA and increasing amounts of DMAEMA.

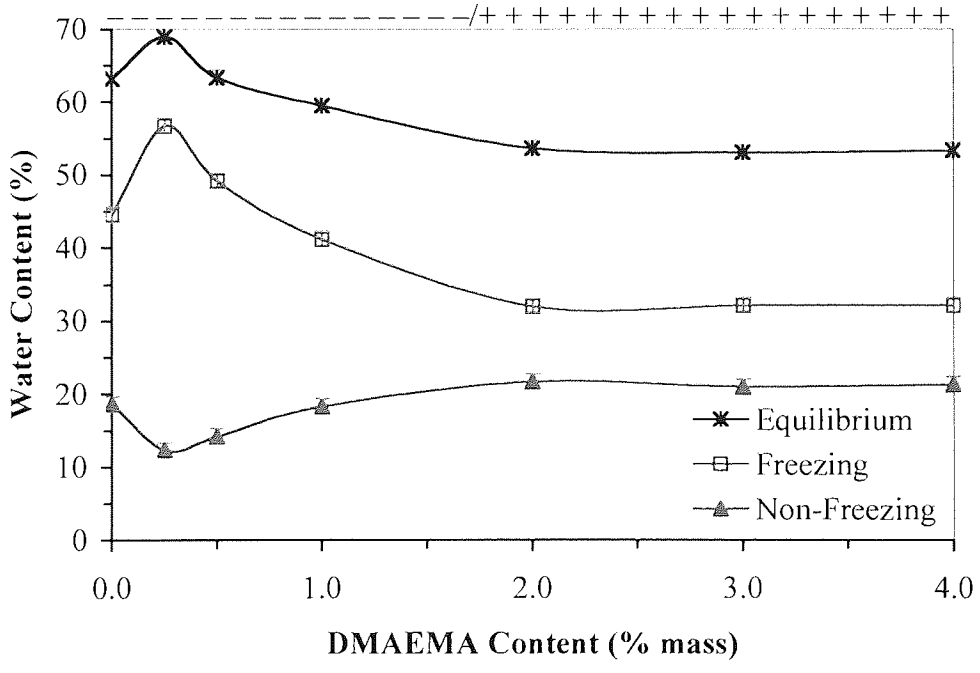

Figure 5.4 The water-binding properties of hydrogels containing 1.5 mol% NaAMPS and increasing amounts of DMAEMA.

The molecular account of wettability is seen in Figures 5.5 through 5.7, where moles of water per mole of monomer unit for SPI, SPA and NaAMPS-based copolymers with increasing DMAEMA are shown.

The small increase seen in the non-freezing water content with increasing DMAEMA is a result of a secondary product of measured total water content and measured freezing water content. In the following figures, it is clear that the moles of non-freezing water per mole of monomer repeat unit for each sulphonate-containing material do not change significantly but do creep slowly upwards and that the sulphonate monomers are themselves similar in their behaviour.

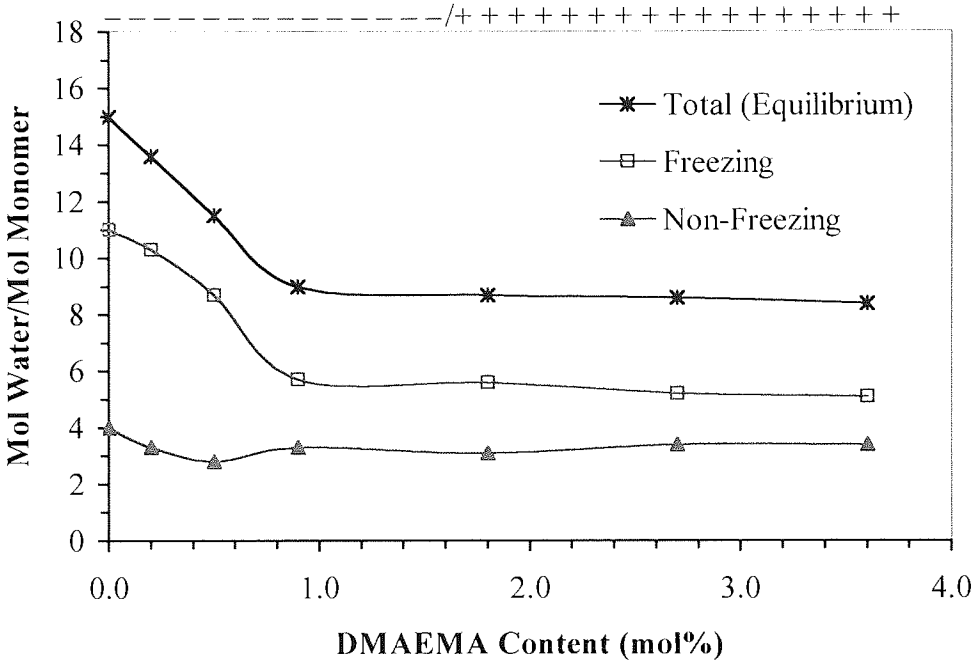

Figure 5.5 The water-binding properties expressed as per mol of monomer repeat unit of hydrogels containing 2.5% w/w SPI and increasing amounts of DMAEMA.

SPA is generally more hydrophilic in the region up to 0.5 mol% DMAEMA, although NaAMPS is very similar, in line with the behaviour seen in the previous chapter. At 0.9 mol% DMAEMA and over, virtually the same total water, freezing water and non-freezing water moles per mole of repeat unit are obtained across all three material groups for each level of DMAEMA. This is indicative of the similarity of the sulphonates and the action of the cation on them. Why the increase is not seen in SPI copolymers must have something to do with the molecule carrying a charge on either side of the copolymer chain and the charge distribution.

Charge shielding has been proposed as a reason for the initial rise in the freezing water and total water content. Post this effect, whilst DMAEMA may not carry a formal

charge, there is at least a charge-dipole interaction that results in a decrease in inter-chain space and a fall in the EWC.

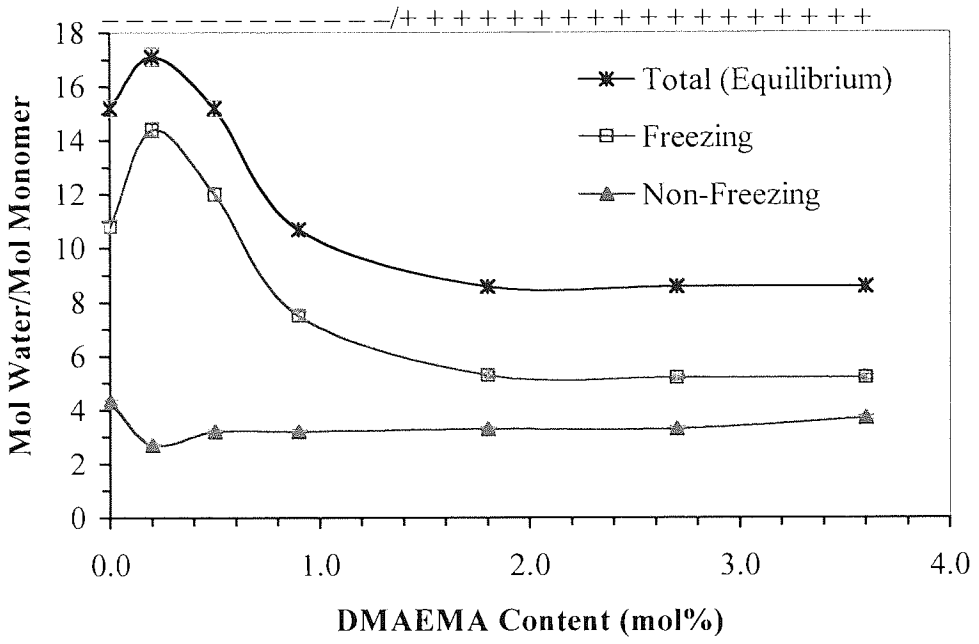

Figure 5.6 The water-binding properties expressed as per mole of monomer repeat unit of hydrogels containing 2.5% w/w SPA and increasing amounts of DMAEMA.

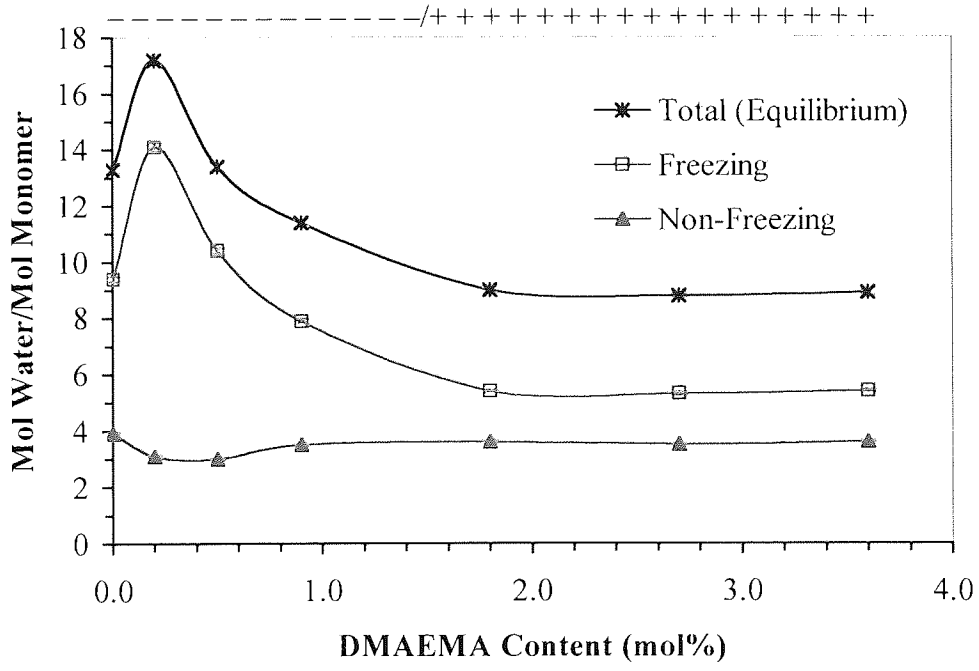

Figure 5.7 The water-binding properties expressed as per mole of monomer repeat unit of hydrogels containing 2.5% w/w NaAMPS and increasing amounts of DMAEMA.

In terms of size, the charge on DMAEMA is of a much reduced size than the one on a sulphonate moiety. As the amount of sulphonate in each copolymer stays the same, after a certain point, the effect of the sulphonate on the hydrophilicity is in effect neutralised. However, the surplus DMAEMA does not then increase the hydrophilicity significantly (in the range tested) because of one or both of the following possibilities:

- The molecules are only partially ionised and the effects on hydrophilicity would only be seen at higher levels of incorporation.
- Over 0.9 mol% of DMAEMA, any additional DMAEMA could interact with the sulphonates groups that already had interacting DMAEMA molecules (i.e. sharing), because of the large size of the sulphonate charge compared to the small/partial positive charge.

5.2.2 Surface Free Energy Properties of Hydrated Hydrogels Containing Anionic and Cationic Monomers

The increasing addition of DMAEMA to the SPI-copolymer can be seen in Figure 5.8 to cause a small increase over the range in the total free energy, driven by the change in the polar component. This would be expected, as the ionicity of the material would be increasing.

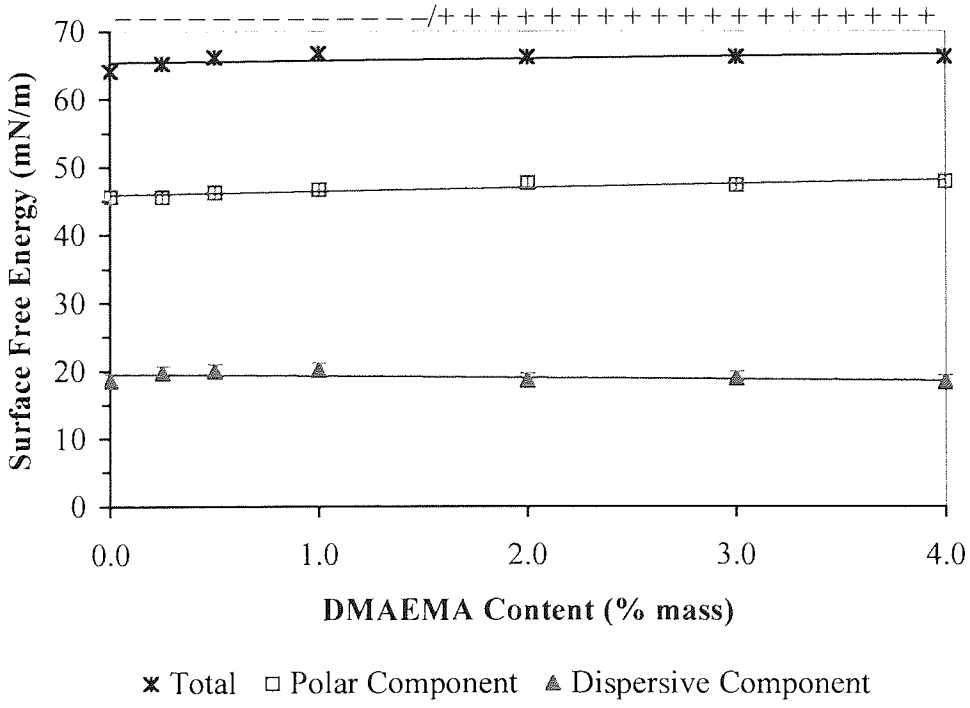

Figure 5.8 The components of surface free energy of hydrogels containing 2.5% w/w SPI and increasing amounts of DMAEMA in the hydrated state.

Examining the fine detail, slight movements in free energy are visible. Whilst the sulphonate groups are present in excess of the molar amounts of DMAEMA, the total, polar and dispersive components of surface free energy all increase. Where DMAEMA becomes present in excess, increasing amounts cause very little change in the free energies. Bulk changes are clearly not reflected in a similar magnitude with measurable surface properties.

The surface free energy components for SPA-based copolymers incorporating DMAEMA are shown below in Figure 5.9. With increasing cation, the total free energy remains fairly constant, with the polar component increasing marginally and the dispersive component decreasing marginally, again a result of increasing ionicity, particularly in the initial stages of addition where the total water content increases.

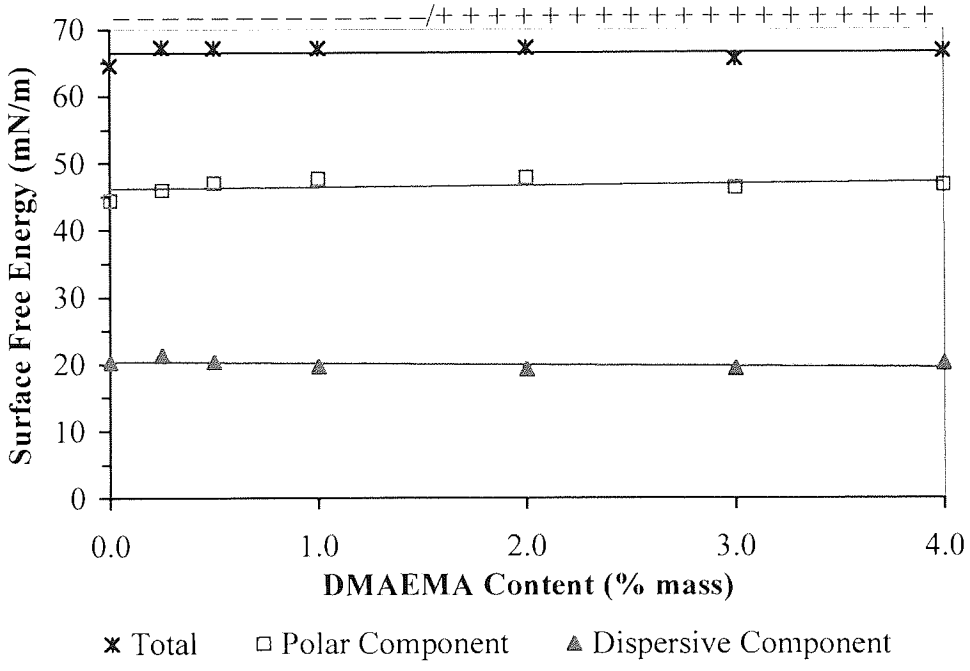

Figure 5.9 The components of surface free energy of hydrogels containing 2.5% w/w SPA and increasing amounts of DMAEMA in the hydrated state.

Figure 5.10 shows the surface free energy components for NaAMPS-based copolymers incorporating DMAEMA. Again, the total surface free energy remains fairly constant, as do the polar and dispersive components, irrespective of the ionic component. A small increase in the total and polar components is seen at low levels of DMAEMA additions, corresponding to the initial increase seen in the water content of the materials.

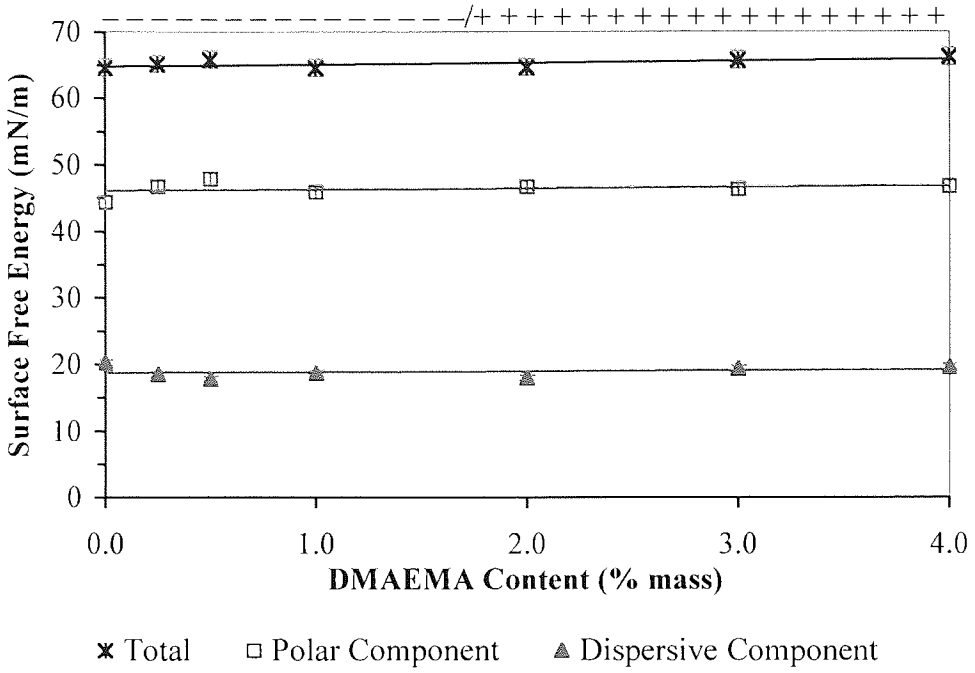

Figure 5.10 The components of surface free energy of hydrogels containing 2.5% w/w NaAMPS and increasing amounts of DMAEMA in the hydrated state.

The surface energy of the SPI/DMAEMA hydrogels show more variability depending on the degree of cationic monomer than do SPA and NaAMPS hydrogels containing DMAEMA, increasing the surface energy as ionicity increases. SPA and NaAMPS are less sterically hindered about the polymer backbone and so may be able to find a more electrostatically favourable conformation where a cation is present, easily changing when more cation is added so that a detectable change in the ionicity using the given techniques is not possible.

The water-binding properties of the hydrogels appear to have more effect on the surface properties of the ionic hydrogels, rather than the individual ionic components. The values for γ_s^t, γ_s^p and γ_s^d for DMAEMA hydrogels at all levels of incorporation are similar to the values for the 2.5% w/w sulphonate copolymer without DMAEMA.

5.2.3 Mechanical Properties Of Hydrogels Containing Anionic and Cationic Monomers

The presence of cations and anions is the same material would be expected to interact and the water-binding properties appear to support this assumption. Such interactions would also be expected to have an effect on the mechanical properties of the copolymers.

Figure 5.11 shows the initial stiffness of the three different sulphonate copolymers with increasing amounts of DMAEMA. In general, all three sets show the same type of behaviour. A suggestion made earlier in this chapter that a small amount of positive charge disrupts the network and causes the amount of plasticising freezing water to increase with respect to the non-freezing water, without introducing retractive forces, would also account for the sharp fall in the stiffness of the material on low addition of the cationic monomer due to increased mobility. The fall is of larger magnitude in the SPA and NaAMPS copolymers because the addition of DMAEMA caused an increase of over 10% in the freezing water component, increasing the mobility of the chains and so decreasing the stiffness more. Retractive forces begin to act on further DMAEMA addition, so increasing the modulus of the materials.

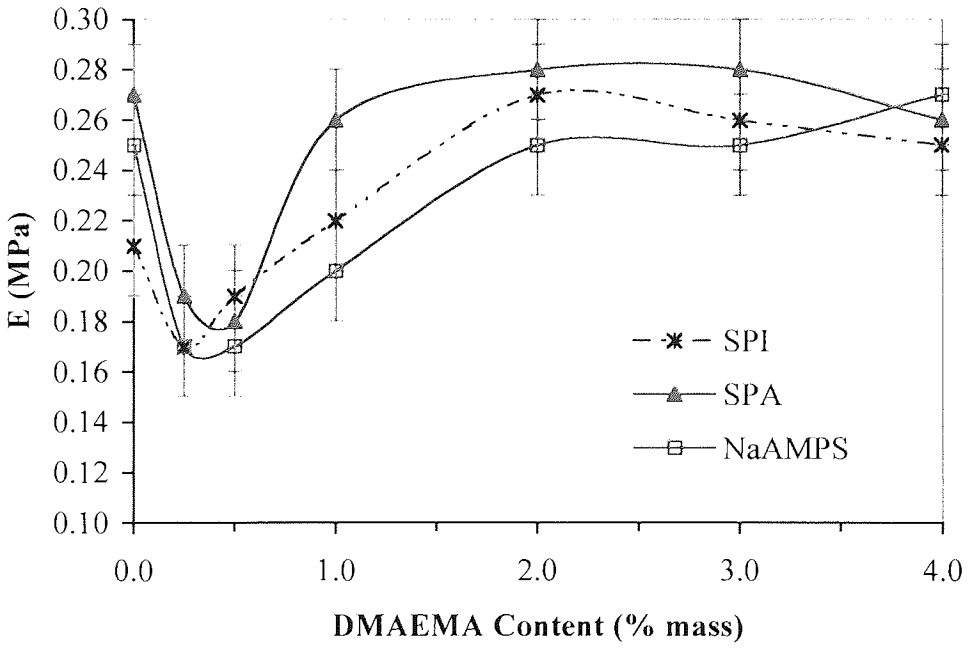

Figure 5.11 The initial modulus of hydrogels containing 2.5% w/w SPI, SPA and NaAMPS and increasing amounts of DMAEMA.

This demonstrates again that although SPI materials contain the same amount of charge as SPA materials, because the charge distribution is different, certain properties reflect

this difference. SPA is less sterically hindered about the polymer backbone than SPI and may be able to achieve more preferential conformations because of it.

NaAMPS shows a lower stiffness than the other two sulphonates with DMAEMA possibly because the cation not only interacts with the sulphonate charge, but also disrupts the hydrogen bonding possible between opposing NaAMPS molecules.

The tensile strength and elongation to break properties for the copolymers are shown in Figures 5.12 and 5.13 respectively. The SPI materials are fairly similar in their tensile strengths across the range. SPA and NaAMPS materials with increasing DMAEMA however see a sharp decrease upon low levels of the cation present and less change on further addition but still decreasing. Ionic interactions are short in terms of the distance they can act over. As such, the application of a pulling force to these materials displays the brittleness that such bonds lend.

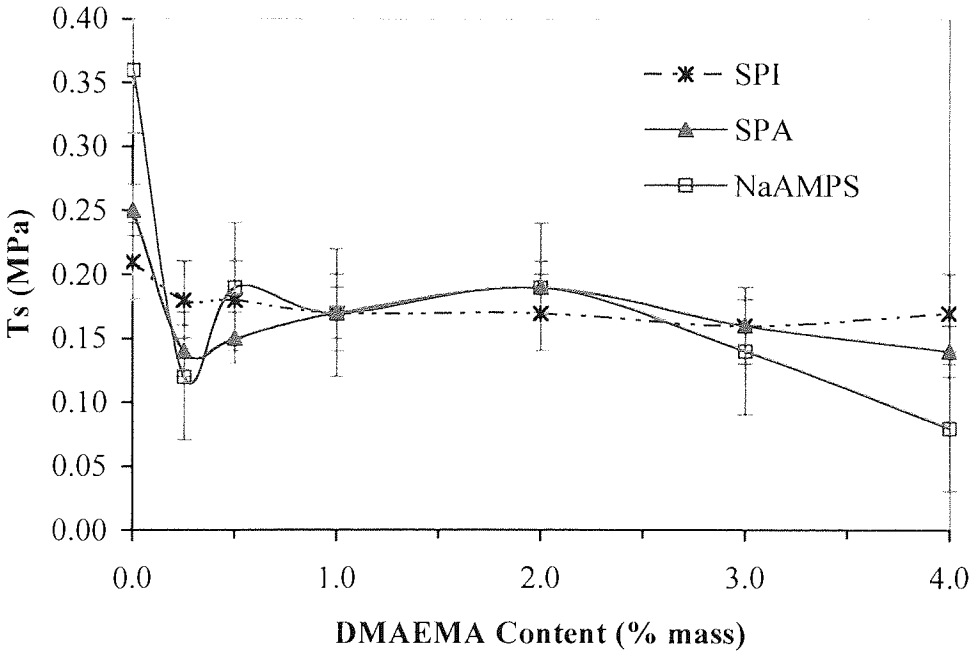

Figure 5.12 The tensile strength of hydrogels containing 2.5% w/w SPI, SPA and NaAMPS and increasing amounts of DMAEMA.

The plasticising water decreases as higher levels of DMAEMA are added and as this reduces chain flexibility, this also affects the deformational properties, namely in reducing tensile strength and elongation to break. SPI is least affected in terms of these two properties, so again charge distribution or rather conformation is having an affect.

The elongation to break of NaAMPS is more affected than SPA by DMAEMA integration possibly due to the simple reason that NaAMPS has more mechanical stabilisation to be disrupted in the first place. The water-binding properties are almost identical for the two sets, so structural conformations and the ability to deal with a cation must be the factors that account for the differences.

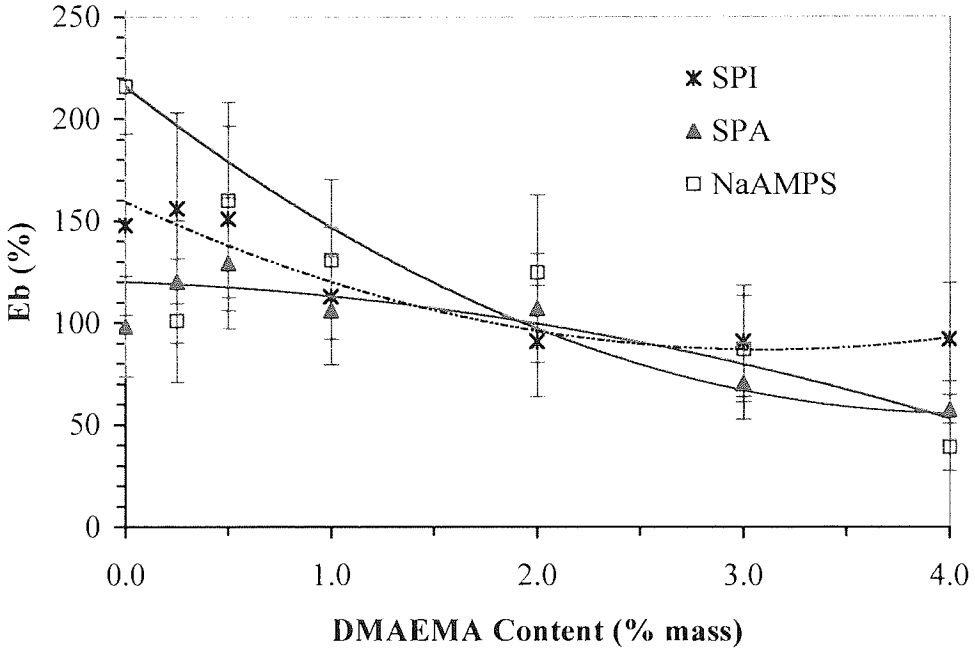

Figure 5.13 The elongation to break of hydrogels containing 2.5% w/w SPI, SPA and NaAMPS and increasing amounts of DMAEMA.

5.2.4 Spoilation Properties Of Hydrogels Containing Anionic and Cationic Monomers

The presence of sulphonates presenting an anionic charge in the previous chapter was shown to reduce the protein deposition characteristics of the hydrogels significantly in comparison to the neutral HEMA/NVP/MMA/MPEGMA hydrogel. The presence of a negative charge alone however would have electrostatically attracted the proteins carrying a positive charge, even though the large hydration shell around the sulphonate charge would be an aid in preventing deposition. If a cation were incorporated in addition to the sulphonate, then the two charges would present and could potentially act to repel proteins of an identical charge and so show changing deposition character.

The total protein spoilation profile for the SPI copolymer with increasing amounts of DMAEMA is shown in Figure 5.14. An interesting trend is observed that mirrors the presence of a dominant charge, whether it be negative or positive. At 0% DMAEMA, only the 2.5% SPI is presenting a negative charge at the surface and this has been shown in the previous chapter to show lower levels of protein spoilation that the 0% SPI copolymer. As DMAEMA is added, protein spoilation increases substantially early in the test period. At 1% DMAEMA, the charges are at the closest point of being equal in quantity and it is here that the highest degree of spoilation is observed. At 4% DMAEMA, once again one charge is dominating in terms of quantity, only here it is a positive charge and with it, deposition has decreased to levels below those seen with the dominant negative charge of SPI.

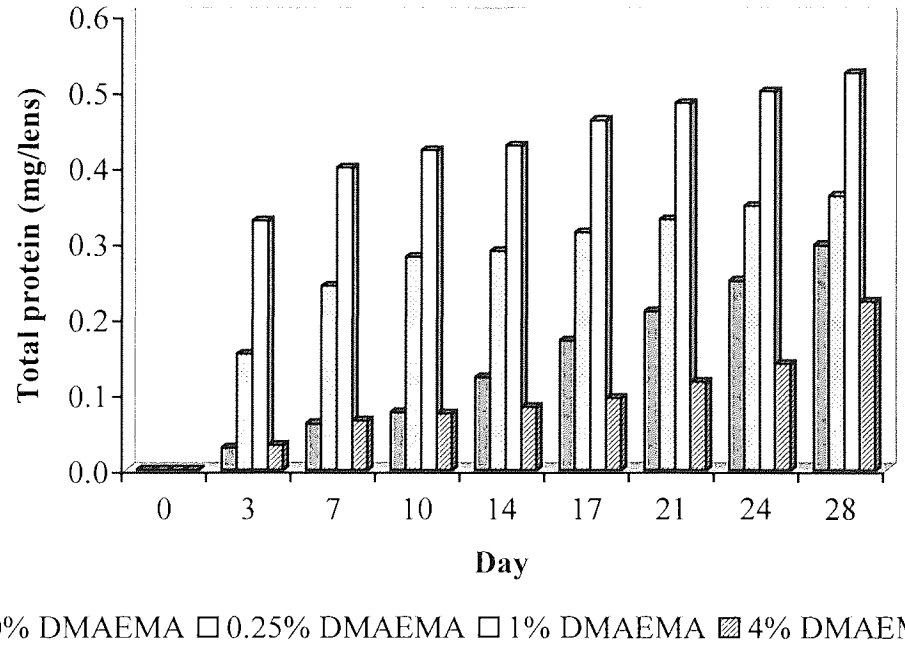

Figure 5.14 The total protein spoilation profile of hydrogels containing 2.5% w/w SPI with increasing amounts of DMAEMA.

The total protein spoilation of SPA copolymers incorporating DMAEMA is shown in Figure 5.16. A similar trend of increasing protein and then decreasing protein on addition of the cation was seen, but all of the materials tested had SPA as the dominant monomer, although decreasing with respect to DMAEMA at each level of addition.

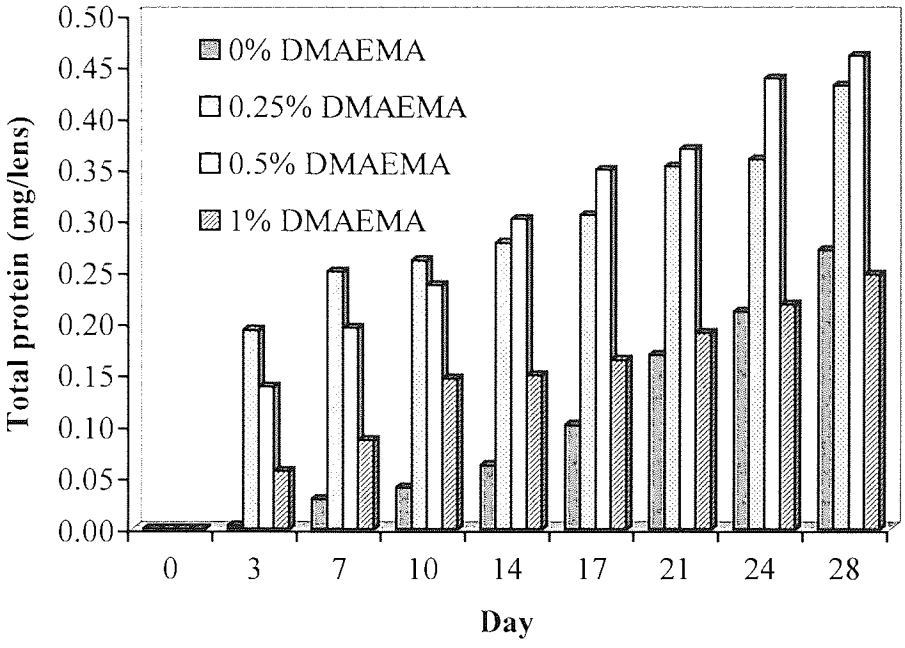

Figure 5.15 The total protein spoilation profile of hydrogels containing 2.5% w/w SPA with increasing amounts of DMAEMA.

The lowest two levels of the cationic monomer caused the highest protein deposition in this case whilst the reduction was observed at 1% DMAEMA, whilst the polymer was still net negative. Although towards the end of the test period, the 0% DMAEMA copolymer and the 4% copolymer were showing almost equal degrees of total protein, they were very close to the reduced levels seen in SPI/DMAEMA and NaAMPS/DMAEMA copolymers where the materials were net positive. Even the highest levels of spoilation seen in Figure 5.15 were significantly less than those in Figure 5.16 and slightly less than in Figure 5.14 for SPI/DMAEMA copolymers.

Figure 5.16 shows the comparable profile for NaAMPS copolymers. Again, up to 1% by weight of DMAEMA, the negative charge of NaAMPS is the dominant charge although to a lesser extent on each level of cation addition and this is what drives the higher levels of deposition; the material surface appearing 'neutral'. The protein deposition seen at the near-neutral charged surface is almost 0.3 mg/lens more than the highest spoiling SPI/DMAEMA material.

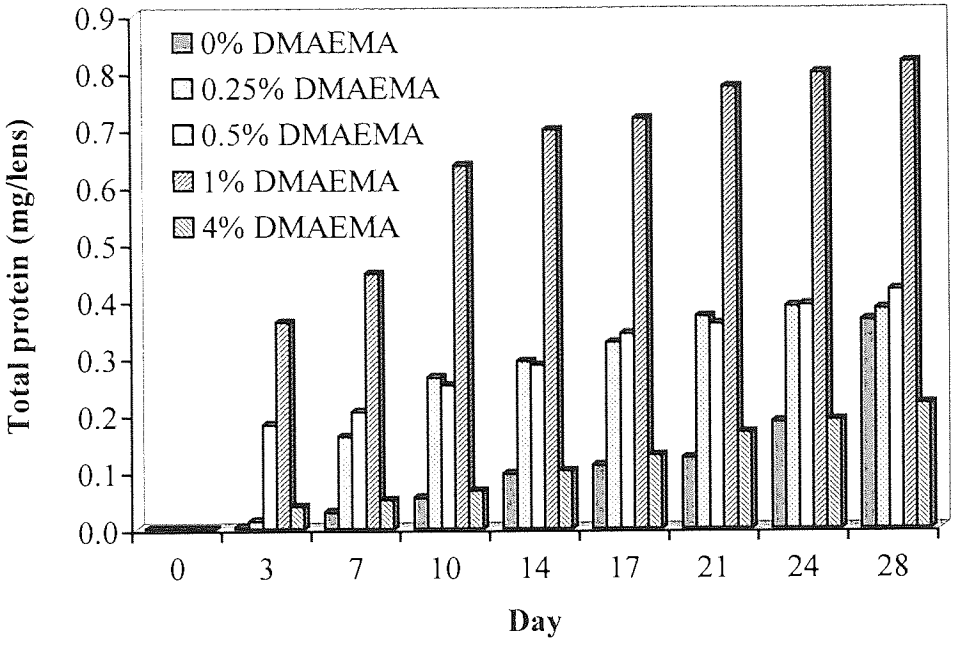

Figure 5.16 The total protein spoilation profile of hydrogels containing 2.5% w/w NaAMPS with increasing amounts of DMAEMA.

At the 4% DMAEMA level of inclusion, the protein deposition is reduced rapidly as once again a charge becomes dominant and at 28 days, this material shows reduced levels of protein than the 2.5% NaAMPS material. At a little over 0.2 mg/lens at 28 days, this material showed almost equivalent levels of deposition as the 4% DMAEMA copolymer including SPI. A wash with ReNu of the 4% cation material revealed a reduction in the total protein of 31%.

Fluorescence spectrophotometry allows the quantification of relative amounts of surface protein to be made. Figure 5.17 shows the surface protein deposition of SPI/DMAEMA copolymers that is similar to but not identical to the trend seen in the total protein spoilation. In this case, as soon as a positive charge becomes the net dominant charge, even though almost equal to the amount of the sulphonates, a decrease in surface protein is observed (at 1% DMAEMA). This could be indicative of differences in the main location of protein spoilation at each level of ionicity. At 4% DMAEMA however, the material still shows a lesser amount of protein deposition than the 0% DMAEMA copolymer.

Almost as important as charge is the EWC, which decreased as DMAEMA content increased. The freezing water fraction was at its highest at the 0.25% level of DMAEMA where the cation was present and it is with this material that the highest degree of surface protein spoilation was observed.

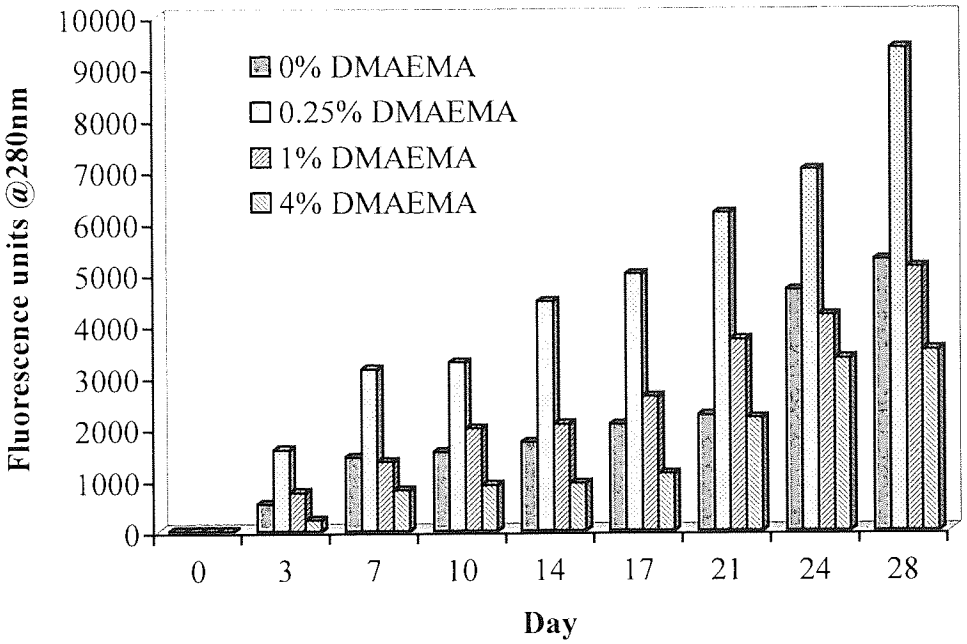

Figure 5.17 The surface protein spoilation profile of hydrogels containing 2.5% w/w SPI with increasing amounts of DMAEMA.

For SPA copolymers, DMAEMA incorporation up to almost net zero charge gave the deposition results shown in Figure 5.18. The 4% DMAEMA material did not survive the 28 day test period and so a net positive material is not available for comparison.

The surface protein increases as the dominance of the negative charge is decreased, in line with the previous results. The surface deposition results for materials incorporating DMAEMA show higher levels of protein than the 2.5% SPA material alone until the 28th day but by this stage, sample fatigue may be playing a major part in the degree of spoilation.

Spoilation during the first half of the test period was again highest at 0.25% DMAEMA where the highest total water and freezing water values were higher than the others in the set. Up to 1% DMAEMA was not enough to reduce the spoilation to below that of 0% cation, although the 1% cation material showed less than the 0.5% cation material (in general).

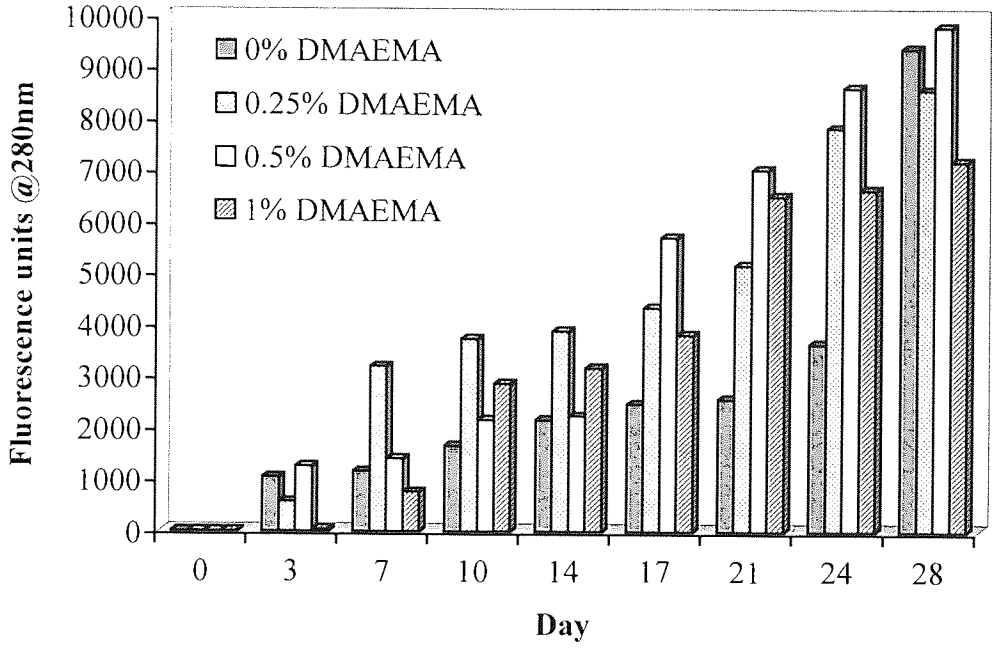

Figure 5.18 The surface protein spoilation profile of hydrogels containing 2.5% w/w SPA with increasing amounts of DMAEMA.

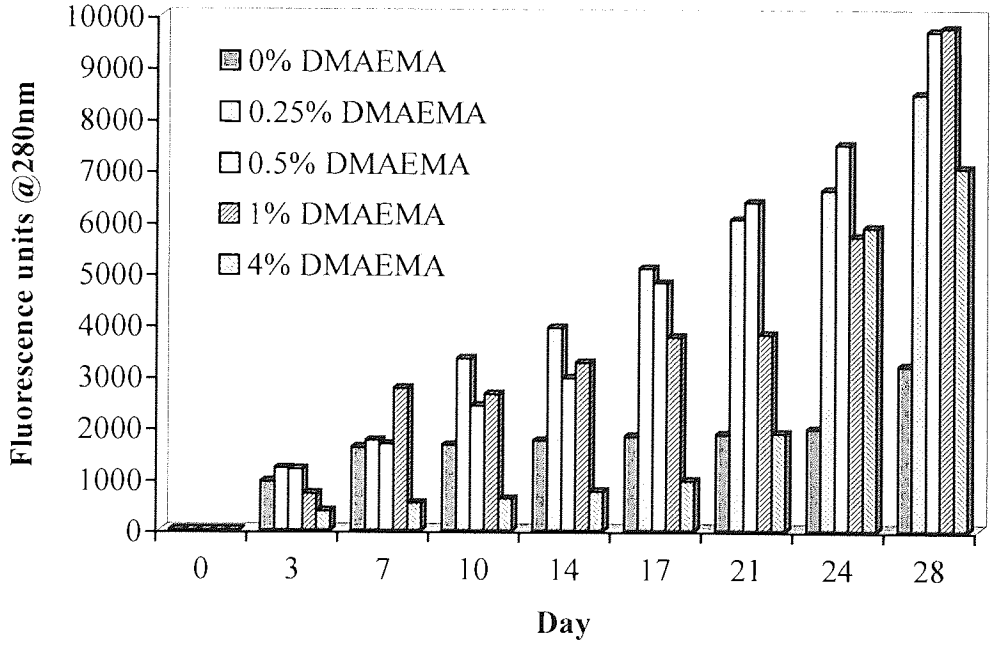

Figure 5.19 The surface protein spoilation profile of hydrogels containing 2.5% w/w NaAMPS with increasing amounts of DMAEMA.

Increasing amounts of DMAEMA into the NaAMPS copolymer have the surface protein deposition effects shown in Figure 5.19. Spoilation was highest for the 0.25%-0.5% DMAEMA copolymers, again where the EWC was highest. Levels over 0.5%

DMAEMA began to reduce the degree of spoilation to levels below that of the 0% cationic material until Day 21. Thereafter, material fatigue may account for the sudden rise in surface spoilation.

The 4% DMAEMA NaAMPS copolymer was washed with ReNu after 28 days in the tear model and a reduction in the surface protein value of 10% was obtained, indicating some reversibility in binding.

In Chapter Four, it appeared that increasing ionicity in terms of increasing sulphonate content caused a substantial increase in the recorded levels of surface lipid deposition. If a net ionic charge were the only driver for this, then the increasing addition of a cation to an anionic material would have a visible effect on the degree of spoilation.

Figure 5.20 shows the surface lipid deposition on 2.5% SPI copolymers with increasing amounts of DMAEMA. Increasing cation content causes the amount of lipid to increase on materials showing reducing water contents in addition to increasing ionic content. Of the materials where a positive charge may be dominant (in 1% and 4% DMAEMA copolymers), in general the levels of lipid deposition were less than the negative net charge of the 0.25% DMAEMA copolymer.

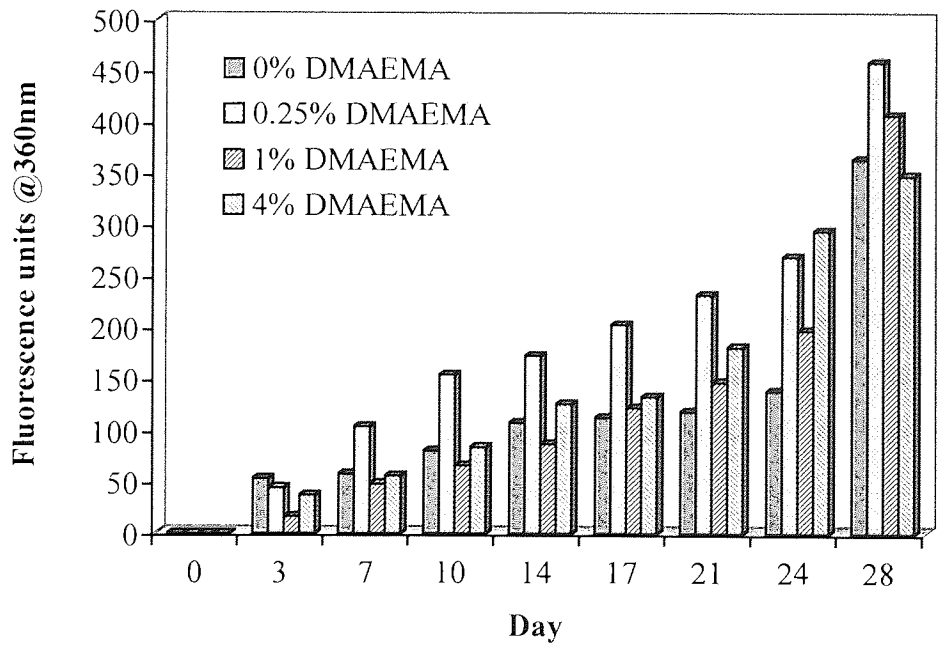

Figure 5.20 The surface lipid spoilation profile of hydrogels containing 2.5% w/w SPI with increasing amounts of DMAEMA.

For the SPA-based copolymers, all of the materials show a net negative charge at the levels of DMAEMA tested in Figure 5.21, although reducing in content relative to the cationic monomer. Again the EWC reduced over the range and it is clear that the lipid deposition increases substantially more than the 0.25% SPA copolymer containing no DMAEMA.

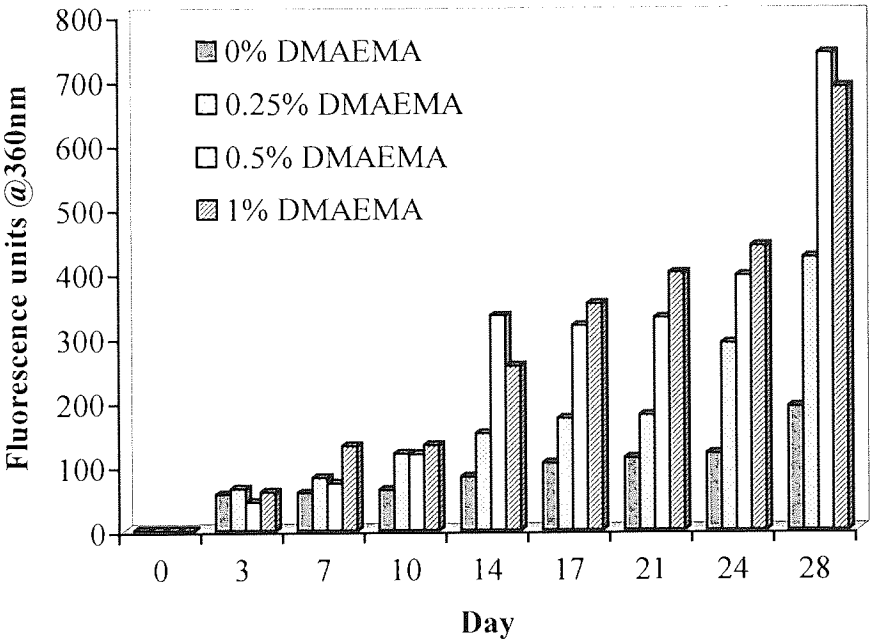

Figure 5.21 The surface lipid spoilation profile of hydrogels containing 2.5% w/w SPA with increasing amounts of DMAEMA.

Almost the same could be said for the NaAMPS copolymers, as the EWC decreases as DMAEMA increases and the lipid deposition appears to increase. Except, that is, for the 4% DMAEMA copolymer where the material is then net positive. For this material, a fall in lipid deposition is observed after Day 10 of the test and the levels throughout the test are equal to or below the levels observed for the 0% cation material. In general though, the values for lipid deposition of the NaAMPS-based copolymers including DMAEMA are slightly higher than those for the equivalent SPA and SPI materials.

The EWC plays an important role, as does the presence of ionicity on the lipid deposition. A net charge will have a part to play as shown by the SPI and NaAMPS materials with 4% DMAEMA compared to lower levels of cation incorporation.

The reversible nature of binding is shown by a wash in ReNu of the 4% DMAEMA copolymer containing NaAMPS reducing the relative amount of surface lipid by 44%.

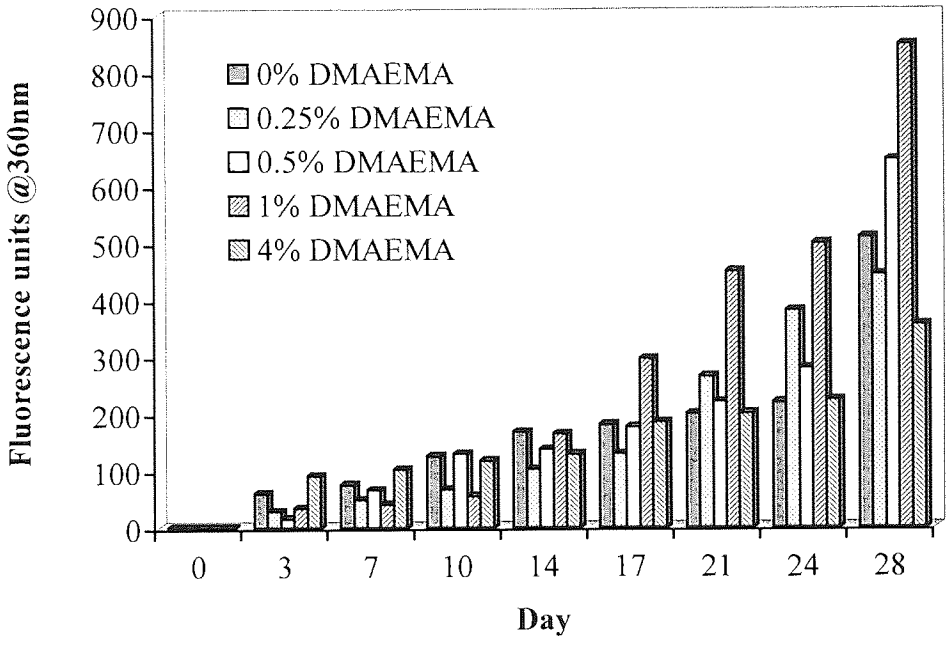

Figure 5.22 The surface lipid spoilation profile of hydrogels containing 2.5% w/w NaAMPS with increasing amounts of DMAEMA.

5.3 Conclusions

As the addition of sulphonates in the previous chapter caused an increase in the hydrophilicity of the resulting materials, in contrast the addition of DMAEMA to sulphonate-containing hydrogels generally caused a decrease in the hydrophilicity. The water-binding studies indicate that the driving component is that of reduced freezing water, whilst non-freezing water creeps upwards slowly.

The suspected cause is that of ionic interactions between groups of opposite polarity acting as secondary cross-links, reducing the mobility of the copolymer network. This is confirmed somewhat by the mechanical properties, which show the stiffness of the sulphonate-based materials increasing with increasing DMAEMA and the tensile strength and elongation to break decreasing over the same range, as the decrease in plasticising water and the short distance of the electrostatic interaction result in sample brittleness.

The dramatic changes that occur in the physical properties of the materials just described occur in the region where the negative charge is the net dominant charge (in terms of quantity of ionic moieties). Approaching and achieving net positive charge materials showed properties differing only slightly from materials with levels of DMAEMA present in further increasing amounts.

SPI again showed differences in water binding compared to equivalent SPA and NaAMPS materials containing DMAEMA, in that small levels of the cation in SPA and NaAMPS copolymers caused an increase in the freezing water and EWC. This resulted in a sharp fall in the stiffness before ionic interactions could play a part in stiffening the material. The stiffness of SPI decreased marginally but nowhere near the magnitude of the decrease seen for the other two, sulphonate copolymers and so the charge conformation must be having an effect.

The size of the charge and the steric hindrance around the charge are both factors affecting the actions of a sulphonate monomer and DMAEMA on each other. The large sulphonate group, randomly distributed across the copolymer is initially greatly affected by incorporated DMAEMA. Once a certain level of incorporation is reached, it could be that further added DMAEMA is only able to interact with the sulphonate groups already interacting with other DMAEMA units, possible because of the larger size and less steric hindrance around the sulphonate charge.

Protein deposition is affected by both the water content and the net charge of the copolymer. As the water content increases, protein deposition increases as the porous nature of the hydrogel increases and vice versa. More significantly is the affect of net charge on the levels of protein deposition. As the charge moves towards neutral, deposition increases and it is clear that the present of a positive charge does not discount a hydrogels use in biomaterials. With a net negative or net positive charge, a reduction in the protein deposition was observed with all sulphonate-based copolymers.

Lipid deposition generally increased with increasing ionic content of all hydrogels but whether this was a consequence of the ionicity or the reducing water content was not clear. The negatively charged fatty acids of lipids would be expected to have an increased interaction with an increasingly cationic surface.

As such, the results show that a net positive charge in a material containing sulphonate groups show deposition characteristics that do not exclude their potential for biomaterials use. The water contents are reduced in comparison to the sulphonate-based copolymers and sample brittleness remains a problem.

CHAPTER 6

Neutral Hydrogels Containing Polyurethane; Semi-Interpenetrating Networks

"Forgive, O Lord, my little jokes on Thee
And I'll forgive Thy great big one on me."
Robert Frost, 1874-1963,
'Cluster Of Faith' (1962).

6.1 Introduction

The major problem facing conventional hydrogels in their application as a biomaterial is their relatively weak mechanical strength, caused predominantly by the plasticising water that governs some of the unique and desirable properties of the hydrogel.

The incorporation of a pre-formed polymer into a hydrogel provides a means for increasing the strength of the inherently weak water swollen hydrogel network. Although monomer combinations and cross-link density are routes to increasing hydrogel strength, the limitations are acutely constrained by the water content.

IPN technology is typically employed in wound covering and prosthetic biomaterials. The flexible, non-antigenic and permeability properties that have been stated as essential requirements for a wound dressing are still insufficient for success until supported by the final requirement, strength, that an interpenetrating network can provide.

The wound dressing Geliperm® was developed and released commercially in the 1980's and was composed of two interlaced networks, of polyacrylamide and of agar[8]. With a water content of 96%, its non-toxicity, elasticity, permeability to biological solutes (but not bacteria) and transparency all acted to show an improvement in wound healing.

Synthetic articular cartilage is another area of IPN research, with semi-IPNs investigated using cellulose acetate or cellulose acetate butyrate as the interpenetrant, forming materials with water contents of 50 - 80%[44].

More recently, a range of polyurethane interpenetrants has become available. In combination with traditional hydrogel copolymers to increase strength, as a semi-IPN, it would allow the unique properties of the conventional hydrogel to present themselves, i.e. hydrophilicity and water transport properties.

The urethane unit is a carbonyl-containing functional group in which the carbonyl carbon is bound to both an ether oxygen and to an amine nitrogen, shown in Figure 6.1.

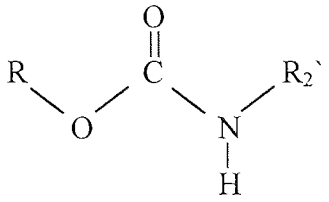

Figure 6.1 The urethane unit.

Polyurethanes are polymers containing urethane linkages. The overall structure of polyurethanes is relatively complex and usually proprietary in nature. However, a structural example of a polyester urethane is shown in Figure 6.2.

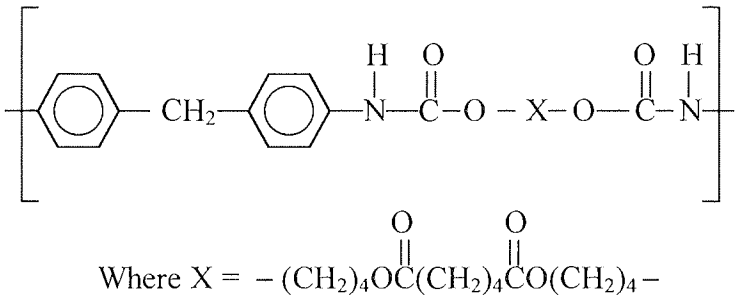

Figure 6.2 A polyester-based aromatic polyurethane

Polyurethane is one of the most important polymers used in biomedical devices and polyurethane hydrogels have been described as soft contact lens materials and surgical implants. Polyurethane-silicone hydrogels containing NNDMA or HEMA have been reported[96] which show much higher oxygen permeability than non-silicone hydrogels and low levels of lysozyme adsorption, which would be expected, as the resultant material was non-ionic. At Aston, polyurethanes have been investigated for the artificial cornea[97].

Previous investigations into six commercially available polyurethanes (proprietary structures) have shown that two, polyester-based aromatic polyurethanes show properties that may of interest in a biomaterial. PU5 showed the highest modulus at 27.4 N mm^{-2} and PU6 showed the highest tensile strength at 55 N mm^{-2} (1 N mm^{-2} = 0.01 MPa). Both possessed good solubility in N-vinyl pyrrolidone[98] but PU5 was chosen as the main polyurethane to investigate as the NVP/PU5 semi-IPN had an EWC of almost 10% higher (of about 82%) than the NVP/PU6 semi-IPN.

As Copolymer X (HEMA:NVP:MMA:MPEGMA) had already been successfully worn in eyes, it was taken as a starting point for semi-IPN modification. As a hydrogel, its development is clear. Starting with a HEMA base, to increase the water content, NVP was added. The mechanically weak and fragile materials produced were strengthened by the addition of the hydrophobic monomer MMA. The PEG-methacrylate (where $[PEG]_n$ is n=400-600 units) was added as a 'swinging arm' to reduce deposition. Adding an interpenetrant to strengthen what is a contact lens material, without a significant loss in the water content, would lead to a material that may be of interest as an artificial cornea. If the flexibility and transparency of the resulting materials are high enough, then use as a contact lens could also be considered.

6.2 Results and Discussion

6.2.1 Semi-IPNs Based Upon Copolymer X and Polyurethane Interpenetrants

The polyurethane interpenetrant, PU5, was incorporated at various levels up to 10% by weight into Copolymer X composition of HEMA:NVP:MMA:MPEGMA and polymerised to form a semi-IPN. PU6 was added at the 2% by weight level to obtain a comparable material with a structurally similar polyurethane with different properties.

The polyurethane was dissolved in 10% by weight of the solvent N-methyl pyrrolidone, plus the N-vinyl pyrrolidone monomer prior to mixing with the remaining monomers, cross-linker and initiator to aid dispersion.

6.2.1.1 The Water-Binding Properties of Semi-IPNs

The semi-IPN materials produced at all levels of PU5 incorporation were opaque in appearance following polymerisation and remained so upon hydration. This indicated, with reference to the four steps of compatibility given in Chapter One, that the problem of incompatibility was that between the monomers and the dissolved polymer (Step ii).

The water-binding properties of the opaque semi-IPNs are shown in Figure 6.3. The material containing PU6 was also opaque.

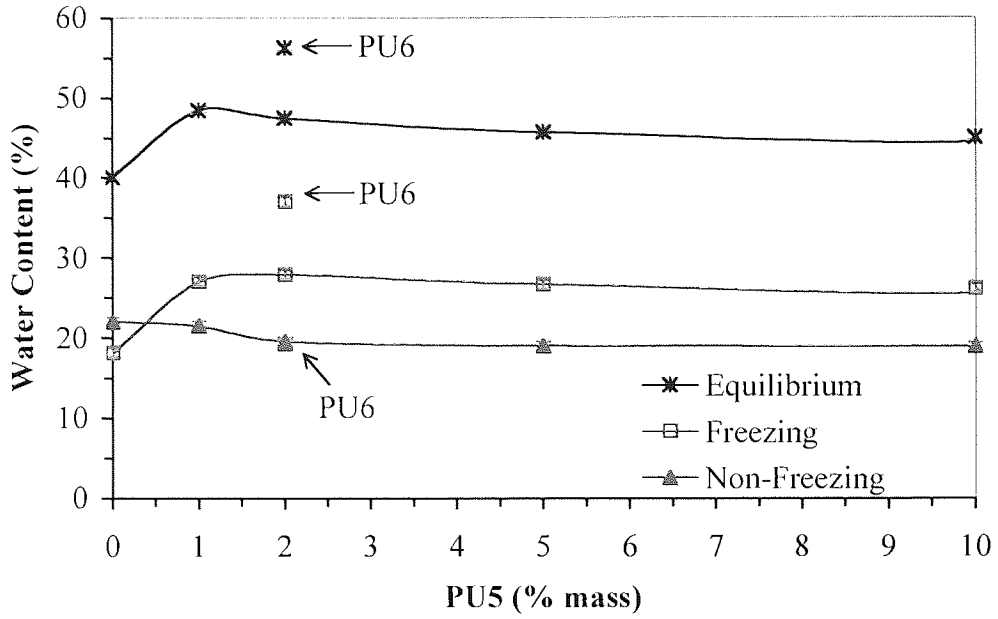

Figure 6.3 The water-binding properties of semi-IPNs based on HEMA:NVP:MMA: MPEGMA, with increasing amounts of interpenetrant.

The incorporation of the interpenetrant PU5 resulted in an increase in the total equilibrium water content at the 1% level but over this level, a gradual decrease was observed. These changes were in the main due to the freezing water fraction decreasing, although the non-freezing fraction did decrease marginally. The magnitude of the change in EWC between 0% and the 1% level of PU5 is due in part to the 0% material being polymerised in the absence of the diluent, NMP.

A low level of PU5 may disrupt the space between the copolymer chains to a small extent and cause more water to be held in the space created and it is seen that the rise is due to loosely bound, freezing water. As the level of interpenetrant increases, the space between the hydrogel copolymer chains available to water decreases and this is seen in the results above. Because of the aromatic groups present in the polyurethane, increased hydrophobicity is also playing a part in reducing the water content.

Surprisingly, the material containing PU6 shows significantly higher hydrophilicity than the corresponding PU5 material. PU5 was chosen as the interpenetrant to investigate because previous work in our laboratories had shown that the PU5/NVP semi-IPN showed a higher EWC than the PU6/NVP semi-IPN. Based upon the results present in this chapter, it could be assumed that PU6 had fewer hydrophobic regions or more

hydrophilic regions than PU5. Alternatively, the presence of HEMA, MMA and/or MPEGMA alters the water interactions between the polyurethanes.

6.2.1.2 Surface Free Energy Properties of Hydrated Semi-IPNs

The surface energy properties of the semi-IPNs are shown below in Figure 6.4. Although a reduction in the water content is seen on increased incorporation of the interpenetrant, γ_s^t remains constant. Small changes are seen in γ_s^p and γ_s^d, although not highly significant given the error bars. The polar component, γ_s^p, appears to follow an upward trend whilst the dispersive component decreases. This was unexpected as the hydrophobic interpenetrant was expected to cause a decrease in γ_s^p. As such, unusual molecular interactions between the polyurethane and the hydrogel may be promoting (or at least not hindering) the expression of hydrophilic groups at the surface. An unusual packing arrangement in semi-IPN polymers has been noted for both NNDMA/PU semi-IPNs and Geliperm® by Corkhill[44], as they also showed higher than expected surface energies.

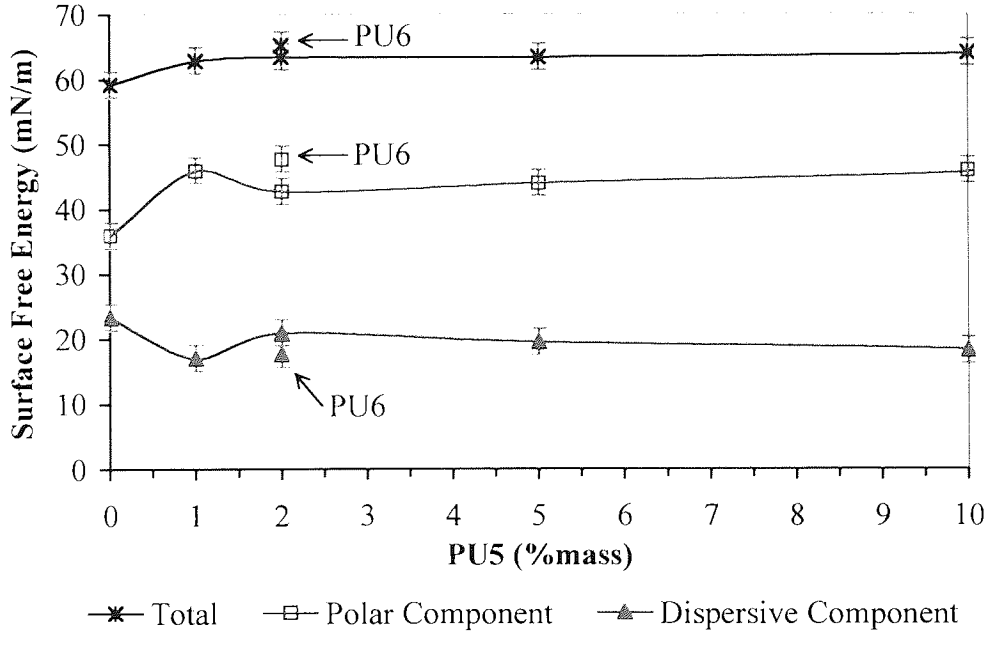

Figure 6.4 The components of surface free energy of semi-IPNs based on Copolymer X and containing increasing amounts of polyurethane interpenetrant in the hydrated state.

The PU6 semi-IPN shows a slightly higher γ_s^I than its PU5 equivalent as expected because of its higher water content. This higher freezing water content is translated into the difference seen for the γ_s^P, which is higher than the PU5 semi-IPN.

Because of the opacity that resulted in the materials produced, they were unsuitable for spoilation analysis as optical clarity is a prerequisite for the measurement techniques involved.

6.2.1.3 Concluding Remarks

Incorporation of the polyurethane interpenetrant into the copolymer material did not adversely affect the EWC of the resulting materials in comparison to the copolymer, although increasing amount of the interpenetrant did cause a fall.

The surface free energies of the materials showed that the surface was dominated by polar groups that were unaffected by the incorporation of the polyurethane, possibly indicative of the incompatibility of the two systems.

6.2.2 Semi-IPNs Based Upon Copolymer X with HEMA Replacements and Polyurethane Interpenetrants

Because the semi-IPNs from the previous section were opaque prior to hydration, a blocky structural arrangement was a possible cause of opacity. Also, the polyurethane interpenetrants were only soluble in organic, non-ionic solvents and the suspicion that HEMA could be responsible for the incompatibility, resulting in phase separation by virtue of its terminal –OH, was investigated. The HEMA fraction of Copolymer X was replaced by an equal mix of THFMA and AMO in the first instance, EEMA and AMO in the second and the resultant semi-IPNs with PU5 characterized. Both THFMA and EEMA are less hydrophilic than HEMA because their oxygen atoms are more sterically hindered within the chain as can be seen in Figure 6.5.

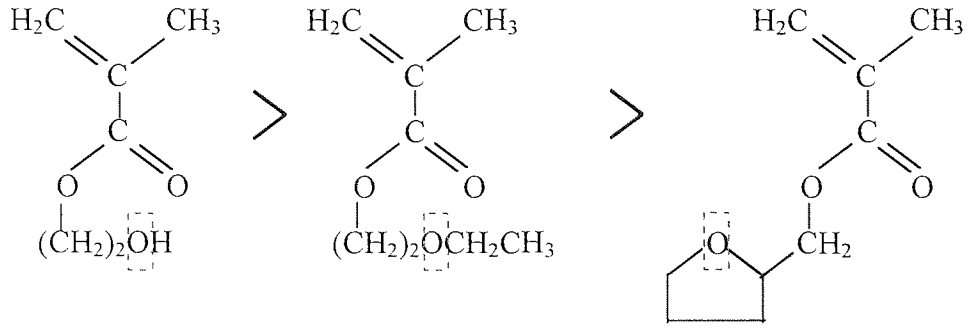

Figure 6.5 The structures of HEMA, EEMA and THFMA in decreasing order of hydrophilicity, with an oxygen involved in hydrogen bonding interactions with water highlighted.

6.2.2.1 The Water-Binding Properties of Semi-IPNs Excluding HEMA

The semi-IPNs including THFMA showed improved compatibility over the HEMA-based materials in that they were transparent when dry but showed increasing opacity with increasing polyurethane content when hydrated. The water-binding properties of this set and notes on their appearance are shown in Figure 6.6.

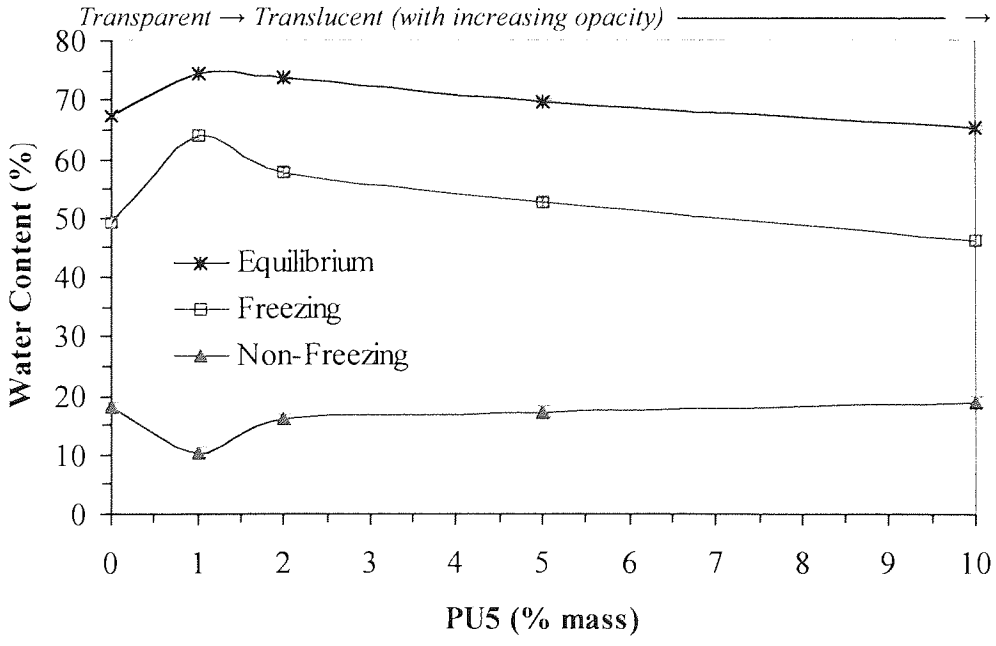

Figure 6.6 The water-binding properties of semi-IPNs based on THFMA:AMO:NVP: MMA:MPEGMA, with increasing amounts of PU5 interpenetrant.

The addition of hydrophilic AMO to the material has resulted in a significant increase in the EWC of the copolymer (67.3%) from Copolymer X (40.1%). Again, a small amount of interpenetrant caused a rise in the water content, a result of an increase in the freezing water and fall in non-freezing water. The interpenetrant probably increased the porosity of the material and so increased the space available for loosely bound, freezing water. Increasing amounts of PU5 resulted in a decrease in the EWC for reasons explained previously.

The semi-IPNs containing EEMA showed the best compatibility in terms of transparency, although at the highest level of PU5 addition, hydrophobic and hydrophilic regions in the material were discernable simply by observing the manner in which water was spreading. The materials were transparent when dry and when hydrated in water. The water-binding properties for the materials are shown in Figure 6.7.

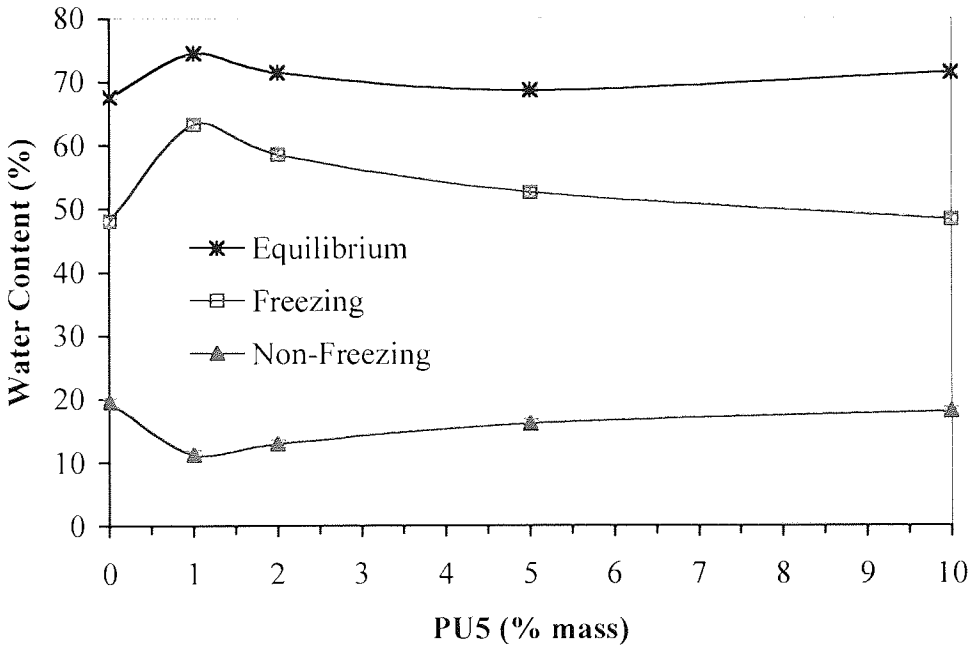

Figure 6.7 The water-binding properties of semi-IPNs based on EEMA:AMO:NVP: MMA:MPEGMA, with increasing amounts of PU5 interpenetrant.

The EWC for the copolymer is on the whole identical to the THFMA copolymer, although subsequently, the AMO copolymer is better able to retain a high water content on increasing addition of interpenetrant. The free space available to freezing water is reduced with increased polyurethane and this is what accounts for the reduction in the freezing water.

6.2.2.2 Surface Free Energy Properties of Semi-IPNs Excluding HEMA

Increasing levels of PU5 appear to have very little effect on all components of the surface free energy of the THFMA-containing semi-IPNs, as can be seen in Figure 6.8, in spite of the reduction seen in the water content. The polar groups appear to be able to express themselves at the surface independent of the hydrophobic interpenetrant increasingly filling the bulk, but at such high water contents, there is less of an effect on this bulk space, i.e., the effect of the polyurethane is diluted. Previously, the surface energies γ_s^p and γ_s^d changed in response to the changes in freezing and non-freezing water fractions changing (in the HEMA-based semi-IPNs).

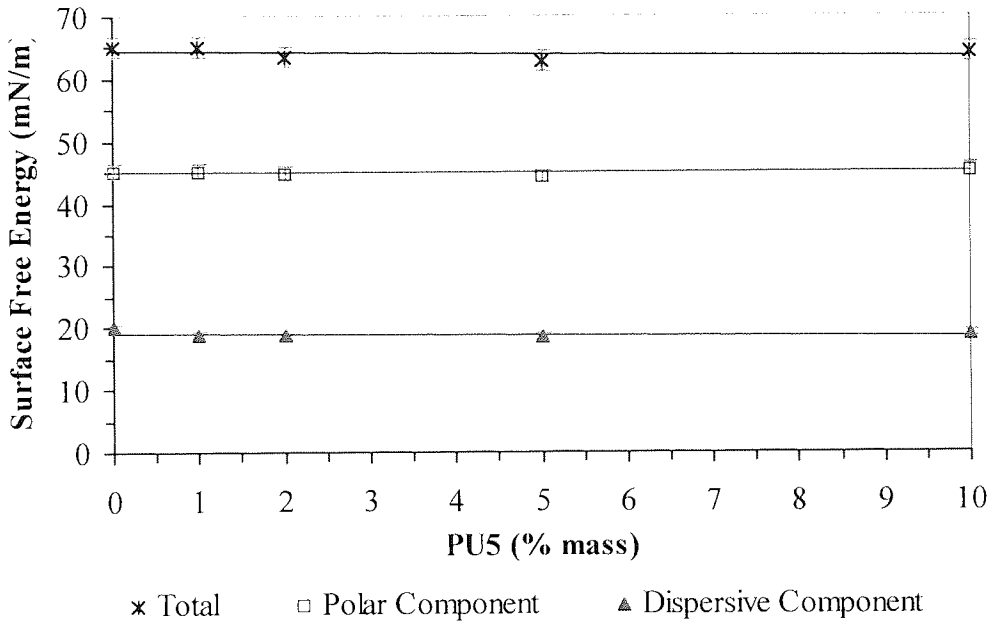

Figure 6.8 The components of surface free energy of semi-IPNs based on THFMA:AMO:NVP:MMA:MPEGMA and containing increasing amounts of polyurethane interpenetrant in the hydrated state.

The trends seen in the components of surface free energy were more like those expected (for increasing hydrophobic content) for EEMA-containing semi-IPNs. Figure 6.9 shows that as the amount of interpenetrant increases, the total free energy falls slightly, the sum of a fall in the polar component, in line with the reduction of freezing water, and an increase in the dispersive component, as the hydrophobic content of the semi-IPN increases. The γ_s^1 reaches a slightly lower level than the equivalent THFMA material as the EEMA material shows a higher interaction with the polyurethane which is reducing the polar component and/or increasing the dispersive component.

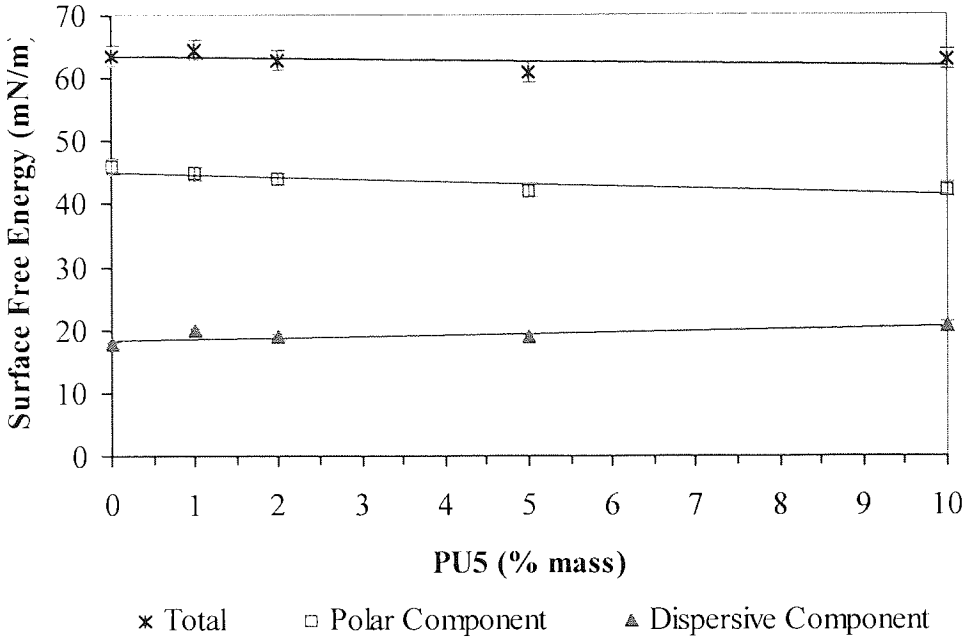

Figure 6.9 The components of surface free energy of semi-IPNs based on EEMA:AMO:NVP:MMA:MPEGMA and containing increasing amounts of polyurethane interpenetrant in the hydrated state.

6.2.2.3 Spoilation Properties of Semi-IPNs Excluding HEMA

As stated earlier, the opacity of the HEMA semi-IPN materials precluded them from undergoing spoilation analysis. However, the modified materials could be tested.

The total protein spoilation for the THFMA-containing semi-IPNs is shown in Figure 6.10 and the EEMA-containing semi-IPNs in Figure 6.11. The anomalous behaviour of the THFMA copolymer makes a striking profile and cannot be satisfactorily explained. Excluding this material, it is apparent that increasing PU5 content causes higher levels of total protein deposition and the levels of protein deposition increases steadily over time following an initial spike.

The EEMA semi-IPNs showed improved chemical compatibility over their THFMA equivalents and it is perhaps for this reason that these materials show less deposition. Reasons such as a higher surface rugosity on the THFMA semi-IPNs would affect the deposition results, although the actual materials yield no obvious, visual differences for

this. The translucent nature of the THFMA semi-IPNs could have inflated the results and this is a possible reason for some of the differences seen.

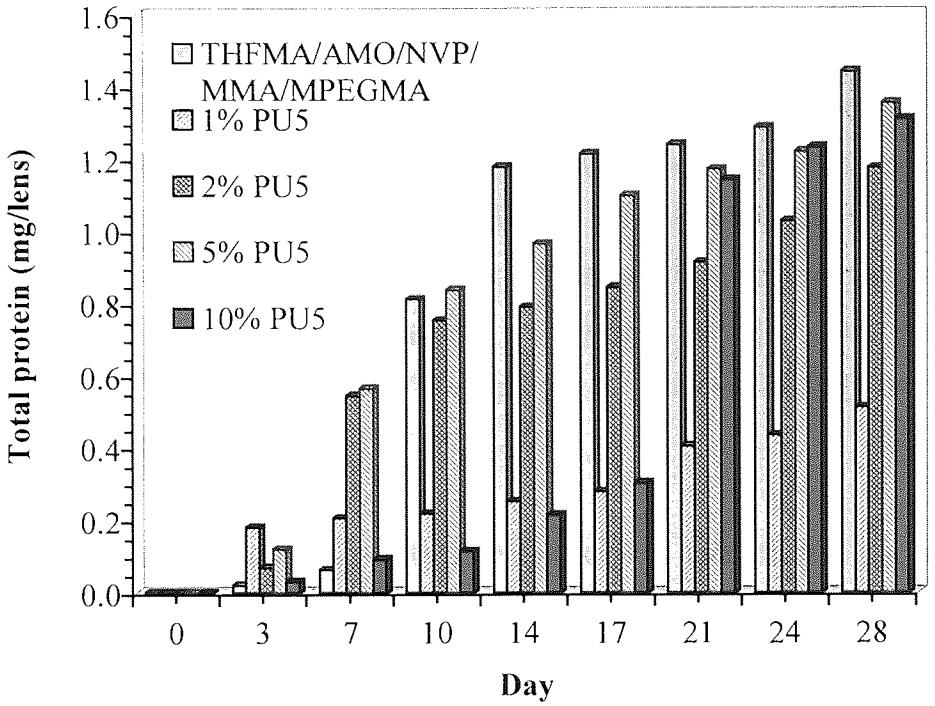

Figure 6.10 The total protein spoilation profile of semi-IPNs containing THFMA and increasing amounts of polyurethane interpenetrant (PU5).

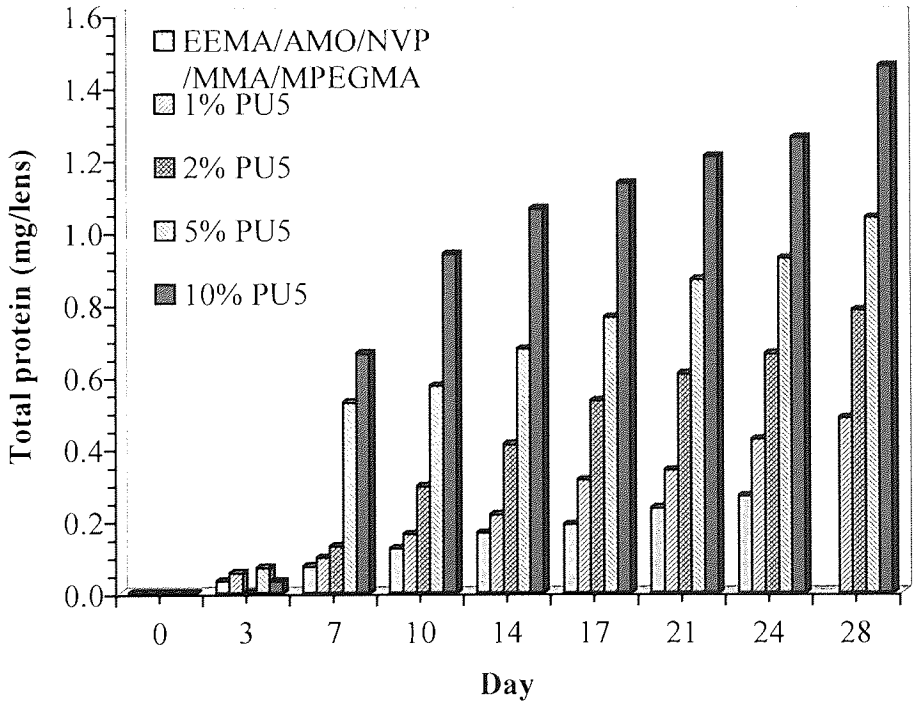

Figure 6.11 The total protein spoilation profile of semi-IPNs containing EEMA and increasing amounts of polyurethane interpenetrant (PU5).

The levels observed in the transparent EEMA materials are higher than the majority of ionic, sulphonate hydrogels investigated in Chapter Four. As these semi-IPNs are non-ionic, a different type of interaction must be responsible for the deposition.

Hydrophobicity in the materials is increased as more polyurethane is incorporated and hydrophobic interactions have been described in Chapter One as a mechanism of protein adsorption (Figure 1.8). The irreversible nature of this binding is somewhat confirmed by the results following a wash with ReNu. Whereas total protein was reduced by upwards of 30% for the ionic sulphonate hydrogels in Chapter Four, the EEMA-containing semi-IPN (with 1% PU5) total protein is reduced by only 10% and the equivalent THFMA semi-IPN by 6%.

The analysis of surface protein deposition gives a clearer indication of the location of protein spoilation. Figures 6.12 and 6.13 show the surface protein deposition of the THFMA- and EEMA-containing semi-IPNs respectively and the levels seen here are similar in magnitude to the sulphonate materials. Where much higher values were found for the sulphonate hydrogel copolymers, this was more a results of sample fatigue due to the high water content than true spoilation.

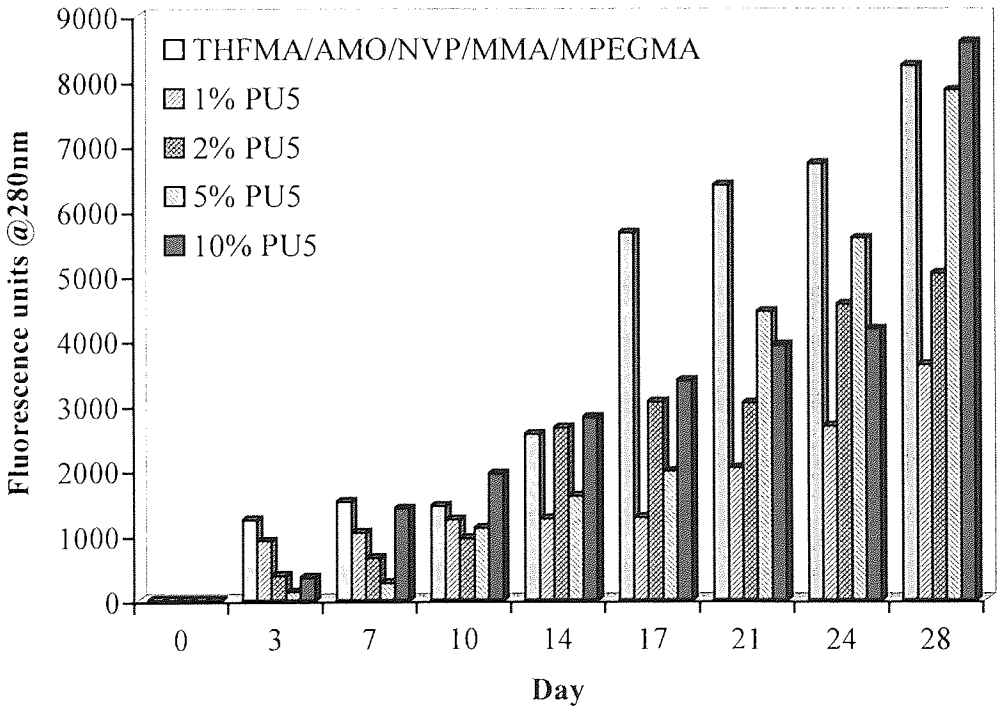

Figure 6.12 The surface protein spoilation profile of semi-IPNs containing THFMA and increasing amounts of polyurethane interpenetrant (PU5).

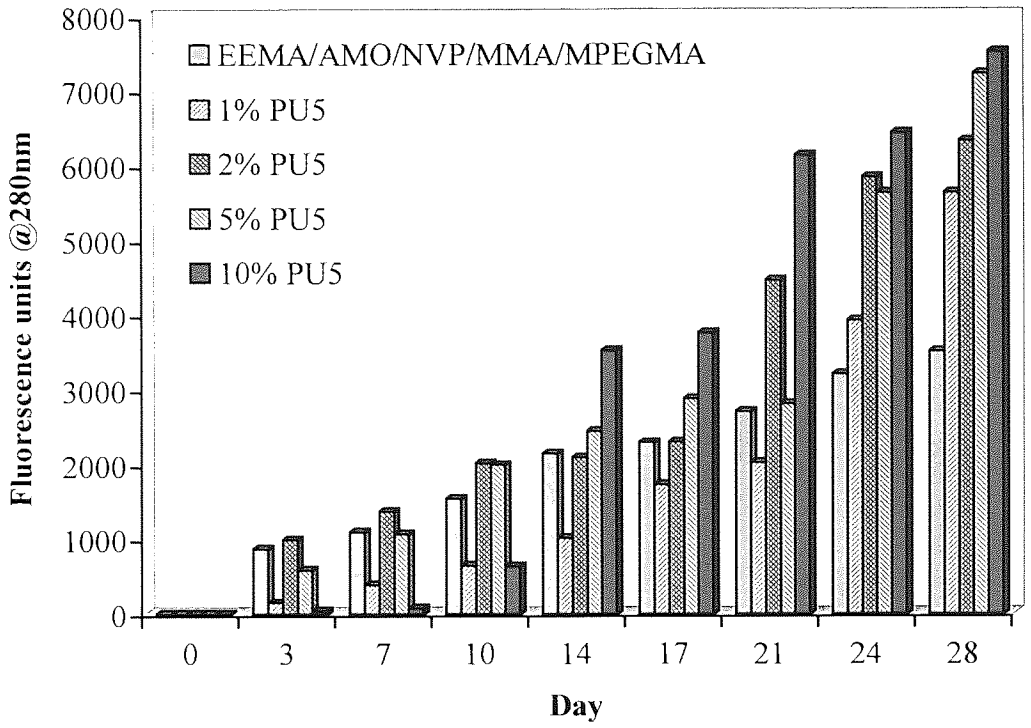

Figure 6.13 The surface protein spoilation profile of semi-IPNs containing EEMA and increasing amounts of polyurethane interpenetrant (PU5).

Interestingly, even though for both, the surface deposition increases with increasing polyurethane incorporation, the THFMA semi-IPNs show less spoilation than the THFMA copolymer hydrogel and the EEMA semi-IPNs show more than the EEMA copolymer hydrogel, similar to the total protein results. For both sets, a longer lag time is observed with the inclusion of 1% PU5.

A wash in ReNu again determines the reversible nature of binding and here, the 1% PU5 semi-IPN that includes THFMA is reduced by 81% and EEMA by 88%. This is significant in that clearly, the majority of protein interaction is in the bulk of the material and not the surface. The porosity caused by the two systems may be such that proteins enter the matrix and irreversibly bind to the polyurethane backbone. It has been shown in the surface free energy results that the polyurethane does not particularly express itself at the surface to the exclusion of polar groups and so its effect is internal rather than surface dominated, which is preferable in the design of a strengthened but surface wettable material.

The results of the lipid deposition analysis are shown in Figures 6.14 and 6.15. Although the trend is less clear, it may still be said that lipid deposition increases with increasing polyurethane and EEMA-containing semi-IPNs spoil to a lesser extent than THFMA semi-IPNs.

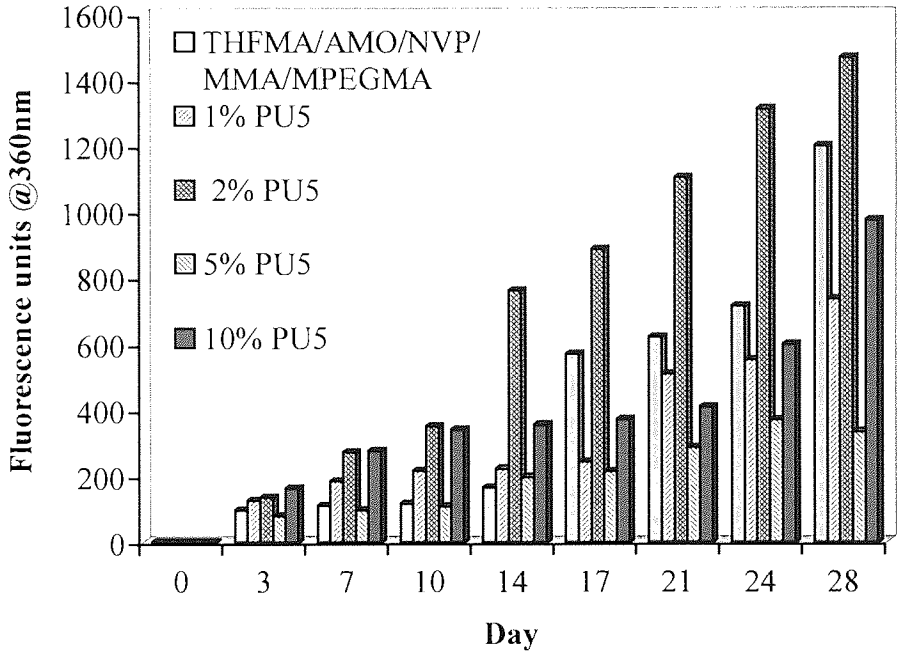

Figure 6.14 The surface lipid spoilation profile of semi-IPNs containing THFMA and increasing amounts of polyurethane interpenetrant (PU5).

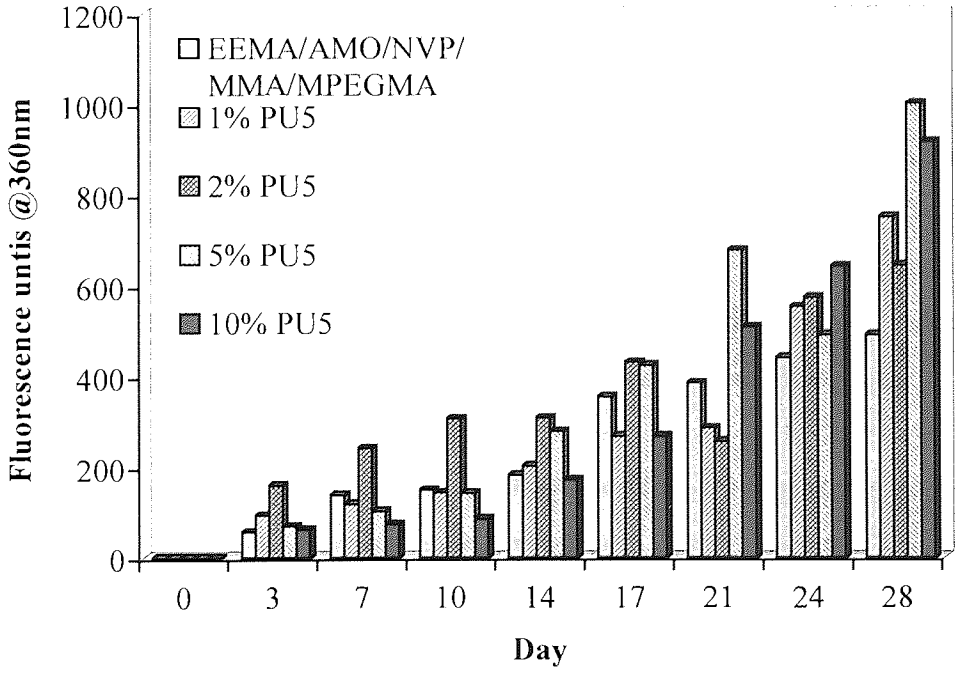

Figure 6.15 The surface lipid spoilation profile of semi-IPNs containing EEMA and increasing amounts of polyurethane interpenetrant (PU5).

Reversibility of the spoilation was demonstrated, again with the 1% PU5 semi-IPNs of THFMA- and EEMA-containing materials, by finding reductions following a ReNu rinse of 86% and 34% respectively.

The levels observed were higher than those containing sulphonate monomers and can be explained by the deposition-enhancing hydrophobic-hydrophobic interaction between lipoidal species and the polyurethane, bearing in mind that the ReNu wash has shown that the deposition is fairly reversible.

6.2.3 Mechanical Properties of Semi-IPNs

All three sets of semi-IPNs will now be discussed regarding their mechanical properties, as all may be included in this section.

Figure 6.16 displays the elastic modulus, or the stiffness of the HEMA-, THFMA- and EEMA-containing semi-IPNs. Firstly, comparing the hydrogel copolymers, the EWC is clearly the most important factor in determining the stiffness. The HEMA copolymer (Copolymer X) had an EWC of approx 40% whilst the THFMA and EEMA copolymers had EWCs of approx. 67%. The increased amount of plasticising water is the driving factor in the nearly 60% reduction in E.

Increasing polyurethane levels in the HEMA semi-IPN results in much higher increases in stiffness than the modest increases seen in the THFMA and EEMA sets. Although the EWC is a major factor in the differences, for the HEMA semi-IPNs, the EWC did not change significantly on higher levels of PU5 and so the effect is an interpenetrant one. The polyurethane appears to have a stronger influence on the material where phase separation had occurred to the extent that the material was completely opaque.

In the high EWC semi-IPNs incorporating THFMA or EEMA, the stiffness does increase slightly as the increasing interpenetrant causes a decrease in the amount of freezing water in the materials, but the strengthening effect seen in the HEMA semi-IPNs is severely diluted. As THFMA and EEMA are less hydrophilic than AMO, which is added to an equal weight amount and is not present in the HEMA semi-IPNs, it must be the significant hydrophilicity introduced by AMO that changes this polyurethane influence.

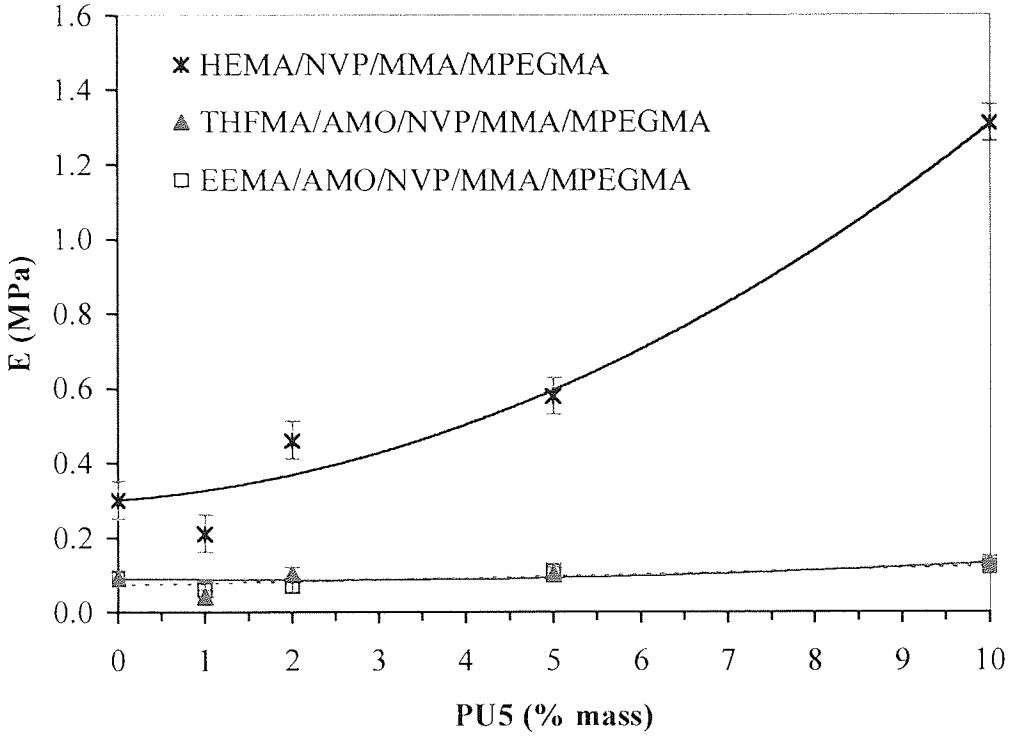

Figure 6.16 The initial modulus of semi-IPN materials containing increasing amounts of polyurethane interpenetrant (PU5).

The tensile strengths of the materials, shown in Figure 6.17, almost duplicate the trends seen above. A more substantial increase in the tensile strength of the THFMA/AMO and EEMA/AMO semi-IPNs is seen on increasing the interpenetrant, although the levels are again nowhere near the magnitude of the tensile strengths seen for the Copolymer X semi-IPNs. EEMA/AMO semi-IPNs have higher tensile strengths than THFMA/AMO semi-IPNs, demonstrating that the polymer matrix does have an effect. The unravelling polyurethane chains confer the tensile strength and have an effect on the elongation to break (Eb), for which the values obtained for the high water content semi-IPNs are shown in Figure 6.18. The HEMA-containing semi-IPN elongation to break results did not show any clear trend.

Whilst at low levels of PU5, the Eb increases to a level that appears to level off or decrease somewhat on further incorporation. As the plasticising water also reaches its lowest levels at the higher PU5 additions, this is a water-driven effect. The initial increase is higher flexibility due to the higher water content some PU5 appears to cause.

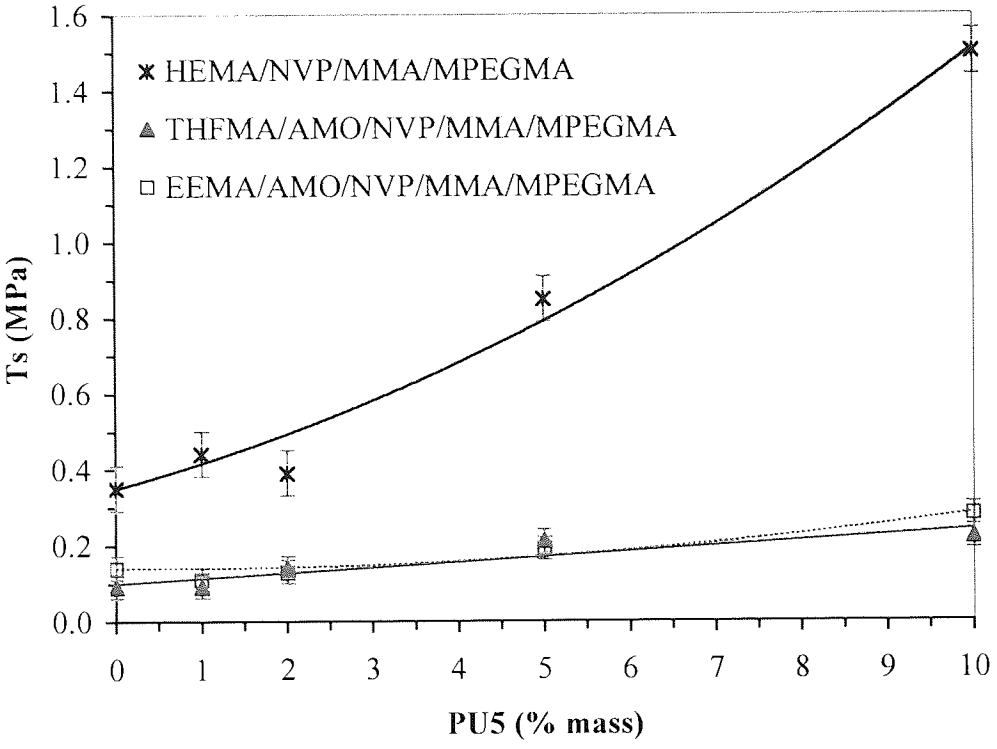

Figure 6.17 The tensile strength of semi-IPN materials containing increasing amounts of polyurethane interpenetrant (PU5).

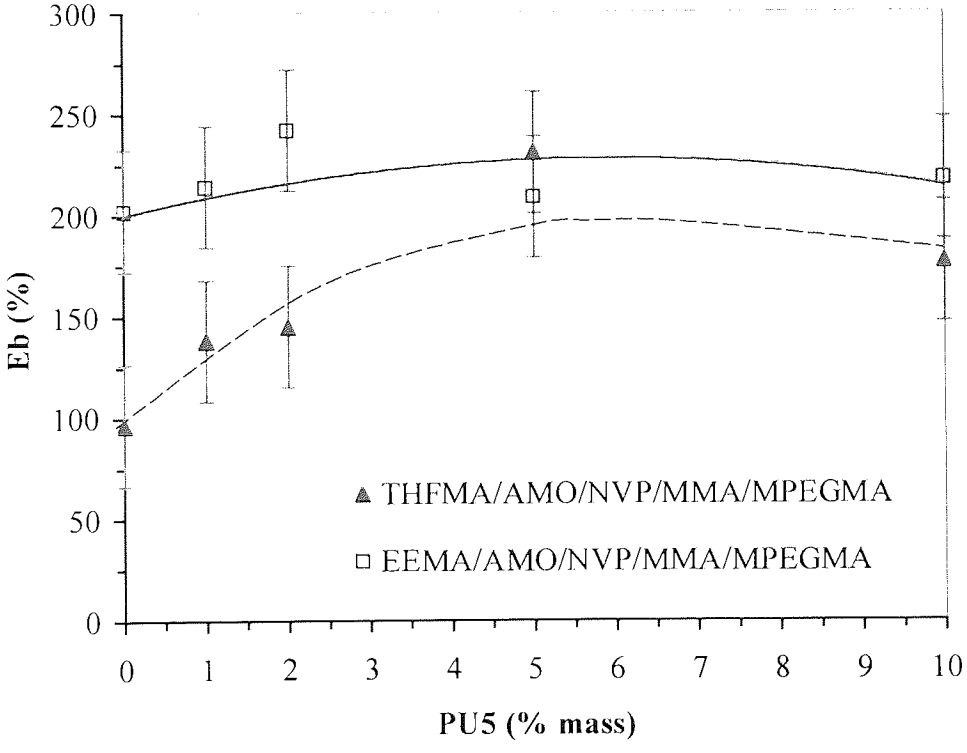

Figure 6.18 The elongation to break of semi-IPN materials containing increasing amounts of polyurethane interpenetrant (PU5).

The THFMA semi-IPNs show a lower Eb than the EEMA equivalents and this may be ascribed to the presence of the bulkier THFMA pendant group in comparison to the linear ethoxyethyl group of EEMA. This reduces the ease of chain rotation on extension and leads to the formation of a more rigid, brittle system, at comparable EWCs and the other monomers included being the same.

6.3 Conclusions

If transparent semi-IPNs are the aim, monomer to polymer compatibility pre-polymerisation, pre-hydration and post-hydration must be viewed to determine where any problems may lie. Otherwise, materials with two distinct phases may result, as occurs with the Copolymer X-based semi-IPN. The increasing translucence of the THFMA-containing semi-IPNs on hydration of a transparent material is where the water is clustering in pores that are larger than the wavelength of light, causing it to scatter, and/or there are blocky components. Only in EEMA-containing materials was transparency upon hydration obtained.

The polar and dispersive components of the surface free energy were more responsive to changes in the amount of PU5 in the EEMA-containing semi-IPNs than THFMA, perhaps an indication of increased interaction between the two systems.

THFMA semi-IPNs indicated that they spoiled more for both protein and lipid in artificial tears than their EEMA equivalent, possibly as a consequence of poorer compatibility and/or the more hydrophobic nature of THFMA. It has been suggested by some that hydrophobic surfaces interact more strongly with proteins than hydrophilic surfaces[99]. Although differences in the surface free energies between THFMA and AMO materials were not of the magnitude to account for the spoilation differences, the contact angle techniques would not be of the sensitivity to account for molecular interactions between complex proteins and the macromolecular structure of the copolymer.

The high EWCs of the semi-IPNs containing AMO had the effect of diluting the effect of the interpenetrant on the strength of the materials. As 10% PU5 did not appear to be the maximum loading possible, perhaps the addition of more would have increased the interaction between the hydrophilic hydrogel and the polyurethane to the extent that

mechanical properties were more similar to the Copolymer X-PU5 materials. The Copolymer X-PU5 materials were completely phase-separated post-polymerisation and had a much lower EWC than the semi-IPNs containing AMO and returned the strongest, stiffest materials. In this case, obviously the interpenetrant was the dominating system.

The effect of EWC on the stiffness of the semi-IPNs is shown in Figure 6.19. The profile of the data points has been described previously be Corkhill[44], who also investigated semi-IPNs. Although material effects are factors in mechanical properties, even with an interpenetrant present, the EWC of the material is the dominant property in determining the mechanical strength of a material.

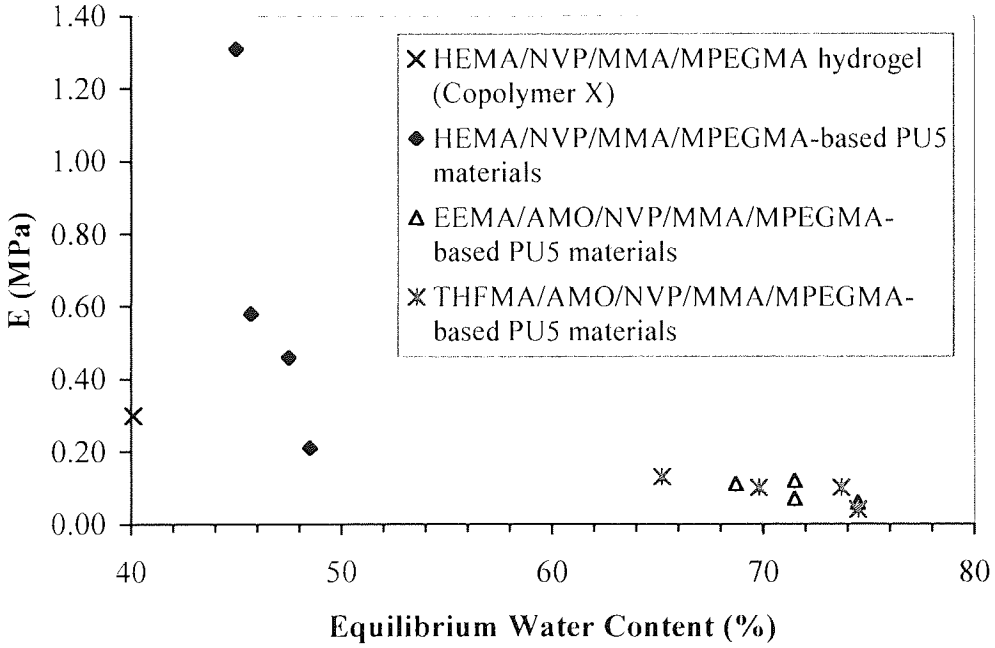

Figure 6.19 The effect of EWC on the stiffness of semi-IPN materials.

CHAPTER 7

Hydrophilic Grafting Of Silicone Elastomers

"If it weren't for marriage, men would spend their lives thinking they had no faults at all."

Anonymous.

7.1 Aim

Previous work in this thesis has focused on developing high water content hydrogels, which include ionic monomers, methoxy-terminated PEG and other, more 'traditional' constituents such as N-vinyl pyrrolidone.

For conventional, high water content hydrogels, water retention and surface wettability are important parameters for success. It could be argued that for a lens to be seen and to behave as an extension of the cornea, it must be as similar to the cornea as possible to reduce biocompatibility problems. As such, a high water content would seem an essential attribute for this situation to complement the 81% water content (approx.) of the cornea.

The physical coating of a hydrogel layer onto the substrate surface would not solve the problem of wettability due to gradual desorption that would occur. Two methods to successfully incorporate hydrophilicity are bulk polymerisation incorporating hydrophilic monomers, or grafting the hydrophilic monomer onto the surface.

The contact lens company Essilor International produce silicone materials and employ grafting technology to obtain a wettable material; glucuronic acid is grafted to cross-linked PDMS with epoxy groups[100]. However, problems with reproducibility and stability exist and is the subject of continued research.

The availability of an Essilor lens material, cross-linked PDMS with epoxy groups (Figure 7.1), allowed an excellent opportunity to graft lightly cross-linked hydrogels developed earlier in this work to a silicone lens. Unfortunately, the exact distribution of the epoxy groups on the surface was not known but as comparative work, this was not an issue.

By activating the surface and grafting various monomers utilized in conventional hydrogel chemistry, an attempt at modifying the surface of the silicone elastomer would be made.

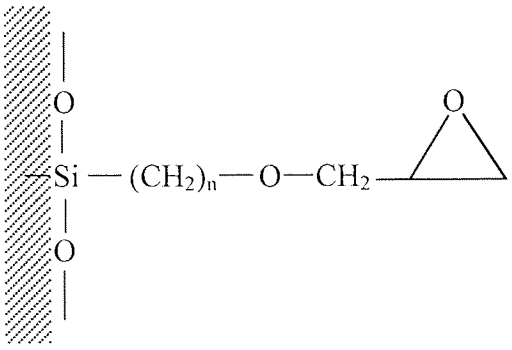

Figure 7.1 Cross-linked poly(dimethyl siloxane) with epoxy groups at the lens surface.

7.2 Introduction: A Brief History of Silicone Lenses

As an initial model, poly(methyl methacrylate), PMMA, was seen as a possible means to providing extended wear. The material had already been used as conventional hard lenses, designed and fitted in a manner so that oxygen supply was possible via tear fluid movement behind the lens. The optical characteristics of PMMA (light weight, discoloration resistance, machining qualities) and its non-irritant behaviour made it a good model to follow. Its disadvantages included mechanical irritation and discomfort.

Silicone rubber, or poly(dimethyl siloxane) (Figure 7.2), was considered as a prospective material due to its high oxygen permeability and transparency but these properties were not enough to overcome the major problems of hydrophobicity, high lipophilicity and lens adhesion (hence no tear exchange under the lens). Surface treatments to improve wettability, at the expense of oxygen permeability, showed no great degree of permanence and was therefore unsuccessful. That it was softer and more flexible than rigid PMMA was, however, a considerable advantage.

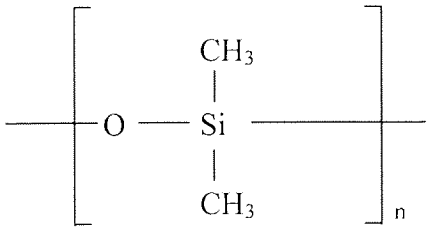

Figure 7.2 The structure of poly(dimethyl siloxane), PDMS.

The drawbacks of conventional hydrogel materials for extended wear stem from poor oxygen permeability and dehydration, which compromise corneal health and pre-condition the cornea to infection. New materials coming onto the market attempted to address these problems by means of applying new chemistry. This chemistry has been developed and protected in many patents to make silicone monomers more hydrophilic, which could then be polymerised with other hydrophilic monomers to give a new class of material, the silicone hydrogel.

Silicone-based hydrogels were seen as a chance to combine the high oxygen permeability of siloxanes with the comfort and biocompatibility of high water hydrogels. Silicone-based monomers, being hydrophobic, were insoluble in hydrophilic monomers and polymerisation resulted in opaque, phase-separated materials. Improved chemistry provided the ability to combine the high oxygen permeability of siloxanes with the comfort and biocompatibility of high water hydrogels. Approaches varied from incorporating hydrophilic monomers into the material to grafting a thin layer of what was essentially a hydrogel onto the lens surface, giving dehydration problems similar to those seen with conventional high water lenses.

Making silicone-containing, wettable materials was the focus of a great deal of subsequent work throughout the 1980's. Tris(trimethylsiloxy)silyl propyl methacrylate, known commonly as TRIS (Figure 7.3), was an important monomer for contact lenses by virtue of its oxygen permeability and machineability but it showed poor wettability and the siloxane was lipophilic. TRIS had already been successfully used in the preparation of RGP lens materials. Combining TRIS with hydrophilic monomers raised difficulties in mixing, due to the formation of phases. Many patents describe modifications to TRIS by incorporation of hydrophilic groups into the monomer to increase its compatibility with hydrophilic monomers, some of which are discussed in a review by Tighe[101].

The synthesis of more hydrophilic silicone monomers has led to minimised phase separation, enabling transparent materials to be produced in conjunction with hydrophilic monomers.

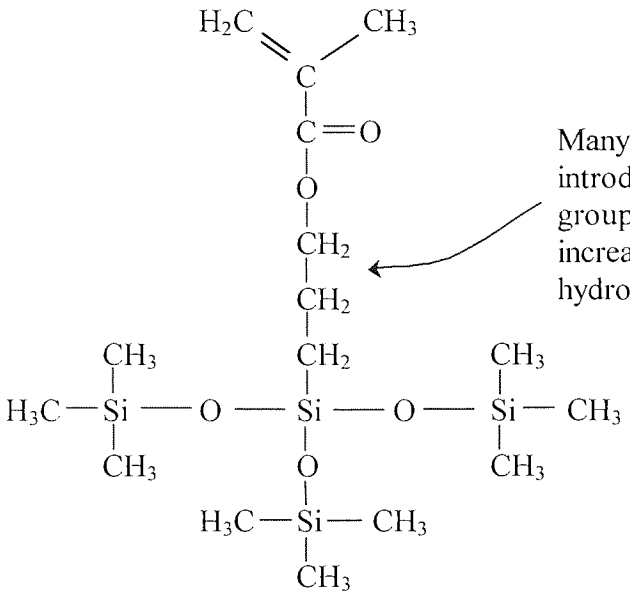

Figure 7.3 Structure of tris(trimethylsiloxy)silyl propyl methacrylate, TRIS.

Silicone-based monomer development has produced a range of candidate materials for both gas permeables and silicone hydrogels. Derivatives of TRIS, the monomers aimed to reduce the phase-separation seen with hydrophilic monomers and to increase biocompatibility, or more simply to increase oxygen permeability.

One of the earliest patents by Tanaka *et al*[102] in 1979 proposed the use of tris(trimethylsiloxy)silyl propyl glycerol methacrylate (SIGMA), a TRIS methacrylate derivative, which was soluble with hydrophilic monomers such as HEMA and NVP and the resulting materials showed a wide range in water contents with high oxygen permeability. A methacrylate substituted by methacrylamide was another approach by Harvey[103] and transparent, hydrophilic, water absorbing materials were achieved by the use of tris(trimethylsiloxy)silyl propyl methacryloxyethylcarbamate (TSMC). TSMC showed significantly improved compatibility over TRIS. More recently by Bambury and Seelye[104], FDA-approved tris(trimethylsiloxy)silyl propyl vinyl carbamate (TPVC) was used in a hydrogel system, based on a vinyl carbamate substituted TRIS-based material.

The difficulties of putting these modifications into practice would explain why two decades would pass before the noisy launch of silicone-hydrogel contact lenses in the late 1990's.

The use of siloxanes containing hydrophilic blocks led to another line of silicone hydrogels. Lai[105], of Bausch & Lomb, was one of the first to use urethane-silicone block copolymers (URE-Si) and compatibility with hydrophilic monomers, mechanical control, water content control and oxygen permeability were stated as advantages. A Kunzler[106] patent, also from Bausch & Lomb, described novel fluorosiloxane-containing monomers and claimed to be especially useful for the preparation of contact lens materials. The monomers were designed to improve the compatibility of TRIS-like monomers in hydrophilic monomers, again referring to the main aim of many patents in overcoming compatibility issues mentioned earlier. The incorporation of fluorine gave enhanced oxygen permeability, a fact known and exploited in patents of the 1970's and early 1980's. Novel difunctional acrylic siloxanes are found at the heart of Bausch & Lomb gas permeable technology, as is the addition of hydrophilic moieties for surface wettability.

Macromers are large monomers formed by pre-assembly of structural units that are designed to bestow particular properties on the final polymer and this technology has been exploited by CIBA[107]. An extensive and important patent refers to an additional parameter to wetting, mechanicals and oxygen permeability in judging a lens and is linked to the lens movement on the eye; hydraulic and ionic permeability. It describes the use of macromers that impart 'oxyperm' and 'ionoperm' properties through formation of a co-continuous biphasic structure that allows necessary transport events to occur sufficient for corneal health. The novelty of this work is in the morphology. Conventional phase-separated materials have phases of different refractive indices and phase dimensions larger than the wavelength of light (ca. 500nm) which results in light scattering and opacity. In this invention, the two phases exist along with optical clarity, possibly due to the presence of interphase regions. The problems of on-eye movement for silicone hydrogels may be overcome through the novel morphology teaching of the CIBA patent.

The actual chemistry involved, including the specifics of monomer structures, and transport mechanics are beyond the scope of this work. What is interesting about this new generation of silicone hydrogels is that they still require surface treatment to become more wettable. PureVision™ (Balafilcon) from Bausch & Lomb has a plasma-treated surface and Focus® Night & Day™ (Lotrafilcon) from Ciba Vision has a 25nm plasma

coating, itself difficult to characterize due to the chemical changes that would occur to the monomers when converted into plasma.

7.3 Plasma Oxidation

The material surface may be physically modified using plasma glow discharge (low pressure). 'Plasma' signifies a mixed state of ionised gases that consists of electrons, ions, gas atoms and molecules in either their ground or excited state. Plasma oxidation renders a surface more wettable to allow subsequent grafting chemistry. The components and physics of plasma may be found in detail in the work by Singh-Gill[108].

Plasma is generated by a high electric potential field and when applied under a reduced pressure, the treatment is performed by the plasma-generated glow discharge. In this work, a low-pressure radio frequency (100kHz - 30MHz) generated discharge (cold r.f.) is used to produce the plasma. An electric field of sufficient magnitude is applied between two electrodes to low-pressure air, causing it to start breaking down[109]. Free electrons, already present in the gas due to processes such as filed emission or photoionisation, are accelerated in the applied electric field and gains kinetic energy. During its procession, it collides with gas atoms and loses energy. Elastic collisions (with neutral species) deflect the path of the electron with little energy loss. Inelastic collisions (where the electron has sufficient energy) such as excitation may occur, causing plasma to 'glow' or ionise. This frees another electron which is accelerated through the field, and so on. Electrons may be regarded as oscillating between the electrodes in RF discharge, not necessarily reaching them and so ionisation through collision removes the dependence of the electron reaching the anode to produce another electron seen in DC (Direct Current) generated discharge with argon gas. Utilizing air, free radicals are produced, such as in Equation 7.1 and bring about oxidation at the material surface to create polar groups. Radicals are atoms, molecules or complexes that have one or more unpaired electron. Both long- and short-lived radicals play major roles by virtue of their highly reactive nature.

$$e^- + O_2 \rightarrow 2O\bullet + e^- \qquad \textit{Equation 7.1}$$

It is well known that plasma exposure alone makes surfaces more hydrophilic and plasma glow has been used to enhance blood compatibility of vascular prosthesis[110]. Its utility in this work comes as a pre-treatment for graft polymerisation of a monomer onto the substrate. Oxygen radicals would attack the surface and produce a combination of radical sites, aldehydes, alcohols and carboxylic acid groups and so reduce the interfacial energy between the elastomer and the aqueous grafting medium.

Initiation for surface graft polymerisation may also be via peroxides, not only free radicals. The radicals introduced onto the surface can react with atmospheric oxygen to yield peroxide groups capable of generating peroxy radicals when heated or brought into contact with a redox reagent.

More difficult procedures for surface treatment include plasma polymerisation, where polymers are deposited in a thin film layer onto the substrate by plasma polymerisation of monomer under glow discharge. This has been used in an attempt to modify the surface properties of contact lenses[111].

7.4 Graft Polymerisation

The redox reagent potassium persulphate ($K_2S_2O_8$) is used in aqueous chemistry as an initiator of grafting chemistry. In this work, it was used to work up the surface of the plasma-treated material prior to grafting, possible due to its degradation into free radicals that can react with water, shown in the equations below.

$$^{-}O_3S–O–O–SO_3^{-}{}_{(aq)} \rightarrow 2SO_4^{-}\bullet \qquad \textit{Equation 7.2}$$

$$2SO_4^{-}\bullet + H_2O \rightarrow HO\bullet + [HSO_4]^{-} \qquad \textit{Equation 7.3}$$

The hydroxyl radical may then react with the radicals present on the material surface, increasing the hydrophilicity of the surface and further reducing the interfacial energy that exists between the relatively hydrophobic material and the aqueous environment that was to be used for the grafting chemistry.

Graft polymerisation of monomers requires the generation of active species to initiate polymerisation. Ammonium cerium (IV) nitrate in aqueous solution has been investigated in grafting acrylamide onto polyurethane[112]. It was proposed that the complexation of the polyurethane substrate with the cerium ion yielded polymer radicals, which initiated free-radical graft polymerisation shown in Equation 7.4 (where UH = polyurethane).

$$UH + Ce^{4+} \rightleftharpoons [complex] \longrightarrow U\bullet + Ce^{3+} + H^{+} \qquad \textit{Equation 7.4}$$

Cerium is a metal agent that facilitates grafting from hydroxyl groups in aqueous solution[113-116]. By this method, vinyl monomers may be grafted onto a polymer surface.

The inability of AZBN to initiate graft polymerisation[117] is considered to be due to the inferior capacity of the resonance stabilized 2-cyano-2-propyl radicals, $Me_2\dot{C}(CN)$, in an environment that could initiate grafting[118].

7.5 Wettability

Performing dynamic contact angle measurements and comparing the results for each treated material, versus each other and against current commercial materials, presented a simple method for evaluating the treated/modified surface. This method has been discussed in Chapters One and Two.

7.6 Method of Grafting

7.6.1 Materials

Reagent	Formula	M.Wt.	Supplier
Ammonium cerium (IV) nitrate a.k.a. ceric ammonium nitrate	$(NH_4)_2Ce(NO_3)_6$	548.23	Aldrich
Potassium persulphate	$K_2S_2O_8$	270.33	Aldrich
Saline (ReNu)	$NaCl_{(aq)}$	n/a	Bausch & Lomb

Table 7.1 Reagents used in grafting work.

AZBN, EGDMA and all monomers used are detailed in Chapter Two (Section 2.1).

7.6.2 Procedure

The silicone material was placed in an r.f.-generated plasma field for approximately 5-10 minutes on each side. Upon removal, the material was washed in a 10% solution of potassium persulphate at 60°C for 45 minutes with a nitrogen bleed. Following persulphate pre-initiation, the material is rinsed in warm saline for about 30 minutes.

In the final step, the material is placed in a grafting mixture and kept at 40°C for 1 hour, again out-gassed with nitrogen. In 100ml of water, the grafting initiator ammonium cerium (IV) nitrate is added to 0.05% by weight and the grafting monomers make up 10 parts by volume.

The material was then placed in distilled water for 3-5 days prior to testing on the DCA measuring system from which a hysteresis could be calculated giving an indication of the relative mobility of the surface in terms of the presentation of hydrophilic and hydrophobic groups in air and water. This was discussed earlier in Chapter One.

7.7 Results and Discussion

The materials were subjected to different treatments to investigate the following:

- The dependence on suitable surface groups affecting the efficacy of grafting
- The effect of plasma treatment on grafting
- The effect of AZBN on grafting
- The effect of grafting AMO vs. NVP on the surface properties
- The effect of monomer hydrophilicity on the resulting surface properties

All materials were evaluated by DCA measurements.

7.7.1 The Effect of Surface Groups on the Efficacy of Grafting

In addition to the PDMS with grafted epoxy groups material, PDMS without surface epoxy groups was available, also from Essilor. To each material, plasma treatment was applied and the procedure outlined in Section 7.6.2 carried out to completion. The monomer grafted to the materials was in this case N,N-dimethyl acrylamide, NNDMA.

The DCA graphical output for the PDMS material is shown in Figure 7.4 and for the PDMS with epoxy groups in Figure 7.5.

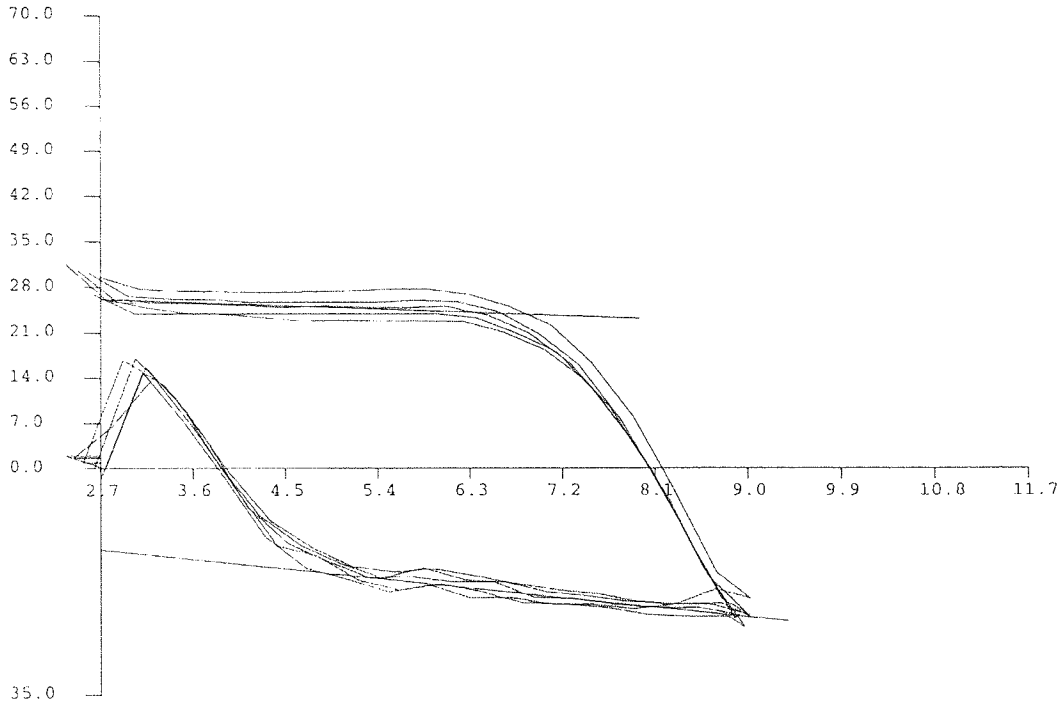

Figure 7.4 Graph showing wetting hysteresis of Essilor silicone lens with no surface epoxy groups, plasma-treated and subject to grafting reaction with NNDMA.

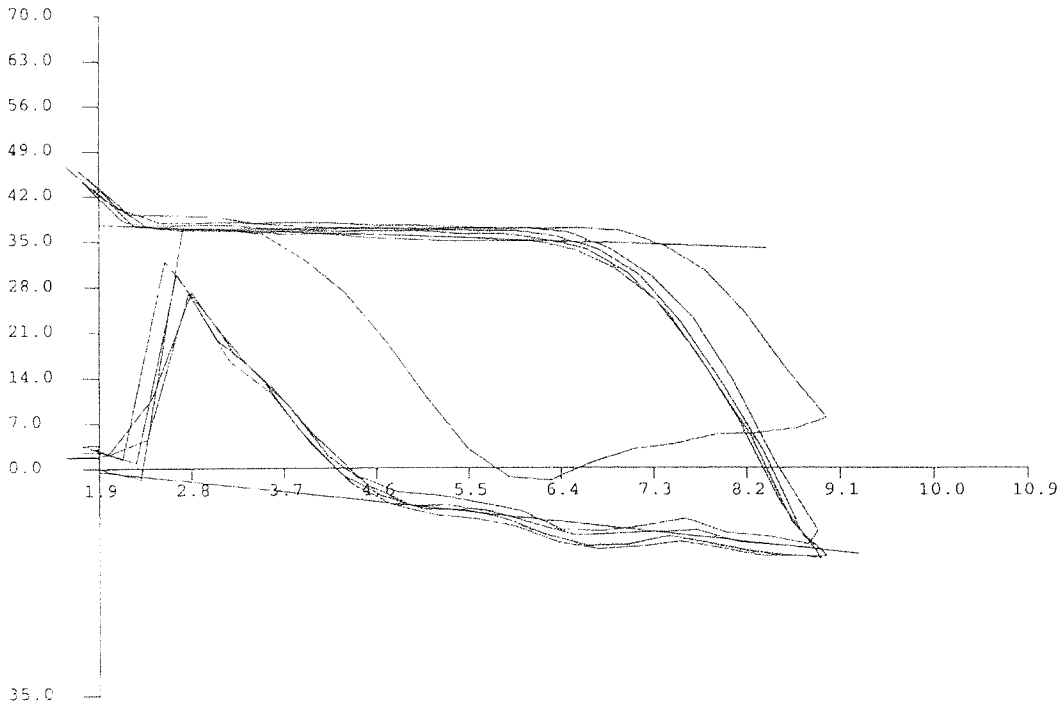

Figure 7.5 Graph showing wetting hysteresis of Essilor silicone lens with surface epoxy groups, plasma-treated and subject to grafting reaction with NNDMA.

The advancing (θ_A) and receding (θ_R) angles for these materials are shown below in Table 7.2.

Epoxy groups	θ_A	θ_R	Hysteresis, θ_H	Surface tension of water, S_T
No	107.5°	51.1°	56.4°	69.1 mN m^{-1}
Yes	90.6°	40.9°	49.7°	70.7 mN m^{-1}

Table 7.2 Dynamic contact angle measurements of silicone elastomer with or without surface epoxy groups, plasma-treated and grafted with NNDMA.

The wetting angles for the silicone elastomer (with no epoxy groups) prior to any treatment are θ_A = 136.4°, θ_R = 77.1° and θ_H = 59.3°. Plasma treatment and grafting treatment with NNDMA has resulted in a more wettable material, causing the advancing angle to decrease by nearly 30° and the receding to decrease by 26°. The surface was still showing the same degree of mobility with similar hystereses.

The wetting angles for the silicone elastomer with epoxy groups prior to any treatment are θ_A = 124.3°, θ_R = 53.0° and θ_H = 71.3° and the graphical output for this and the two new, commercially available silicone hydrogels, Pure Vision and Focus Night & Day are shown in Appendix F. Following plasma treatment and grafting with NNDMA, a significant improvement in the wettability of the material is observed. The hydrophobicity of the material has been reduced as the advancing angle falls from 124.3° to 90.6° and the hydrophilicity of the immersed hydrated material has increased as the receding angle is reduced from 53.0° to 40.9°. The hysteresis calculated from these figures shows that the surface mobility of the material has been reduced following plasma and grafting treatment.

The results in Table 7.2 indicate that the surface containing grafted epoxy groups has undergone a higher degree of grafting than the PDMS material. This was to be expected and since confirmed by the figures as the outward projecting epoxy groups would be more easily oxidized by plasma and so have more pronounced effect in reducing the interfacial energy between the hydrophobic bulk material and the aqueous grafting medium. Where the plasma had only the PDMS backbone to oxidize, this resulted in an oxidized surface area smaller in size than where epoxy groups were present. Also,

PDMS would be less sterically hindered in rotating the radicals produced into the bulk in an effort to reduce any surface charge on a hydrophobic material, so reducing the oxidized sites available for grafting. The higher hydrophobic character of the plasma-treated/NNDMA-grafted PDMS is shown in a higher θ_A and higher θ_R, although the hysteresis (surface mobility) is only a few degrees larger in magnitude. Even so, this material has undergone a treatment that has made it more wettable and less surface mobile than untreated PDMS with epoxy groups.

7.7.2 The Effect of Plasma Treatment on Grafting

To test whether the plasma treatment was having an effect on the wettability of the final product, an attempt to graft NNDMA to silicone elastomer with epoxy groups that had not been plasma-treated was made and the wetting angles compared to the corresponding plasma-treated material.

Figure 7.6 shows the graphical output obtained on the DCA for this material and it may be compared to Figure 7.5 which was the output for the plasma-treated material. Table 7.2 shows the wetting angles for these two materials and allows the differences to be seen.

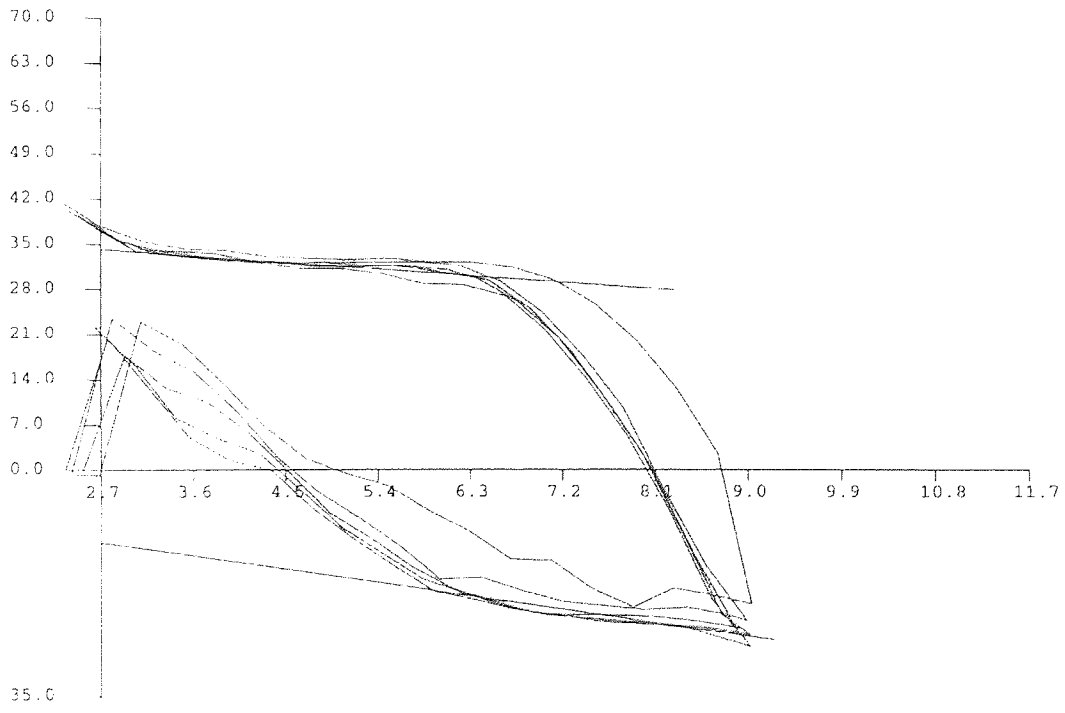

Figure 7.6 Graph showing wetting hysteresis of Essilor silicone lens with surface epoxy groups subject to grafting reaction with NNDMA.

Plasma-treated	θ_A	θ_R	θ_H	Surface tension of water, S_T
No	103.2°	45.8°	57.4°	69.2 mN m^{-1}
Yes	90.6°	40.9°	49.7°	70.7 mN m^{-1}

Table 7.3 Dynamic contact angle measurements of silicone elastomer (with surface epoxy groups), that has or has not been plasma-treated, followed by aqueous grafting chemistry with NNDMA.

For like materials, the effect of plasma-treatment is similar to the effect that the surface epoxy groups have on the wettability of the final material. Plasma oxidation has clearly resulted in a more wettable surface by allowing a greater degree of grafting to take place. This confirms the importance of the following two points that have had roles to play in the reaction chemistry:

- Plasma oxidizes surface groups and so provides hydrophilic sites for the initiators of grafting to attack.
- Plasma oxidation prepares a surface that will have a reduced interfacial tension between the hydrophobic silicone elastomer and the aqueous medium in which the grafting chemistry will take place.

The non-plasma-treated PDMS with epoxy groups, grafted with NNDMA, still shows higher wettability than the original PDMS material, indicating that the aqueous chemistry is still able to oxidize and graft to the material to some degree. The advancing and receding angles are both reduced in comparison (i.e. material is more wettable), although the mobility of the surfaces is almost identical.

7.7.3 The Effect of AZBN on Grafting

As mentioned earlier, AZBN is unable to initiate grafting chemistry. It is however, the initiator used in other chapters in this work for copolymerisation chemistry. With an activation temperature of approximately 50°C (where $k_d = 1.56 \times 10^{-6}$ s^{-1} in water), it was expected that the initiator would still decompose at the 40°C level used in the final grafting medium, to a lesser extent but continuing to have an effect.

Adding AZBN to the grafting medium would provide a competing copolymerisation reaction to the cerium ion initiated grafting reaction, as both initiators would be seeking to react the monomers in the solution. AZBN was dissolved in an organic carrier monomer (usually NVP or AMO) prior to its addition to the aqueous phase.

Three monomer compositions were selected from the hydrogels that have been investigated throughout the course of this work for meeting the following criteria:

- High EWC
- Optical clarity
- Good mechanical properties in relation to the EWC
- Miscibility with the cerium ion reaction medium

A cross-linking molecule (EGDMA) was also to be included in an effort to produce a lightly cross-linked hydrogel graft to help stabilize the surface more than linear grafts could alone.

The three graft compositions that were attempted are shown in Table 7.4 along with the wetting angles obtained on analysis. Cross-linker was added to 1% by weight and where AZBN was added, it was to 0.5% by weight. The silicone elastomer with epoxy groups was used in each case and plasma treatment applied prior to aqueous chemistry.

Initial indications from the results obtained showed that the presence of AZBN did have an effect on the final wettability of the sample, in that a more wettable material with a lower surface mobility was obtained where AZBN was not present. The visual evidence that AZBN was competing with the cerium ion initiator for monomer was confirmed by the presence of copolymer precipitating out of solution.

The graphical outputs for the epoxy elastomer grafted with acrylamide/hydroxypropyl acrylate/N-vinyl pyrrolidone in the presence of AZBN and in the absence of AZBN are shown in Figures 7.7 and 7.8 respectively. A slight reduction in the advancing angle is seen without AZBN, improving the advancing wettability by only 3°. The receding angle increases by 2°, changes that are almost insignificant. Only the difference of almost 5° between the hysteresis of each material leads us to assume the AA/HPA/NVP (no AZBN) grafted elastomer is marginally more wettable.

Monomers grafted (% weight addition)	AZBN	θ_A	θ_R	θ_H	Surface tension of water, S_T
AA : HPA : NVP $23^1/_6 : 66^1/_2 : 10^1/_3$	✓	65.6°	40.2°	25.4°	69.8 mN m^{-1}
AA : HPA : NVP $23^1/_6 : 66^1/_2 : 10^1/_3$	✗	62.6°	42.2°	20.3°	67.9 mN m^{-1}
AA : HPA : AMO $22^1/_2 : 64^7/_{10} : 12^3/_4$	✓	100.8°	43.7°	57.1°	70.7 mN m^{-1}
AA : HPA : AMO $22^1/_2 : 64^7/_{10} : 12^3/_4$	✗	79.1°	49.7°	29.4°	69.5 mN m^{-1}
NVP : SPA 95 : 5	✓	62.5°	43.8°	18.6°	70.4 mN m^{-1}
NVP : SPA 95 : 5	✗	50.3°	41.0°	9.3°	70.6 mN m^{-1}

Table 7.4 Dynamic contact angle measurements of silicone elastomer (with surface epoxy groups), plasma-treated, followed by aqueous grafting chemistry with or without AZBN present.

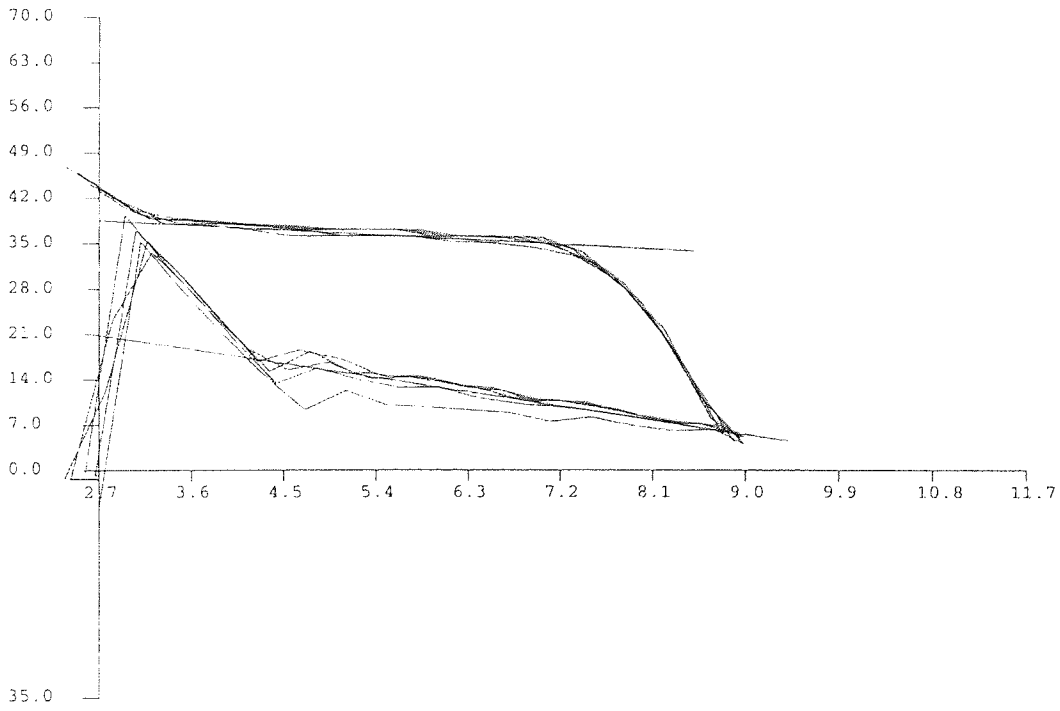

Figure 7.7 Graph showing wetting hysteresis of Essilor silicone lens with surface epoxy groups, plasma-treated and subject to grafting reaction with AA/HPA/NVP/EGDMA in presence of AZBN.

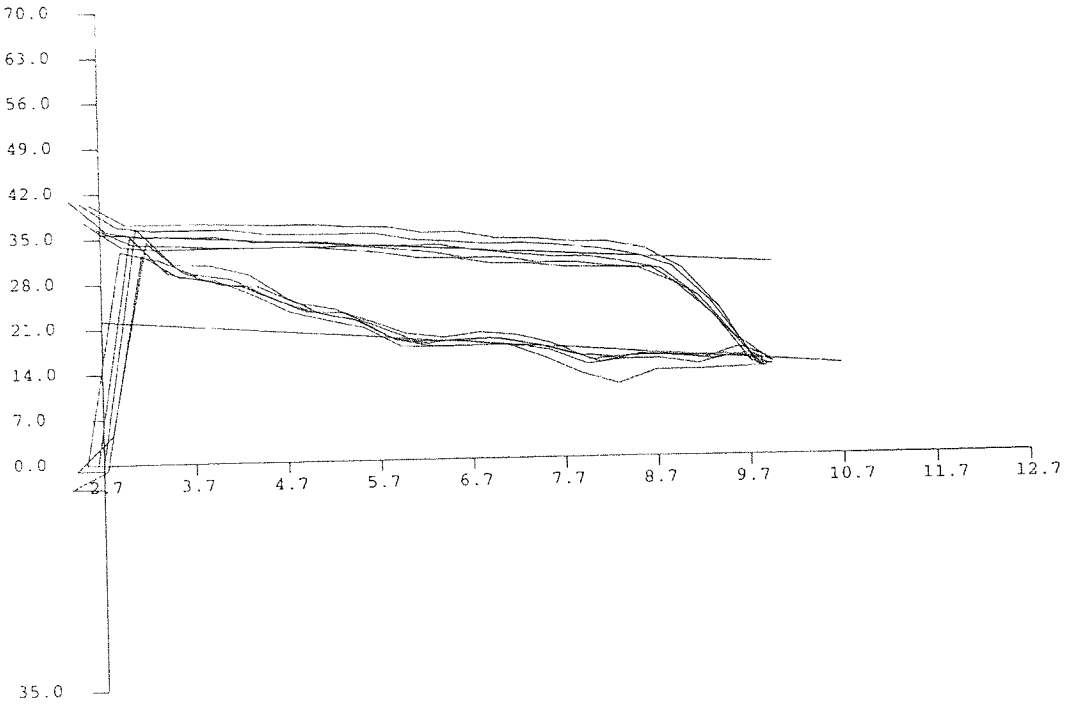

Figure 7.8 Graph showing wetting hysteresis of Essilor silicone lens with surface epoxy groups, plasma-treated and subject to grafting reaction with AA/HPA/NVP/EGDMA.

A more pronounced effect is seen in the grafting of acrylamide/hydroxypropyl acrylate/acryloyl morpholine with and without AZBN present, seen in Figures 7.9 and 7.10 respectively. A decrease in the advancing angle of about 20° is obtained where AZBN is not present, resulting in a hysteresis of 29.4°, much reduced from a hysteresis of 57.1° where AZBN is present. Whether this is saying something about the interaction between AMO and AZBN and/or between AMO and the cerium initiator is not clear.

A clear effect is also seen on the grafting of the final monomer composition, SPA and NVP, seen in Figure 7.11 in the presence of AZBN and in Figure 7.12 without. A large reduction in the advancing angle causes the resulting hysteresis to fall from 18.6° to 9.3° in the absence of AZBN.

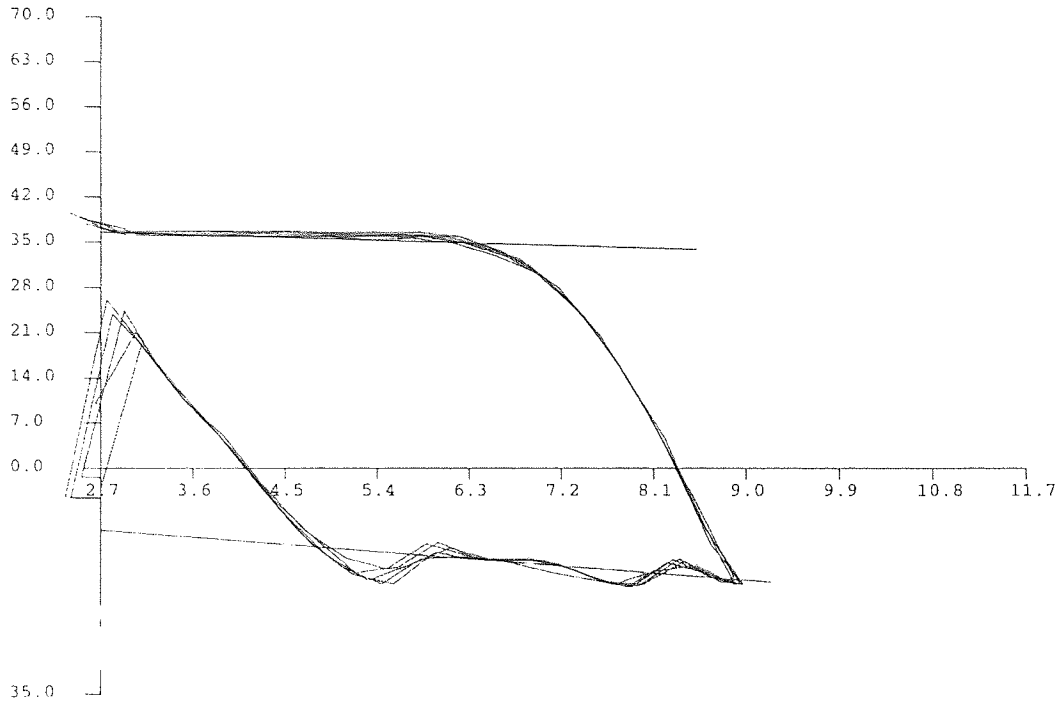

Figure 7.9 Graph showing wetting hysteresis of Essilor silicone lens with surface epoxy groups, plasma-treated and subject to grafting reaction with AA/HPA/AMO/EGDMA in presence of AZBN.

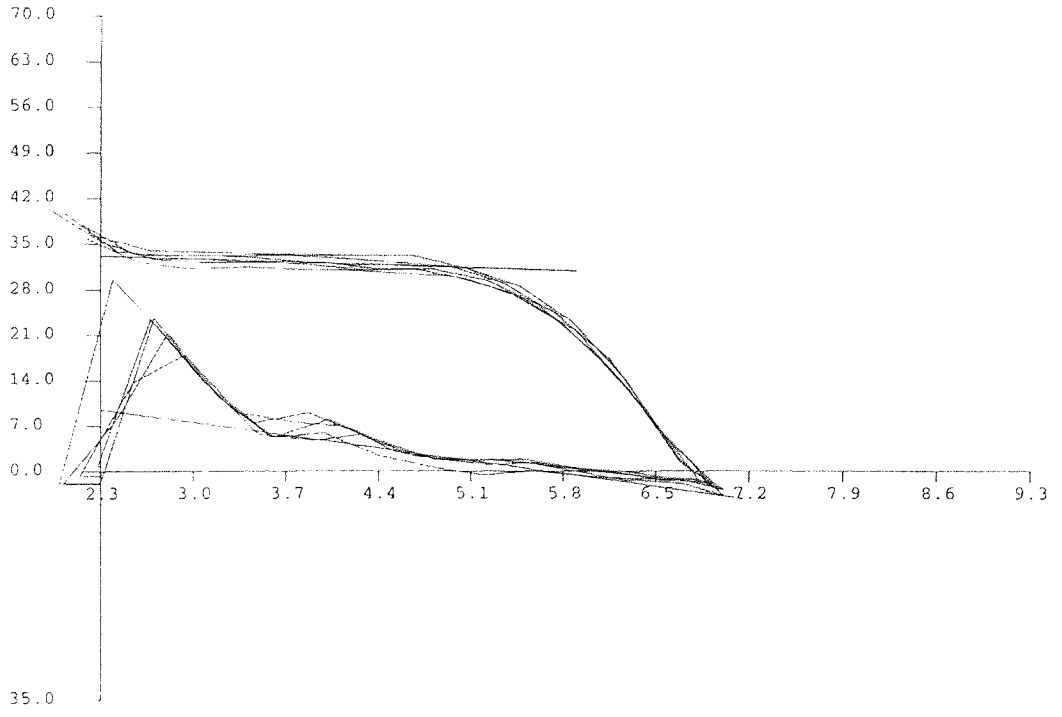

Figure 7.10 Graph showing wetting hysteresis of Essilor silicone lens with surface epoxy groups, plasma-treated and subject to grafting reaction with AA/HPA/AMO/EGDMA.

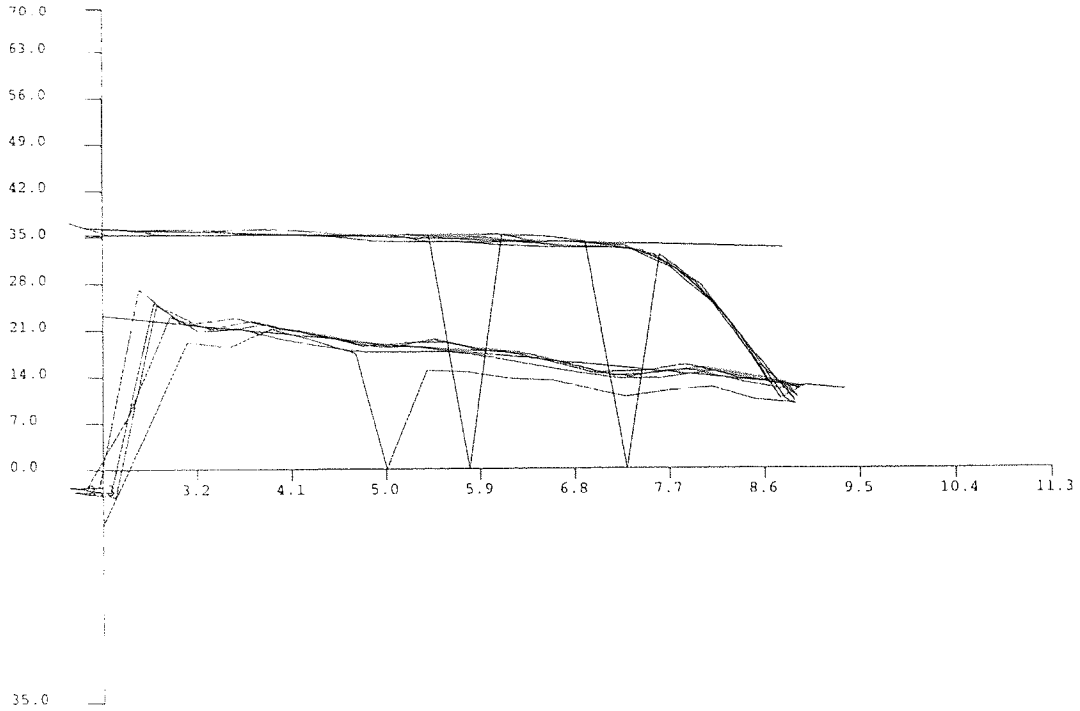

Figure 7.11 Graph showing wetting hysteresis of Essilor silicone lens with surface epoxy groups, plasma-treated and subject to grafting reaction with SPA/NVP/EGDMA in presence of AZBN.

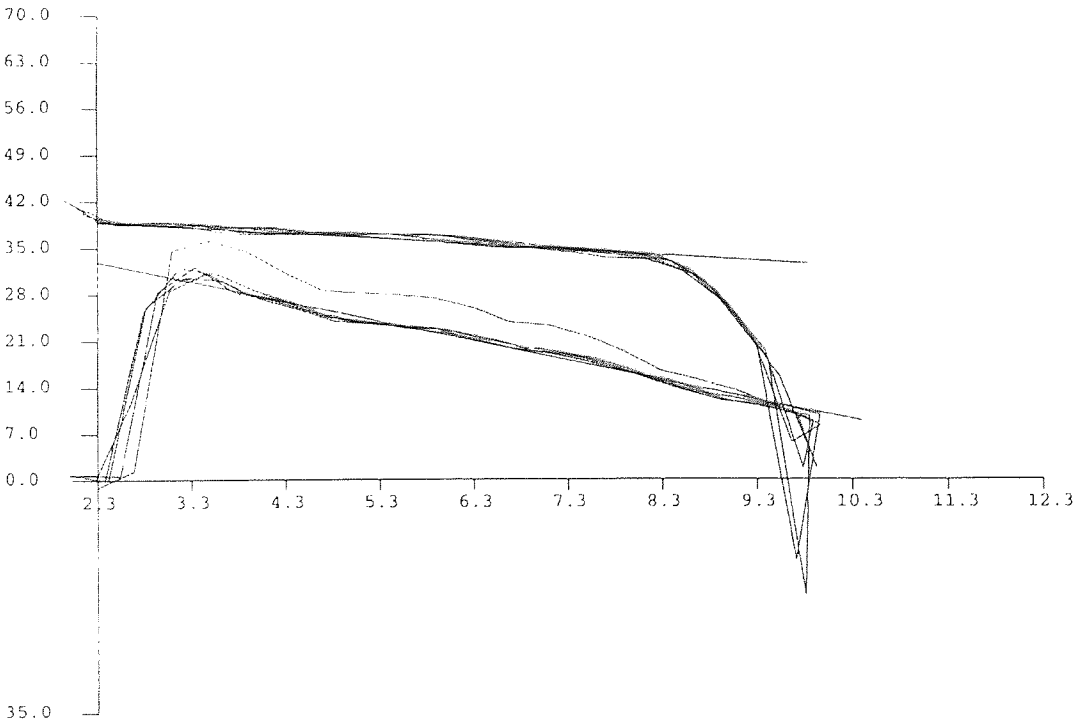

Figure 7.12 Graph showing wetting hysteresis of Essilor silicone lens with surface epoxy groups, plasma-treated and subject to grafting reaction with SPA/NVP/EGDMA.

7.7.3 The Effect of Grafting Monomer Properties on Wettability

The SPA/NVP monomers grafted elastomer shows the highest wettability and lowest surface mobility (hysteresis) of the three compositions, followed by AA/HPA/NVP and then finally AA/HPA/AMO.

The ionicity of SPA easily explains the higher wetting properties of the grafted elastomer over the other two, but the large difference seen between AMO and NVP, assuming that AA and HPA have the same influence on the grafting reaction in each case, raises interesting points for discussion. In Chapter Three, the hydrogels containing equal molar parts of either AMO or NVP showed almost identical properties even though differences towards vinyl polymerisation reactions existed. The possible enhancement of the NVP radical by water was also discussed. This suspected interaction of NVP/water, the reactivity of AMO with cerium ammonium nitrate or its miscibility and interaction with the elastomer surface that accounts for the improved wettability of the NVP-grafted elastomer with AA and HPA as comonomers are all tenable explanations.

The addition of an ionic monomer to the surface is responsible for the much reduced advancing angle seen on the silicone elastomer compared to the other grafted surfaces, showing a more ideal wetting action that is aimed for with biomaterials – that is, a low advancing angle, a low receding angle and a small hysteresis, indicating a wettable, relatively non-mobile surface.

At an interfacial boundary (lens and air), the hydrophilic groups will attempt to orient themselves in such a way as to be away from the hydrophobic air environment. This is a result of an interfacial free-energy minimisation process, a process also seen at conventional hydrogel surfaces and also likely where the use of thin coatings of conventional hydrogels on more hydrophobic substrates occurs. Phase separation and siloxane rearrangement may occur (e.g., in siloxane-based urethane block copolymers) in another instance of interfacial free-energy minimisation. Such reorientation of hydrophilic groups encourages tear break-up and lens deposition, and is a problem inherent in many conventional high water hydrogels. Ionic monomers may be less prone to re-orientation though because it would be energetically unfavourable for it to bury into the non-polar silicone bulk material.

7.8 Discussion

The work contained in this chapter has shown that simple chemistry may be employed to improve the wettability of a silicone elastomer grafted with epoxy groups. These provide a scaffold for plasma oxidation and subsequent aqueous grafting with chosen monomers. The ability of an ionic monomer, SPA, to significantly improve the advancing angle in comparison to hydrophilic monomers such as acrylamide and N-vinyl pyrrolidone has also been shown, but the implications on ocular spoilation of a SPA/NVP graft are not known. Work in Chapter Four has shown that an anionic charge does not necessarily mean disadvantageous protein spoilation, in particular when a sulphonate group, possibly due to a large hydration shell facilitating dynamic exchange.

Two extended wear silicone hydrogel lenses, Focus Night & Day (Ciba Vision) and Pure Vision (Bausch & Lomb), have recently been released commercially. The Pure Vision material, Balafilcon, is treated by plasma oxidation to produce wettable silicate 'islands' on the surface. The Ciba material, Lotrafilcon, has a dense, high refractive index plasma coating applied. In Ciba's case, reactive precursors fed into the plasma undergo structural change before being deposited onto the polymer surface and so precise characterisation of the final coating is difficult.

Early clinical studies report[67] that both materials produce the so called 'mucin balls' (mucin rolled up), which is likely to be due to the shearing effect of the eyelid over the lens. The long-term effect that this phenomenon may have on corneal health has yet to be determined. No doubt further improvements will be effected in the future to enhance the surface.

The monomers used to induce a degree of wettability in silicone patents are still unable to prevent protein deposition from occurring. Recent work has shown that some silicone hydrogel extended wear patients exhibit standard classical lens deposits[119].

Although silicone hydrogels may give transparency, flexibility, high oxygen permeability and a degree of wettability, true biocompatibility has yet to be achieved. An obstacle remaining is essentially that of the surface problem. Clearly, high oxygen permeability is

not enough for successful wear. Wettability is the key word and approaches vary as have been discussed.

The consequential paradox is therefore that achievement of truly successful extended wear still depends upon the ability to control the dehydration and interfacial behaviour of a thin layer of a high water content hydrogel.

CHAPTER 8

Concluding Discussion And Suggestions For Further Work

"How these curiosities would be quite forgot,
did not such idle fellows as I am put them down."
John Aubrey, 1626-97,
Brief Lives.

8.1 Concluding Discussion

From the outset, the aim of this research was to produce high water content hydrogels for biomedical applications, particularly ophthalmic applications. For biocompatibility and biological exchange, it is a widely held belief that a water content matching or close to that of the tissue would produce optimal performance. As the cornea has a water content of approximately 81%, this was a clear target range.

Initial work focused on the patented copolymer materials based on acrylamide, hydroxypropyl acrylate and N-vinyl pyrrolidone (NVP), more specifically, updating the composition with newer synthetic analogues that changed bulk properties. Acryloyl morpholine was shown to produce a more regular sequence distribution using the Polsim software than N-vinyl pyrrolidone, although the reactivity of NVP had been reported to improve significantly in the presence of water. Substituting acrylamide with N-isopropyl acrylamide (NIPA) led to hydrogels that could show smart effects, that is, a water content dependent on the temperature. NIPA is playing an ever-increasing role in hydrogels for drug delivery and many researchers include ionic switches in addition to the temperature switch to achieve maximum volume transition.

The advantage of modifying an existing composition that had found success as a contact lens material was that the general composition had already been approved for biomedical use. As such, incorporating monomers that had been studied in other biomaterial-related work would not raise many questions on toxicology and safety.

The work on these materials highlighted problems of solubility of the acrylamides in the other organic monomers, which were overcome with the addition of water and N-methyl pyrrolidone as a type of solvent bridge between aqueous and organic systems. Another result was that mechanical strength combined with integrity at high water content was obviously difficult to obtain in neutral materials. Although increasing the cross-linking concentration would have had some beneficial effects on the strength, as a means to increased strength it is not ideal for accepted reasons of cross-linker toxicity if leached out.

The role of proteoglycans in nature is quite complex and focus on an appetite for water. The functional groups involved in the high hydrophilicity include sulphonates, carboxylates, amides, and alcohols. The relatively new, commercially available monomers SPI, SPA and NaAMPS possessed functional groups that could potentially produce highly hydrophilic materials, harnessing the ionicity to drive hydration. Again, the monomers were added to a composition that had achieved success as a contact lens but this time based on 2-hydroxyethyl methacrylate (HEMA).

Indeed, highly hydrophilic hydrogels were produced and although mechanical properties suffered in the usual way with high amounts of plasticising water, the structural integrity showed improvement over the neutral acrylamide-based hydrogels studied earlier. Additionally, as charge is thought to detrimentally affect spoilation, it was interesting to find that sulphonate inclusion showed a lower amount of protein spoilation than the neutral, HEMA-based copolymer, although increasing ionicity still meant increasing spoilation. Potentially, sulphonates could show reduced protein adsorption over copolymers containing methacrylic acid, the usual monomer incorporated to produce anionic contact lenses, by virtue of its increased size and hydration shells and hence more dynamic exchange at the interface.

Again, solubility of the solid sulphonates SPI and SPA restricted the amounts that could be incorporated, although for the 10% by weight that was used as the maximum level, dissolution was easily achieved on prolonged mixing in water.

Adding a cationic monomer to sulphonate-containing hydrogels had the effect of bringing the water content back down as ionic interactions within the matrix acted as secondary cross-links as so reducing the volume available for plasticising water. Spoilation studies demonstrated that the dominant presence of a charge acted to show reduced protein spoilation over the copolymers that contained negative and positive groups in almost equal amounts, which presented a near-neutral surface.

Interpenetrants were investigated in an attempt to significantly improve the mechanical strength of hydrogels and it was seen that the effect of an interpenetrant on such properties were determined by, if not restricted by, the hydrophilicity of the surrounding hydrogel. The dilution of the strengthening effect of the interpenetrant is clearly shown

in Figure 6.19. Issues of compatibility were complex, even after obtaining a miscible mix of monomers and the interpenetrant. The compatibility of the polymerised copolymer around the interpenetrant and the water clustering in and around the hydrated semi-IPN were extremely sensitive to the location of hydrophilic moieties in the monomer molecules. Incompatibility of PU5 with HEMA resulted by what appeared to be the presence of the terminal hydroxyl group, as substitution with ethoxyethyl methacrylate produced transparent hydrated materials.

Of the conventional hydrogels produced, a clear effect of water content could be seen on the initial stiffness of the hydrated copolymers. Increasing plasticising water produced less stiff materials. However, clear structural effects could also be seen as materials with the same or similar water contents showing different values of stiffness, seen below in Figure 8.1.

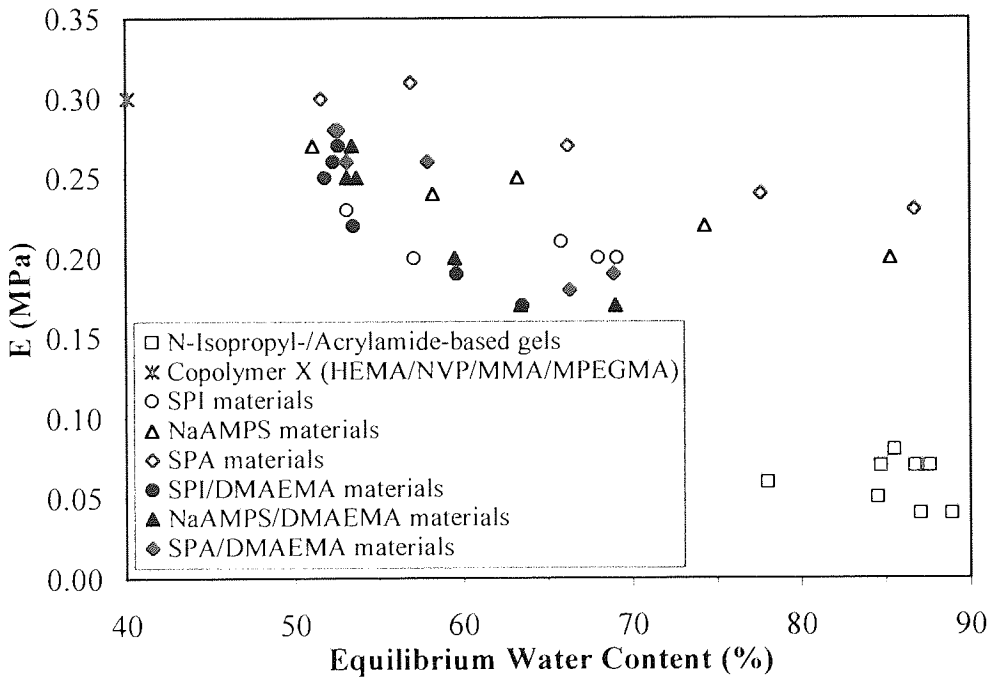

Figure 8.1 Graph showing the effect of equilibrium water content and material composition on the initial stiffness of the hydrogel copolymers studied in this work.

A higher degree of variability was seen in the tensile strengths of the hydrogels, as expected due to the longer test time to obtain tensile strength data and being a measure of

the extent of the material's lengthening network on an applied load. The benefits of the self-association seen in NaAMPS materials are clearly visible, as shown in Figure 8.2.

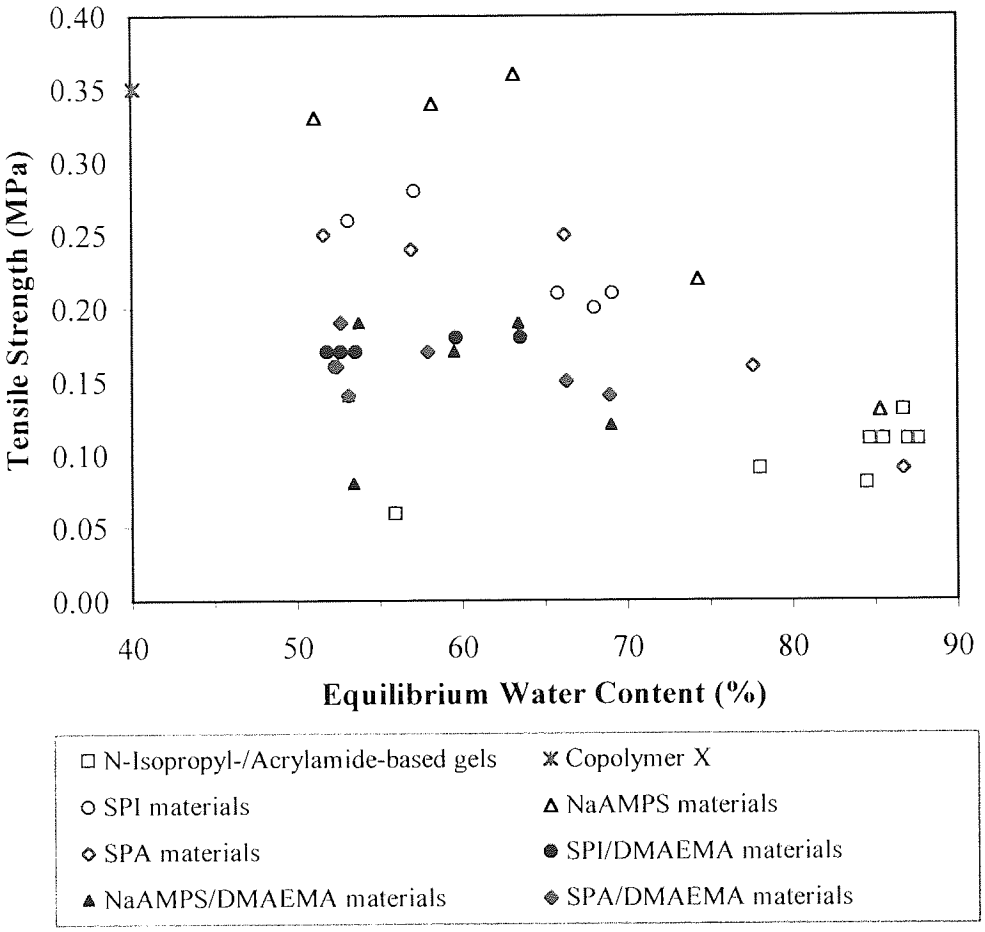

Figure 8.2 Graph showing the effect of equilibrium water content and material composition on the tensile strength of the hydrogel copolymers studied in this work.

The extent of surface energy change on increasing amounts of ionic monomer was minimal. Although clearly a rise in the γ_s^l and γ_s^p (towards those of water) were seen when moving from a non-ionic surface to an ionic surface, once an ionic surface was present, further changes in the surface energies were minimal as discernable by the droplet technique. Obviously surface changes were occurring, as apparent from the spoilation data which reflected the charge component composition, but the presence of charged species and/or a high water content were the factors that controlled and presented the surface properties measured.

In contrast to the bulk production of hydrogels, the problems encountered with solid monomer solubility in other organic monomers meant that these same monomers lent themselves to aqueous grafting chemistry. So, acrylamide, SPA and SPI could be incorporated easily, alongside the other water-soluble liquid monomers such as NNDMA, NVP, HPA and AMO.

A frequently overlooked step in successful grafting onto a hydrophobic substrate is to first reduce the interfacial energy between the surface and the grafting medium, so plasma oxidation was performed for this reason and was shown to have an effect on the efficacy of grafting. The monomers that played a part in producing the most hydrophilic hydrogels produced grafts that substantially increased the wettability of silicone elastomer substrates. In particular, the SPA graft produced a material that showed a very low hysteresis due to the ionic potential of the graft layer. As the material dehydrated on leaving the wetting water, the ionic potential of the surface increased and so on re-insertion into the water, an osmotic drive for re-hydration occurred.

Monomers that in a bulk hydrogel would display dimensional instability in response to pH, tonicity and temperature effects for example, but show hydrophilic character, were then easily applied to grafting. As the substrate was a dimensionally stable silicone elastomer, a grafted layer would result in a material that did not suffer from dimensional instability and so acrylamide and the sulphonates tested were good candidates for biomaterial use as a graft.

Only by characterizing and understanding bulk hydrogels can the effects of neutral, anionic and cationic monomers be applied to a graft layer expected to perform at a biological interface. Even as the dimensionally unstable bulk hydrogels are unsuitable for contact lens applications, their sensitivity to various switches (temperature, pH) lend themselves to biological uses where easily controllable substrate binding and release, as well as volume changes, are required.

8.2 Suggestions For Further Work

Many opportunities for further study have become apparent from this work. Firstly, the temperature-sensitive materials studied were neutral in nature. Published work examines the incorporation of ionic monomers to produce pH and temperature sensitive materials which are able to show larger volume transitions. The acidic monomers typically added are the likes of methacrylic acid, acrylic acid and AMPS, but studies including SPA, which shows similar hydrophilicity to NaAMPS, and SPI have not yet been published.

The dynamic contact angle measurements of the SPA-grafted elastomer seemed to suggest that there was an osmotic drive for re-hydration when the surface re-entered the wetting liquid. The ionic monomers SPI, SPA and NaAMPS, show some structural analogy with natural proteoglycans which must remain hydrated to function properly. Dehydration/rehydration studies of the bulk, HEMA-based hydrogels containing sulphonates may highlight advantageous hydration ability in the face of the thermal drive for dehydration when the temperature rises from room temperature to that of physiological temperature. Use of the Dynamic Vapour Sorption (DVS) apparatus allows the temperature and humidity of the environment of the atmosphere surrounding the test sample to be accurately controlled and the resulting weight changes of the sample in response to temperature and humidity changes measured. Higher levels of sulphonate monomer addition would be possible and could be subsequently tested.

The spoilation studies of the ionic hydrogels were encouraging in that high deposition did not follow ionicity. Whilst this was postulated to be due to the level of hydration shells of water around the sulphonate groups in comparison to methacrylic acid, direct comparisons between such hydrogels, containing similar incorporation of methacrylic acid, were not made. To produce materials with equivalent amounts of the sulphonate acids and methacrylic acid and to repeat the deposition studies would be useful. Also, at each stage of the deposition study, if measurements of protein and lipid deposition were made pre- and post-wash with ReNu, the accumulation that was not due to true material-driven responses, somewhat diminished using the technique, would be reduced.

The effect of pH on the hydrogels containing ionic monomers, particularly the anionic and cationic monomers, was not investigated. Were two opposite charges are present, it

would be expected that pH changes would changes the effect that one charge has on the expression of the other and dimensional and other property changes would result. Whilst not ideal for contact lenses, 'smart' switches in hydrogels are playing an increasingly important role in other biological applications.

The success of the grafting work meant that the effect of many other monomer combinations on the wettability could be investigated. Long-term stability of the grafts could not be tested in this work due to time constraints but is an important factor in future success. Spoilation of grafted whole lenses and subsequent cleaning procedures would give an indication of grafting stability.

The measurement of sample friction has been correlated to comfort[120] in recent years and if the sulphonate grafts do possess a drive for rehydration (or equally, an ability to resist dehydration), then a comparative technique such as friction measurement could go someway to confirm any such claims.

Clearly, the presumed strengthening effect of polyurethane incorporation in high water content hydrogels did not occur as the hydrophilicity of the hydrogel diluted the mechanical properties to levels similar to bulk hydrogels. Adding an interpenetrant with stronger and more specific hydrogen bonding potential such as poly(acrylamido-co-acrylic acid) or poly(acrylamide), whose structures are shown in Figure 8.3, may have a beneficial effect on strength.

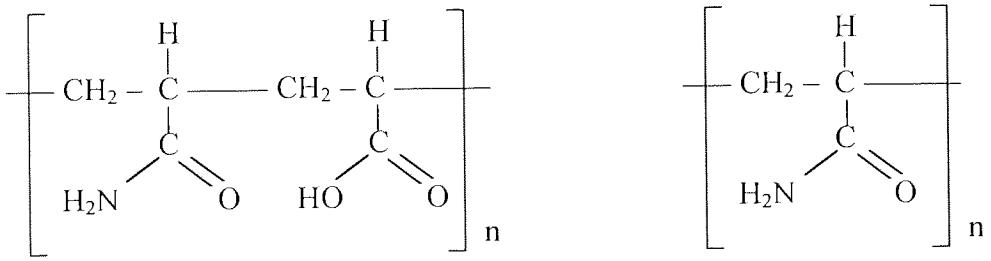

Poly(acrylamido-co-acrylic acid) Poly(acrylamide)

Figure 8.3 Structures of poly(acrylamido-co-acrylic acid) and poly(acrylamide).

The effect of cross-linker and cross-link density opens up another area of study for both bulk hydrogels and grafted layers. DATr was used in bulk hydrogels in this work and EGDMA in the grafted layers. Changing amounts were not investigated and other cross-linkers such as the water-soluble cross-linker methylene-bis-acrylamide would have a part to play in changing water and mechanical properties.

References

"You will find it a very good practice
always to verify your references, sir!"
Martin Joseph Routh (attributed), 1755-1854.

1. Wichterle, O. and Lim, D., Hydrophilic gels for biological use. Nature; 185: 117-118 (1960)

2. General Aniline and Film Corp., PVP: An annotated bibliography II. 21-27 (1951-1966)

3. Sasaki, H, Kojima, M., Mori, Y., Enhancing effect of pyrrolidone derivatives on transdermal penetration of 5-fluorouracil, triamanolone acetonide, indomethacin and fluriprofen. J. Pharm. Sci.; 80: 533-538 (1991)

4. Larke, J. R., Pedley, D. G. and Tighe, B. J., Hydrogels. UK Pat. 1,566,249 (1980)

5. Tighe, B. J. and Gee, H. J., Fluorine-containing hydrogel-forming polymeric materials. US Pat. 4,433,111 (1984)

6. Vanderlaan, Ophthalmic lens polymer incorporating acyclic monomer. US Pat. 5,311,223 (1994)

7. Corkhill, P. H., Fitton, J. H. and Tighe, B. J., Towards a synthetic articular cartilage. J. Biomater. Sci. Polymer Edn; 4(6): 615-630 (1993)

8. Kickhofen, B., Wokalek, H., Scheel, D. and Ruh, H., Chemical and physical properties of a hydrogel wound dressing. Biomaterials; 7: 67-72 (1986)

9. Venkatraman, S. and Gale, R., Skin adhesives and skin adhesion 1. Transdermal drug delivery systems. Biomaterials; 19: 1119-1136 (1998)

10. Galaev, I. Y., 'Smart' polymers in biotechnology and medicine. Russian Chemical Reviews; 64(5): 471-489 (1995)

11. Corkhill, P. H., Hamilton, C. J. and Tighe, B. J., The design of hydrogels for medical applications. Critical Reviews in Biocompatibility; 5(4): 363-436 (1990)

12. Williams, D. F., A model for biocompatibility and its evaluation. J. Biomed. Eng; 11: 185-191 (1989)

13. Sperling, L. H., Interpenetrating networks and related materials. Plenum Press, New York (1981)

14. Frommer, M. A. and Lancet, D., Freezing and non-freezing water in cellulose acetate membranes. J. Appl. Polym. Sci.; 16: 1295-1303 (1972)

15. Taniguchi, Y. and Horigome, S., The states of water in cellulose acetate membranes. J. Appl. Polym. Sci.; 19: 2743-2748 (1975)

16. Lai, Y. C., Free and bound water in water swollen polymer systems/hydrogels and their correlation with water evaporation from hydrogel lenses. Report for Bausch & Lomb Inc. New York (1990)

17. Muller-Plathe, F., Different states of water in hydrogels? Macromol.; 31: 6721-6723 (1998)

18. Mathur, A. M. and Scranton, A. B., Characterization of hydrogels using nuclear magnetic resonance spectroscopy. Biomaterials; 17: 547-557 (1996)

19. Larsen, D. W., Huff, J. W. and Holden, B. A., Proton NMR relaxation in hydrogel contact lenses: correlation with *in vivo* lens dehydration data. Current Eye Research; 9(7): 697-706 (1990)

20. Sung, Y. K., Gregonis, D. E., John, M. S. and Andrade, J. D., Thermal and pulse NMR analysis of water in poly(2-hydroxyethyl methacrylate). J. Appl. Polym. Sci.; 26: 3719-3728 (1981)

21. Yamada-Nosaka, A., Ishikiriyama, K. *et al*, ^{1}H-NMR studies on water in methacrylate hydrogels I. J. Appl. Polym. Sci.; 39: 2443-2452 (1990)

22. Roorda, W. E., de Bleyser, J., Junginger, H. E. and Leyte, J. C., Nuclear magnetic relxation of water in hydrogels. Biomaterials; 11: 17-23 (1990)

23. Pathmanathan, K. and Johari, G. P., Dielectric and conductivity relaxations in poly (HEMA) and of water in its hydrogel. J. Polym. Sci.: Part B: Polym. Physics; 28: 675-689 (1990)

24. Roorda, W. E., Bouwstra, J. A., de Vries, M. A. and Junginger, H. E., Thermal analysis of water in p(HEMA) hydrogels. Biomaterials; 9: 494-499 (1998)

25. Cha, W.-I., Hyon, S.-H. and Ikada, Y., Microstructure of poly(vinyl alcohol) hydrogels investigated with differential scanning calorimetry. Makromol. Chem.; 194: 2433-2441 (1993)

26. Khare, A. R. and Peppas, N. A., Investigation of hydrogel water in polyelectrolyte gels using differential scanning calorimetry. Polymer; 34(22): 4736-4739 (1993)

27. Takigami, S., Kimura, T. and Nakamura, Y., The state of water in nylon-6 membranes grafted with hydrophilic monomers: 2. Water in acrylic acid, acrylamide and *p*-styrenesulphonic acid grafted nylon-6 membranes. Polymer; 34(3): 604-609 (1993)

28. Hatakeyema, T., Yamaucho, A. and Hatakeyema, H., Studies on bound water in poly(vinyl alcohol). Eur. Polym. J.; 20(1): 61-64 (1984)

29. Holly, F. J. and Refojo, M. F., Wettability of hydrogels I. Poly(2-hydroxyethyl methacrylate). J. Biomed. Mater. Res.; 9: 315-326 (1975)

30. Smith, L., Doyle, C., Gregonis, D. E. and Andrade J. D., Surface oxidation of cis-trans polybutadiene. J. Appl. Polym. Sci.; 26: 1269-1276 (1982)

31. Andrade, J. D., Smith, L. M. and Gregonis, D. E., The contact angle and interfacial energetics in biomedical polymers, Vol. 1. J. D. Andrade Ed., Plenum, New York: 249-292 (1985)

32. Morra, M., Occhiello, E. and Garbassi, F., On the wettability of poly(2-hydroxyethyl methacrylate). J. Colloid and Interface Sci.; 149(1): 84-91 (1992)

33. Okano, T., Katayama, M. and Shinohara, I., The interface of hydrophilic and hydrophobic domains on water wettability of 2-hydroxyethyl methacrylate-styrene copolymers. J. Appl. Polym. Sci.; 22: 369-377 (1978)

34. Young, T., An essay on the cohesion of fluids. Phil. Trans. Roy. Soc. (London); 95: 65-87 (1805)

35. Dupre, A., Theorie mechanique de la chaleur. Guthier Villars; Paris: 369 (1869)

36. Owens, D. K. and Wendt, R. C., Estimation of the surface free energy of polymers. J. Appl. Polym. Sci.; 13: 1741-1747 (1969)

37. Fowkes, F. M., Determination of interfacial tensions, contact angles and dispersion forces in surfaces by assuming additivity of intermolecular interactions in surfaces. J. Phys. Chem; 66: 382 (1962)

38. Hamilton, W. C., A technique for the characterization of hydrophilic solid surfaces. J. Colloid and Interface Sci.; 40(2): 219-222 (1972)

39. Hamilton, W. C., Measurement of the polar force contribution to adhesive bonding. J. Colloid and Interface Sci.; 47(3): 672-675 (1974)

40. Fowkes, F. M., Attractive forces at interfaces. Ind. Eng. Chem.; 56: 40 (1964)

41. Tamai, Y., Makuuchi, K. and Suzuki, M., Experimental analysis of interfacial forces at the plane surface of solids. J. Phys. Chem.; 72(13): 4176-4179 (1967)

42. Adamson, A. W., Physical chemistry of surfaces, 3rd Edn., Wiley-Interscience, New York (1976)

43. Andrade, J. D., King, R. N., Gregonis, D. E. and Coleman, D. L., Surface characterization of p(HEMA) and related polymers I. Contact angle methods in water. J. Appl. Polym. Sci., Polym. Symp.; 66: 313-336 (1979)

44. Corkhill, P. H., Novel hydrogel polymers. Ph.D. thesis, Aston University (1988)

45. Franklin, V. J., Bright, A. M. and Tighe, B., Hydrogel polymers and ocular spoilation processes. TRIP; 1(1): 9-16(1993)

46. Baker, D. and Tighe, B. J., Polymers in contact lens applications (VIII) the problem of biocompatibility. Contact Lens J.; 10(30): 3-14 (1981)

47. Ikada, Y., Suzuki, M. and Tamada, Y., Polymer surfaces possessing minimal interaction with blood components, in Polymers As Biomaterials, Shalaby, S. and Hoffman, A., Ratner, B. and Horbett, T., Eds., Plenum, New York: 135-147 (1984)

48. Baier, R. E., and Dutton, R. C., J. Biomater. Res.; 3: 191 (1969)

49. Ruben, M., Soft Lenses, Balliere Tindall, London & J. Wiley Inc., New York (1978)

50. Mirejovsky, D., Patel, A. S. and Rodriguez, B. S., Effect of proteins on water and transport properties of various hydrogel contact lens materials. Current Eye Res.; 10(3): 187-196 (1991)

51. Ashraf, N., Sequence distribution in free radical polymerisations. Ph.D. thesis, Aston University (1995)

52. Ma, J. J., Franklin, V. J., Tonge, S. R. and Tighe, B. J., Ocular compatibility of biomimetic hydrogels. Poster presented at the British Contact Lens Association 9th annual clinical conference, Torquay (1994)

53. Franklin, V. J., Lipoidal species in ocular spoilation processes. Ph.D. thesis, Aston University (1990)

54. Alfrey, T. and Price, C. C., Relative reactivities in vinyl copolymerization. J. Polym. Sci.; 2(1): 101-106 (1947)

55. Alfrey, T. and Goldfinger, G., The mechanism of copolymerization. J. Chem. Phys.; 12: 205-209 (1944)

56. Laurier, G. C., O'Driscoll, K. F. and Reilly, P. M., Estimating reactivity in free radical copolymerizations. J. Polym. Sci.: Polym. Symp.; 72: 17-26 (1985)

57. O'Driscoll, K. F., Comments on 'Relative reactivities in vinyl copolymerization,' Turner Alfrey, Jr. and Charles C. Price, J. Polym. Sci., 2, 101 (1947)., J. Polym. Sci.: Part A: Polym. Chem.; 34: 155-156 (1996)

58. Frank, H. P., Studies on the binary system N-vinyl pyrrolidone-water. J. Polym. Sci.; 13: 187-188 (1954)

59. Senogles, E., Thomas, R. A., Hydrogen bonding effects in the polymerization of N-vinyl pyrrolidone. J. Polym. Sci.: Polym. Letters Edn.; 16: 555-562 (1978)

60. Huglin, M. B. and Rehab, M. M. A.-M., Some observations on monomer reactivity ratios in aqueous and non-aqueous media. Eur. Polym. J.; 23(10): 825-828 (1987)

61. Kaim, A. and Oracz, P., Solvent effects on true terminal reactivity ratios for styrene-methyl methacrylate copolymerization system. Polymer; 40: 6925-6935 (1999)

62. Perec, L., Solvent effect on the radiochemical copolymerization of acrylamide with acrylonitrile. Polym. Letters Edn.; 11: 267-270 (1973)

63. Cameron, G. G. and Esslemont, G. F., Solvent effects in free radical copolymerization of styrene and methacrylonitrile. Polymer; 13: 435-438 (1972)

64. Czerwinski, W. K., Solvent effects on free radical polymerization, 1. Solvent effect on initiation of methyl methacrylate and N-vinyl-2-pyrrolidone. Makromol. Chem.; 192: 1285-1296 (1991)

65. Czerwinski, W. K., Solvent effects on free radical polymerization, 3a. Solvent effect on polymerization rate of methyl methacrylate and N-vinyl-2-pyrrolidone. Makromol. Chem.; 192: 1285-1296 (1991)

66. Maissa, C., Franklin, V., Guillon, M. and Tighe, B., Influence of contact lens material surface characteristics and replacement frequency on protein and lipid deposition. Optom. Vis. Sci.; 75(9): 697-705 (1998)

67. Sweeney, D., Clinical performance of silicone hydrogels. Presented at the British Contact Lens Association Continuing Education Day, Silicone hydrogels – the rebirth of extended wear, Birmingham (1999)

68. Corkhill, P. J., Jolly, A. M., Ng, C. O. and Tighe, B. J., Synthetic hydrogels: 1. Hydroxyalkyl acrylate and methacrylate copolymers – water binding studies. Polymer; 28: 1758-1766 (1987)

69. Trevett, A. S., The mechanical properties of hydrogel copolymers. Ph.D. thesis, Aston University (1991)

70. Pedley, D. G., Hydrophilic polymers. Ph.D. thesis, Aston University (1976)

71. Middleton, I. P., Acrylamide based hydrogels for continuous wear contact lenses. Ph.D. thesis, Aston University (1981)

72. Tighe, B. J. and Gee, H. J., Hydrogel-forming polymeric materials. US Pat. 4,430,458 (1984)

73. Goulding, K., Some aspects of the polymers of acrylamide. B.Sc. project, Aston University (1978)

74. Hirokawa, Y. and Tanaka, T., Volume phase transition in a non-ionic gel. J. Chem. Phys.; 81(12) pt.2: 6379-6380 (1984)

75. Inomata, H., Wada, N., Yagi, Y., Goto, S. and Saito, S., Swelling behaviours of N-alkylacrylamide gels in water: effects of copolymerization and crosslinking density. Polymer; 36(40: 875-877 (1995)

76. Otake, K., Inomata, H., Konna, M. and Saito, S., Thermal analysis of the volume phase transition with N-isopropyl acrylamide gels. Macromolecules; 23: 283-289 (1990)

77. Percot, A., Zhu, X. X. and Lafleur, M., A simple FTIR spectroscopic method for the determination of the lower critical solution temperature of N-isopropyl acrylamide copolymers and related hydrogels. J. Polym. Sci.: Pt. B: Polym. Physics; 38: 907-915 (2000)

78. Huglin, M. B., Liu, Y. and Velada, J. L., Thermoreversible swelling behaviour of hydrogels based on N-isopropyl acrylamide with acidic comonomers. Polymer; 38(23): 5785-5791 (1997)

79. Uchida, K., Sakai, K., *et al*, Temperature-dependent modulation of blood platelet movement and morphology on poly(N-isopropyl acrylamide)-grafted surfaces. Biomaterials; 21: 923-929 (2000)

80. Lee, W.-F., Shieh, C.-H., pH-thermoreversible hydrogels. I. Synthesis and swelling behaviors of the (N-isopropyl acrylamide-co-acrylamide-co-2-hydroxytheyl methacrylate) copolymeric hydrogels. J. Appl. Polym. Sci.; 71: 221-231 (1999)

81. Velada, J. L., Liu, Y. and Huglin, M. B., Effect of pH on the swelling behaviour of hydrogels based on N-isopropyl acrylamide with acidic comonomers. Macromol. Chem. Phys.; 199: 1127-1134 (1998)

82. Artoni, G., Gianazza, E., *et al*, Fractionation techniques in a hydro-organic environment. Analytical Biochem.; 137: 420-428 (1984)

83. Greenley, R. Z., Determination of Q and e values by a least squares technique. J. Macromol. Sci. – Chem.; A9(4): 505-516 (1975)

84. Osman, M. B. S., Dakroury, A. Z. and Mokhtar, S. M., Study on acrylamide-vinyl pyrrolidone copolymer. Polymer Bull.; 28: 181-188 (1992)

85. Kaneko, Y., Nakamura, S., *et al*, Rapid deswelling response of poly(N-isopropyl acrylamide) hydrogels by the formation of water release channels using poly(ethylene oxide) graft chains. Macromolecules; 31: 6099-6105 (1998)

86. Schulz, D. N., Kitano, K., Danik, J. A. and Kaladas, J. J., Copolymers of N-vinyl pyrrolidone and sulfonate monomers, ACS; 165-173 (1989)

87. Benning, B. K., Novel hydrogels for extended wear. Presented at Chemical Engineering and Applied Chemistry Annual Symposium (1999)

88. Durmaz, S. and Okay, O., Acrylamide/2-acrylamido-2-methylpropane sulfonic acid sodium salt-based hydrogels: synthesis and characterization. Polymer; 41: 3693-3704 (2000)

89. Liu, X., Ting, Z. and Hu, O., Swelling equilibria of hydrogels with sulfonate groups in water and in aqueous salt solutions. Macromolecules; 28: 3813-3817 (1995)

90. Oxley, H. R., Hydrogel polymers containing linear and cyclic polyethers. Ph.D. thesis, Aston University (1990)

91. Jones, L., Evans, K., Sariri, R., Franklin, V. and Tighe, B., Lipid and protein deposition of N-vinyl pyrrolidone-containing group II and group IV frequent replacement contact lenses. CLAO J.; 23(2): 122-126 (1997)

92. Franklin, V. J. and Tighe, B. J., Spoilation profiles on high Dk fluorosilicone hydrogel lenses during continuous wear. Presented at Academy 6th International Meeting, Madrid (2000)

93. Franklin, V. J. and Tighe, B. J., A study of spoilation profiles of high Dk fluorosilicone hydrogel lenses. Presented at British Contact Lens Association 24th Annual Clinical Conference, Birmingham (2000)

94. French, K., Novel cationic polymers for use at biological interfaces. Ph.D. thesis, Aston University (1996)

95. Wall, C. A., A study of polycationic disinfectant absorption into the polymer matrix of a contact lens. B.Sc. Chemistry project, Aston University (1995)

96. Lai, Y.-C., Novel polyurethane-silicone hydrogels. J. Appl. Polym. Sci.; 56: 301-310 (1995)

97. Young, R., Lydon, F. and Tighe, B., Polyurethane based hydrogel IPNs for ophthalmic application. Presented at the 8th symposium on the materials science and chemistry of contact lenses, New Orleans (1996)

98. Young, R. A., Synthetic articular cartilage production using semi-IPN technology. B.Sc. Appl. Chemistry project, Aston University (1994)

99. Castillo, E. J., Koenig, J. L., Anderson, J. M. and Lo, J., Characterization of proteins adsorption on soft contact lenses I. Conformational changes of adsorbed serum albumin. Biomaterials; 5: 319-325 (1984)

100. Frances, J. M. and Wajs, G., Elastomere de silicone mouillable conveant a la fabrication de lentilles de contact. Eur. Pat. EP 317,377 (1989)

101. Tighe, B. J., Silicone hydrogels – how do they work? In Silicone hydrogels, the rebirth of continuous wear contact lenses, D. Sweeney Eds., Butterworth-Heinemann, Oxford (2000)

102. Tanaka, K., Takahashi, K., Kanada, M., *et al*, Copolymers for soft contact lenses, its preparation and soft contact lens made therefrom. US Pat. 4,139,513 (1979)

103. Harvey, T. B., Preparation of hydrophilic siloxysilylalkylacrylamide monomers and dimmers for contact lens materials and contact lenses fabricated therefrom. US Pat. 4,711,943 (1987)

104. Bambury, R. E. and Seelye, D. E., Eur. Pat. EP 396,364 (1990)

105. Lay, Y. C., Friends, G. D. and Valint, P. L., Wettable silicone hydrogel compositions and methods for their manufacture. WO 93/09155 (1993)

106. Kunzler, J. and Ozark, R., Fluorosilicone hydrogels. US Pat. 5,321,108 (1994)

107. Griesser, H. J., Laycock, B. G., Papaspiliotopoulos, E., *et al*, Extended wear ophthalmic lens. WO 96/31792 (1996)

108. Singh-Gill, U., A novel plasma-etching and emission monitoring system (PEEMS) to assess protein and lipid spoilation for hydrogel contact lenses. Ph.D. thesis, Aston University (1997)

109. Biederman, H. and Osada, Y., Plasma polymerization processes, Plasma technology 3, Elsevier Science, New York (1992)

110. Chandy, T., Das, G. S., Wilson, R. F. and Rao, G. H. R., Use of plasma glow for surface-engineering biomolecules to enhance blood compatibility of Dacron and PTFE vascular prosthesis. Biomaterials; 21: 699-712 (2000)

111. Yasuda, H., Baumgartner, M. O., *et al*, Ultrathin coating by plasma polymerization applied to corneal contact lens. J. Biomed. Mater. Res.; 9: 629-643 (1975)

112. Feng, X. D., Sun, Y. H. and Qiu, K. Y., Reactive site and mechanism of graft copolymerization onto poly(ether urethane) with ceric ion as initiator. Macromolecules; 18: 2105-2109 (1985)

113. Iranpoor, N., Baltork, M., Zardaloo, F. S., Ceric ammonium nitrate, an efficient catalyst for mild and selective opening of epoxides in the presence of water thiols and acetic acid. Tetrahedron; 47(47): 9861-9866 (1991)

114. Bamford, C. H. and Al-Lamee, K. G., Studies in polymer surface functionalization and grafting for biomedical and other applications. Polymer; 35(13): 2844-2852 (1994)

115. Gurdag, G., Yasar, M. and Gurkaynak, M. A., Graft copolymerization of acrylic acid on cellulose: reaction kinetics of copolymerization. J. Appl. Polym. Sci.; 66: 929-934 (1997)

116. Athawale, V. D., Rathi, S. C. and Lele, V., Graft copolymerization on to maize starch – I. Grafting of methacrylamide using ceric ammonium nitrate as an initiation. Eur. Polym. J.; 34(2): 159-161 (1998)

117. Allen, P. W. and Merrett, F. M., Polymerization of methyl methacrylate in polyisoprene solutions. J. Polym. Sci.; 22: 193-201 (1956)

118. Ceresa, R. J., Block and graft copolymers. Butterworth & Co., London (1962)

119. Fonn, D., The ageing silicone hydrogel. Presented at the British Contact Lens Association Continuing Education Day, Silicone hydrogels – the rebirth of extended wear, Birmingham (1999)

120. Young, R. A., Synthesis and characterisation of hydrogel polymers for medical applications. Ph.D. thesis, Aston University (1998)

Appendix A

Derivations Applied In Study

The Q and e Approximation For N-Isopropyl Acrylamide.

Reactions where Q and e values for monomer 1 are known, determine Q and e of N-isopropyl acrylamide working back from reactivity ratio equations,

$$e_2 = e_1 \pm (-\ln r_1 r_2)^{1/2}$$

$$Q_2 = Q_1/r_1 . \exp(-e_1(e_1-e_2))$$

Monomer 1	Monomer 2	r_1	r_2	N-Isopropyl acrylamide	
				Q_2	e_2
Acrylamide	N-Isopropyl acrylamide	0.5	1.00	0.23	0.54
Butyl acrylate	N-Isopropyl acrylamide	0.8	0.4	0.38	0.85
Methyl acrylate	N-Isopropyl acrylamide	1.2	0.26	0.45	0.64

Plot Q and e values on following axes and derive average values for Q and e by Greenley approximation,

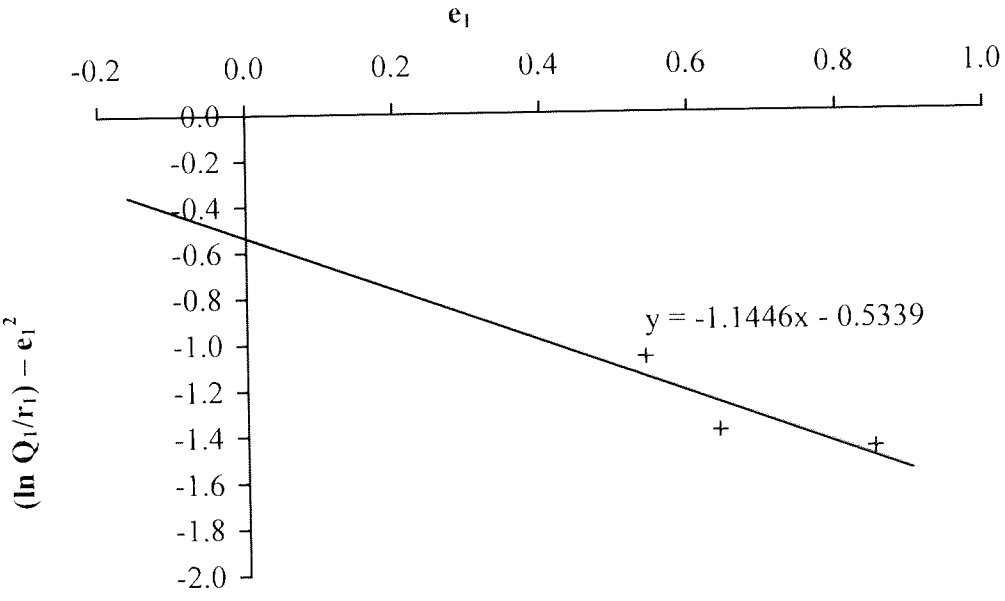

slope = $-e_2$

y-intercept = $\ln Q_2$

→ $e_2 = 1.14$ and $Q_2 = 0.59$ for NIPA

The Q and e Approximation For Hydroxypropyl Acrylate.

Hydroxypropyl acrylate (HPA) is a mix of isomers:

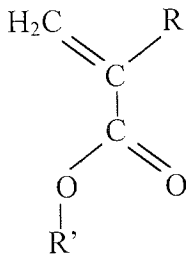

R = H R' = $CH_2CH_2CH_2OH$

and R' = $CH_2CH(OH)CH_3$

Data on Q and e values for glycidyl acrylate of similar structure exists, where

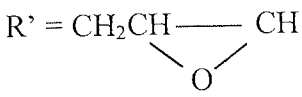

and Q = 0.48, e = 1.28.

These values are used for HPA as the approximated Q and e for reactivity calculations.

An example of the spreadsheet layout used to calculate the moles of water per mole of polymer upon entry of data (shaded fields).

The calculations required are programmed into the appropriate cells.

monomer	mol wt	%mass
HEMA	130.1	52.8
NVP	111.1	11.2
MMA	100.1	12
MPEGMA	300	19.2
SPA	232	4.8

%EWC	% freezing	% non-freezing
77.6	64	13.6

In 1g of hydrated polymer have:

g water	g freezing water	g non-freezing water	g polymer
0.776	0.64	0.136	0.224

In 0.224 **g polymer:**

	mass (g)	no. moles
HEMA	0.118	0.000909
NVP	0.025	0.000226
MMA	0.027	0.000269
MPEGMA	0.043	0.000143
SPA	0.011	0.000046
total no. mol polymer -		0.00159

Mol wt of water:
18

		no. moles
0.776	**g water:**	0.0431
0.64	**g freezing water:**	0.0356
0.136	**g non-freezing water:**	0.00756
	check sum	0.0431
	=	0.0431
	difference	0

Therefore:

mol total water/mol polymer =	27.06
mol freezing water/mol polymer =	22.32
mol non-freezing water/mol polymer =	4.74

check sum	27.06
=	27.06
difference	0.00

Appendix B

Water-Binding Properties Of Hydrated Materials

Copolymer Composition (Approx. % by mass)	EWC (%)	% Freezing water	% Non-freezing water
Copolymer X (=HEMA:NVP:MMA:$MPEG_{200}MA$)	40.1 ± 0.2	18.1 ± 0.6	22.0
Copolymer X + SPI			
$^1/_2$	53.1 ± 0.3	30.3 ± 1.0	22.8
1	57.1 ± 0.7	37.8 ± 0.5	19.3
$2^1/_2$	65.8 ± 0.2	48.1 ± 1.6	17.7
$4^4/_5$	68.0 ± 0.2	49.2 ± 1.2	18.8
$9^1/_5$	69.1 ± 0.3	51.5 ± 0.7	17.6
Copolymer X + NaAMPS			
$^1/_2$	51.1 ± 0.7	30.3 ± 0.1	21.1
1	58.2 ± 0.2	37.3 ± 1.0	20.9
$2^1/_2$	63.2 ± 0.2	44.6 ± 1.2	18.9
$4^4/_5$	74.3 ± 0.2	60.4 ± 1.1	13.9
$9^1/_5$	85.3 ± 0.1	75.6 ± 0.6	9.7
Copolymer X + SPA			
$^1/_2$	51.6 ± 0.1	31.6 ± 1.9	20.0
1	56.9 ± 0.2	37.3 ± 0.4	19.6
$2^1/_2$	66.2 ± 0.2	47.3 ± 0.7	18.9
$4^4/_5$	77.6 ± 0.3	64.0 ± 0.8	13.6
$9^1/_5$	86.7 ± 0.2	80.4 ± 1.1	6.3

Copolymer Composition (Approx. % by mass)	Mol water / Mol monomer repeat unit	Mol freezing water / Mol monomer repeat unit	Mol non-freezing water / Mol monomer repeat unit
Copolymer X (=HEMA:NVP:MMA:$MPEG_{200}MA$)	5.1	2.3	2.8
Copolymer X + SPI			
$^1/_2$	8.8	5.0	3.8
1	10.3	6.8	3.5
$2^1/_2$	14.8	10.8	4.0
$4^4/_5$	16.8	12.2	4.7
$9^1/_5$	18.3	13.6	4.7
Copolymer X + NaAMPS			
$^1/_2$	9.4	5.4	4.0
1	10.7	6.9	3.8
$2^1/_2$	13.3	9.4	3.9
$4^4/_5$	22.6	18.4	4.2
$9^1/_5$	52.2	46.2	6.0
Copolymer X + SPA			
$^1/_2$	8.2	5.0	3.2
1	10.2	6.9	3.5
$2^1/_2$	15.2	10.8	4.4
$4^4/_5$	27.0	22.3	4.7
$9^1/_5$	58.6	54.4	4.2

Copolymer Composition (Approx. % by mass)	EWC (%)	% Freezing water	% Non-freezing water
Copolymer X + $2^1/_2$ SPI + DMAEMA			
0	65.8 ± 0.2	48.1 ± 1.6	17.7
$^1/_4$	63.5 ± 0.4	48.2 ± 0.2	15.3
$^1/_2$	59.6 ± 0.8	45.0 ± 0.3	14.6
1	53.5 ± 0.9	34.0 ± 0.9	19.5
2	52.6 ± 0.3	33.8 ± 0.8	18.8
3	52.3 ± 0.6	31.5 ± 0.4	21.6
4	51.8 ± 0.6	31.2 ± 0.6	20.7
Copolymer X + $2^1/_2$ NaAMPS + DMAEMA			
0	63.2 ± 0.2	44.6 ± 1.2	18.6
$^1/_4$	69.0 ± 0.3	56.7 ± 0.5	12.3
$^1/_2$	63.4 ± 0.4	49.2 ± 1.1	14.2
1	59.5 ± 0.3	41.2 ± 1.3	18.3
2	53.7 ± 0.6	32.0 ± 1.6	21.7
3	53.1 ± 0.8	32.1 ± 1.1	21.0
4	53.4 ± 0.6	32.1 ± 0.2	21.3
Copolymer X + $2^1/_2$ SPA + DMAEMA			
0	66.2 ± 0.2	47.3 ± 0.7	18.9
$^1/_4$	68.9 ± 0.5	57.8 ± 0.7	11.1
$^1/_2$	66.3 ± 0.3	52.5 ± 1.0	13.8
1	57.9 ± 0.5	40.8 ± 0.3	17.1
2	52.6 ± 0.8	32.5 ± 0.4	20.1
3	52.4 ± 0.8	31.9 ± 1.1	20.5
4	53.1 ± 0.4	31.1 ± 0.7	22.0

Copolymer Composition (Approx. % by mass)	Mol water / Mol monomer repeat unit	Mol freezing water / Mol monomer repeat unit	Mol non-freezing water / Mol monomer repeat unit
Copolymer X + $2^1/_2$ SPI + DMAEMA			
0	15.0	11.0	4.0
$^1/_4$	13.6	10.3	3.3
$^1/_2$	11.5	8.7	2.8
1	9.0	5.7	3.3
2	8.7	5.6	3.1
3	8.6	5.2	3.4
4	8.4	5.1	3.4
Copolymer X + $2^1/_2$ NaAMPS + DMAEMA			
0	13.3	9.4	3.9
$^1/_4$	17.2	14.1	3.1
$^1/_2$	13.4	10.4	3.0
1	11.4	7.9	3.5
2	9.0	5.4	3.6
3	8.8	5.3	3.5
4	8.9	5.4	3.6
Copolymer X + $2^1/_2$ SPA + DMAEMA			
0	15.2	10.8	4.3
$^1/_4$	17.1	14.4	2.7
$^1/_2$	15.2	12.0	3.2
1	10.7	7.5	3.2
2	8.6	5.3	3.3
3	8.6	5.2	3.3
4	8.8	5.2	3.7

Copolymer Composition (Approx. % by mass)	EWC (%)	% Freezing water	% Non-freezing water
Copolymer X + PU5			
0%	40.1 ± 0.2	18.1 ± 0.6	22.0
1%	48.5 ± 0.4	27.0 ± 1.0	21.5
2%	47.5 ± 0.3	27.9 ± 0.0	19.6
5%	45.7 ± 0.5	26.7 ± 0.0	19.0
10%	45.0 ± 0.5	26.1 ± 0.7	18.9
HEMA:AMO:MMA:$MPEG_{200}MA$ + 2% PU5	44.9 ± 0.4	27.4 ± 0.1	17.5
HEMA:NVP:MMA:$MPEG_{200}MA$ + 2% PU6	56.3 ± 0.3	37.0 ± 0.0	19.3
THFMA:AMO:NVP:MMA:$MPEG_{200}MA$ + PU5			
0%	67.3 ± 0.6	49.3 ± 0.9	18.0
1%	74.5 ± 0.3	64.1 ± 0.8	10.4
2%	73.7 ± 0.3	57.8 ± 0.8	15.9
5%	69.8 ± 0.2	52.6 ± 1.0	17.2
10%	65.2 ± 0.3	46.3 ± 0.1	18.9
EEMA:AMO:NVP:MMA:$MPEG_{200}MA$ + PU5			
0%	67.6 ± 0.2	48.1 ± 1.4	19.5
1%	74.5 ± 0.1	63.3 ± 0.5	11.2
2%	71.5 ± 0.3	58.6 ± 0.1	12.9
5%	68.7 ± 1.0	52.6 ± 0.1	16.1
10%	71.5 ± 0.3	48.3 ± 0.4	18.0

Copolymer Composition (Approx. % by mass)	EWC (%)				
	20°C	25°C	30°C	35°C	40°C
AA : HPA : NVP					
$23^{1}/_{6} : 66^{1}/_{2} : 10^{1}/_{3}$ *(35:55:10 by molar parts)*	85.5 ± 0.3	83.5 ± 0.4	83.0 ± 0.6	81.1 ± 1.0	79.7 ± 0.7
$40^{5}/_{6} : 47^{11}/_{20} : 11^{3}/_{5}$ *(55:35:10 by molar pts.)*	87.6 ± 0.4	88.4 ± 0.4	88.7 ± 0.1	88.0 ± 0.1	87.4 ± 0.1
AA : HPA : AMO					
$22^{1}/_{2} : 64^{7}/_{10} : 12^{3}/_{4}$ *(35:55:10 by molar pts.)*	84.7 ± 0.3	81.8 ± 0.1	80.9 ± 0.1	80.0 ± 0.4	78.8 ± 0.1
$39^{3}/_{5} : 46^{1}/_{10} : 14^{3}/_{10}$ *(55:35:10 by molar pts.)*	86.7 ± 0.1	87.2 ± 0.1	88.4 ± 0.0	87.1 ± 0.5	85.8 ± 0.1
NIPA : HPA : NVP					
$32^{2}/_{5} : 58^{1}/_{2} : 9^{1}/_{10}$ *(35:55:10 by molar pts.)*	84.5 ± 0.1	64.0 ± 0.6	51.7 ± 0.9	41.9 ± 0.4	42.5 ± 0.8
$52^{1}/_{3} : 38^{1}/_{3} : 9^{1}/_{3}$ *(55:35:10 by molar pts.)*	88.9 ± 0.2	73.4 ± 0.9	59.7 ± 1.0	49.0 ± 1.5	50.9 ± 0.3
NIPA : HPA : AMO					
$31^{3}/_{5} : 57^{1}/_{10} : 11^{1}/_{4}$ *(35:55:10 by molar pts.)*	78.0 ± 0.3	50.5 ± 0.6	42.0 ± 0.1	36.6 ± 0.9	38.6 ± 1.6
$51^{1}/_{10} : 37^{1}/_{3} : 11^{3}/_{5}$ *(55:35:10 by molar pts.)*	87.0 ± 0.2	65.7 ± 1.0	50.2 ± 1.3	36.7 ± 1.6	38.3 ± 0.2

Appendix C

Mechanical Properties Of Hydrated Materials

Copolymer Composition (Approx. % by mass)	E (MPa)	Ts (MPa)	Eb (%)
Copolymer X (=HEMA:NVP:MMA:MPEG$_{200}$MA)	0.30 ± 0.03	0.35 ± 0.06	214 ± 51
Copolymer X + SPI			
$^1/_2$	0.23 ± 0.02	0.26 ± 0.02	159 ± 17
1	0.20 ± 0.02	0.28 ± 0.07	229 ± 24
$2^1/_2$	0.21 ± 0.02	0.21 ± 0.05	148 ± 43
$4^4/_5$	0.20 ± 0.03	0.20 ± 0.05	148 ± 47
$9^1/_5$	0.20 ± 0.02	0.21 ± 0.03	144 ± 24
Copolymer X + NaAMPS			
$^1/_2$	0.27 ± 0.01	0.33 ± 0.04	188 ± 23
1	0.24 ± 0.02	0.34 ± 0.02	219 ± 15
$2^1/_2$	0.25 ± 0.05	0.36 ± 0.04	216 ± 24
$4^4/_5$	0.22 ± 0.03	0.22 ± 0.05	129 ± 33
$9^1/_5$	0.20 ± 0.02	0.13 ± 0.03	99 ± 10
Copolymer X + SPA			
$^1/_2$	0.30 ± 0.02	0.25 ± 0.02	124 ± 12
1	0.31 ± 0.04	0.24 ± 0.08	120 ± 51
$2^1/_2$	0.27 ± 0.02	0.25 ± 0.02	98 ± 12
$4^4/_5$	0.24 ± 0.01	0.16 ± 0.03	92 ± 12
$9^1/_5$	0.23 ± 0.02	0.09 ± 0.02	48 ± 13

Copolymer Composition (Approx. % by mass)	E (MPa)	Ts (MPa)	Eb (%)
Copolymer X + $2^1/_2$ SPI + DMAEMA			
0	0.21 ± 0.02	0.21 ± 0.05	148 ± 43
$^1/_4$	0.17 ± 0.03	0.18 ± 0.04	156 ± 51
$^1/_2$	0.19 ± 0.03	0.18 ± 0.05	151 ± 70
1	0.22 ± 0.02	0.17 ± 0.01	119 ± 18
2	0.27 ± 0.05	0.17 ± 0.05	91 ± 40
3	0.26 ± 0.01	0.16 ± 0.02	91 ± 17
4	0.25 ± 0.03	0.17 ± 0.03	92 ± 20
Copolymer X + $2^1/_2$ NaAMPS + DMAEMA			
0	0.25 ± 0.05	0.36 ± 0.04	216 ± 24
$^1/_4$	0.17 ± 0.01	0.12 ± 0.03	101 ± 37
$^1/_2$	0.17 ± 0.02	0.19 ± 0.06	160 ± 66
1	0.20 ± 0.02	0.17 ± 0.07	131 ± 63
2	0.25 ± 0.05	0.19 ± 0.05	125 ± 37
3	0.25 ± 0.02	0.14 ± 0.03	87 ± 17
4	0.27 ± 0.03	0.08 ± 0.04	39 ± 7
Copolymer X + $2^1/_2$ SPA + DMAEMA			
0	0.27 ± 0.02	0.25 ± 0.02	98 ± 12
$^1/_4$	0.19 ± 0.03	0.14 ± 0.02	120 ± 18
$^1/_2$	0.18 ± 0.01	0.15 ± 0.02	129 ± 26
1	0.26 ± 0.01	0.17 ± 0.02	106 ± 25
2	0.28 ± 0.02	0.19 ± 0.06	107 ± 45
3	0.28 ± 0.04	0.16 ± 0.03	70 ± 17
4	0.26 ± 0.03	0.14 ± 0.02	57 ± 16

Copolymer Composition (Approx. % by mass)	E (MPa)	Ts (MPa)	Eb (%)
Copolymer X + PU5			
0%	0.30 ± 0.03	0.35 ± 0.06	214 ± 51
1%	0.21 ± 0.03	0.44 ± 0.08	278 ± 60
2%	0.46 ± 0.04	0.39 ± 0.01	179 ± 14
5%	0.58 ± 0.05	0.85 ± 0.07	250 ± 21
10%	1.31 ± 0.18	1.50 ± 0.10	235 ± 17
HEMA:AMO:MMA:$MPEG_{200}MA$ + 2% PU5	0.42 ± 0.01	0.36 ± 0.04	193 ± 19
HEMA:NVP:MMA:$MPEG_{200}MA$ + 2% PU6	0.19 ± 0.01	0.35 ± 0.04	262 ± 27
THFMA:AMO:NVP:MMA:$MPEG_{200}MA$ + PU5			
0%	0.09 ± 0.01	0.09 ± 0.02	96 ± 35
1%	0.04 ± 0.00	0.09 ± 0.02	138 ± 20
2%	0.10 ± 0.01	0.14 ± 0.03	145 ± 25
5%	0.10 ± 0.00	0.21 ± 0.05	231 ± 29
10%	0.13 ± 0.02	0.22 ± 0.04	177 ± 23
EEMA:AMO:NVP:MMA:$MPEG_{200}MA$ + PU5			
0%	0.09 ± 0.01	0.14 ± 0.02	202 ± 28
1%	0.06 ± 0.01	0.11 ± 0.02	214 ± 43
2%	0.07 ± 0.00	0.13 ± 0.02	242 ± 35
5%	0.11 ± 0.01	0.19 ± 0.04	209 ± 32
10%	0.12 ± 0.00	0.28 ± 0.04	218 ± 30

Appendix D

Surface Properties
Of Hydrated Materials

Copolymer Composition (Approx. % by mass)	Air contact angle (°)	Octane contact angle (°)	γ_s^d (mN m^{-1})	γ_s^p (mN m^{-1})	γ_s^t (mN m^{-1})
Copolymer X (=HEMA:NVP:MMA:MPEG$_{200}$MA)	38 ± 2	133 ± 3	23.3	35.9	59.2
Copolymer X + SPI					
$^1/_2$	32 ± 2	141 ± 2	22.6	40.1	62.8
1	30 ± 3	153 ± 3	17.5	45.7	63.6
$2^1/_2$	29 ± 3	153 ± 3	18.5	45.6	64.1
$4^4/_5$	28 ± 1	153 ± 1	19.0	45.6	64.7
$9^1/_5$	28 ± 3	154 ± 3	18.3	46.1	64.4
Copolymer X + NaAMPS					
$^1/_2$	28 ± 2	143 ± 2	23.7	41.2	65.0
1	29 ± 3	152 ± 2	18.9	45.2	64.1
$2^1/_2$	28 ± 1	150 ± 4	20.2	44.4	64.6
$4^4/_5$	28 ± 3	152 ± 2	19.5	45.2	64.6
$9^1/_5$	28 ± 1	149 ± 1	20.7	44.0	64.7
Copolymer X + SPA					
$^1/_2$	29 ± 3	144 ± 3	22.5	41.8	64.3
1	28 ± 2	143 ± 2	23.7	41.2	65.0
$2^1/_2$	28 ± 2	150 ± 2	20.2	44.4	64.6
$4^4/_5$	28 ± 2	152 ± 2	19.5	45.2	64.6
$9^1/_5$	29 ± 1	155 ± 2	17.8	46.3	64.1

Copolymer Composition (Approx. % by mass)	Air contact angle (°)	Octane contact angle (°)	γ_s^d (mN m^{-1})	γ_s^p (mN m^{-1})	γ_s^t (mN m^{-1})
Copolymer X + $2^1/_2$ SPI + DMAEMA					
0	29 ± 3	153 ± 3	18.5	45.6	64.1
$^1/_4$	27 ± 3	153 ± 1	19.6	45.6	65.2
$^1/_2$	25 ± 1	155 ± 1	19.9	46.3	66.2
1	24 ± 2	156 ± 1	20.1	46.7	66.8
2	25 ± 2	159 ± 1	18.6	47.7	66.3
3	25 ± 1	158 ± 2	18.9	47.4	66.3
4	25 ± 1	160 ± 2	18.3	47.9	66.3
Copolymer X + $2^1/_2$ NaAMPS + DMAEMA					
0	28 ± 1	150 ± 4	20.2	44.4	64.6
$^1/_4$	27 ± 1	156 ± 1	18.5	46.7	65.2
$^1/_2$	26 ± 1	160 ± 2	17.8	47.9	65.8
1	28 ± 3	154 ± 2	18.7	45.9	64.6
2	28 ± 2	156 ± 2	18.0	46.7	64.7
3	26 ± 1	155 ± 1	19.4	46.3	65.7
4	25 ± 1	156 ± 1	19.6	46.7	66.2
Copolymer X + $2^1/_2$ SPA + DMAEMA					
0	28 ± 2	150 ± 2	20.2	44.4	64.6
$^1/_4$	23 ± 0	154 ± 1	21.3	45.9	67.3
$^1/_2$	23 ± 1	157 ± 0	20.3	47.0	67.2
1	23 ± 1	159 ± 1	19.6	47.7	67.2
2	23 ± 0	160 ± 2	19.3	47.9	67.3
3	26 ± 1	155 ± 1	19.4	46.3	65.7
4	24 ± 0	156 ± 0	20.1	46.7	66.8

Copolymer Composition (Approx. % by mass)	Air contact angle (°)	Octane contact angle (°)	γ_s^d (mN m^{-1})	γ_s^p (mN m^{-1})	γ_s^t (mN m^{-1})
Copolymer X + PU5					
0%	38 ± 3	133 ± 3	23.3	35.9	59.2
1%	31 ± 1	154 ± 2	17.0	45.9	62.9
2%	30 ± 2	146 ± 1	20.9	42.7	63.5
5%	30 ± 2	149 ± 2	19.5	44.0	63.5
10%	29 ± 2	154 ± 2	18.2	45.9	64.1
HEMA:AMO:MMA:$MPEG_{200}MA$ + 2% PU5	32 ± 1	144 ± 2	20.6	41.8	62.3
HEMA:NVP:MMA:$MPEG_{200}MA$ + 2% PU6	27 ± 2	159 ± 1	17.6	47.7	65.3
THFMA:AMO:NVP:MMA:$MPEG_{200}MA$ + PU5					
0%	27 ± 1	152 ± 1	20.0	45.2	65.2
1%	27 ± 1	155 ± 1	18.9	45.2	65.2
2%	30 ± 1	151 ± 2	18.7	44.8	63.5
5%	31 ± 1	150 ± 1	18.5	44.4	62.9
10%	29 ± 1	152 ± 2	18.9	45.2	64.1
EEMA:AMO:NVP:MMA:$MPEG_{200}MA$ + PU5					
0%	30 ± 2	154 ± 1	17.6	45.9	63.5
1%	28 ± 2	151 ± 2	19.8	44.8	64.6
2%	31 ± 1	149 ± 1	18.9	44.0	62.9
5%	34 ± 2	145 ± 2	18.8	42.2	61.0
10%	31 ± 1	145 ± 2	20.7	42.2	62.9

Silicone hydrogel with surface epoxy groups	Plasma-treated	Grafting monomers (weight %)	Advancing contact angle, θ_A (°)	Receding contact angle, θ_R (°)	Hysteresis, θ_H (°)	Surface tension of water, S_T (mN m^{-1})
No	Yes	NNDMA, 100	107.5	51.1	56.4	69.1
Yes	No	NNDMA, 100	103.2	45.8	57.4	69.2
Yes	Yes	NNDMA, 100	90.6	40.9	49.7	70.7
Yes	Yes	AA:HPA:NVP:EGDMA:AZBN $23^1/_6 : 66^1/_2 : 10^1/_3 : 1 : {}^1/_2$	65.6	40.2	25.4	69.8
Yes	Yes	AA:HPA:NVP:EGDMA $23^1/_6 : 66^1/_2 : 10^1/_3 : 1$	62.6	42.2	20.3	67.9
Yes	Yes	AA:HPA:AMO:EGDMA:AZBN $22^1/_2 : 64^7/_{10} : 12^3/_4 : 1 : {}^1/_2$	100.8	43.7	57.1	70.7
Yes	Yes	AA:HPA:AMO:EGDMA $22^1/_2 : 64^7/_{10} : 12^3/_4 : 1$	79.1	49.7	29.4	69.5
Yes	Yes	NVP:SPA:EGDMA:AZBN $95 : 5 : 1 : {}^1/_2$	62.5	43.8	18.6	70.4
Yes	Yes	NVP:SPA:EGDMA 95 : 5 : 1	50.3	41.0	9.3	70.6

Appendix E

Spoilation Properties Of Hydrogel Materials

Total Protein Spoilation (mg/lens)								
Copolymer (Approx. % by mass)	Day							
	3	7	10	14	17	21	24	28
Copolymer X [HEMA:NVP: MMA:$MPEG_{200}MA$]	0.020	0.036	0.057	0.104	0.126	0.245	0.449	0.580
Copolymer X + SPI								
$^1/_2$	0.024	0.041	0.068	0.077	0.098	0.105	0.140	0.155
1	0.006	0.016	0.037	0.051	0.093	0.113	0.122	0.126
$2^1/_2$	0.029	0.061	0.076	0.122	0.171	0.209	0.250	0.297
$4^4/_5$	0.025	0.035	0.050	0.080	0.107	0.127	0.286	0.374
$9^1/_5$	0.014	0.042	0.081	0.111	0.130	0.142	0.143	0.229
Copolymer X + NaAMPS								
$^1/_2$	0.041	0.058	0.062	0.071	0.080	0.110	0.121	0.130
1	0.025	0.035	0.050	0.098	0.110	0.119	0.123	0.164
$2^1/_2$	0.003	0.029	0.054	0.096	0.111	0.124	0.187	0.365
$4^4/_5$	0.022	0.151	0.195	0.230	0.257	0.263	0.266	0.323
Copolymer X + SPA								
$^1/_2$	0.015	0.032	0.033	0.056	0.086	0.093	0.123	0.146
1	0.015	0.061	0.065	0.095	0.101	0.107	0.116	0.161
$2^1/_2$	0.003	0.029	0.040	0.062	0.101	0.169	0.211	0.217
$4^4/_5$	0.006	0.028	0.168	0.287	0.314	0.398	0.479	0.529

Surface Protein Spoilation (fluorescence units)								
Copolymer (Approx. % by mass)	Day							
	3	7	10	14	17	21	24	28
Copolymer X [HEMA:NVP: MMA:$MPEG_{200}MA$]	349	898	1462	2520	3046	3254	5559	9787
Copolymer X + SPI								
$^1/_2$	1739	2045	2146	2454	2795	3059	3316	4823
1	665	1230	1486	1739	1978	2081	3230	3665
$2^1/_2$	533	1436	1534	1723	2068	2248	4072	5282
$4^4/_5$	1263	1868	2452	3518	3834	4770	6242	6821
$9^1/_5$	747	945	1820	2391	2564	4320	3398	3648
Copolymer X + NaAMPS								
$^1/_2$	895	927	1022	3247	3652	4648	7669	9292
1	814	1327	1942	3110	3322	4204	4152	4433
$2^1/_2$	947	1616	1656	1747	1827	1864	1969	3198
$4^4/_5$	736	1518	1749	3122	3482	4045	5606	6280
Copolymer X + SPA								
$^1/_2$	451	1675	1912	2527	2590	3359	5137	9828
1	1296	1710	2664	2954	3095	4089	6638	6870
$2^1/_2$	1046	1159	1658	2163	2473	2564	3632	9.85
$4^4/_5$	1815	3756	4296	6767	9421	9809	9881	9899

Surface Lipid Spoilation (fluorescence units)								
Copolymer (Approx. % by mass)	Day							
	3	7	10	14	17	21	24	28
Copolymer X [HEMA:NVP: MMA:$MPEG_{200}MA$]	5	114	142	166	200	279	542	753
Copolymer X + SPI								
$^1/_2$	0	23	62	65	168	235	272	658
1	135	105	222	238	266	305	299	338
$2^1/_2$	54	58	81	108	113	119	139	364
$4^4/_5$	76	96	160	182	189	220	276	282
$9^1/_5$	42	60	62	138	232	257	290	313
Copolymer X + NaAMPS								
$^1/_2$	34	115	179	209	222	303	287	369
1	104	227	243	312	353	390	494	601
$2^1/_2$	60	76	126	168	182	201	220	510
$4^4/_5$	68	110	125	134	152	475	207	249
Copolymer X + SPA								
$^1/_2$	69	79	118	141	327	302	446	845
1	125	155	237	251	235	384	413	554
$2^1/_2$	56	58	63	83	104	112	119	192
$4^4/_5$	84	213	526	539	957	1179	1217	909

Total Protein Spoilation (mg/lens)								
Copolymer (Approx. % by mass)	Day							
	3	7	10	14	17	21	24	28
Copolymer X + 2.5% SPI + DMAEMA								
0	0.029	0.061	0.076	0.122	0.171	0.209	0.250	0.297
1/4	0.153	0.243	0.281	0.289	0.314	0.331	0.349	0.362
1	0.329	0.399	0.422	0.428	0.462	0.485	0.500	0.524
4	0.032	0.065	0.074	0.083	0.095	0.116	0.140	0.222
Copolymer X + 2.5% NaAMPS + DMAEMA								
0	0.003	0.029	0.054	0.096	0.111	0.124	0.187	0.365
1/4	0.013	0.161	0.265	0.293	0.326	0.371	0.389	0.384
1/2	0.182	0.205	0.251	0.286	0.341	0.358	0.391	0.417
1	0.362	0.447	0.636	0.698	0.717	0.773	0.797	0.816
4	0.039	0.050	0.066	0.101	0.128	0.168	0.190	0.218
Copolymer X + 2.5% SPA + DMAEMA								
0	0.003	0.029	0.040	0.062	0.101	0.169	0.211	0.271
1/4	0.193	0.250	0.261	0.278	0.305	0.352	0.359	0.431
1/2	0.138	0.195	0.237	0.301	0.349	0.369	0.438	0.460
1	0.056	0.086	0.146	0.149	0.164	0.190	0.218	0.247

Surface Protein Spoilation (fluorescence units)								
Copolymer (Approx. % by mass)	Day							
	3	7	10	14	17	21	24	28
Copolymer X + 2.5% SPI + DMAEMA								
0	533	1436	1534	1723	2068	2248	4672	5262
1/4	1582	3144	3272	4402	4986	6172	7011	9378
1	750	1347	1987	2073	2605	3710	4181	5116
4	216	797	890	919	1106	2193	3346	3507
Copolymer X + 2.5% NaAMPS + DMAEMA								
0	947	1616	1656	1747	1827	1864	1969	3198
1/4	1204	1744	3339	3941	5102	6054	6623	8490
1/2	1181	1670	2419	2954	4819	6386	7504	9708
1	706	2757	2644	3262	3765	3818	5716	9777
4	365	524	614	758	955	1886	5892	7051
Copolymer X + 2.5% SPA + DMAEMA								
0	1046	1159	1658	2163	2473	2564	3632	9385
1/4	568	3203	3738	3887	4342	5160	7831	8575
1/2	1257	1410	2164	2229	5697	7022	8617	9801
1	33	761	2870	3170	3813	6506	6631	7181

Surface Lipid Spoilation (fluorescence units)								
Copolymer (Approx. % by mass)	Day							
	3	7	10	14	17	21	24	28
Copolymer X + 2.5% SPI + DMAEMA								
0	54	58	81	108	113	119	139	364
1/4	44	104	154	172	203	232	269	459
1	16	48	66	87	122	147	197	407
4	37	56	84	126	133	181	294	348
Copolymer X + 2.5% NaAMPS + DMAEMA								
0	60	76	126	168	182	201	220	510
1/4	28	49	67	102	130	266	381	444
1/2	15	66	130	137	177	220	280	645
1	34	41	55	165	297	450	499	848
4	91	102	118	129	186	201	224	356
Copolymer X + 2.5% SPA + DMAEMA								
0	56	58	63	83	104	112	119	192
1/4	65	82	119	150	173	178	291	423
1/2	43	73	118	333	317	329	395	741
1	60	131	133	255	352	400	441	689

Total Protein Spoilation (mg/lens)								
Copolymer (Approx. % by mass)	Day							
	3	7	10	14	17	21	24	28
Copolymer X Modification # 1 HEMA→THFMA:AMO + PU5								
0	0.020	0.062	0.812	1.179	1.215	1.240	1.287	1.442
1%	0.180	0.206	0.218	0.252	0.279	0.405	0.434	0.511
2%	0.068	0.545	0.752	0.790	0.846	0.917	1.028	1.175
5%	0.119	0.564	0.838	0.956	1.099	1.172	1.220	1.355
10%	0.030	0.092	0.114	0.214	0.303	1.143	1.233	1.311
Copolymer X Modification # 2 HEMA→EEMA:AMO + PU5								
0	0.032	0.072	0.121	0.164	0.187	0.233	0.266	
1%	0.054	0.097	0.161	0.215	0.311	0.338	0.424	0.482
2%	0.000	0.128	0.294	0.410	0.531	0.605	0.661	0.781
5%	0.068	0.527	0.572	0.674	0.762	0.866	0.925	1.037
10%	0.032	0.662	0.937	1.063	1.133	1.207	1.259	1.457

Surface Protein Spoilation (fluorescence units)								
Copolymer (Approx. % by mass)	Day							
	3	7	10	14	17	21	24	28
Copolymer X Modification # 1 HEMA→THFMA:AMO + PU5								
0	1232	1508	1441	2545	5656	6392	6718	8235
1%	909	1037	1235	1247	1267	2026	2667	3417
2%	375	645	947	2645	3049	3029	4548	5027
5%	123	256	1101	1594	1974	4440	5570	7852
10%	345	1407	1940	2804	3373	3925	4167	8595
Copolymer X Modification # 2 HEMA→EEMA:AMO + PU5								
0	873	1094	1547	2150	2301	2715	3214	3513
1%	148	386	648	1015	1731	2029	3927	5634
2%	994	1370	2021	2097	2304	4465	5846	6326
5%	581	1072	1999	2450	2886	2818	5632	7222
10%	38	75	634	3536	3768	6135	6439	7517

Surface Lipid Spoilation (fluorescence units)								
Copolymer (Approx. % by mass)	Day							
	3	7	10	14	17	21	24	28
Copolymer X Modification # 1 HEMA→THFMA:AMO + PU5								
0	97	110	116	165	571	622	716	1200
1%	125	184	216	223	243	509	553	736
2%	135	272	351	763	887	1105	1313	1469
5%	79	96	109	197	215	287	371	334
10%	164	276	342	356	373	409	599	976
Copolymer X Modification # 2 HEMA→EEMA:AMO + PU5								
0	57	139	149	183	355	386	442	492
1%	94	119	143	203	268	286	554	752
2%	160	242	308	308	432	257	575	646
5%	70	103	143	279	425	679	492	1003
10%	62	74	86	172	268	510	644	919

Appendix F

Dynamic Contact Angle Measurements Of Some Silicone Materials

Lens material (Company)	EWC (%)	Advancing contact angle θ_A (°)	Receding contact angle θ_R (°)	Hysteresis θ_H (°)	Surface tension of water, S_T (mN m^{-1})
Silicone elastomer PDMS (Essilor)	-	136.4	77.1	59.3	89.7
PDMS with surface epoxy groups (Essilor)	-	124.3	53.0	71.3	70.7
Focus Night & Day (CIBA)	24	85.2	41.8	43.4	70.4
Pure Vision (B&L)	35	114.0	35.4	78.6	71.7

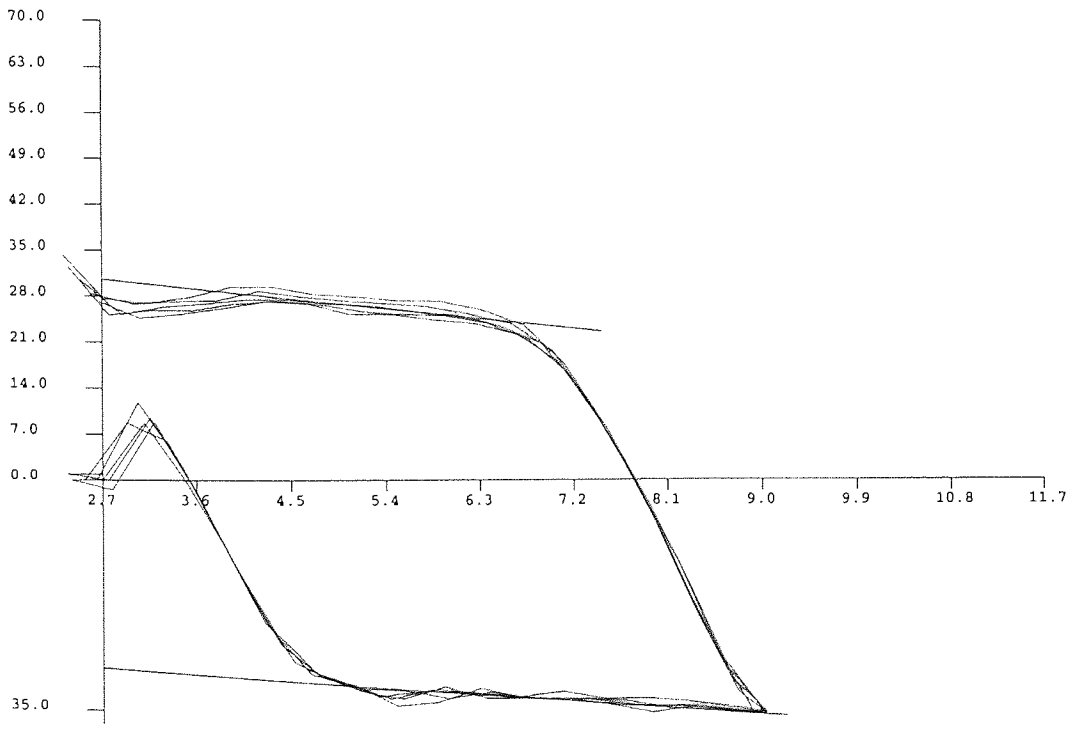

Graph showing wetting hysteresis of Essilor silicone elastomer with surface epoxy groups.

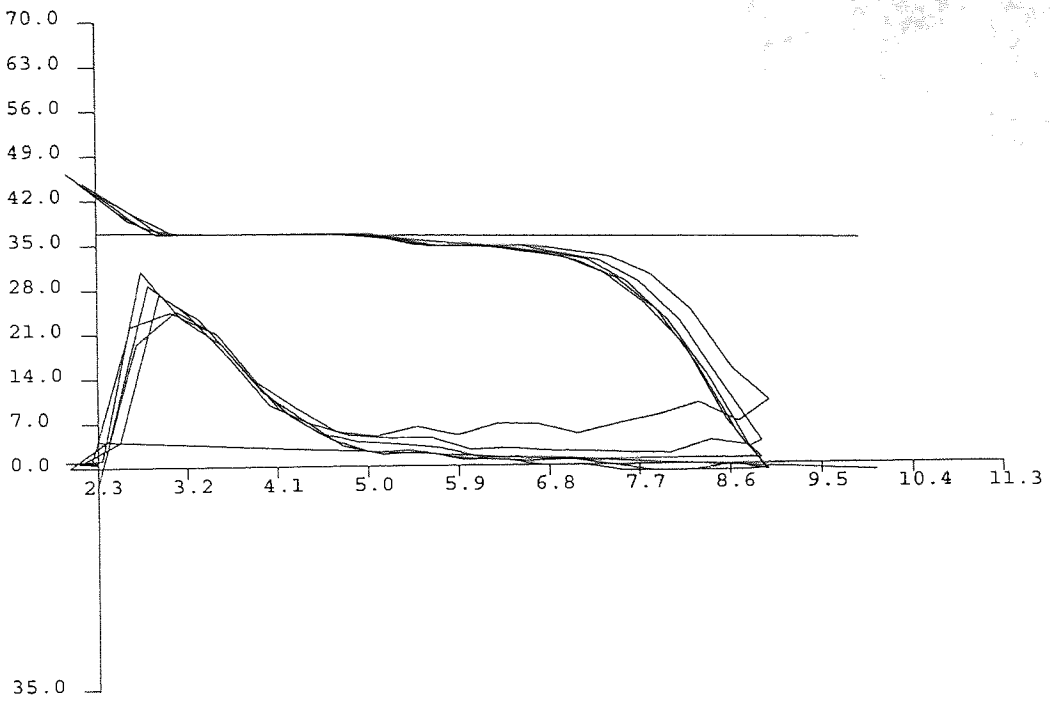

Graph showing wetting hysteresis of CIBA Focus Night & Day silicone hydrogel material.

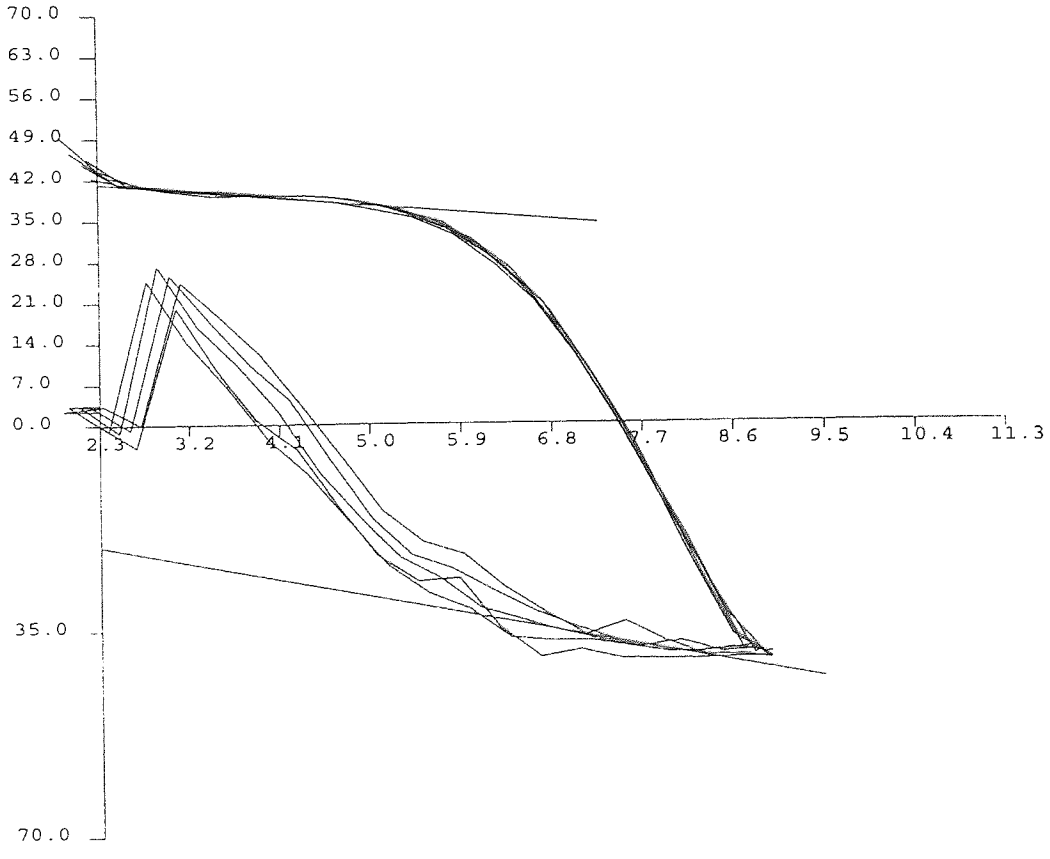

Graph showing wetting hysteresis of Bausch & Lomb Pure Vision silicone hydrogel material.